Title
Energy Systems Optimization

Author
Albassam, Abdulrahman M.

Publication Date
2016

Peer reviewed|Thesis/dissertation

University of California
Los Angeles

Energy Systems Optimization

A dissertation submitted in partial satisfaction
of the requirements for the degree
Doctor of Philosophy in Chemical Engineering

by

Abdulrahman Musaed Albassam

2017

Abstract of the Dissertation

Energy Systems Optimization

by

Abdulrahman Musaed Albassam

Doctor of Philosophy in Chemical Engineering

University of California, Los Angeles, 2017

Professor Vasilios Manousiouthakis, Chair

This dissertation presents novel realizations in balancing the economical and environmental constraints in an energy intense world using process network synthesis, energetic process enhancement, carbon dioxide utilization and the deployment of renewable energy resources. Such balance is achieved through effective control and planning of resources and conditions. The mathematical optimization framework developed in this body of work can be found in chapters 1 and 2 while their applications are developed in chapters 3 and 4.

Chapter 1, introduce for the first time the Infinite Dimensional State-Space (IDEAS) based synthesis of reactor networks featuring multiple residence time distribution (MRTD). IDEAS is shown to be applicable to the MRTD synthesis problem containing a combination of Plug Flow reactor (PFR), Continuous Stirred-Tank Reactor (CSTR) and Segregated Laminar Flow Reactor (SLFR). The formulation which synthesize reactor networks featuring multiple residence time distribution (MRTD) guarantees global optimality through IDEAS based properties. Case studies featuring the Trambouze reaction scheme are carried out using the different reactor combinations and multiple selectivity and economical constraints.

Chapter 2, presents for the first time a design and synthesis framework for the minimum number of units reactor networks problem with multiple Residence time density functions. The works combines Plug Flow Reactor (PFR) and Continuous Stirred-Tank Reactor (CSTR) in constructing reactor networks using an IDEAS based Mixed Integer Linear Pro-

graming (MILP) formulation. Case studies featuring the Trambouze reaction scheme are carried out based on multiple process specification. This work expands the real life application potential of the work presented in chapter 1.

In chapter 3, the newly developed concept of process energetics is applied to Steam Methane Reforming (SMR) to address the highly endothermic load challenge. The resulting process termed Energetically Enhanced Steam Methane Reforming (EESMR) is a non combustion process which means that the process related GHG emissions will receive favorable treatment in national carbon pricing programs.

Chapter 4 presents an energetically self-sufficient process with zero carbon dioxide emissions for the production of electricity and chemicals from natural gas. The choice of product can be made based on environmental and economical constraints explained within the chapter. Natural Gas Chemical Power System (NGCPS) provides flexibility of choice when it comes to producing electricity, formic acid and hydrogen. The work further covers the environmental impact of thermochemical cycles in power production.

The dissertation of Abdulrahman Musaed Albassam is approved.

Reza H. Ahmadi

James Davis

Selim M. Senkan

Vasilios Manousiouthakis, Committee Chair

University of California, Los Angeles

2017

To my family, your support and encouragement is more than what I can express on paper...

Table of Contents

List of Figures

List of Tables

Acknowledgments

Undertaking this PhD has been nothing short of a life changing experience for me and it would not have been possible without the guidance and support that I received from many people.

First, I would like to acknowledge my advisor and mentor Vasilios Manousiouthakis who went the extra mile to assist me. I must thank you for the patience and understanding you gave me, I have reaped many benefits from my time with you. Thank you for your powerful, well-thought-out advice and for pushing me towards my goal.

I would like to dedicate this work to my family whose support throughout my life has allowed me to be the person I am today. Words cannot express how grateful I am to my mother, my father and my little sister for their prayers for me which was what sustained me thus far.

I would like express my sincere appreciation to my friends Badr, Ahmed, Khalil, Nasser, Fawaz, Rayan, Ali, Abdulaziz, Fahad, Faisal, Mansour, Talal, Abdulrahman, Mohammed, Bassam, Abdullah, Zaid, Flavio, Patricia and Sultan without whom this work would have been completed a year earlier.

I would like to thank Saudi Aramco Research & Development Center for the generous financial support and the valuable advice from my chief technologist Ali Alsomali. From Saudi Aramco I would like to express my deepest gratitude to Ahmad Alkhowaiter, Abdullah Alnaim and Amir Alsulaim for their perspective and encouragement in support of my endeavors, it means a lot that you have taken time out of your busy schedules to help me succeed. The time you invested in me will have a significant impact on my life for years to come.

Finally, Chapter 4 is dedicated to the burglars in Los Angeles who broke into my house and stole my computer, which contained the original contents of the chapter. Losing such content forced me to rethink, retool and redo the project with a new mantra.

Vita

2008	B.S with First Honors in Chemical Engineering, King Fahd University of Petroleum and Minerals (KFUPM) Dhahran, Saudi Arabia
2008-2011	Research Engineer, Saudi Aramco R&D Center Dhahran, Saudi Arabia
2010-2011	Process Engineer, Saudi Aramco Shell Refinery (SASREF) Jubail, Saudi Arabia

Publications

Albassam, A. and Manousiouthakis, V. Green Power Production From Natural Gas. In AIChE Annual Meeting, paper 698b, Pittsburgh, PA; 2012

Albassam, A. and Manousiouthakis, V. The Power of Electricity & Chemicals Co-Production. In AIChE Annual Meeting, paper 381c, Atlanta, GA; 2014

Albassam, A. and Manousiouthakis, V. Difficulties in Separation: A Unique Thermodynamic Approach. In AIChE Annual Meeting, paper 359b, Atlanta, GA; 2014

Conner, J. , Albassam, A. and Manousiouthakis, V. On Quantification of the Attainable Region for Separator Networks with Varying Network Outlet Flowrates. In AIChE Annual Meeting, paper 555f, Salt Lake, UT; 2015

Albassam, A. and Manousiouthakis, V. Synthesis of Reactor Networks Featuring Minimum Number of Units and Network Volume Constraints. In AIChE Annual Meeting, paper 291d, Salt Lake, UT; 2015

Albassam, A. and Manousiouthakis, V. Synthesis of Networks of Reactors Featuring Multiple Residence Time Distribution. In AIChE Annual Meeting, paper 156b, Salt Lake, UT; 2015

CHAPTER 1

IDEAS based synthesis of reactor networks featuring multiple residence time distribution (RTD) models

1.1 Introduction

In reactor modeling, parameters can be estimated for various reactors using basic information such as the rate of the reaction, this however leaves a lot to be desired when it comes to truly understanding the reaction kinetics . This fact is further magnified when we look at the problem at the system level to design reactor networks. In order to address such problem, the synthesis of reactor networks models the behavior of individual reactor units using Residence Time density/Distribution (RTd/RTD) mathematical models. Residence Time Distribution (RTD) was first introduced in 1935 as a tool to analyze reactor performance, and improve the process of reactor design[7]. RTD functions are typically measured using impulse (step) function tracer experiments[8], and are thus limited to reactors with a single feed and a single exit stream [9] . Aside from these limitations, RTD based reactor modeling is carried out under the assumptions that the reactor operates at steady state, and the reacting phase is homogeneous, and isothermal. These assumptions are employed throughout this work[10]. The RTD's of many common reactor types have been identified and are now included in most reaction engineering textbooks[11, 12, 13, 14]. Mixing can be examined at two levels: *micromixing* and *macromixing* with an intermediate state in between termed as mesomixing, and attributed to two mechanisms: turbulent dispersion, and inertial convective disintegration of large eddies[15]. Danckwerts discussed the functions of multiple RTDs highlighting the importance of mixing, micromixing and degree of segregation[16]. The con-

cept of maximum mixedness introduced by Zwietering is a mixing pattern at the opposite extreme of segregation, and showed that RTD knowledge must be combined with mixing pattern information (e.g. segregation, maximum mixedness) to capture reactor performance (i.e. identify reactor outlet concentrations given inlet concentrations) [17, 18]. A reactor with one inlet and one outlet, operating at steady state, having a homogeneous, isothermal, constant density, reacting phase in which only a single reaction takes place, and having an arbitrary RTD, the following holds: Conversion is maximized, with a mixing-pattern of maximum mixedness (segregation) if the limiting reactant's consumption rate is a positive, concave (convex) function of that reactant's concentration[19]. More recently, RTD theory was used to characterize the performance of water disinfection contact systems in the presence of mixing and disinfection kinetics effects[20].

Reactor network studies involving RTd models for the reactor units are scarce in the literature. Glasser demonstrated through an example that conversions above those attained with the segregation and maximum mixedness mixing patterns are possible[21]. Hocine used locally optimal MINLP techniques to identify networks of PFR's and CSTR's whose overall RTD approximates an a-priori known RTD[22]. Al-Husseini synthesized globally optimal reactor networks where all the units features the same normalized RTd (NRTd), and the same mixing pattern (Segregation or Maximum Mixedness)[23]. Nevertheless, no prior work has considered the optimization of reactor networks featuring units with normalized residence time density (NRTd) function and mixing-pattern belong to an a-priori known, finite cardinality set, whose elements are known NRTd function mixing-pattern pairs.

An alternative process network synthesis methodology that guarantees global optimality has been put forward by Manousiouthakis and coworkers and has been termed the Infinite DimEnsionAl State-space(IDEAS) approach to process network synthesis. IDEAS has been applied to the attainable region (AR) quantification problem for reactor networks ([24, 25, 26]), and general process networks ([27]). The IDEAS conceptual framework aims to develop precise approximations of the true AR, by solving a sequence of linear programs of ever increasing size. The IDEAS framework has also been applied to other reactor network

synthesis problems, such as the quantification of the attainable region for batch reactors ([28]), non-ideal reactors ([29]), isothermal reactors ([30, 31]), non-isothermal reactors ([32]) and variable density fluid reactors ([33]). IDEAS has also been applied to mass exchange networks ([34]), separation networks ([35]), power cycle synthesis ([36]) and distillation networks ([37, 38, 39, 40]).

The remaining sections of this chapter are as follows: First, Residence Time density/Distribution (RTd/RTD) and mixing-pattern concepts are briefly reviewed, and the equivalence of continuous stirred tank (CSTR) behavior with that of a particular RTd/mixing-pattern combination is established. Then, the IDEAS mathematical framework is shown to be applicable to the synthesis of reactor networks that feature reactor units whose normalized residence time density (NRTd) function and mixing-pattern belong to an a-priori known, finite cardinality set, whose elements are known NRTd function mixing-pattern pairs. The proposed synthesis method is illustrated with a case study featuring the Trambouze reaction scheme. It is shown that networks featuring multiple NRTd's can exhibit superior performance to that of networks featuring a single RTd. Finally, the obtained results are discussed and conclusions are drawn.

1.2 Residence Time density/Distribution (RTd/RTD) concepts

A brief review of basic RTd/RTD concepts is given below, prior to establishing the equivalence of a common reactor model to an RTd/mixing-pattern combination.

Residence time t of a fluid element is the difference between the time the fluid element exits the system t_{out} and the time that it entered the system t_{in} , (i.e.,) $t = t_{out} - t_{in}$

Life expectancy λ of a fluid element at a given time t_g is the difference between the time that the fluid element will exit the system t_{out} and the given time t_g

Residence time density (RTd) $E := \mathbb{R}^+ \to \mathbb{R}^+; E : t \to E(t); \int_0^\infty E(t)dt = 1$ where $E(t)dt$ is the volume fraction of the exit stream that has resided in the system for a time between t and $t + dt$.

Residence time distribution (RTD)$F := \mathbb{R}^+ \to \mathbb{R}^+; F : t \to E(t); \int_0^t E(t)dt$ where $F(t)dt$ is the volume fraction of the exit stream with residence time between time 0 and t.

Mean Residence Time $\bar{t}$

Normalized Residence Time density (NRTd): $E := \mathbb{R}^+ \to \mathbb{R}^+; E : \theta \hat{=} \frac{t}{\bar{t}} \to E(\theta) \hat{=} \bar{t}E(t)$

C_{out}^i

1.2.1 Segregated Flow Reactor (SFR) model

Consider a reactor with RTd function $E := \mathbb{R}^+ \to \mathbb{R}^+$, and segregated flow mixing-pattern. Then the reactor inlet, and outlet species concentrations $\{C_i^{in}\}_{i=1}^n \left(\frac{kmol}{m^3}\right)$, $\{C_i^{out}\}_{i=1}^n \left(\frac{kmol}{m^3}\right)$ respectively, satisfy the following:

$$C_i^{out}(\tau) = \int_0^\infty C_i(t) E(t) dt \quad \forall i = 1, ..., n \tag{1.1}$$

$$\bar{t} \triangleq \int_0^\infty tE(t) dt = \frac{V}{F} \triangleq \tau \tag{1.2}$$

$$\frac{dC_i(t')}{dt'} = R_i\left(\{C_j(t')\}_{j=1}^n\right) \ \forall t' \in [0, t] \ \forall t \in [0, \infty) \ \forall i = 1, ..., n \tag{1.3}$$

$$C_i(0) = C_i^{in}; \forall i = 1, ..., n \tag{1.4}$$

1.2.2 Maximum Mixedness Reactor (MMR) model

Consider a reactor with RTd function $E := \mathbb{R}^+ \to \mathbb{R}^+$, and maximum mixedness flow mixing-pattern. Then the reactor inlet, and outlet species concentrations $\{C_i^{in}\}_{i=1}^n \left(\frac{kmol}{m^3}\right)$, $\{C_i^{out}\}_{i=1}^n \left(\frac{kmol}{m^3}\right)$ respectively, satisfy the following:

$$\frac{dC(\lambda)}{d\lambda} = -R(C(\lambda)) + (C(\lambda) - C^{in}) \frac{E(\lambda)}{1 - \int_0^\lambda E(\lambda)d(\lambda)} \tag{1.5}$$

$$\frac{dC_i(\lambda)}{d\lambda} = -R_i\left(\{C_j(\lambda)\}_1^n\right) + \left(C_i(\lambda) - C_i^{in}\right)\frac{E(\lambda)}{1 - \int_0^{\lambda} E(\lambda')\,d\lambda'} \;\; \forall\lambda \in [0,\infty) \;\; \forall i = 1,....,n \tag{1.6}$$

$$\frac{dC_i}{d\lambda}(\lambda = \infty) = 0 \;\; \forall i = 1,....,n \tag{1.7}$$

$$\bar{t} \triangleq \int_0^{\infty} tE(t)\,dt = \frac{V}{F} \triangleq \tau \tag{1.8}$$

$$C_i(\lambda = 0) = C_i^{out}(\tau) \;\forall i = 1,....,n \tag{1.9}$$

Where, for both models, $F\left(\frac{m^3}{s}\right)$ is the reactor′s volumetric flowrate,$V\,(m^3)$ is the reactor′s volume (excluding dead-volume), and $\{R_i\}_{i=1}^n\left(\frac{kmol}{m^3 s}\right)$ is the i^{th} species′ generation rate.$R_i : \{C_j\}_1^n \to R_i\left(\{C_j\}_1^n\right) \;\; i = 1,n$

Proposition Consider a reactor with normalized residence time density function $E : \mathbb{R}^+ \to \mathbb{R}^+; E : \theta \to E(\theta) = e^{-\theta}$ and a maximum mixedness mixing-pattern. In addition, consider that the species generation rate functions $R_i : \mathbb{R}^n \to \mathbb{R}; R_i : \{C_j\}_1^n \to R_i\left(\{C_j\}_1^n\right) \;\; i = 1,n$ are Lipschitz continuous functions. Then this reactor can be modeled as a steady-state, isothermal, constant fluid density continuously stirred tank reactor (CTSR) whose constitutive equations are:

$$C_i^{in} - C_i^{out,CSTR} + R_i\left(\left\{C_i^{out,CSTR}\right\}_{i=1}^n\right)\tau = 0 \;\; \forall i = 1,....,n \tag{1.10}$$

Proof The general residence time density based model of a reactor with a maximum mixedness pattern of mixing is listed as:

$$\frac{dC_i(\lambda)}{d\lambda} = -R_i\left(\{C_j(\lambda)\}_1^n\right) + \left(C_i(\lambda) - C_i^{in}\right)\frac{E(\lambda)}{1-F(\lambda)} \quad \forall\lambda \in [0,\infty) \;\; \forall i = 1,....,n \quad (1.11)$$

$$C_i(\lambda = 0) = C_i^{out,MMR} \forall i = 1,....,n \quad (1.12)$$

$$\frac{dC_i}{d\lambda}(\lambda = \infty) = 0 \; \forall i = 1,....,n \quad (1.13)$$

Let the reactor under consideration have mean residence time τ. Since the normalized residence time density function of the reactor is $E : \mathbb{R}^+ \to \mathbb{R}^+; E : \theta \to E(\theta) \hat{=} e^{-\theta}$, then the residence time density function of the reactor with mean residence time τ is $E : \mathbb{R}^+ \to \mathbb{R}^+; E : t \to E(t) \hat{=} \frac{e^{\frac{-t}{\tau}}}{\tau}$. In turn this implies that the reactor residence time distribution function is $F := \mathbb{R}^+ \to \mathbb{R}^+; F : t \to F(t) \stackrel{\wedge}{=} \int_0^t E(t')\,dt' = \int_0^t \frac{e^{-t'/\tau}}{\tau} dt' = 1 - e^{-t/\tau}$. Since the reactor′s mixing pattern is that of maximum mixedness, then the inlet and outlet species concentrations satisfy the following:

$$\frac{dC_i(\lambda)}{d\lambda} = -R_i\left(\{C_j(\lambda)\}_1^n\right) + \left(C_i(\lambda) - C_i^{in}\right)\frac{\frac{e^{-\lambda/\tau}}{\tau}}{1-(1-e^{-\lambda/\tau})} \quad \forall\lambda \in [0,\infty) \;\; \forall i = 1,....,n \quad (1.14)$$

$$C_i(\lambda = 0) = C_i^{out,\,MMR} \forall i = 1,....,n \quad (1.15)$$

$$\frac{dC_i}{d\lambda}(\lambda = \infty) = 0 \; \forall i = 1,....,n \quad (1.16)$$

Considering that the species generation rate function $R_i : \mathbb{R}^n \to \mathbb{R}; R_i : \{C_j\}_1^n \to R_i\left(\{C_j\}_1^n\right) \;\; i = 1,n$ are Lipschitz continuous, then the initial value problem $\frac{dC_i(\lambda)}{d\lambda} = -R_i\left(\{C_j(\lambda)\}_1^n\right) + (C_i(\lambda) - C_i^{in})\frac{1}{\tau} \;\; \forall\lambda \in [0,\infty) \;\; \forall i = 1,....,n; C_i(\lambda = 0) = C_i^{out,\,MMR} \forall i =$

$1, ..., n$ has a unique solution. Then the assumption $\frac{dC_i}{d\lambda}(\lambda = \infty) = 0 \ \forall i = 1, ..., n$ ensures that $\lim_{\lambda \to \infty} C_i(\lambda)$ exists, and is defined as $C_i^{\infty} \stackrel{\wedge}{=} \lim_{\lambda \to \infty} C_i(\lambda)$. In turn, this implies that the following holds: $0 = -R_i\left(\left\{C_j^{\infty}\right\}_1^n\right) + (C_i^{\infty} - C_i^{in})\frac{1}{\tau} \quad \forall i = 1, ..., n$. Thus $C_i^{\infty} \quad \forall i = 1, ..., n$ satisfy the constitutive equations $C_i^{in} - C_i^{out,CSTR} + R_i\left(\left\{C_i^{out,CSTR}\right\}_{i=1}^n\right)\tau = 0 \quad \forall i = 1, ..., n$ of an isothermal constant fluid density continuously stirred tank reactor (CTSR).

Substituting the above derived expression into the reactor's maximum mixedness model then yields:

$$\frac{dC_i(\lambda)}{d\lambda} = -R_i\left(\{C_j(\lambda)\}_1^n\right) + \left(C_i(\lambda) - C_i^{in}\right)\frac{1}{\tau} \quad \forall \lambda \in [0, \infty) \quad \forall i = 1, ..., n \tag{1.17}$$

$$C_i(\lambda = 0) = C_i^{out,MMR} \forall i = 1, ..., n \tag{1.18}$$

$$C_i = \lim_{\lambda \to \infty} C_i(\lambda) \quad \forall i = 1, ..., n \tag{1.19}$$

It is then clear that $C_i^{out,MMR} = C_i^{\infty} \lim_{\lambda \to \infty} C_i(\lambda) \quad \forall i = 1, ..., n$ implies that the solution to the above equation satisfies $C_i(\lambda) = C_i^{out,MMR} = C_i^{\infty} = \lim_{\lambda \to \infty} C_i(\lambda) \quad \forall \lambda \in [0, \infty) \quad \forall i = 1, ..., n$ satisfy the constitutive equations $C_i^{in} - C_i^{out,CSTR} + R_i\left(\left\{C_i^{out,CSTR}\right\}_{i=1}^n\right)\tau = 0 \quad \forall i = 1, ..., n$ of an isothermal constant fluid density continuously stirred tank reactor (CTSR), so do $C_i^{out,MMR}$. Therefore, $C_i^{out,CSTR} = C_i^{out,MMR} = C_i^{\infty} = \lim_{\lambda \to \infty} C_i(\lambda) = C_i(\lambda) \quad \forall \lambda \in [0, \infty) \quad \forall i = 1, ..., n$. $O.E.\Delta$.

1.3 Infinite Dimensional State Space (IDEAS)

Process network synthesis problems have traditionally been pursued through super structure based optimization methods[41, 42] which give rise to non linear programming (NLP) and mixed integer non linear programming (MINLP) formulations. The non convex nature of these formulations limits guarantees of global optimality to problem instances of small size.

[43] introduced the concept of attainable region (AR) for reactor networks and presented it as the collection of objective variables in the concentration space for possible steady-state reactor networks. Glasser quantified the ARs using a geometric approach for plug-flow reactor (PFR) and continuous stirred tank reactor (CSTR) using trajectories and loci[21]. So far most of the prior work in the field of reactor network synthesis investigated attainable region (AR) targeting. The purpose of this work is to illustrate the applicability of IDEAS to the globally optimal synthesis of reactor networks featuring units whose mixing pattern and normalized RTd belong to an a-priori known set of finite cardinality.

For this work, the following assumptions are considered:

- Reactor network at steady state
- Single inlet and outlet to the network
- Reactor network is isothermal i.e all the reactors, streams are at the same temperature
- Reactor network is isobaric i.e all the reactors, streams are at the same pressure.
- Reacting mixture throughout the network has constant density and a single-phase.

The purpose of this work is to illustrate the applicability of IDEAS to the globally optimal synthesis of reactor networks featuring units whose mixing pattern and normalized RTd belong to an a-priori known set of finite cardinality. Figure 1.1 illustrates the IDEAS representation of the reactor network, which consists of two subnetworks: the operator network (OP) consisting of an infinite number of units with known NRTd and mixing pattern, and a distribution network (DN), where all splitting, mixing, and recycling operations take place.

As stated earlier, each reactor network unit has a known NRTd and mixing pattern.

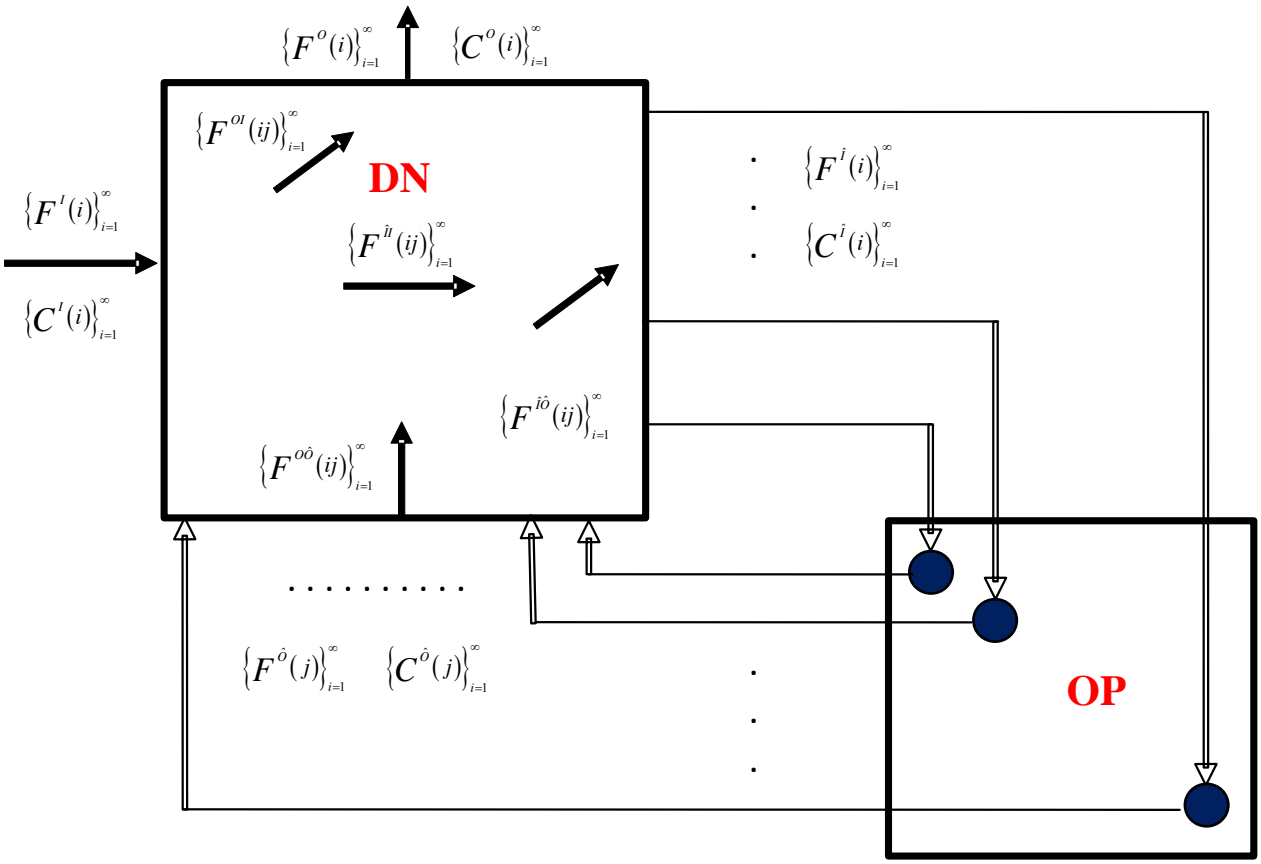

Figure 1.1: IDEAS representation of reactor network

Consider the set:

$$S \triangleq \left\{ \begin{array}{l} (E_l, \gamma_l) \;\; l = 1, N_S \leq 2N_E : \\ E_l \in S_E \triangleq \left\{ \begin{array}{l} E_m : \mathbb{R}^+ \to \mathbb{R}^+;\; E_m : \theta \to E_m(\theta), \\ \int_0^\infty E_m(\theta')\, d\theta' = 1, \;\; \lim_{\theta \to \infty} \frac{E_m(\theta)}{1 - \int_0^\theta E_m(\theta') d\theta'} > 0, \;\; m = 1, N_E \end{array} \right\} \wedge \\ \gamma_l \in S_\Gamma \triangleq \left\{ \begin{array}{l} \gamma_m \in \{0, 1\}; \\ \gamma_m = 0 \;\; if \;\; mixing\, pattern\, is\, maximum\, mixedness \\ \gamma_m = 1 \;\; if \;\; mixing\, pattern\, is\, segregated\, flow \end{array} \right\} \end{array} \right\} \quad (1.20)$$

The above suggests that the i^{th} reactor unit, where $i = 1, \text{inf}$, possesses a NRTd that is known and is one of the N_E elements of the set S_E, and one of two mixing patterns: maximum mixedness or segregated flow.

Applicability of IDEAS requires that each unit's information map:

$B : D_1 \times D_2 \subset \mathbb{R}^{n+1} \times \mathbb{R} \to \mathbb{R}^{n+1} \times \mathbb{R}^2$

$$B: \quad u = \begin{bmatrix} u_1 \\ u_2 \end{bmatrix} \to y = \begin{bmatrix} y_1 \\ y_2 \end{bmatrix} = B\left(u_1, u_2\right) = \begin{bmatrix} B_1\left(u_1, u_2\right) \\ B_2\left(u_1, u_2\right) \end{bmatrix}$$

Property 1. $y_1 = B_1\left(u_1, u_2\right) = \bar{B}_1\left(u_2\right) u_1$, i.e. the first part y_1 of the output vector y is related in a linear manner to the first part u_1 of the input vector u, through an operator $\bar{B}_1$ that maps the second part u_2 of the input vector u to a linear matrix $\bar{B}_1(u_2)$ that then pre-multiplies u_1 to y_1 form .

Property 2. $y_2 = B_2\left(u_1, u_2\right) = \bar{B}_2\left(u_2\right)$, i.e. the first part y_2 of the output vector y is related in a linear manner to the first part u_2 of the input vector u, under a (possibly nonlinear) operator $\bar{B}_2$.

Consider any one of the units with known NRTd $\boldsymbol{E} \in S_E$,and maximum mixedness mixing pattern,$\gamma = 0$.

This unit's input-output information map satisfies the above properties, since:

$$u \stackrel{\wedge}{=} \begin{bmatrix} F \\ C_1^{in} \\ \vdots \\ C_n^{in} \\ \bar{t} \end{bmatrix}, u_1 \stackrel{\wedge}{=} \begin{bmatrix} F \end{bmatrix}, u_2 \stackrel{\wedge}{=} \begin{bmatrix} C_1^{in} \\ \vdots \\ C_n^{in} \\ \bar{t} \end{bmatrix}, y_1 \stackrel{\wedge}{=} \begin{bmatrix} F \\ V \end{bmatrix}, y_2 \stackrel{\wedge}{=} \begin{bmatrix} C_1^{out} \\ \vdots \\ C_n^{out} \\ \tau \end{bmatrix} = \begin{bmatrix} C_1\left(\lambda = 0\right) \\ \vdots \\ C_n\left(\lambda = 0\right) \\ \bar{t} \end{bmatrix}$$

Where,

$$u_1 \in D_1 \stackrel{\wedge}{=} \{u_1 = [F] \in \mathbb{R} : F \geq 0\}$$

And,

$$u_2 \in D_2 \stackrel{\wedge}{=} \left\{ u_2 = \left[\begin{array}{cccc} C_1^{in} & \cdots & C_n^{in} & \bar{t} \end{array} \right]^T \in \mathbb{R}^{n+1} : \ C_i^{in} \geq 0 \ \forall i = 1, n, \ \bar{t} \geq 0 \right\}, \boldsymbol{E} \in S_E$$

$$\left\{ \begin{array}{l} \frac{dC_i(\lambda)}{d\lambda} = -R_i \left(\{C_j(\lambda)\}_1^n \right) + \left(C_i(\lambda) - C_i^{in} \right) \frac{\frac{1}{\bar{t}} E\left(\frac{\lambda}{\bar{t}}\right)}{1 - \frac{1}{\bar{t}} \int\limits_0^{\lambda} E\left(\frac{\lambda'}{\bar{t}}\right) d\lambda'} \ \ \forall \lambda \in [0, \infty) \ \ \forall i = 1, ..., n \\ \\ \frac{dC_i}{d\lambda}(\lambda = \infty) = 0 \ \ \forall i = 1, ..., n \end{array} \right\}$$

Similarly, the input-output information map for a unit with known NRTd $\boldsymbol{E} \in S_E$,and segregated flow mixing pattern,$\gamma = 1$.

$$u \stackrel{\wedge}{=} \left[\begin{array}{c} F \\ C_1^{in} \\ \vdots \\ C_n^{in} \\ \bar{t} \end{array} \right], u_1 \stackrel{\wedge}{=} \left[\begin{array}{c} F \end{array} \right], u_2 \stackrel{\wedge}{=} \left[\begin{array}{c} C_1^{in} \\ \vdots \\ C_n^{in} \\ \bar{t} \end{array} \right], y_1 \stackrel{\wedge}{=} \left[\begin{array}{c} F \\ V \end{array} \right], = \bar{B}_1(u_2) u_1 = \left[\begin{array}{c} 1 \\ \bar{t} \end{array} \right] \left[\begin{array}{c} F \end{array} \right]$$

,

$$y_2 \stackrel{\wedge}{=} \left[\begin{array}{c} C_1^{out} \\ \vdots \\ C_n^{out} \\ \tau \end{array} \right] = \left[\begin{array}{c} \int\limits_0^{\infty} C_1(t) \frac{1}{\bar{t}} E\left(\frac{t}{\bar{t}}\right) dt \\ \vdots \\ \int\limits_0^{\infty} C_n(t) E\left(\frac{t}{\bar{t}}\right) dt \\ \bar{t} \end{array} \right]$$

Where,

$$u_1 \in D_1 \stackrel{\wedge}{=} \{u_1 = [F] \in \mathbb{R} : F \geq 0\}$$

And,

$$u_2 \in D_2 \stackrel{\wedge}{=} \left\{ u_2 = \left[\begin{array}{cccc} C_1^{in} & \cdots & C_n^{in} & \bar{t} \end{array} \right]^T \in \mathbb{R}^{n+1} : \; C_i^{in} \geq 0 \; \forall i = 1, n, \; \bar{t} \geq 0 \right\}, \boldsymbol{E} \in S_E$$

$$\left\{ \begin{array}{ll} \frac{dC_i(t')}{dt'} = R_i \left(\left\{ C_j \left(t' \right) \right\}_{j=1}^{n} \right) & \forall t' \in [0, t] \;\; \forall t \in [0, \infty) \;\; \forall i = 1, ..., n \\ C_i \left(0 \right) = C_i^{in}; & \forall i = 1, ..., n \end{array} \right\}$$

Having established the applicability of IDEAS to the problem under consideration, we next present the resulting IDEAS mathematical formulation.

1.3.1 IDEAS formulation

The problem solved in this chapter will feature a single network inlet and outlet where the inlet flow has two choices once it enters the network, it can bypass the states (and thus all possible reactors) and leave the network (this is represented by F^{OI}) or it can travel to any number of different states (this is represented by $F^{I\hat{I}}$), as illustrated in Figure 1.2. This coincides with the flow balance on the network inlet (presented in FBIN constraint in the problem formulation). For state crossflow $F^{\hat{I}\hat{O}}$ and reactor flow $F^{\hat{I}}$, the state the flow originates from is given a -1 for the SFB constraint and the state where the flow ends up is given a 1.

Construction of the constraint matrix A for the optimization framework is done by inputting the scalar value (coefficient) associated with each flow variable whenever the variable appears in the objective function or any of the constraints. For example, the flow from the network inlet to a state ($F^{\hat{I}\hat{O}}$) appears in three constraints (FBIN, SFB1 and SCB). Therefore, under the $F^{\hat{I}\hat{O}}$ column a -1 is put in the FBIN row, -1 is put in the SFB1 row and -C_A^I is put in the SCB row. The completed constraint matrix is shown in Table 1.1:

In this section we will present and the various objective functions and the constrains used in solving the problems presented in this chapter.

Table 1.1: Constraint Matrix (A)

	F^{I}	$F^{\hat{I}}$	$F^{I\hat{I}}$	F^{OI}	F^{O}	$F^{\hat{O}}$	$F^{\hat{I}\hat{O}}$	$F^{\hat{O}\hat{O}}$
OBJ	0	τ	0	0	0	0	0	0
FBIN	1	0	-1	-1	0	0	0	0
FBOUT	0	0	0	-1	1	0	0	1
CBOUT	0	0	0	-C_A^I	C_A^O	1	1	-C_A^O
SFB1	0	1	-1	0	0	0	-1	0
SFB2	0	0	0	0	0	1	-1	-1
SCB	0	C_A^I	-C_A^I	0	0	0	-C_A^O	0

The objective function for the minimum volume problem is:

$$minimize \;\; V = \sum_{i=1}^{\infty} \tau\left(i\right) F^{\hat{I}}\left(i\right) \tag{1.21}$$

The objective function for the selectivity problem is:

$$F^{OI}\left(1,1\right) + C_A^I\left(1\right) + \sum_{i=1}^{N_R} F^{O\hat{O}}\left(1,j\right) C_A^{\hat{O}}\left(j\right) \tag{1.22}$$

DN total mass balance mixing equations:

$$F^{O}\left(i\right) = \sum_{j=1}^{N_I} F^{OI}\left(i,j\right) + \sum_{j=1}^{\infty} F^{O\hat{O}}\left(i,j\right) \forall i = 1, ..., N_O \tag{1.23}$$

$$F^{\hat{I}}\left(i\right) = \sum_{j=1}^{N_I} F^{\hat{I}I}\left(i,j\right) + \sum_{j=1}^{\infty} F^{\hat{I}\hat{O}}\left(i,j\right) \forall i = 1, ..., \infty \tag{1.24}$$

DN total mass balance splitting equations:

$$F^{I}\left(j\right) = \sum_{i=1}^{N_O} F^{OI}\left(i,j\right) + \sum_{i=1}^{\infty} F^{\hat{I}I}\left(i,j\right) \forall j = 1, ..., N_I \tag{1.25}$$

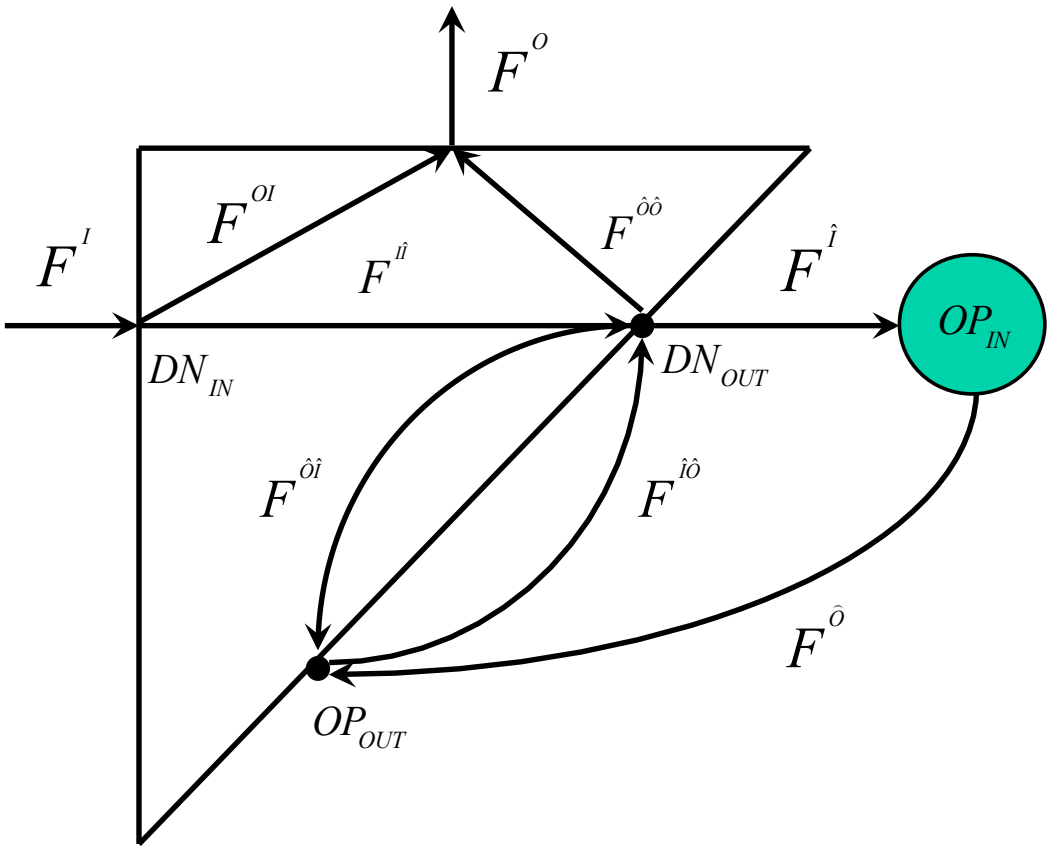

Figure 1.2: IDEAS representation of reactor network

$$F^{\hat{O}}(j) = \sum_{i=1}^{N_O} F^{O\hat{O}}(i,j) + \sum_{i=1}^{\infty} F^{\hat{I}\hat{O}}(i,j) \forall j = 1, ..., \infty \tag{1.26}$$

DN component mass balance mixing equations:

$$C_A^{\hat{I}}(i) F^{\hat{I}}(i) = \sum_{j=1}^{N_I} C_A^I(j) F^{\hat{I}I}(i,j) + \sum_{j=1}^{\infty} C_A^{\hat{O}}(j) F^{\hat{I}\hat{O}}(i,j) \quad \forall i = 1, ..., \infty \tag{1.27}$$

DN outlet specifications:

$$\left(F^O(i)\right)^l \leq F^O(i) \leq \left(F^O(i)\right)^u \quad \forall i = 1, ..., N_O \tag{1.28}$$

$$\left(C_C^O(i)\right)^l F^O(i) \leq \sum_{j=1}^{N_I} C_C^I(j) F^{OI}(i,j) + \sum_{j=1}^{\infty} C_C^{\hat{O}}(j) F^{O\hat{O}}(i,j) \leq \left(C_C^O(i)\right)^u F^O(i) \quad \forall i = 1, ..., N_O \tag{1.29}$$

OP balance equations:

$$F^{\hat{O}}(i) = F^{\hat{I}}(i) \, \forall i = 1, ..., \infty \tag{1.30}$$

Overall network component mass balance mixing equations:

$$C_A^O(i) F^O(i) = \sum_{j=1}^{N_I} C_A^I(j) F^{OI}(i,j) + \sum_{j=1}^{\infty} C_A^{\hat{O}}(j) F^{O\hat{O}}(i,j) \;\; \forall k = 1, ..., n \;\; \forall i = 1, ..., N_O \tag{1.31}$$

Selectivity constraint:

$$\left[C_C^{\hat{O}}(i) - X_s C_B^{\hat{O}}(i)\right] F^O(i) \geq 0 \tag{1.32}$$

Non-negativity constraints:

$$F^I \geq 0; \; F^O \geq 0; F^{\hat{I}} \geq 0; F^{\hat{O}} \geq 0; F^{OI} \geq 0; F^{\hat{I}I} \geq 0; F^{\hat{I}\hat{O}} \geq 0; F^{O\hat{O}} \geq 0; V \geq 0 \tag{1.33}$$

1.4 Case studies

In this case study, the IDEAS conceptual framework is applied to the solution of the minimum volume problem for a reactor network, the units of which feature a mixing pattern and a normalized RTd which belong to an a-priori known set of finite cardinality. Additional network constraints are considered in various subcases. The Trambouze reaction scheme is considered to take place inside every reactor. The corresponding kinetic rate, and reactor network inlet information is:

$$A \overset{k_1}{\rightarrow} B \ , \ k_1 = 0.025 \frac{kmol}{m^3 \cdot s}; \ A \overset{k_2}{\rightarrow} C \ , \ k_2 = 0.2 \frac{1}{s}; \ A \overset{k_3}{\rightarrow} D \ , \ k_3 = 0.4 \frac{m^3}{kmol \cdot s}$$

where,

$$k_2{}^2 = 4k_1k_3; \quad \alpha = \frac{k_2}{2k_3} = 0.25 > 0$$

And

$$C_A^I = 1 \frac{kmol}{m^3}, \ C_C^I = 0 \frac{kmol}{m^3}$$

Three normalized RTd, mixing pattern sets are considered. They are defined as follows:

$$S_1 \triangleq \{(E_1, \gamma_1), (E_2, \gamma_2)\}, S_2 \triangleq \{(E_2, \gamma_2), (E_3, \gamma_3)\}, S_3 \triangleq \{(E_3, \gamma_3)\}$$

$$E_1 : \mathbb{R}^+ \rightarrow \mathbb{R}^+; \ E_1 : \theta \rightarrow E_1(\theta) = \delta(\theta - 1), \gamma_1 = 1$$

$$E_2 : \mathbb{R}^+ \rightarrow \mathbb{R}^+; \ E_2 : \theta \rightarrow E_2(\theta) = e^{-\theta}, \gamma_2 = 0$$

$$E_3 : \mathbb{R}^+ \rightarrow \mathbb{R}^+; \ E_3 : \theta \rightarrow E_3(\theta) = \left\{ \begin{array}{ll} 0 & if \ \theta < \frac{1}{2} \\ \frac{1}{2\theta^3} & if \ \theta \geq \frac{1}{2} \end{array} \right\}, \gamma_3 = 1$$

$$S_E \triangleq \{E_1, E_2, E_3\}, S_\Gamma \triangleq \left\{ \gamma_m \in \{0, 1\}; \ \gamma_m = \left\{ \begin{array}{l} 0 \ if \ mixing \, pattern \, is \, maximum \, mixedness \\ 1 \ if \ mixing \, pattern \, is \, segregated \, flow \end{array} \right\} \right\}$$

The above three NRTd, mixing pattern combinations are equivalent to the following familiar reactor types:

Plug Flow Reactor (PFR):

$$(E_1, \gamma_1)$$

, Continuously Stirred Tank Reactor (CSTR):

$$(E_2, \gamma_2)$$

Segregated Laminar Flow Reactor (SLFR):

$$(E_3, \gamma_3)$$

Carrying out the relevant computations for the three aforementioned reactor models and the considered reaction scheme, yields the following mathematical models:

The PFR model for the Trambouze reaction scheme is:

$$\left\{ \begin{array}{ll} \frac{dC_A}{d\tau'} = -\left(k_1 + k_2 C_A + k_3 {C_A}^2\right), & C_A\left(\tau' = 0\right) = C_A^{in} \\ \frac{dC_C}{d\tau'} = k_2 C_A, & C_C\left(\tau' = 0\right) = C_C^{in} \end{array} \right\} \begin{array}{c} {k_2}^2 = 4 k_1 k_3 \\ \Leftrightarrow \\ \alpha = \frac{k_2}{2 \cdot k_3} \end{array}$$

$$\left\{ \begin{array}{l} C_A(\tau) = \left\{ \begin{array}{ll} -\alpha + \frac{1}{k_3\tau + \frac{1}{C_A^{in}+\alpha}} & if \tau \leq \tau_c \triangleq \frac{1}{k_3} \frac{C_A^{in}}{\alpha\left(\alpha + C_A^{in}\right)} \\ 0 & if \tau > \tau_c \triangleq \frac{1}{k_3} \frac{C_A^{in}}{\alpha\left(\alpha + C_A^{in}\right)} \end{array} \right\} \\ C_C(\tau) = \left\{ \begin{array}{ll} C_C^{in} - 2\alpha^2 k_3 \tau + 2\alpha \ln\left(k_3 \tau \left(C_A^{in} + \alpha\right) + 1\right) & if \quad \tau \leq \tau_c \triangleq \frac{1}{k_3} \frac{C_A^{in}}{\alpha\left(\alpha + C_A^{in}\right)} \\ C_C^{in} - 2\alpha \frac{C_A^{in}}{\left(\alpha + C_A^{in}\right)} + 2\alpha \ln\left(\frac{C_A^{in}+\alpha}{\alpha}\right) & if \ \tau > \tau_c \triangleq \frac{1}{k_3} \frac{C_A^{in}}{\alpha\left(\alpha + C_A^{in}\right)} \end{array} \right\} \end{array} \right\}$$

The CSTR model for the Trambouze reaction scheme is:

$$\left\{ \begin{array}{l} 0 = C_A^{in} - C_A - \tau\left(k_1 + k_2 C_A + k_3 (C_A)^2\right) \\ 0 = C_C^{in} - C_C + \tau\left(k_2 C_A\right) \end{array} \right\} \begin{array}{c} {k_2}^2 = 4 k_1 k_3 \\ \Leftrightarrow \\ \alpha = \frac{k_2}{2 \cdot k_3} \end{array}$$

$$\left\{ \begin{array}{l} C_A(\tau) = \left\{ \begin{array}{ll} -\alpha - \frac{1}{2k_3\tau} + \sqrt{\left(\frac{1}{2k_3\tau}\right)^2 + \alpha \frac{1}{k_3\tau} + \frac{C_A^{in}}{k_3\tau}} & if \ \tau \leq \tau_c \triangleq \frac{C_A^{in}}{k_3 \alpha^2} \\ 0 & if \ \tau \geq \tau_c \triangleq \frac{C_A^{in}}{k_3 \alpha^2} \end{array} \right\} \\ C_C(\tau) = \left\{ \begin{array}{ll} C_C^{in} + 2\tau k_3 \alpha \left(-\alpha - \frac{1}{2k_3\tau} + \sqrt{\left(\frac{1}{2k_3\tau}\right)^2 + \alpha \frac{1}{k_3\tau} + \frac{C_A^{in}}{k_3\tau}}\right) & if \ \tau \leq \tau_c \triangleq \frac{C_A^{in}}{k_3 \alpha^2} \\ C_C^{in} & if \ \tau \geq \tau_c \triangleq \frac{C_A^{in}}{k_3 \alpha^2} \end{array} \right\} \end{array} \right\}$$

The SLFR model for the Trambouze reaction scheme is[23]:

$$\left\{\begin{array}{l} C_A(\tau)=\left\{\begin{array}{l} C_A^{in}\left(1-\frac{\tau^2}{4\tau_c^2}\right)+k_3\frac{\tau}{2}\left(\frac{\tau}{\tau_c}-2\right)\left(C_A^{in}+\alpha\right)^2+ \\ +k_3^2\frac{\tau^2}{2}\left(C_A^{in}+\alpha\right)^3\ln\left(\frac{\tau_c\left(k_3\left(C_A^{in}+\alpha\right)\frac{\tau}{2}+1\right)}{\frac{\tau}{2}\left(k_3\left(C_A^{in}+\alpha\right)\tau_c+1\right)}\right) \quad if\ \tau\le 2\tau_c=\frac{2}{k_3}\frac{C_A^{in}}{\alpha\left(\alpha+C_A^{in}\right)} \\ 0 \qquad\qquad if\ \tau\ge 2\tau_c=\frac{2}{k_3}\frac{C_A^{in}}{\alpha\left(\alpha+C_A^{in}\right)} \end{array}\right\} \\ C_B(\tau)=\left\{\begin{array}{l} \frac{\tau^2}{4{\tau_c}^2}\left(C_B^{in}+k_1\tau_c\right)\ if\frac{\tau}{2}\ge\tau_c \\ \frac{\tau^2 C_B^{in}}{4{\tau_c}^2}+\frac{\tau^2 k_1}{4\tau_c}\ if\frac{\tau}{2}\le\tau_c \end{array}\right\} \\ C_C(\tau)=\left\{\begin{array}{l} C_C^{in}+k_3\alpha\tau\left(C_A^{in}\left(1-\frac{\tau}{2\tau_c}\right)-\alpha\right)+2\alpha\ln\left(k_3\left(C_A^{in}+\alpha\right)\frac{\tau}{2}+1\right)+ \\ +\frac{1}{2}\alpha\tau^2k_3^2\left(C_A^{in}+\alpha\right)^2\ln\left(\frac{\frac{\tau}{2}\left(k_3\left(C_A^{in}+\alpha\right)\tau_c+1\right)}{\tau_c\left(k_3\left(C_A^{in}+\alpha\right)\frac{\tau}{2}+1\right)}\right) \quad if\ \tau\le 2\tau_c=\frac{2}{k_3}\frac{C_A^{in}}{\alpha\left(\alpha+C_A^{in}\right)} \\ C_C^{in}-2\alpha\frac{C_A^{in}}{\left(\alpha+C_A^{in}\right)}+2\alpha\ln\left(\frac{C_A^{in}+\alpha}{\alpha}\right) \qquad if\ \tau\ge 2\tau_c=\frac{2}{k_3}\frac{C_A^{in}}{\alpha\left(\alpha+C_A^{in}\right)} \end{array}\right\} \end{array}\right\}$$

Given the above three reactor models, we can now proceed to synthesize the reactor networks for the following cases:

- Minimum volume objective function (Case Study 1)
- Selectivity objective function (Case Study 2)
- Selectivity objective function with recycle constraint (Case Study 3)

In these case studies, the IDEAS conceptual framework is applied to the solution of the reactor network synthesis, the units of which feature a mixing pattern and a normalized RTd which belong to an a-priori known set of finite cardinality. Additional network constraints are considered in various subcases.

1.4.1 Case study 1A: $C_A = 0\,\frac{kmol}{m^3}$, $C_A \ge 0.47157\,\frac{kmol}{m^3}$

In this case we consider that all reactor units belong to the set:

$$S_1 \triangleq \{(E_1,\gamma_1),(E_2,\gamma_2)\}$$

.

The network details are summarized in Table 1.2. In this case, the obtained IDEAS minimum volume network features a total network volume of $V = 12.5$ and it consists of a CSTR followed by a PFR.

Table 1.2: Case 1A Network Data

Reactor Number	Reactor Type	C_A^{in}	C_A^{out}	τ	ΔC_C	V
1	CSTR	1.0000	0.2500	7.50	0.3750	7.50
2	PFR	0.2500	0	5.00	0.09657	5.00

1.4.2 Case study 1B: $C_A = 0\,\frac{kmol}{m^3}$, $C_A \geq 0.47157\,\frac{kmol}{m^3}$

In this case we consider that all reactor units belong to the set:

$$S_2 \triangleq \{(E_2, \gamma_2), (E_3, \gamma_3)\}$$

The network details are summarized in Table 1.3. In this case, the obtained IDEAS minimum volume network features a total network volume of $V = 17.5$ and it consists of 3 CSTR followed by a SLFR.

Table 1.3: Case 1B Network Data

Reactor Number	Reactor Type	C_A^{in}	C_A^{out}	τ	ΔC_C	V
1	CSTR	0.65625	0.2500	4.0625	0.203125	3.74
2	CSTR	0.5000	0.2500	2.500	0.1250	3.45
3	CSTR	0.28125	0.2500	0.3125	0.015625	0.3125
4	SLFR	0.2500	0	10.0	0.09657	10.0

1.4.3 Case study 2A:X_s=4.1

In this case we consider that all reactor units belong to the set:

$$S_1 \triangleq \{(E_1, \gamma_1), (E_2, \gamma_2)\}$$

. The optimum network based on a selectivity of 4.1 will produce an objective function=0.2489

Table 1.4: Case 2A Network Data

Reactor Number	Reactor Type	C_A^{in}	C_A^{out}	τ	ΔC_C	F
1	PFR	1.0000	0.2500	3.0000	0.3081	1.0000
2	PFR	0.2500	0.21875	0.3333	0.0156	0.0348

1.4.4 Case study 2B:X_s=4.1

In this case we consider that all reactor units belong to the set:

$$S_2 \stackrel{\wedge}{=} \{(E_2, \gamma_2), (E_3, \gamma_3)\}$$

For these specifications, a feasible network featuring an optimum objective function value=0.2688.

1.4.5 Case study 2C:X_s=4.1

Next consider that all reactor units belong to the set:

$$S_3 \stackrel{\wedge}{=} \{(E_3, \gamma_3)\}$$

For these specifications, a feasible network featuring an optimum objective function value=0.2711

1.4.6 Case study 2D:X_s=4.1

In this case we consider that all reactor units belong to the set:

$$S_4 \stackrel{\wedge}{=} \{(E_2, \gamma_2)\}$$

The optimum network based on a selectivity of 4.1 will produce an objective function=0.2697

Table 1.5: Case 2B Network Data

Reactor Number	Reactor Type	C_A^{in}	C_A^{out}	τ	ΔC_C	F
1	SLFR	0.3750	0.3438	0.2225	0.0151	1.0000
2	SLFR	0.3438	0.3125	0.2477	0.0153	1.0000
3	SLFR	0.3125	0.2813	0.2775	0.0155	1.0000
4	SLFR	0.2813	0.2500	0.3131	0.0155	0.3972
5	CSTR	1.0000	0.9688	0.0526	0.0102	1.0000
6	CSTR	0.9688	0.9375	0.0554	0.0104	1.0000
7	CSTR	0.9375	0.9063	0.0584	0.0106	1.0000
8	CSTR	0.9063	0.8750	0.0617	0.0108	1.0000
9	CSTR	0.8750	0.8438	0.0653	0.0110	1.0000
10	CSTR	0.8438	0.8125	0.0692	0.0112	1.0000
11	CSTR	0.8125	0.7813	0.0735	0.0115	1.0000
12	CSTR	0.7813	0.7500	0.0781	0.0117	1.0000
13	CSTR	0.7500	0.7188	0.0832	0.0120	1.0000
14	CSTR	0.7188	0.6875	0.0889	0.0122	1.0000
15	CSTR	0.6875	0.6563	0.0951	0.0125	1.0000
16	CSTR	0.6563	0.6250	0.1020	0.0128	1.0000
17	CSTR	0.6250	0.5938	0.1097	0.0130	1.0000
18	CSTR	0.5938	0.5625	0.1183	0.0133	1.0000
19	CSTR	0.5625	0.5313	0.1280	0.0136	1.0000
20	CSTR	0.5313	0.5000	0.1389	0.0139	1.0000
21	CSTR	0.5000	0.4688	0.1512	0.0142	1.0000
22	CSTR	0.4688	0.4375	0.1653	0.0145	1.0000
23	CSTR	0.4375	0.4063	0.1814	0.0147	1.0000
24	CSTR	0.4063	0.3750	0.2000	0.0150	1.0000

Table 1.6: Case 2C Network Data

Reactor Number	Reactor Type	C_A^{in}	C_A^{out}	τ	ΔC_C	F
1	SLFR	1.0000	0.9688	0.0531	0.0102	1.0000
2	SLFR	0.9688	0.9375	0.0559	0.0104	1.0000
3	SLFR	0.9375	0.9063	0.0589	0.0106	1.0000
4	SLFR	0.9063	0.8750	0.0623	0.0108	1.0000
5	SLFR	0.8750	0.8438	0.0659	0.0110	1.0000
6	SLFR	0.8438	0.8125	0.0698	0.0112	1.0000
7	SLFR	0.8125	0.7813	0.0741	0.0115	1.0000
8	SLFR	0.7813	0.7500	0.0788	0.0117	1.0000
9	SLFR	0.7500	0.7188	0.0839	0.0119	1.0000
10	SLFR	0.7188	0.6875	0.0896	0.0122	1.0000
11	SLFR	0.6875	0.6563	0.0959	0.0125	1.0000
12	SLFR	0.6563	0.6250	0.1028	0.0127	1.0000
13	SLFR	0.6250	0.5938	0.1105	0.0130	1.0000
14	SLFR	0.5938	0.5625	0.1192	0.0133	1.0000
15	SLFR	0.5625	0.5313	0.1289	0.0135	1.0000
16	SLFR	0.5313	0.5000	0.1398	0.0138	1.0000
17	SLFR	0.5000	0.4688	0.1521	0.0141	1.0000
18	SLFR	0.4688	0.4375	0.1662	0.0144	1.0000
19	SLFR	0.4375	0.4063	0.1823	0.0147	1.0000
20	SLFR	0.4063	0.3750	0.2009	0.0149	1.0000
21	SLFR	0.3750	0.3438	0.2225	0.0151	1.0000
22	SLFR	0.3438	0.3125	0.2477	0.0153	1.0000
23	SLFR	0.3125	0.2813	0.2775	0.0155	1.0000
24	SLFR	0.2813	0.2500	0.3131	0.0155	0.3242

Table 1.7: Case 2D Network Data

Reactor Number	Reactor Type	C_A^{in}	C_A^{out}	τ	ΔC_C	F
1	CSTR	1.0000	0.9688	0.0526	0.0102	1.0000
2	CSTR	0.9688	0.9375	0.0554	0.0104	1.0000
3	CSTR	0.9375	0.9063	0.0584	0.0106	1.0000
4	CSTR	0.9063	0.8750	0.0617	0.0108	1.0000
5	CSTR	0.8750	0.8438	0.0653	0.0110	1.0000
6	CSTR	0.8438	0.8125	0.0692	0.0112	1.0000
7	CSTR	0.8125	0.7813	0.0735	0.0115	1.0000
8	CSTR	0.7813	0.7500	0.0781	0.0117	1.0000
9	CSTR	0.7500	0.7188	0.0832	0.0120	1.0000
10	CSTR	0.7188	0.6875	0.0889	0.0122	1.0000
11	CSTR	0.6875	0.6563	0.0951	0.0125	1.0000
12	CSTR	0.6563	0.6250	0.1020	0.0128	1.0000
13	CSTR	0.6250	0.5938	0.1097	0.0130	1.0000
14	CSTR	0.5938	0.5625	0.1183	0.0133	1.0000
15	CSTR	0.5625	0.5313	0.1280	0.0136	1.0000
16	CSTR	0.5313	0.5000	0.1389	0.0139	1.0000
17	CSTR	0.5000	0.4688	0.1512	0.0142	1.0000
18	CSTR	0.4688	0.4375	0.1653	0.0145	1.0000
19	CSTR	0.4375	0.4063	0.1814	0.0147	1.0000
20	CSTR	0.4063	0.3750	0.2000	0.0150	1.0000
21	CSTR	0.3750	0.3438	0.2216	0.0152	1.0000
22	CSTR	0.3438	0.3125	0.2469	0.0154	1.0000
23	CSTR	0.3125	0.2813	0.2768	0.0156	1.0000
24	CSTR	0.2813	0.2500	0.3125	0.0156	0.3708

Cases 1 and 2 showed that the type of reactor doesn't matter if we are working with constraints related to volume, selectivity and convergence. However, we tend to see the following trends:

- a sequence of SLFR would recreate the behavior of a PFR by aligning multiple SLFR in series.
- A sequence of CSTRs would mirror the behavior of a PFR.

now a final case study will be presented that governs and limit the recycle behavior of the reactors at hand in order to limit the economical impacts of high pumping cost related to higher flow rates.

1.4.7 Case study 3A:X_s=4.1 PFR+CSTR:

In this case we consider that all reactor units belong to the set:

$$S_1 \triangleq \{(E_1, \gamma_1), (E_2, \gamma_2)\}$$

. The optimum network based on a selectivity of 4.1 will produce an objective function=0.2489.

1.4.8 Case study 3B:X_s=4.1 SLFR+CSTR:

In this case we consider that all reactor units belong to the set:

$$S_2 \triangleq \{(E_2, \gamma_2), (E_3, \gamma_3)\}$$

For these specifications, a feasible network featuring an optimum objective function value=0.3214.

1.4.9 Case study 3C:X_s=4.1 SLFR:

Next consider that all reactor units belong to the set:

$$S_3 \triangleq \{(E_3, \gamma_3)\}$$

Table 1.8: Case 3A Network Data

Reactor Number	Reactor Type	C_A^{in}	C_A^{out}	τ	ΔC_C	F
1	PFR	1.0000	0.9688	0.0513	0.0101	0.1065
2	PFR	1.0000	0.2500	3.0000	0.3081	0.8935
3	PFR	0.9688	0.8438	0.2344	0.0424	0.1065
4	PFR	0.8438	0.8125	0.0672	0.0111	0.1065
5	PFR	0.8125	0.5938	0.6100	0.0848	0.0717
6	PFR	0.8125	0.3438	1.8576	0.1981	0.0348
7	PFR	0.5938	0.5625	0.1140	0.0132	0.0717
8	PFR	0.5625	0.5313	0.1231	0.0135	0.0717
9	PFR	0.5313	0.5000	0.1333	0.0137	0.0717
10	PFR	0.5000	0.4688	0.1449	0.0140	0.0717
11	PFR	0.4688	0.4375	0.1581	0.0143	0.0717
12	PFR	0.4375	0.3438	0.5742	0.0446	0.0717
13	PFR	0.3438	0.3125	0.2339	0.0153	0.0717
14	PFR	0.3438	0.2188	1.1228	0.0621	0.0348
15	PFR	0.3125	0.2813	0.2614	0.0155	0.0717
16	PFR	0.2813	0.2500	0.2941	0.0156	0.0717

Table 1.9: Case 3B Network Data

Reactor Number	Reactor Type	C_A^{in}	C_A^{out}	τ	ΔC_C	F
1	SLFR	1.0000	0.6250	1.0072	0.1377	1.0000
2	SLFR	0.6250	0.3438	1.6058	0.1262	0.2846
3	SLFR	0.6250	0.3125	1.9044	0.1411	0.7154

For these specifications, a feasible network featuring an optimum objective function value=0.3214.

Table 1.10: Case 3C Network Data

Reactor Number	Reactor Type	C_A^{in}	C_A^{out}	τ	ΔC_C	F
1	SLFR	1.0000	0.6250	1.0072	0.1377	1.0000
2	SLFR	0.6250	0.3438	1.6058	0.1262	0.2846
3	SLFR	0.6250	0.3125	1.9044	0.1411	0.7154

1.4.10 Case study 3D:X_s=4.1 CSTR:

In this case we consider that all reactor units belong to the set:

$$S_4 \stackrel{\wedge}{=} \{(E_2, \gamma_2)\}$$

The optimum network based on a selectivity of 4.1 will produce an objective function=0.405.

Table 1.11: Case 3D Network Data

Reactor Number	Reactor Type	C_A^{in}	C_A^{out}	τ	ΔC_C	F
1	CSTR	1.0000	0.6250	1.2245	0.1531	0.9643
2	CSTR	1.0000	0.5938	1.4266	0.1694	0.0357
3	CSTR	0.6250	0.4063	1.2698	0.1032	0.9643
4	CSTR	0.5938	0.3750	1.4000	0.1050	0.0357

1.5 Discussion and conclusions

MRTD can potentially may or may not provide an advantage and that depends on the types of consideration that are incorporated into the design procedure. Here we have demonstrated that when you try to max conversion while maintaining selectivity specs then the use of MRTD may not be beneficial since the optimization emulates the behavior of one RTD mixing pattern. One RTD mixing pattern emulated by another RTD mixing pattern for example a CSTR is emulated with PFR or SLFR with a large recycle. A PFR is emulated by a sequence

of CSTRs or SLFRs. however, when other consideration are incorporated into the design producer such as the network total flow rate the emulation capabilities of various technologies may be limited and this is shown when the SLFR optimum is distinctly different from the CSTR/PFR and SLFR/CSTR optimum in the second case study presented. Formal proof of the maximum mixedness CSTR RTD model being equivalent to a CSTR is given. The residence time disruption belongs to a reactor who's contents are considered to be specially uniform and who's dimensionless. the proposed methodology are applicable to arbitrary RTDs that can be experimentally obtain and thus can aid the designer to synthesize reactor networks that are not limited to ideal models such as PFR and CSTRs only.

1.6 Appendix A

$$E(t) = \left\{ \begin{array}{ll} \frac{8}{9}\frac{\tau^3}{t^4} & if\theta \geq \frac{2}{3} \\ 0 & if\theta < \frac{2}{3} \end{array} \right\} \tag{1.34}$$

The exit concentration $\overline{C}_A(\tau)$ of a segregated laminar flow reactor (SLFR) employing the Trambouze reaction scheme is:

$$\overline{C}_A(\tau) = \left\{ \begin{array}{ll} \int\limits_{\frac{2\tau}{3}}^{\tau_c} \left(-\alpha + \frac{C_A^{in}+\alpha}{k_3\left(C_A^{in}+\alpha\right)t+1} \right) \frac{8\tau^3}{9t^4} dt \ if \ \theta \geq \frac{2}{3} \\ 0 \qquad\qquad if \ if\theta < \frac{2}{3} \end{array} \right\} \tag{1.35}$$

let $A = [k_3(C_A^{in} + \alpha)]$ then

$$\frac{1}{(At+1)\,t^4} = \frac{A^4}{(At+1)} + \frac{1}{t^4} - \frac{A}{t^3} + \frac{A^2}{t^2} - \frac{A^3}{t} \tag{1.36}$$

Similarly,

$$\int\limits_{\frac{2\tau}{3}}^{\tau_c} \frac{1}{(At+1)\,t^4} dt = A^3 \ln\left(\frac{2\tau\,(A\tau_c+1)}{\tau_c\,(2A\tau+3)}\right) + A^2\left(\frac{3}{2\tau} - \frac{1}{\tau_c}\right) + A\left(\frac{1}{2\tau_c^2} - \frac{9}{8t^2}\right) + \left(-\frac{9}{8t^3} - \frac{1}{3\tau_c^3}\right) \tag{1.37}$$

Then,

$$\overline{C}_A(\tau) = \left\{ \begin{array}{ll} -\frac{8\alpha\tau^3}{9} \cdot \frac{t^{-3}}{-3}\Big|_{\frac{2\tau}{3}}^{\tau_c} + \frac{8\tau^3}{9} \cdot (C_A^{in}+\alpha) \int\limits_{\frac{2\tau}{3}}^{\tau_c} \frac{1}{\left(k_3(C_A^{in}+\alpha)t+1\right)t^4} dt \ if \ \theta \geq \frac{2}{3} \\ 0 \qquad\qquad if \ \theta < \frac{2}{3} \end{array} \right\} \tag{1.38}$$

which gives us:

$$\overline{C}_A(\tau) = \left\{ \begin{array}{ll} \frac{8\alpha\tau^3}{27\tau_c^3} - \alpha + \frac{8\tau^3}{9} \cdot \frac{A}{k_3} \int\limits_{\frac{2\tau}{3}}^{\tau_c} \frac{1}{\left(k_3(C_A^{in}+\alpha)t+1\right)t^4} dt \ if \ \theta \geq \frac{2}{3} \\ 0 \qquad\qquad if \ \theta < \frac{2}{3} \end{array} \right\} \tag{1.39}$$

And so,

$$\frac{8\tau^3}{9}\frac{A}{k_3}\int\limits_{\frac{2\tau}{3}}^{\tau_c}\frac{1}{(k_3(C_A^{in}+\alpha)t+1)\,t^4}dt =$$

$$\left\{\ \tfrac{8\tau^3}{9}\cdot\tfrac{A}{k_3}\left(A^3\ln\left(\tfrac{2\tau(A\tau_c+1)}{\tau_c(2A\tau+3)}\right)+A^2\left(\tfrac{3}{2\tau}-\tfrac{1}{\tau_c}\right)+A\left(\tfrac{1}{2\tau_c^2}-\tfrac{9}{8t^2}\right)+\left(-\tfrac{9}{8t^3}-\tfrac{1}{3\tau_c^3}\right)\right)\ \right\} \quad (1.40)$$

$$\overline{C}_A(\tau)=\begin{cases} =\frac{8\tau^3}{9k_3}[k_3(C_A^{in}+\alpha)]^4\ln\left(\frac{2\tau\left([k_3(C_A^{in}+\alpha)]\tau_c+1\right)}{\tau_c\left(2[k_3(C_A^{in}+\alpha)]\tau+3\right)}\right)+[k_3(C_A^{in}+\alpha)]^3\left(\frac{12\tau^2}{9k_3}-\frac{8\tau^3}{9k_3\tau_c}\right) & \\ +[k_3(C_A^{in}+\alpha)]^2\left(\frac{4\tau^3}{9k_3\tau_c^2}-\frac{\tau}{k_3}\right)+[k_3(C_A^{in}+\alpha)]\left(-\frac{1}{k_3}-\frac{8\tau^3}{27k_3\tau_c^3}\right)+\frac{8\alpha\tau^3}{27\tau_c^3}-\alpha & if\ \theta\geq\frac{2}{3} \\ 0 & if\ \theta<\frac{2}{3} \end{cases} \quad (1.41)$$

1.7 Appendix B

The exit concentration $\overline{C}_C(\tau)$ of a segregated laminar flow reactor (SLFR) employing the Trambouze reaction scheme is:

$$\overline{C}_C(\tau) = \left\{ \begin{array}{l} \frac{8\tau^3}{9} \int\limits_{\frac{2\tau}{3}}^{\tau_c} \left[C_C^{in} - 2\alpha^2 k_3 t + 2\alpha \ln\left(k_3 t\left(C_A^{in}+\alpha\right)+1\right)\right] t^{-4} dt + \\ + \frac{8\tau^3}{9}\left[C_C^{in} - 2\alpha^2 k_3 \tau_c + 2\alpha \ln\left(k_3 \tau_c\left(C_A^{in}+\alpha\right)+1\right)\right] \int\limits_{\tau_c}^{\infty} t^{-4} dt \quad if\theta \geq \frac{2}{3} \\ \frac{8\tau^3}{9}\left[C_C^{in} - 2\alpha^2 k_3 \tau_c + 2\alpha \ln\left(k_3 \tau_c\left(C_A^{in}+\alpha\right)+1\right)\right] \int\limits_{\frac{2\tau}{3}}^{\infty} t^{-4} dt \quad if\theta < \frac{2}{3} \end{array} \right\}$$

where, $\int\limits_{\frac{2\tau}{3}}^{\tau_c} \ln\left(k_3\left(C_A^{in}+\alpha\right)t+1\right) t^{-4} dt = \int\limits_{\frac{2\tau}{3}}^{\tau_c} \ln\left(At+1\right) t^{-4} dt = \left[\frac{9A}{8\tau^2} + \frac{9}{8\tau^3} - \frac{A}{2\tau_c^2} - \frac{1}{3\tau_c^3}\right]\Big|$

$$\overline{C}_C(\tau) = \left\{ \begin{array}{l} \frac{8\tau^3}{9} C_C^{in} \left.\frac{t^{-3}}{-3}\right|_{\frac{2\tau}{3}}^{\tau_c} + \frac{8\tau^3}{9}\left(-2\alpha^2 k_3\right) \left.\frac{t^{-2}}{-2}\right|_{\frac{2\tau}{3}}^{\tau_c} + \frac{8\tau^3}{9}\left(2\alpha\right) \int\limits_{\frac{2\tau}{3}}^{\tau_c} \ln\left(k_3 t\left(C_A^{in}+\alpha\right)+1\right) t^{-4} dt + \\ + \frac{8\tau^3}{9}\left[C_C^{in} - 2\alpha^2 k_3 \tau_c + 2\alpha \ln\left(k_3 \tau_c\left(C_A^{in}+\alpha\right)+1\right)\right] \left.\frac{t^{-3}}{-3}\right|_{\tau_c}^{\infty} \quad if\theta \geq \frac{2}{3} \\ \frac{8\tau^3}{9}\left[C_C^{in} - 2\alpha^2 k_3 \tau_c + 2\alpha \ln\left(k_3 \tau_c\left(C_A^{in}+\alpha\right)+1\right)\right] \left.\frac{t^{-3}}{-3}\right|_{\frac{2\tau}{3}}^{\infty} \quad if\theta < \frac{2}{3} \end{array} \right\}$$

$$\overline{C}_C(\tau) = \left\{ \begin{array}{l} \frac{8\tau^3}{9} C_c^{in} \left(\frac{1}{-3\tau_c{}^3} + \frac{9}{8\tau^3}\right) - \frac{8\tau^3}{9}(-2\alpha^2 k_3)\left(\frac{1}{-2\tau_c^2} + \frac{9}{8\tau^2}\right) + \frac{16\tau^3\alpha}{9}\left[\frac{9A}{8\tau^2} + \frac{9}{8\tau^3} - \frac{A}{2\tau_c^2} - \frac{1}{3\tau_c^3}\right] + \\ + \frac{8\tau^3}{27\tau_c{}^3}\left[C_C^{in} - 2\alpha^2 k_3 \tau_c + 2\alpha \ln\left(k_3 \tau_c\left(C_A^{in}+\alpha\right)+1\right)\right] \quad if\theta \geq \frac{2}{3} \\ + \left[C_C^{in} - 2\alpha^2 k_3 \tau_c + 2\alpha \ln\left(k_3 \tau_c\left(C_A^{in}+\alpha\right)+1\right)\right] \quad if\theta < \frac{2}{3} \end{array} \right\}$$

$$\overline{C}_C(\tau) = \left\{ \begin{array}{l} -\frac{8\tau^3}{9}(-2\alpha^2 k_3)\left(\frac{1}{-2\tau_c^2} + \frac{9}{8\tau^2}\right) \\ + \frac{16\tau^3\alpha}{9}\left[\frac{9\left[k_3\left(C_A^{in}+\alpha\right)\right]}{8\tau^2} + \frac{9}{8\tau^3} - \frac{\left[k_3\left(C_A^{in}+\alpha\right)\right]}{2\tau_c^2} - \frac{1}{3\tau_c^3}\right] + \\ + \frac{8\tau^3}{27\tau_c{}^3}\left[C_C^{in} - 2\alpha^2 k_3 \tau_c + 2\alpha \ln\left(k_3 \tau_c\left(C_A^{in}+\alpha\right)+1\right)\right] \quad if\theta \geq \frac{2}{3} \\ + \left[C_C^{in} - 2\alpha^2 k_3 \tau_c + 2\alpha \ln\left(k_3 \tau_c\left(C_A^{in}+\alpha\right)+1\right)\right] \quad if\theta < \frac{2}{3} \end{array} \right\}$$

$$\overline{C}_C(\tau) = \left\{ \begin{array}{l} 2\alpha^2 k_3 \tau - \frac{8\alpha^2 k_3 \tau^3}{9\tau_c^2} + 2\alpha\tau A + 2\alpha - \frac{8\alpha\tau^3 A}{9T_c^2} \\ + \frac{16\tau^3\alpha}{9}\left[\frac{9\left[k_3\left(C_A^{in}+\alpha\right)\right]}{8\tau^2} + \frac{9}{8\tau^3} - \frac{\left[k_3\left(C_A^{in}+\alpha\right)\right]}{2\tau_c^2} - \frac{1}{3\tau_c^3}\right] + \\ - \frac{16\alpha^2 k_3 \tau^3}{27 t_c^2} + \frac{16\alpha\tau^3}{27\tau_c^3} \ln(k_3\tau_c(C_A^{in}+\alpha)+1) \quad if\theta \geq \frac{2}{3} \\ -2\alpha^2 k_3 \tau_c + 2\alpha \ln\left(k_3 \tau_c\left(C_A^{in}+\alpha\right)+1\right) \quad if\theta < \frac{2}{3} \end{array} \right\}$$

1.8 Appendix C

Here we will show all the combinations of the multiple reactors involved in this study:

- SLFR
- PFR
- CSTR

Table 1.12: SLFR Reactors 1

i	$x(i)$	$y(i)$	$\tau(i)$	$\Delta C_c(i)$	i	$x(i)$	$y(i)$	$\tau(i)$	$\Delta C_c(i)$
1	1.0000	0.9688	0.0513	0.0101	26	1.0000	0.1875	3.7143	0.3392
2	1.0000	0.9375	0.1053	0.0204	27	1.0000	0.1563	4.1538	0.3543
3	1.0000	0.9063	0.1622	0.0309	28	1.0000	0.1250	4.6667	0.3687
4	1.0000	0.8750	0.2222	0.0416	29	1.0000	0.0938	5.2727	0.3819
5	1.0000	0.8438	0.2857	0.0525	30	1.0000	0.0625	6.0000	0.3931
6	1.0000	0.8125	0.3529	0.0636	31	1.0000	0.0313	6.8889	0.4014
7	1.0000	0.7813	0.4242	0.0750	32	1.0000	0.0000	8.0000	0.4047
8	1.0000	0.7500	0.5000	0.0866	33	0.9688	0.9375	0.0540	0.0103
9	1.0000	0.7188	0.5806	0.0984	34	0.9688	0.9063	0.1109	0.0208
10	1.0000	0.6875	0.6667	0.1105	35	0.9688	0.8750	0.1709	0.0315
11	1.0000	0.6563	0.7586	0.1229	36	0.9688	0.8438	0.2344	0.0424
12	1.0000	0.6250	0.8571	0.1355	37	0.9688	0.8125	0.3017	0.0535
13	1.0000	0.5938	0.9630	0.1484	38	0.9688	0.7813	0.3730	0.0649
14	1.0000	0.5625	1.0769	0.1615	39	0.9688	0.7500	0.4487	0.0765
15	1.0000	0.5313	1.2000	0.1750	40	0.9688	0.7188	0.5294	0.0883
16	1.0000	0.5000	1.3333	0.1887	41	0.9688	0.6875	0.6154	0.1004
17	1.0000	0.4688	1.4783	0.2028	42	0.9688	0.6563	0.7073	0.1128
18	1.0000	0.4375	1.6364	0.2171	43	0.9688	0.6250	0.8059	0.1254
19	1.0000	0.4063	1.8095	0.2317	44	0.9688	0.5938	0.9117	0.1383
20	1.0000	0.3750	2.0000	0.2466	45	0.9688	0.5625	1.0256	0.1515
21	1.0000	0.3438	2.2105	0.2617	46	0.9688	0.5313	1.1487	0.1649
22	1.0000	0.3125	2.4444	0.2770	47	0.9688	0.5000	1.2821	0.1787
23	1.0000	0.2813	2.7059	0.2925	48	0.9688	0.4688	1.4270	0.1927
24	1.0000	0.2500	3.0000	0.3081	49	0.9688	0.4375	1.5851	0.2070
25	1.0000	0.2188	3.3333	0.3237	50	0.9688	0.4063	1.7582	0.2216

Table 1.13: SLFR Reactors 2

i	$x(i)$	$y(i)$	$\tau(i)$	$\Delta C_c(i)$	i	$x(i)$	$y(i)$	$\tau(i)$	$\Delta C_c(i)$
51	0.9688	0.3750	1.9487	0.2365	76	0.9375	0.5313	1.0947	0.1546
52	0.9688	0.3438	2.1592	0.2516	77	0.9375	0.5000	1.2281	0.1684
53	0.9688	0.3125	2.3932	0.2669	78	0.9375	0.4688	1.3730	0.1824
54	0.9688	0.2813	2.6546	0.2824	79	0.9375	0.4375	1.5311	0.1967
55	0.9688	0.2500	2.9487	0.2981	80	0.9375	0.4063	1.7043	0.2113
56	0.9688	0.2188	3.2821	0.3137	81	0.9375	0.3750	1.8947	0.2262
57	0.9688	0.1875	3.6630	0.3291	82	0.9375	0.3438	2.1053	0.2413
58	0.9688	0.1563	4.1026	0.3442	83	0.9375	0.3125	2.3392	0.2566
59	0.9688	0.1250	4.6154	0.3586	84	0.9375	0.2813	2.6006	0.2722
60	0.9688	0.0938	5.2214	0.3718	85	0.9375	0.2500	2.8947	0.2878
61	0.9688	0.0625	5.9487	0.3831	86	0.9375	0.2188	3.2281	0.3034
62	0.9688	0.0313	6.8376	0.3913	87	0.9375	0.1875	3.6090	0.3188
63	0.9688	0.0000	7.9487	0.3946	88	0.9375	0.1563	4.0486	0.3339
64	0.9375	0.9063	0.0569	0.0105	89	0.9375	0.1250	4.5614	0.3483
65	0.9375	0.8750	0.1170	0.0212	90	0.9375	0.0938	5.1675	0.3615
66	0.9375	0.8438	0.1805	0.0321	91	0.9375	0.0625	5.8947	0.3728
67	0.9375	0.8125	0.2477	0.0432	92	0.9375	0.0313	6.7836	0.3810
68	0.9375	0.7813	0.3190	0.0546	93	0.9375	0.0000	7.8947	0.3843
69	0.9375	0.7500	0.3947	0.0662	94	0.9063	0.8750	0.0601	0.0107
70	0.9375	0.7188	0.4754	0.0780	95	0.9063	0.8438	0.1236	0.0216
71	0.9375	0.6875	0.5614	0.0901	96	0.9063	0.8125	0.1908	0.0327
72	0.9375	0.6563	0.6534	0.1025	97	0.9063	0.7813	0.2621	0.0441
73	0.9375	0.6250	0.7519	0.1151	98	0.9063	0.7500	0.3378	0.0557
74	0.9375	0.5938	0.8577	0.1280	99	0.9063	0.7188	0.4185	0.0675
75	0.9375	0.5625	0.9717	0.1412	100	0.9063	0.6875	0.5045	0.0796

Table 1.14: SLFR Reactors 3

i	$x(i)$	$y(i)$	$\tau(i)$	$\Delta C_c(i)$	i	$x(i)$	$y(i)$	$\tau(i)$	$\Delta C_c(i)$
101	0.9063	0.6563	0.5965	0.0920	126	0.8750	0.7500	0.2778	0.0450
102	0.9063	0.6250	0.6950	0.1046	127	0.8750	0.7188	0.3584	0.0568
103	0.9063	0.5938	0.8008	0.1175	128	0.8750	0.6875	0.4444	0.0689
104	0.9063	0.5625	0.9148	0.1307	129	0.8750	0.6563	0.5364	0.0813
105	0.9063	0.5313	1.0378	0.1441	130	0.8750	0.6250	0.6349	0.0939
106	0.9063	0.5000	1.1712	0.1579	131	0.8750	0.5938	0.7407	0.1068
107	0.9063	0.4688	1.3161	0.1719	132	0.8750	0.5625	0.8547	0.1200
108	0.9063	0.4375	1.4742	0.1862	133	0.8750	0.5313	0.9778	0.1334
109	0.9063	0.4063	1.6474	0.2008	134	0.8750	0.5000	1.1111	0.1472
110	0.9063	0.3750	1.8378	0.2157	135	0.8750	0.4688	1.2560	0.1612
111	0.9063	0.3438	2.0484	0.2308	136	0.8750	0.4375	1.4141	0.1755
112	0.9063	0.3125	2.2823	0.2462	137	0.8750	0.4063	1.5873	0.1901
113	0.9063	0.2813	2.5437	0.2617	138	0.8750	0.3750	1.7778	0.2050
114	0.9063	0.2500	2.8378	0.2773	139	0.8750	0.3438	1.9883	0.2201
115	0.9063	0.2188	3.1712	0.2929	140	0.8750	0.3125	2.2222	0.2355
116	0.9063	0.1875	3.5521	0.3083	141	0.8750	0.2813	2.4837	0.2510
117	0.9063	0.1563	3.9917	0.3234	142	0.8750	0.2500	2.7778	0.2666
118	0.9063	0.1250	4.5045	0.3378	143	0.8750	0.2188	3.1111	0.2822
119	0.9063	0.0938	5.1106	0.3510	144	0.8750	0.1875	3.4921	0.2976
120	0.9063	0.0625	5.8378	0.3623	145	0.8750	0.1563	3.9316	0.3127
121	0.9063	0.0313	6.7267	0.3705	146	0.8750	0.1250	4.4444	0.3271
122	0.9063	0.0000	7.8378	0.3738	147	0.8750	0.0938	5.0505	0.3403
123	0.8750	0.8438	0.0635	0.0109	148	0.8750	0.0625	5.7778	0.3516
124	0.8750	0.8125	0.1307	0.0220	149	0.8750	0.0313	6.6667	0.3598
125	0.8750	0.7813	0.2020	0.0334	150	0.8750	0.0000	7.7778	0.3631

Table 1.15: SLFR Reactors 4

i	$x(i)$	$y(i)$	$\tau(i)$	$\Delta C_c(i)$	i	$x(i)$	$y(i)$	$\tau(i)$	$\Delta C_c(i)$
151	0.8438	0.8125	0.0672	0.0111	176	0.8438	0.0313	6.6032	0.3489
152	0.8438	0.7813	0.1385	0.0225	177	0.8438	0.0000	7.7143	0.3522
153	0.8438	0.7500	0.2143	0.0341	178	0.8125	0.7813	0.0713	0.0114
154	0.8438	0.7188	0.2949	0.0459	179	0.8125	0.7500	0.1471	0.0230
155	0.8438	0.6875	0.3810	0.0580	180	0.8125	0.7188	0.2277	0.0348
156	0.8438	0.6563	0.4729	0.0704	181	0.8125	0.6875	0.3137	0.0469
157	0.8438	0.6250	0.5714	0.0830	182	0.8125	0.6563	0.4057	0.0592
158	0.8438	0.5938	0.6772	0.0959	183	0.8125	0.6250	0.5042	0.0719
159	0.8438	0.5625	0.7912	0.1091	184	0.8125	0.5938	0.6100	0.0848
160	0.8438	0.5313	0.9143	0.1225	185	0.8125	0.5625	0.7240	0.0979
161	0.8438	0.5000	1.0476	0.1363	186	0.8125	0.5313	0.8471	0.1114
162	0.8438	0.4688	1.1925	0.1503	187	0.8125	0.5000	0.9804	0.1251
163	0.8438	0.4375	1.3506	0.1646	188	0.8125	0.4688	1.1253	0.1392
164	0.8438	0.4063	1.5238	0.1792	189	0.8125	0.4375	1.2834	0.1535
165	0.8438	0.3750	1.7143	0.1941	190	0.8125	0.4063	1.4566	0.1681
166	0.8438	0.3438	1.9248	0.2092	191	0.8125	0.3750	1.6471	0.1830
167	0.8438	0.3125	2.1587	0.2246	192	0.8125	0.3438	1.8576	0.1981
168	0.8438	0.2813	2.4202	0.2401	193	0.8125	0.3125	2.0915	0.2134
169	0.8438	0.2500	2.7143	0.2557	194	0.8125	0.2813	2.3529	0.2289
170	0.8438	0.2188	3.0476	0.2713	195	0.8125	0.2500	2.6471	0.2445
171	0.8438	0.1875	3.4286	0.2867	196	0.8125	0.2188	2.9804	0.2601
172	0.8438	0.1563	3.8681	0.3018	197	0.8125	0.1875	3.3613	0.2756
173	0.8438	0.1250	4.3810	0.3162	198	0.8125	0.1563	3.8009	0.2907
174	0.8438	0.0938	4.9870	0.3294	199	0.8125	0.1250	4.3137	0.3050
175	0.8438	0.0625	5.7143	0.3407	200	0.8125	0.0938	4.9198	0.3182

Table 1.16: SLFR Reactors 5

i	$x(i)$	$y(i)$	$\tau(i)$	$\Delta C_c(i)$	i	$x(i)$	$y(i)$	$\tau(i)$	$\Delta C_c(i)$
201	0.8125	0.0625	5.6471	0.3295	226	0.7813	0.0625	5.5758	0.3182
202	0.8125	0.0313	6.5359	0.3378	227	0.7813	0.0313	6.4646	0.3264
203	0.8125	0.0000	7.6471	0.3411	228	0.7813	0.0000	7.5758	0.3297
204	0.7813	0.7500	0.0758	0.0116	229	0.7500	0.7188	0.0806	0.0118
205	0.7813	0.7188	0.1564	0.0234	230	0.7500	0.6875	0.1667	0.0239
206	0.7813	0.6875	0.2424	0.0355	231	0.7500	0.6563	0.2586	0.0363
207	0.7813	0.6563	0.3344	0.0479	232	0.7500	0.6250	0.3571	0.0489
208	0.7813	0.6250	0.4329	0.0605	233	0.7500	0.5938	0.4630	0.0618
209	0.7813	0.5938	0.5387	0.0734	234	0.7500	0.5625	0.5769	0.0750
210	0.7813	0.5625	0.6527	0.0866	235	0.7500	0.5313	0.7000	0.0884
211	0.7813	0.5313	0.7758	0.1000	236	0.7500	0.5000	0.8333	0.1022
212	0.7813	0.5000	0.9091	0.1138	237	0.7500	0.4688	0.9783	0.1162
213	0.7813	0.4688	1.0540	0.1278	238	0.7500	0.4375	1.1364	0.1305
214	0.7813	0.4375	1.2121	0.1421	239	0.7500	0.4063	1.3095	0.1451
215	0.7813	0.4063	1.3853	0.1567	240	0.7500	0.3750	1.5000	0.1600
216	0.7813	0.3750	1.5758	0.1716	241	0.7500	0.3438	1.7105	0.1751
217	0.7813	0.3438	1.7863	0.1867	242	0.7500	0.3125	1.9444	0.1905
218	0.7813	0.3125	2.0202	0.2021	243	0.7500	0.2813	2.2059	0.2060
219	0.7813	0.2813	2.2816	0.2176	244	0.7500	0.2500	2.5000	0.2216
220	0.7813	0.2500	2.5758	0.2332	245	0.7500	0.2188	2.8333	0.2372
221	0.7813	0.2188	2.9091	0.2488	246	0.7500	0.1875	3.2143	0.2526
222	0.7813	0.1875	3.2900	0.2642	247	0.7500	0.1563	3.6538	0.2677
223	0.7813	0.1563	3.7296	0.2793	248	0.7500	0.1250	4.1667	0.2821
224	0.7813	0.1250	4.2424	0.2937	249	0.7500	0.0938	4.7727	0.2953
225	0.7813	0.0938	4.8485	0.3069	250	0.7500	0.0625	5.5000	0.3066

Table 1.17: SLFR Reactors 6

i	$x(i)$	$y(i)$	$\tau(i)$	$\Delta C_c(i)$	i	$x(i)$	$y(i)$	$\tau(i)$	$\Delta C_c(i)$
251	0.7500	0.0313	6.3889	0.3148	276	0.6875	0.6563	0.0920	0.0124
252	0.7500	0.0000	7.5000	0.3181	277	0.6875	0.6250	0.1905	0.0250
253	0.7188	0.6875	0.0860	0.0121	278	0.6875	0.5938	0.2963	0.0379
254	0.7188	0.6563	0.1780	0.0244	279	0.6875	0.5625	0.4103	0.0510
255	0.7188	0.6250	0.2765	0.0371	280	0.6875	0.5313	0.5333	0.0645
256	0.7188	0.5938	0.3823	0.0500	281	0.6875	0.5000	0.6667	0.0782
257	0.7188	0.5625	0.4963	0.0631	282	0.6875	0.4688	0.8116	0.0923
258	0.7188	0.5313	0.6194	0.0766	283	0.6875	0.4375	0.9697	0.1066
259	0.7188	0.5000	0.7527	0.0903	284	0.6875	0.4063	1.1429	0.1212
260	0.7188	0.4688	0.8976	0.1044	285	0.6875	0.3750	1.3333	0.1361
261	0.7188	0.4375	1.0557	0.1187	286	0.6875	0.3438	1.5439	0.1512
262	0.7188	0.4063	1.2289	0.1333	287	0.6875	0.3125	1.7778	0.1665
263	0.7188	0.3750	1.4194	0.1482	288	0.6875	0.2813	2.0392	0.1820
264	0.7188	0.3438	1.6299	0.1633	289	0.6875	0.2500	2.3333	0.1976
265	0.7188	0.3125	1.8638	0.1786	290	0.6875	0.2188	2.6667	0.2132
266	0.7188	0.2813	2.1252	0.1941	291	0.6875	0.1875	3.0476	0.2287
267	0.7188	0.2500	2.4194	0.2097	292	0.6875	0.1563	3.4872	0.2438
268	0.7188	0.2188	2.7527	0.2253	293	0.6875	0.1250	4.0000	0.2581
269	0.7188	0.1875	3.1336	0.2408	294	0.6875	0.0938	4.6061	0.2713
270	0.7188	0.1563	3.5732	0.2559	295	0.6875	0.0625	5.3333	0.2826
271	0.7188	0.1250	4.0860	0.2702	296	0.6875	0.0313	6.2222	0.2909
272	0.7188	0.0938	4.6921	0.2834	297	0.6875	0.0000	7.3333	0.2942
273	0.7188	0.0625	5.4194	0.2947	298	0.6563	0.6250	0.0985	0.0126
274	0.7188	0.0313	6.3082	0.3030	299	0.6563	0.5938	0.2043	0.0255
275	0.7188	0.0000	7.4194	0.3063	300	0.6563	0.5625	0.3183	0.0387

Table 1.18: SLFR Reactors 7

i	$x(i)$	$y(i)$	$\tau(i)$	$\Delta C_c(i)$	i	$x(i)$	$y(i)$	$\tau(i)$	$\Delta C_c(i)$
301	0.6563	0.5313	0.4414	0.0521	326	0.6250	0.3750	1.1429	0.1111
302	0.6563	0.5000	0.5747	0.0659	327	0.6250	0.3438	1.3534	0.1262
303	0.6563	0.4688	0.7196	0.0799	328	0.6250	0.3125	1.5873	0.1416
304	0.6563	0.4375	0.8777	0.0942	329	0.6250	0.2813	1.8487	0.1571
305	0.6563	0.4063	1.0509	0.1088	330	0.6250	0.2500	2.1429	0.1727
306	0.6563	0.3750	1.2414	0.1237	331	0.6250	0.2188	2.4762	0.1883
307	0.6563	0.3438	1.4519	0.1388	332	0.6250	0.1875	2.8571	0.2037
308	0.6563	0.3125	1.6858	0.1542	333	0.6250	0.1563	3.2967	0.2188
309	0.6563	0.2813	1.9473	0.1697	334	0.6250	0.1250	3.8095	0.2332
310	0.6563	0.2500	2.2414	0.1853	335	0.6250	0.0938	4.4156	0.2464
311	0.6563	0.2188	2.5747	0.2009	336	0.6250	0.0625	5.1429	0.2577
312	0.6563	0.1875	2.9557	0.2163	337	0.6250	0.0313	6.0317	0.2659
313	0.6563	0.1563	3.3952	0.2314	338	0.6250	0.0000	7.1429	0.2692
314	0.6563	0.1250	3.9080	0.2458	339	0.5938	0.5625	0.1140	0.0132
315	0.6563	0.0938	4.5141	0.2590	340	0.5938	0.5313	0.2370	0.0266
316	0.6563	0.0625	5.2414	0.2703	341	0.5938	0.5000	0.3704	0.0404
317	0.6563	0.0313	6.1303	0.2785	342	0.5938	0.4688	0.5153	0.0544
318	0.6563	0.0000	7.2414	0.2819	343	0.5938	0.4375	0.6734	0.0687
319	0.6250	0.5938	0.1058	0.0129	344	0.5938	0.4063	0.8466	0.0833
320	0.6250	0.5625	0.2198	0.0261	345	0.5938	0.3750	1.0370	0.0982
321	0.6250	0.5313	0.3429	0.0395	346	0.5938	0.3438	1.2476	0.1133
322	0.6250	0.5000	0.4762	0.0533	347	0.5938	0.3125	1.4815	0.1287
323	0.6250	0.4688	0.6211	0.0673	348	0.5938	0.2813	1.7429	0.1442
324	0.6250	0.4375	0.7792	0.0816	349	0.5938	0.2500	2.0370	0.1598
325	0.6250	0.4063	0.9524	0.0962	350	0.5938	0.2188	2.3704	0.1754

Table 1.19: SLFR Reactors 8

i	$x(i)$	$y(i)$	$\tau(i)$	$\Delta C_c(i)$	i	$x(i)$	$y(i)$	$\tau(i)$	$\Delta C_c(i)$
351	0.5938	0.1875	2.7513	0.1908	376	0.5313	0.5000	0.1333	0.0137
352	0.5938	0.1563	3.1909	0.2059	377	0.5313	0.4688	0.2783	0.0278
353	0.5938	0.1250	3.7037	0.2203	378	0.5313	0.4375	0.4364	0.0421
354	0.5938	0.0938	4.3098	0.2335	379	0.5313	0.4063	0.6095	0.0567
355	0.5938	0.0625	5.0370	0.2448	380	0.5313	0.3750	0.8000	0.0716
356	0.5938	0.0313	5.9259	0.2530	381	0.5313	0.3438	1.0105	0.0867
357	0.5938	0.0000	7.0370	0.2563	382	0.5313	0.3125	1.2444	0.1020
358	0.5625	0.5313	0.1231	0.0135	383	0.5313	0.2813	1.5059	0.1175
359	0.5625	0.5000	0.2564	0.0272	384	0.5313	0.2500	1.8000	0.1331
360	0.5625	0.4688	0.4013	0.0412	385	0.5313	0.2188	2.1333	0.1487
361	0.5625	0.4375	0.5594	0.0556	386	0.5313	0.1875	2.5143	0.1642
362	0.5625	0.4063	0.7326	0.0702	387	0.5313	0.1563	2.9538	0.1793
363	0.5625	0.3750	0.9231	0.0850	388	0.5313	0.1250	3.4667	0.1937
364	0.5625	0.3438	1.1336	0.1001	389	0.5313	0.0938	4.0727	0.2069
365	0.5625	0.3125	1.3675	0.1155	390	0.5313	0.0625	4.8000	0.2181
366	0.5625	0.2813	1.6290	0.1310	391	0.5313	0.0313	5.6889	0.2264
367	0.5625	0.2500	1.9231	0.1466	392	0.5313	0.0000	6.8000	0.2297
368	0.5625	0.2188	2.2564	0.1622	393	0.5000	0.4688	0.1449	0.0140
369	0.5625	0.1875	2.6374	0.1777	394	0.5000	0.4375	0.3030	0.0284
370	0.5625	0.1563	3.0769	0.1927	395	0.5000	0.4063	0.4762	0.0430
371	0.5625	0.1250	3.5897	0.2071	396	0.5000	0.3750	0.6667	0.0578
372	0.5625	0.0938	4.1958	0.2203	397	0.5000	0.3438	0.8772	0.0729
373	0.5625	0.0625	4.9231	0.2316	398	0.5000	0.3125	1.1111	0.0883
374	0.5625	0.0313	5.8120	0.2398	399	0.5000	0.2813	1.3725	0.1038
375	0.5625	0.0000	6.9231	0.2432	400	0.5000	0.2500	1.6667	0.1194

Table 1.20: SLFR Reactors 9

i	$x(i)$	$y(i)$	$\tau(i)$	$\Delta C_c(i)$	i	$x(i)$	$y(i)$	$\tau(i)$	$\Delta C_c(i)$
401	0.5000	0.2188	2.0000	0.1350	426	0.4375	0.3438	0.5742	0.0446
402	0.5000	0.1875	2.3810	0.1505	427	0.4375	0.3125	0.8081	0.0599
403	0.5000	0.1563	2.8205	0.1655	428	0.4375	0.2813	1.0695	0.0754
404	0.5000	0.1250	3.3333	0.1799	429	0.4375	0.2500	1.3636	0.0910
405	0.5000	0.0938	3.9394	0.1931	430	0.4375	0.2188	1.6970	0.1066
406	0.5000	0.0625	4.6667	0.2044	431	0.4375	0.1875	2.0779	0.1221
407	0.5000	0.0313	5.5556	0.2126	432	0.4375	0.1563	2.5175	0.1372
408	0.5000	0.0000	6.6667	0.2160	433	0.4375	0.1250	3.0303	0.1516
409	0.4688	0.4375	0.1581	0.0143	434	0.4375	0.0938	3.6364	0.1648
410	0.4688	0.4063	0.3313	0.0289	435	0.4375	0.0625	4.3636	0.1760
411	0.4688	0.3750	0.5217	0.0438	436	0.4375	0.0313	5.2525	0.1843
412	0.4688	0.3438	0.7323	0.0589	437	0.4375	0.0000	6.3636	0.1876
413	0.4688	0.3125	0.9662	0.0743	438	0.4063	0.3750	0.1905	0.0149
414	0.4688	0.2813	1.2276	0.0898	439	0.4063	0.3438	0.4010	0.0300
415	0.4688	0.2500	1.5217	0.1054	440	0.4063	0.3125	0.6349	0.0453
416	0.4688	0.2188	1.8551	0.1210	441	0.4063	0.2813	0.8964	0.0608
417	0.4688	0.1875	2.2360	0.1364	442	0.4063	0.2500	1.1905	0.0764
418	0.4688	0.1563	2.6756	0.1515	443	0.4063	0.2188	1.5238	0.0920
419	0.4688	0.1250	3.1884	0.1659	444	0.4063	0.1875	1.9048	0.1075
420	0.4688	0.0938	3.7945	0.1791	445	0.4063	0.1563	2.3443	0.1226
421	0.4688	0.0625	4.5217	0.1904	446	0.4063	0.1250	2.8571	0.1370
422	0.4688	0.0313	5.4106	0.1986	447	0.4063	0.0938	3.4632	0.1502
423	0.4688	0.0000	6.5217	0.2019	448	0.4063	0.0625	4.1905	0.1614
424	0.4375	0.4063	0.1732	0.0146	449	0.4063	0.0313	5.0794	0.1697
425	0.4375	0.3750	0.3636	0.0295	450	0.4063	0.0000	6.1905	0.1730

Table 1.21: SLFR Reactors 10

i	$x(i)$	$y(i)$	$\tau(i)$	$\Delta C_c(i)$	i	$x(i)$	$y(i)$	$\tau(i)$	$\Delta C_c(i)$
451	0.3750	0.3438	0.2105	0.0151	476	0.3125	0.2188	0.8889	0.0467
452	0.3750	0.3125	0.4444	0.0305	477	0.3125	0.1875	1.2698	0.0622
453	0.3750	0.2813	0.7059	0.0460	478	0.3125	0.1563	1.7094	0.0772
454	0.3750	0.2500	1.0000	0.0616	479	0.3125	0.1250	2.2222	0.0916
455	0.3750	0.2188	1.3333	0.0772	480	0.3125	0.0938	2.8283	0.1048
456	0.3750	0.1875	1.7143	0.0926	481	0.3125	0.0625	3.5556	0.1161
457	0.3750	0.1563	2.1538	0.1077	482	0.3125	0.0313	4.4444	0.1244
458	0.3750	0.1250	2.6667	0.1221	483	0.3125	0.0000	5.5556	0.1277
459	0.3750	0.0938	3.2727	0.1353	484	0.2813	0.2500	0.2941	0.0156
460	0.3750	0.0625	4.0000	0.1466	485	0.2813	0.2188	0.6275	0.0312
461	0.3750	0.0313	4.8889	0.1548	486	0.2813	0.1875	1.0084	0.0467
462	0.3750	0.0000	6.0000	0.1581	487	0.2813	0.1563	1.4480	0.0617
463	0.3438	0.3125	0.2339	0.0153	488	0.2813	0.1250	1.9608	0.0761
464	0.3438	0.2813	0.4954	0.0308	489	0.2813	0.0938	2.5668	0.0893
465	0.3438	0.2500	0.7895	0.0465	490	0.2813	0.0625	3.2941	0.1006
466	0.3438	0.2188	1.1228	0.0621	491	0.2813	0.0313	4.1830	0.1088
467	0.3438	0.1875	1.5038	0.0775	492	0.2813	0.0000	5.2941	0.1122
468	0.3438	0.1563	1.9433	0.0926	493	0.2500	0.2188	0.3333	0.0156
469	0.3438	0.1250	2.4561	0.1070	494	0.2500	0.1875	0.7143	0.0311
470	0.3438	0.0938	3.0622	0.1202	495	0.2500	0.1563	1.1538	0.0461
471	0.3438	0.0625	3.7895	0.1315	496	0.2500	0.1250	1.6667	0.0605
472	0.3438	0.0313	4.6784	0.1397	497	0.2500	0.0938	2.2727	0.0737
473	0.3438	0.0000	5.7895	0.1430	498	0.2500	0.0625	3.0000	0.0850
474	0.3125	0.2813	0.2614	0.0155	499	0.2500	0.0313	3.8889	0.0932
475	0.3125	0.2500	0.5556	0.0311	500	0.2500	0.0000	5.0000	0.0966

Table 1.22: SLFR Reactors 11

i	$x(i)$	$y(i)$	$\tau(i)$	$\Delta C_c(i)$	i	$x(i)$	$y(i)$	$\tau(i)$	$\Delta C_c(i)$
501	0.2188	0.1875	0.3810	0.0154	515	0.1563	0.0938	1.1189	0.0276
502	0.2188	0.1563	0.8205	0.0305	516	0.1563	0.0625	1.8462	0.0389
503	0.2188	0.1250	1.3333	0.0449	517	0.1563	0.0313	2.7350	0.0471
504	0.2188	0.0938	1.9394	0.0581	518	0.1563	0.0000	3.8462	0.0504
505	0.2188	0.0625	2.6667	0.0694	519	0.1250	0.0938	0.6061	0.0132
506	0.2188	0.0313	3.5556	0.0776	520	0.1250	0.0625	1.3333	0.0245
507	0.2188	0.0000	4.6667	0.0810	521	0.1250	0.0313	2.2222	0.0327
508	0.1875	0.1563	0.4396	0.0151	522	0.1250	0.0000	3.3333	0.0361
509	0.1875	0.1250	0.9524	0.0295	523	0.0938	0.0625	0.7273	0.0113
510	0.1875	0.0938	1.5584	0.0427	524	0.0938	0.0313	1.6162	0.0195
511	0.1875	0.0625	2.2857	0.0540	525	0.0938	0.0000	2.7273	0.0229
512	0.1875	0.0313	3.1746	0.0622	526	0.0625	0.0313	0.8889	0.0082
513	0.1875	0.0000	4.2857	0.0655	527	0.0625	0.0000	2.0000	0.0116
514	0.1563	0.1250	0.5128	0.0144	528	0.0313	0.0000	1.1111	0.0033

Table 1.23: PFR Reactors 1

i	$x(i)$	$y(i)$	$\tau(i)$	$\Delta C_c(i)$	i	$x(i)$	$y(i)$	$\tau(i)$	$\Delta C_c(i)$
1	1.0000	0.9688	0.0513	0.0101	26	1.0000	0.1875	3.7143	0.3392
2	1.0000	0.9375	0.1053	0.0204	27	1.0000	0.1563	4.1538	0.3543
3	1.0000	0.9063	0.1622	0.0309	28	1.0000	0.1250	4.6667	0.3687
4	1.0000	0.8750	0.2222	0.0416	29	1.0000	0.0938	5.2727	0.3819
5	1.0000	0.8438	0.2857	0.0525	30	1.0000	0.0625	6.0000	0.3931
6	1.0000	0.8125	0.3529	0.0636	31	1.0000	0.0313	6.8889	0.4014
7	1.0000	0.7813	0.4242	0.0750	32	1.0000	0.0000	8.0000	0.4047
8	1.0000	0.7500	0.5000	0.0866	33	0.9688	0.9375	0.0540	0.0103
9	1.0000	0.7188	0.5806	0.0984	34	0.9688	0.9063	0.1109	0.0208
10	1.0000	0.6875	0.6667	0.1105	35	0.9688	0.8750	0.1709	0.0315
11	1.0000	0.6563	0.7586	0.1229	36	0.9688	0.8438	0.2344	0.0424
12	1.0000	0.6250	0.8571	0.1355	37	0.9688	0.8125	0.3017	0.0535
13	1.0000	0.5938	0.9630	0.1484	38	0.9688	0.7813	0.3730	0.0649
14	1.0000	0.5625	1.0769	0.1615	39	0.9688	0.7500	0.4487	0.0765
15	1.0000	0.5313	1.2000	0.1750	40	0.9688	0.7188	0.5294	0.0883
16	1.0000	0.5000	1.3333	0.1887	41	0.9688	0.6875	0.6154	0.1004
17	1.0000	0.4688	1.4783	0.2028	42	0.9688	0.6563	0.7073	0.1128
18	1.0000	0.4375	1.6364	0.2171	43	0.9688	0.6250	0.8059	0.1254
19	1.0000	0.4063	1.8095	0.2317	44	0.9688	0.5938	0.9117	0.1383
20	1.0000	0.3750	2.0000	0.2466	45	0.9688	0.5625	1.0256	0.1515
21	1.0000	0.3438	2.2105	0.2617	46	0.9688	0.5313	1.1487	0.1649
22	1.0000	0.3125	2.4444	0.2770	47	0.9688	0.5000	1.2821	0.1787
23	1.0000	0.2813	2.7059	0.2925	48	0.9688	0.4688	1.4270	0.1927
24	1.0000	0.2500	3.0000	0.3081	49	0.9688	0.4375	1.5851	0.2070
25	1.0000	0.2188	3.3333	0.3237	50	0.9688	0.4063	1.7582	0.2216

Table 1.24: PFR Reactors 2

i	$x(i)$	$y(i)$	$\tau(i)$	$\Delta C_c(i)$	i	$x(i)$	$y(i)$	$\tau(i)$	$\Delta C_c(i)$
51	0.9688	0.3750	1.9487	0.2365	76	0.9375	0.5313	1.0947	0.1546
52	0.9688	0.3438	2.1592	0.2516	77	0.9375	0.5000	1.2281	0.1684
53	0.9688	0.3125	2.3932	0.2669	78	0.9375	0.4688	1.3730	0.1824
54	0.9688	0.2813	2.6546	0.2824	79	0.9375	0.4375	1.5311	0.1967
55	0.9688	0.2500	2.9487	0.2981	80	0.9375	0.4063	1.7043	0.2113
56	0.9688	0.2188	3.2821	0.3137	81	0.9375	0.3750	1.8947	0.2262
57	0.9688	0.1875	3.6630	0.3291	82	0.9375	0.3438	2.1053	0.2413
58	0.9688	0.1563	4.1026	0.3442	83	0.9375	0.3125	2.3392	0.2566
59	0.9688	0.1250	4.6154	0.3586	84	0.9375	0.2813	2.6006	0.2722
60	0.9688	0.0938	5.2214	0.3718	85	0.9375	0.2500	2.8947	0.2878
61	0.9688	0.0625	5.9487	0.3831	86	0.9375	0.2188	3.2281	0.3034
62	0.9688	0.0313	6.8376	0.3913	87	0.9375	0.1875	3.6090	0.3188
63	0.9688	0.0000	7.9487	0.3946	88	0.9375	0.1563	4.0486	0.3339
64	0.9375	0.9063	0.0569	0.0105	89	0.9375	0.1250	4.5614	0.3483
65	0.9375	0.8750	0.1170	0.0212	90	0.9375	0.0938	5.1675	0.3615
66	0.9375	0.8438	0.1805	0.0321	91	0.9375	0.0625	5.8947	0.3728
67	0.9375	0.8125	0.2477	0.0432	92	0.9375	0.0313	6.7836	0.3810
68	0.9375	0.7813	0.3190	0.0546	93	0.9375	0.0000	7.8947	0.3843
69	0.9375	0.7500	0.3947	0.0662	94	0.9063	0.8750	0.0601	0.0107
70	0.9375	0.7188	0.4754	0.0780	95	0.9063	0.8438	0.1236	0.0216
71	0.9375	0.6875	0.5614	0.0901	96	0.9063	0.8125	0.1908	0.0327
72	0.9375	0.6563	0.6534	0.1025	97	0.9063	0.7813	0.2621	0.0441
73	0.9375	0.6250	0.7519	0.1151	98	0.9063	0.7500	0.3378	0.0557
74	0.9375	0.5938	0.8577	0.1280	99	0.9063	0.7188	0.4185	0.0675
75	0.9375	0.5625	0.9717	0.1412	100	0.9063	0.6875	0.5045	0.0796

Table 1.25: PFR Reactors 3

i	$x(i)$	$y(i)$	$\tau(i)$	$\Delta C_c(i)$	i	$x(i)$	$y(i)$	$\tau(i)$	$\Delta C_c(i)$
101	0.9063	0.6563	0.5965	0.0920	126	0.8750	0.7500	0.2778	0.0450
102	0.9063	0.6250	0.6950	0.1046	127	0.8750	0.7188	0.3584	0.0568
103	0.9063	0.5938	0.8008	0.1175	128	0.8750	0.6875	0.4444	0.0689
104	0.9063	0.5625	0.9148	0.1307	129	0.8750	0.6563	0.5364	0.0813
105	0.9063	0.5313	1.0378	0.1441	130	0.8750	0.6250	0.6349	0.0939
106	0.9063	0.5000	1.1712	0.1579	131	0.8750	0.5938	0.7407	0.1068
107	0.9063	0.4688	1.3161	0.1719	132	0.8750	0.5625	0.8547	0.1200
108	0.9063	0.4375	1.4742	0.1862	133	0.8750	0.5313	0.9778	0.1334
109	0.9063	0.4063	1.6474	0.2008	134	0.8750	0.5000	1.1111	0.1472
110	0.9063	0.3750	1.8378	0.2157	135	0.8750	0.4688	1.2560	0.1612
111	0.9063	0.3438	2.0484	0.2308	136	0.8750	0.4375	1.4141	0.1755
112	0.9063	0.3125	2.2823	0.2462	137	0.8750	0.4063	1.5873	0.1901
113	0.9063	0.2813	2.5437	0.2617	138	0.8750	0.3750	1.7778	0.2050
114	0.9063	0.2500	2.8378	0.2773	139	0.8750	0.3438	1.9883	0.2201
115	0.9063	0.2188	3.1712	0.2929	140	0.8750	0.3125	2.2222	0.2355
116	0.9063	0.1875	3.5521	0.3083	141	0.8750	0.2813	2.4837	0.2510
117	0.9063	0.1563	3.9917	0.3234	142	0.8750	0.2500	2.7778	0.2666
118	0.9063	0.1250	4.5045	0.3378	143	0.8750	0.2188	3.1111	0.2822
119	0.9063	0.0938	5.1106	0.3510	144	0.8750	0.1875	3.4921	0.2976
120	0.9063	0.0625	5.8378	0.3623	145	0.8750	0.1563	3.9316	0.3127
121	0.9063	0.0313	6.7267	0.3705	146	0.8750	0.1250	4.4444	0.3271
122	0.9063	0.0000	7.8378	0.3738	147	0.8750	0.0938	5.0505	0.3403
123	0.8750	0.8438	0.0635	0.0109	148	0.8750	0.0625	5.7778	0.3516
124	0.8750	0.8125	0.1307	0.0220	149	0.8750	0.0313	6.6667	0.3598
125	0.8750	0.7813	0.2020	0.0334	150	0.8750	0.0000	7.7778	0.3631

Table 1.26: PFR Reactors 4

i	$x(i)$	$y(i)$	$\tau(i)$	$\Delta C_c(i)$	i	$x(i)$	$y(i)$	$\tau(i)$	$\Delta C_c(i)$
151	0.8438	0.8125	0.0672	0.0111	176	0.8438	0.0313	6.6032	0.3489
152	0.8438	0.7813	0.1385	0.0225	177	0.8438	0.0000	7.7143	0.3522
153	0.8438	0.7500	0.2143	0.0341	178	0.8125	0.7813	0.0713	0.0114
154	0.8438	0.7188	0.2949	0.0459	179	0.8125	0.7500	0.1471	0.0230
155	0.8438	0.6875	0.3810	0.0580	180	0.8125	0.7188	0.2277	0.0348
156	0.8438	0.6563	0.4729	0.0704	181	0.8125	0.6875	0.3137	0.0469
157	0.8438	0.6250	0.5714	0.0830	182	0.8125	0.6563	0.4057	0.0592
158	0.8438	0.5938	0.6772	0.0959	183	0.8125	0.6250	0.5042	0.0719
159	0.8438	0.5625	0.7912	0.1091	184	0.8125	0.5938	0.6100	0.0848
160	0.8438	0.5313	0.9143	0.1225	185	0.8125	0.5625	0.7240	0.0979
161	0.8438	0.5000	1.0476	0.1363	186	0.8125	0.5313	0.8471	0.1114
162	0.8438	0.4688	1.1925	0.1503	187	0.8125	0.5000	0.9804	0.1251
163	0.8438	0.4375	1.3506	0.1646	188	0.8125	0.4688	1.1253	0.1392
164	0.8438	0.4063	1.5238	0.1792	189	0.8125	0.4375	1.2834	0.1535
165	0.8438	0.3750	1.7143	0.1941	190	0.8125	0.4063	1.4566	0.1681
166	0.8438	0.3438	1.9248	0.2092	191	0.8125	0.3750	1.6471	0.1830
167	0.8438	0.3125	2.1587	0.2246	192	0.8125	0.3438	1.8576	0.1981
168	0.8438	0.2813	2.4202	0.2401	193	0.8125	0.3125	2.0915	0.2134
169	0.8438	0.2500	2.7143	0.2557	194	0.8125	0.2813	2.3529	0.2289
170	0.8438	0.2188	3.0476	0.2713	195	0.8125	0.2500	2.6471	0.2445
171	0.8438	0.1875	3.4286	0.2867	196	0.8125	0.2188	2.9804	0.2601
172	0.8438	0.1563	3.8681	0.3018	197	0.8125	0.1875	3.3613	0.2756
173	0.8438	0.1250	4.3810	0.3162	198	0.8125	0.1563	3.8009	0.2907
174	0.8438	0.0938	4.9870	0.3294	199	0.8125	0.1250	4.3137	0.3050
175	0.8438	0.0625	5.7143	0.3407	200	0.8125	0.0938	4.9198	0.3182

Table 1.27: PFR Reactors 5

i	$x(i)$	$y(i)$	$\tau(i)$	$\Delta C_c(i)$	i	$x(i)$	$y(i)$	$\tau(i)$	$\Delta C_c(i)$
201	0.8125	0.0625	5.6471	0.3295	226	0.7813	0.0625	5.5758	0.3182
202	0.8125	0.0313	6.5359	0.3378	227	0.7813	0.0313	6.4646	0.3264
203	0.8125	0.0000	7.6471	0.3411	228	0.7813	0.0000	7.5758	0.3297
204	0.7813	0.7500	0.0758	0.0116	229	0.7500	0.7188	0.0806	0.0118
205	0.7813	0.7188	0.1564	0.0234	230	0.7500	0.6875	0.1667	0.0239
206	0.7813	0.6875	0.2424	0.0355	231	0.7500	0.6563	0.2586	0.0363
207	0.7813	0.6563	0.3344	0.0479	232	0.7500	0.6250	0.3571	0.0489
208	0.7813	0.6250	0.4329	0.0605	233	0.7500	0.5938	0.4630	0.0618
209	0.7813	0.5938	0.5387	0.0734	234	0.7500	0.5625	0.5769	0.0750
210	0.7813	0.5625	0.6527	0.0866	235	0.7500	0.5313	0.7000	0.0884
211	0.7813	0.5313	0.7758	0.1000	236	0.7500	0.5000	0.8333	0.1022
212	0.7813	0.5000	0.9091	0.1138	237	0.7500	0.4688	0.9783	0.1162
213	0.7813	0.4688	1.0540	0.1278	238	0.7500	0.4375	1.1364	0.1305
214	0.7813	0.4375	1.2121	0.1421	239	0.7500	0.4063	1.3095	0.1451
215	0.7813	0.4063	1.3853	0.1567	240	0.7500	0.3750	1.5000	0.1600
216	0.7813	0.3750	1.5758	0.1716	241	0.7500	0.3438	1.7105	0.1751
217	0.7813	0.3438	1.7863	0.1867	242	0.7500	0.3125	1.9444	0.1905
218	0.7813	0.3125	2.0202	0.2021	243	0.7500	0.2813	2.2059	0.2060
219	0.7813	0.2813	2.2816	0.2176	244	0.7500	0.2500	2.5000	0.2216
220	0.7813	0.2500	2.5758	0.2332	245	0.7500	0.2188	2.8333	0.2372
221	0.7813	0.2188	2.9091	0.2488	246	0.7500	0.1875	3.2143	0.2526
222	0.7813	0.1875	3.2900	0.2642	247	0.7500	0.1563	3.6538	0.2677
223	0.7813	0.1563	3.7296	0.2793	248	0.7500	0.1250	4.1667	0.2821
224	0.7813	0.1250	4.2424	0.2937	249	0.7500	0.0938	4.7727	0.2953
225	0.7813	0.0938	4.8485	0.3069	250	0.7500	0.0625	5.5000	0.3066

Table 1.28: PFR Reactors 6

i	$x(i)$	$y(i)$	$\tau(i)$	$\Delta C_c(i)$	i	$x(i)$	$y(i)$	$\tau(i)$	$\Delta C_c(i)$
251	0.7500	0.0313	6.3889	0.3148	276	0.6875	0.6563	0.0920	0.0124
252	0.7500	0.0000	7.5000	0.3181	277	0.6875	0.6250	0.1905	0.0250
253	0.7188	0.6875	0.0860	0.0121	278	0.6875	0.5938	0.2963	0.0379
254	0.7188	0.6563	0.1780	0.0244	279	0.6875	0.5625	0.4103	0.0510
255	0.7188	0.6250	0.2765	0.0371	280	0.6875	0.5313	0.5333	0.0645
256	0.7188	0.5938	0.3823	0.0500	281	0.6875	0.5000	0.6667	0.0782
257	0.7188	0.5625	0.4963	0.0631	282	0.6875	0.4688	0.8116	0.0923
258	0.7188	0.5313	0.6194	0.0766	283	0.6875	0.4375	0.9697	0.1066
259	0.7188	0.5000	0.7527	0.0903	284	0.6875	0.4063	1.1429	0.1212
260	0.7188	0.4688	0.8976	0.1044	285	0.6875	0.3750	1.3333	0.1361
261	0.7188	0.4375	1.0557	0.1187	286	0.6875	0.3438	1.5439	0.1512
262	0.7188	0.4063	1.2289	0.1333	287	0.6875	0.3125	1.7778	0.1665
263	0.7188	0.3750	1.4194	0.1482	288	0.6875	0.2813	2.0392	0.1820
264	0.7188	0.3438	1.6299	0.1633	289	0.6875	0.2500	2.3333	0.1976
265	0.7188	0.3125	1.8638	0.1786	290	0.6875	0.2188	2.6667	0.2132
266	0.7188	0.2813	2.1252	0.1941	291	0.6875	0.1875	3.0476	0.2287
267	0.7188	0.2500	2.4194	0.2097	292	0.6875	0.1563	3.4872	0.2438
268	0.7188	0.2188	2.7527	0.2253	293	0.6875	0.1250	4.0000	0.2581
269	0.7188	0.1875	3.1336	0.2408	294	0.6875	0.0938	4.6061	0.2713
270	0.7188	0.1563	3.5732	0.2559	295	0.6875	0.0625	5.3333	0.2826
271	0.7188	0.1250	4.0860	0.2702	296	0.6875	0.0313	6.2222	0.2909
272	0.7188	0.0938	4.6921	0.2834	297	0.6875	0.0000	7.3333	0.2942
273	0.7188	0.0625	5.4194	0.2947	298	0.6563	0.6250	0.0985	0.0126
274	0.7188	0.0313	6.3082	0.3030	299	0.6563	0.5938	0.2043	0.0255
275	0.7188	0.0000	7.4194	0.3063	300	0.6563	0.5625	0.3183	0.0387

Table 1.29: PFR Reactors 7

i	$x(i)$	$y(i)$	$\tau(i)$	$\Delta C_c(i)$	i	$x(i)$	$y(i)$	$\tau(i)$	$\Delta C_c(i)$
301	0.6563	0.5313	0.4414	0.0521	326	0.6250	0.3750	1.1429	0.1111
302	0.6563	0.5000	0.5747	0.0659	327	0.6250	0.3438	1.3534	0.1262
303	0.6563	0.4688	0.7196	0.0799	328	0.6250	0.3125	1.5873	0.1416
304	0.6563	0.4375	0.8777	0.0942	329	0.6250	0.2813	1.8487	0.1571
305	0.6563	0.4063	1.0509	0.1088	330	0.6250	0.2500	2.1429	0.1727
306	0.6563	0.3750	1.2414	0.1237	331	0.6250	0.2188	2.4762	0.1883
307	0.6563	0.3438	1.4519	0.1388	332	0.6250	0.1875	2.8571	0.2037
308	0.6563	0.3125	1.6858	0.1542	333	0.6250	0.1563	3.2967	0.2188
309	0.6563	0.2813	1.9473	0.1697	334	0.6250	0.1250	3.8095	0.2332
310	0.6563	0.2500	2.2414	0.1853	335	0.6250	0.0938	4.4156	0.2464
311	0.6563	0.2188	2.5747	0.2009	336	0.6250	0.0625	5.1429	0.2577
312	0.6563	0.1875	2.9557	0.2163	337	0.6250	0.0313	6.0317	0.2659
313	0.6563	0.1563	3.3952	0.2314	338	0.6250	0.0000	7.1429	0.2692
314	0.6563	0.1250	3.9080	0.2458	339	0.5938	0.5625	0.1140	0.0132
315	0.6563	0.0938	4.5141	0.2590	340	0.5938	0.5313	0.2370	0.0266
316	0.6563	0.0625	5.2414	0.2703	341	0.5938	0.5000	0.3704	0.0404
317	0.6563	0.0313	6.1303	0.2785	342	0.5938	0.4688	0.5153	0.0544
318	0.6563	0.0000	7.2414	0.2819	343	0.5938	0.4375	0.6734	0.0687
319	0.6250	0.5938	0.1058	0.0129	344	0.5938	0.4063	0.8466	0.0833
320	0.6250	0.5625	0.2198	0.0261	345	0.5938	0.3750	1.0370	0.0982
321	0.6250	0.5313	0.3429	0.0395	346	0.5938	0.3438	1.2476	0.1133
322	0.6250	0.5000	0.4762	0.0533	347	0.5938	0.3125	1.4815	0.1287
323	0.6250	0.4688	0.6211	0.0673	348	0.5938	0.2813	1.7429	0.1442
324	0.6250	0.4375	0.7792	0.0816	349	0.5938	0.2500	2.0370	0.1598
325	0.6250	0.4063	0.9524	0.0962	350	0.5938	0.2188	2.3704	0.1754

Table 1.30: PFR Reactors 8

i	$x(i)$	$y(i)$	$\tau(i)$	$\Delta C_c(i)$	i	$x(i)$	$y(i)$	$\tau(i)$	$\Delta C_c(i)$
351	0.5938	0.1875	2.7513	0.1908	376	0.5313	0.5000	0.1333	0.0137
352	0.5938	0.1563	3.1909	0.2059	377	0.5313	0.4688	0.2783	0.0278
353	0.5938	0.1250	3.7037	0.2203	378	0.5313	0.4375	0.4364	0.0421
354	0.5938	0.0938	4.3098	0.2335	379	0.5313	0.4063	0.6095	0.0567
355	0.5938	0.0625	5.0370	0.2448	380	0.5313	0.3750	0.8000	0.0716
356	0.5938	0.0313	5.9259	0.2530	381	0.5313	0.3438	1.0105	0.0867
357	0.5938	0.0000	7.0370	0.2563	382	0.5313	0.3125	1.2444	0.1020
358	0.5625	0.5313	0.1231	0.0135	383	0.5313	0.2813	1.5059	0.1175
359	0.5625	0.5000	0.2564	0.0272	384	0.5313	0.2500	1.8000	0.1331
360	0.5625	0.4688	0.4013	0.0412	385	0.5313	0.2188	2.1333	0.1487
361	0.5625	0.4375	0.5594	0.0556	386	0.5313	0.1875	2.5143	0.1642
362	0.5625	0.4063	0.7326	0.0702	387	0.5313	0.1563	2.9538	0.1793
363	0.5625	0.3750	0.9231	0.0850	388	0.5313	0.1250	3.4667	0.1937
364	0.5625	0.3438	1.1336	0.1001	389	0.5313	0.0938	4.0727	0.2069
365	0.5625	0.3125	1.3675	0.1155	390	0.5313	0.0625	4.8000	0.2181
366	0.5625	0.2813	1.6290	0.1310	391	0.5313	0.0313	5.6889	0.2264
367	0.5625	0.2500	1.9231	0.1466	392	0.5313	0.0000	6.8000	0.2297
368	0.5625	0.2188	2.2564	0.1622	393	0.5000	0.4688	0.1449	0.0140
369	0.5625	0.1875	2.6374	0.1777	394	0.5000	0.4375	0.3030	0.0284
370	0.5625	0.1563	3.0769	0.1927	395	0.5000	0.4063	0.4762	0.0430
371	0.5625	0.1250	3.5897	0.2071	396	0.5000	0.3750	0.6667	0.0578
372	0.5625	0.0938	4.1958	0.2203	397	0.5000	0.3438	0.8772	0.0729
373	0.5625	0.0625	4.9231	0.2316	398	0.5000	0.3125	1.1111	0.0883
374	0.5625	0.0313	5.8120	0.2398	399	0.5000	0.2813	1.3725	0.1038
375	0.5625	0.0000	6.9231	0.2432	400	0.5000	0.2500	1.6667	0.1194

Table 1.31: PFR Reactors 9

i	$x(i)$	$y(i)$	$\tau(i)$	$\Delta C_c(i)$	i	$x(i)$	$y(i)$	$\tau(i)$	$\Delta C_c(i)$
401	0.5000	0.2188	2.0000	0.1350	426	0.4375	0.3438	0.5742	0.0446
402	0.5000	0.1875	2.3810	0.1505	427	0.4375	0.3125	0.8081	0.0599
403	0.5000	0.1563	2.8205	0.1655	428	0.4375	0.2813	1.0695	0.0754
404	0.5000	0.1250	3.3333	0.1799	429	0.4375	0.2500	1.3636	0.0910
405	0.5000	0.0938	3.9394	0.1931	430	0.4375	0.2188	1.6970	0.1066
406	0.5000	0.0625	4.6667	0.2044	431	0.4375	0.1875	2.0779	0.1221
407	0.5000	0.0313	5.5556	0.2126	432	0.4375	0.1563	2.5175	0.1372
408	0.5000	0.0000	6.6667	0.2160	433	0.4375	0.1250	3.0303	0.1516
409	0.4688	0.4375	0.1581	0.0143	434	0.4375	0.0938	3.6364	0.1648
410	0.4688	0.4063	0.3313	0.0289	435	0.4375	0.0625	4.3636	0.1760
411	0.4688	0.3750	0.5217	0.0438	436	0.4375	0.0313	5.2525	0.1843
412	0.4688	0.3438	0.7323	0.0589	437	0.4375	0.0000	6.3636	0.1876
413	0.4688	0.3125	0.9662	0.0743	438	0.4063	0.3750	0.1905	0.0149
414	0.4688	0.2813	1.2276	0.0898	439	0.4063	0.3438	0.4010	0.0300
415	0.4688	0.2500	1.5217	0.1054	440	0.4063	0.3125	0.6349	0.0453
416	0.4688	0.2188	1.8551	0.1210	441	0.4063	0.2813	0.8964	0.0608
417	0.4688	0.1875	2.2360	0.1364	442	0.4063	0.2500	1.1905	0.0764
418	0.4688	0.1563	2.6756	0.1515	443	0.4063	0.2188	1.5238	0.0920
419	0.4688	0.1250	3.1884	0.1659	444	0.4063	0.1875	1.9048	0.1075
420	0.4688	0.0938	3.7945	0.1791	445	0.4063	0.1563	2.3443	0.1226
421	0.4688	0.0625	4.5217	0.1904	446	0.4063	0.1250	2.8571	0.1370
422	0.4688	0.0313	5.4106	0.1986	447	0.4063	0.0938	3.4632	0.1502
423	0.4688	0.0000	6.5217	0.2019	448	0.4063	0.0625	4.1905	0.1614
424	0.4375	0.4063	0.1732	0.0146	449	0.4063	0.0313	5.0794	0.1697
425	0.4375	0.3750	0.3636	0.0295	450	0.4063	0.0000	6.1905	0.1730

Table 1.32: PFR Reactors 10

i	$x(i)$	$y(i)$	$\tau(i)$	$\Delta C_c(i)$	i	$x(i)$	$y(i)$	$\tau(i)$	$\Delta C_c(i)$
451	0.3750	0.3438	0.2105	0.0151	476	0.3125	0.2188	0.8889	0.0467
452	0.3750	0.3125	0.4444	0.0305	477	0.3125	0.1875	1.2698	0.0622
453	0.3750	0.2813	0.7059	0.0460	478	0.3125	0.1563	1.7094	0.0772
454	0.3750	0.2500	1.0000	0.0616	479	0.3125	0.1250	2.2222	0.0916
455	0.3750	0.2188	1.3333	0.0772	480	0.3125	0.0938	2.8283	0.1048
456	0.3750	0.1875	1.7143	0.0926	481	0.3125	0.0625	3.5556	0.1161
457	0.3750	0.1563	2.1538	0.1077	482	0.3125	0.0313	4.4444	0.1244
458	0.3750	0.1250	2.6667	0.1221	483	0.3125	0.0000	5.5556	0.1277
459	0.3750	0.0938	3.2727	0.1353	484	0.2813	0.2500	0.2941	0.0156
460	0.3750	0.0625	4.0000	0.1466	485	0.2813	0.2188	0.6275	0.0312
461	0.3750	0.0313	4.8889	0.1548	486	0.2813	0.1875	1.0084	0.0467
462	0.3750	0.0000	6.0000	0.1581	487	0.2813	0.1563	1.4480	0.0617
463	0.3438	0.3125	0.2339	0.0153	488	0.2813	0.1250	1.9608	0.0761
464	0.3438	0.2813	0.4954	0.0308	489	0.2813	0.0938	2.5668	0.0893
465	0.3438	0.2500	0.7895	0.0465	490	0.2813	0.0625	3.2941	0.1006
466	0.3438	0.2188	1.1228	0.0621	491	0.2813	0.0313	4.1830	0.1088
467	0.3438	0.1875	1.5038	0.0775	492	0.2813	0.0000	5.2941	0.1122
468	0.3438	0.1563	1.9433	0.0926	493	0.2500	0.2188	0.3333	0.0156
469	0.3438	0.1250	2.4561	0.1070	494	0.2500	0.1875	0.7143	0.0311
470	0.3438	0.0938	3.0622	0.1202	495	0.2500	0.1563	1.1538	0.0461
471	0.3438	0.0625	3.7895	0.1315	496	0.2500	0.1250	1.6667	0.0605
472	0.3438	0.0313	4.6784	0.1397	497	0.2500	0.0938	2.2727	0.0737
473	0.3438	0.0000	5.7895	0.1430	498	0.2500	0.0625	3.0000	0.0850
474	0.3125	0.2813	0.2614	0.0155	499	0.2500	0.0313	3.8889	0.0932
475	0.3125	0.2500	0.5556	0.0311	500	0.2500	0.0000	5.0000	0.0966

Table 1.33: PFR Reactors 11

i	$x(i)$	$y(i)$	$\tau(i)$	$\Delta C_c(i)$	i	$x(i)$	$y(i)$	$\tau(i)$	$\Delta C_c(i)$
501	0.2188	0.1875	0.3810	0.0154	515	0.1563	0.0938	1.1189	0.0276
502	0.2188	0.1563	0.8205	0.0305	516	0.1563	0.0625	1.8462	0.0389
503	0.2188	0.1250	1.3333	0.0449	517	0.1563	0.0313	2.7350	0.0471
504	0.2188	0.0938	1.9394	0.0581	518	0.1563	0.0000	3.8462	0.0504
505	0.2188	0.0625	2.6667	0.0694	519	0.1250	0.0938	0.6061	0.0132
506	0.2188	0.0313	3.5556	0.0776	520	0.1250	0.0625	1.3333	0.0245
507	0.2188	0.0000	4.6667	0.0810	521	0.1250	0.0313	2.2222	0.0327
508	0.1875	0.1563	0.4396	0.0151	522	0.1250	0.0000	3.3333	0.0361
509	0.1875	0.1250	0.9524	0.0295	523	0.0938	0.0625	0.7273	0.0113
510	0.1875	0.0938	1.5584	0.0427	524	0.0938	0.0313	1.6162	0.0195
511	0.1875	0.0625	2.2857	0.0540	525	0.0938	0.0000	2.7273	0.0229
512	0.1875	0.0313	3.1746	0.0622	526	0.0625	0.0313	0.8889	0.0082
513	0.1875	0.0000	4.2857	0.0655	527	0.0625	0.0000	2.0000	0.0116
514	0.1563	0.1250	0.5128	0.0144	528	0.0313	0.0000	1.1111	0.0033

Table 1.34: CSTR Reactors 1

i	$x(i)$	$y(i)$	$\tau(i)$	$\Delta C_c(i)$	i	$x(i)$	$y(i)$	$\tau(i)$	$\Delta C_c(i)$
1	1.0000	0.9688	0.0526	0.0102	26	1.0000	0.1875	10.6122	0.3980
2	1.0000	0.9375	0.1108	0.0208	27	1.0000	0.1563	12.7811	0.3994
3	1.0000	0.9063	0.1753	0.0318	28	1.0000	0.1250	15.5556	0.3889
4	1.0000	0.8750	0.2469	0.0432	29	1.0000	0.0938	19.1736	0.3595
5	1.0000	0.8438	0.3265	0.0551	30	1.0000	0.0625	24.0000	0.3000
6	1.0000	0.8125	0.4152	0.0675	31	1.0000	0.0313	30.6173	0.1914
7	1.0000	0.7813	0.5142	0.0803	32	1.0000	0.0000	40.0000	0.0000
8	1.0000	0.7500	0.6250	0.0938	33	0.9688	0.9375	0.0554	0.0104
9	1.0000	0.7188	0.7492	0.1077	34	0.9688	0.9063	0.1169	0.0212
10	1.0000	0.6875	0.8889	0.1222	35	0.9688	0.8750	0.1852	0.0324
11	1.0000	0.6563	1.0464	0.1373	36	0.9688	0.8438	0.2612	0.0441
12	1.0000	0.6250	1.2245	0.1531	37	0.9688	0.8125	0.3460	0.0562
13	1.0000	0.5938	1.4266	0.1694	38	0.9688	0.7813	0.4408	0.0689
14	1.0000	0.5625	1.6568	0.1864	39	0.9688	0.7500	0.5469	0.0820
15	1.0000	0.5313	1.9200	0.2040	40	0.9688	0.7188	0.6660	0.0957
16	1.0000	0.5000	2.2222	0.2222	41	0.9688	0.6875	0.8000	0.1100
17	1.0000	0.4688	2.5709	0.2410	42	0.9688	0.6563	0.9512	0.1249
18	1.0000	0.4375	2.9752	0.2603	43	0.9688	0.6250	1.1224	0.1403
19	1.0000	0.4063	3.4467	0.2800	44	0.9688	0.5938	1.3169	0.1564
20	1.0000	0.3750	4.0000	0.3000	45	0.9688	0.5625	1.5385	0.1731
21	1.0000	0.3438	4.6537	0.3199	46	0.9688	0.5313	1.7920	0.1904
22	1.0000	0.3125	5.4321	0.3395	47	0.9688	0.5000	2.0833	0.2083
23	1.0000	0.2813	6.3668	0.3581	48	0.9688	0.4688	2.4197	0.2268
24	1.0000	0.2500	7.5000	0.3750	49	0.9688	0.4375	2.8099	0.2459
25	1.0000	0.2188	8.8889	0.3889	50	0.9688	0.4063	3.2653	0.2653

Table 1.35: CSTR Reactors 2

i	$x(i)$	$y(i)$	$\tau(i)$	$\Delta C_c(i)$	i	$x(i)$	$y(i)$	$\tau(i)$	$\Delta C_c(i)$
51	0.9688	0.3750	3.8000	0.2850	76	0.9375	0.5313	1.6640	0.1768
52	0.9688	0.3438	4.4321	0.3047	77	0.9375	0.5000	1.9444	0.1944
53	0.9688	0.3125	5.1852	0.3241	78	0.9375	0.4688	2.2684	0.2127
54	0.9688	0.2813	6.0900	0.3426	79	0.9375	0.4375	2.6446	0.2314
55	0.9688	0.2500	7.1875	0.3594	80	0.9375	0.4063	3.0839	0.2506
56	0.9688	0.2188	8.5333	0.3733	81	0.9375	0.3750	3.6000	0.2700
57	0.9688	0.1875	10.2041	0.3827	82	0.9375	0.3438	4.2105	0.2895
58	0.9688	0.1563	12.3077	0.3846	83	0.9375	0.3125	4.9383	0.3086
59	0.9688	0.1250	15.0000	0.3750	84	0.9375	0.2813	5.8131	0.3270
60	0.9688	0.0938	18.5124	0.3471	85	0.9375	0.2500	6.8750	0.3438
61	0.9688	0.0625	23.2000	0.2900	86	0.9375	0.2188	8.1778	0.3578
62	0.9688	0.0313	29.6296	0.1852	87	0.9375	0.1875	9.7959	0.3673
63	0.9688	0.0000	38.7500	0.0000	88	0.9375	0.1563	11.8343	0.3698
64	0.9375	0.9063	0.0584	0.0106	89	0.9375	0.1250	14.4444	0.3611
65	0.9375	0.8750	0.1235	0.0216	90	0.9375	0.0938	17.8512	0.3347
66	0.9375	0.8438	0.1959	0.0331	91	0.9375	0.0625	22.4000	0.2800
67	0.9375	0.8125	0.2768	0.0450	92	0.9375	0.0313	28.6420	0.1790
68	0.9375	0.7813	0.3673	0.0574	93	0.9375	0.0000	37.5000	0.0000
69	0.9375	0.7500	0.4688	0.0703	94	0.9063	0.8750	0.0617	0.0108
70	0.9375	0.7188	0.5827	0.0838	95	0.9063	0.8438	0.1306	0.0220
71	0.9375	0.6875	0.7111	0.0978	96	0.9063	0.8125	0.2076	0.0337
72	0.9375	0.6563	0.8561	0.1124	97	0.9063	0.7813	0.2938	0.0459
73	0.9375	0.6250	1.0204	0.1276	98	0.9063	0.7500	0.3906	0.0586
74	0.9375	0.5938	1.2071	0.1433	99	0.9063	0.7188	0.4995	0.0718
75	0.9375	0.5625	1.4201	0.1598	100	0.9063	0.6875	0.6222	0.0856

Table 1.36: CSTR Reactors 3

i	$x(i)$	$y(i)$	$\tau(i)$	$\Delta C_c(i)$	i	$x(i)$	$y(i)$	$\tau(i)$	$\Delta C_c(i)$
101	0.9063	0.6563	0.7610	0.0999	126	0.8750	0.7500	0.3125	0.0469
102	0.9063	0.6250	0.9184	0.1148	127	0.8750	0.7188	0.4162	0.0598
103	0.9063	0.5938	1.0974	0.1303	128	0.8750	0.6875	0.5333	0.0733
104	0.9063	0.5625	1.3018	0.1464	129	0.8750	0.6563	0.6659	0.0874
105	0.9063	0.5313	1.5360	0.1632	130	0.8750	0.6250	0.8163	0.1020
106	0.9063	0.5000	1.8056	0.1806	131	0.8750	0.5938	0.9877	0.1173
107	0.9063	0.4688	2.1172	0.1985	132	0.8750	0.5625	1.1834	0.1331
108	0.9063	0.4375	2.4793	0.2169	133	0.8750	0.5313	1.4080	0.1496
109	0.9063	0.4063	2.9025	0.2358	134	0.8750	0.5000	1.6667	0.1667
110	0.9063	0.3750	3.4000	0.2550	135	0.8750	0.4688	1.9660	0.1843
111	0.9063	0.3438	3.9889	0.2742	136	0.8750	0.4375	2.3140	0.2025
112	0.9063	0.3125	4.6914	0.2932	137	0.8750	0.4063	2.7211	0.2211
113	0.9063	0.2813	5.5363	0.3114	138	0.8750	0.3750	3.2000	0.2400
114	0.9063	0.2500	6.5625	0.3281	139	0.8750	0.3438	3.7673	0.2590
115	0.9063	0.2188	7.8222	0.3422	140	0.8750	0.3125	4.4444	0.2778
116	0.9063	0.1875	9.3878	0.3520	141	0.8750	0.2813	5.2595	0.2958
117	0.9063	0.1563	11.3609	0.3550	142	0.8750	0.2500	6.2500	0.3125
118	0.9063	0.1250	13.8889	0.3472	143	0.8750	0.2188	7.4667	0.3267
119	0.9063	0.0938	17.1901	0.3223	144	0.8750	0.1875	8.9796	0.3367
120	0.9063	0.0625	21.6000	0.2700	145	0.8750	0.1563	10.8876	0.3402
121	0.9063	0.0313	27.6543	0.1728	146	0.8750	0.1250	13.3333	0.3333
122	0.9063	0.0000	36.2500	0.0000	147	0.8750	0.0938	16.5289	0.3099
123	0.8750	0.8438	0.0653	0.0110	148	0.8750	0.0625	20.8000	0.2600
124	0.8750	0.8125	0.1384	0.0225	149	0.8750	0.0313	26.6667	0.1667
125	0.8750	0.7813	0.2204	0.0344	150	0.8750	0.0000	35.0000	0.0000

Table 1.37: CSTR Reactors 4

i	$x(i)$	$y(i)$	$\tau(i)$	$\Delta C_c(i)$	i	$x(i)$	$y(i)$	$\tau(i)$	$\Delta C_c(i)$
151	0.8438	0.8125	0.0692	0.0112	176	0.8438	0.0313	25.6790	0.1605
152	0.8438	0.7813	0.1469	0.0230	177	0.8438	0.0000	33.7500	0.0000
153	0.8438	0.7500	0.2344	0.0352	178	0.8125	0.7813	0.0735	0.0115
154	0.8438	0.7188	0.3330	0.0479	179	0.8125	0.7500	0.1563	0.0234
155	0.8438	0.6875	0.4444	0.0611	180	0.8125	0.7188	0.2497	0.0359
156	0.8438	0.6563	0.5707	0.0749	181	0.8125	0.6875	0.3556	0.0489
157	0.8438	0.6250	0.7143	0.0893	182	0.8125	0.6563	0.4756	0.0624
158	0.8438	0.5938	0.8779	0.1043	183	0.8125	0.6250	0.6122	0.0765
159	0.8438	0.5625	1.0651	0.1198	184	0.8125	0.5938	0.7682	0.0912
160	0.8438	0.5313	1.2800	0.1360	185	0.8125	0.5625	0.9467	0.1065
161	0.8438	0.5000	1.5278	0.1528	186	0.8125	0.5313	1.1520	0.1224
162	0.8438	0.4688	1.8147	0.1701	187	0.8125	0.5000	1.3889	0.1389
163	0.8438	0.4375	2.1488	0.1880	188	0.8125	0.4688	1.6635	0.1560
164	0.8438	0.4063	2.5397	0.2063	189	0.8125	0.4375	1.9835	0.1736
165	0.8438	0.3750	3.0000	0.2250	190	0.8125	0.4063	2.3583	0.1916
166	0.8438	0.3438	3.5457	0.2438	191	0.8125	0.3750	2.8000	0.2100
167	0.8438	0.3125	4.1975	0.2623	192	0.8125	0.3438	3.3241	0.2285
168	0.8438	0.2813	4.9827	0.2803	193	0.8125	0.3125	3.9506	0.2469
169	0.8438	0.2500	5.9375	0.2969	194	0.8125	0.2813	4.7059	0.2647
170	0.8438	0.2188	7.1111	0.3111	195	0.8125	0.2500	5.6250	0.2813
171	0.8438	0.1875	8.5714	0.3214	196	0.8125	0.2188	6.7556	0.2956
172	0.8438	0.1563	10.4142	0.3254	197	0.8125	0.1875	8.1633	0.3061
173	0.8438	0.1250	12.7778	0.3194	198	0.8125	0.1563	9.9408	0.3107
174	0.8438	0.0938	15.8678	0.2975	199	0.8125	0.1250	12.2222	0.3056
175	0.8438	0.0625	20.0000	0.2500	200	0.8125	0.0938	15.2066	0.2851

Table 1.38: CSTR Reactors 5

i	$x(i)$	$y(i)$	$\tau(i)$	$\Delta C_c(i)$	i	$x(i)$	$y(i)$	$\tau(i)$	$\Delta C_c(i)$
201	0.8125	0.0625	19.2000	0.2400	226	0.7813	0.0625	18.4000	0.2300
202	0.8125	0.0313	24.6914	0.1543	227	0.7813	0.0313	23.7037	0.1481
203	0.8125	0.0000	32.5000	0.0000	228	0.7813	0.0000	31.2500	0.0000
204	0.7813	0.7500	0.0781	0.0117	229	0.7500	0.7188	0.0832	0.0120
205	0.7813	0.7188	0.1665	0.0239	230	0.7500	0.6875	0.1778	0.0244
206	0.7813	0.6875	0.2667	0.0367	231	0.7500	0.6563	0.2854	0.0375
207	0.7813	0.6563	0.3805	0.0499	232	0.7500	0.6250	0.4082	0.0510
208	0.7813	0.6250	0.5102	0.0638	233	0.7500	0.5938	0.5487	0.0652
209	0.7813	0.5938	0.6584	0.0782	234	0.7500	0.5625	0.7101	0.0799
210	0.7813	0.5625	0.8284	0.0932	235	0.7500	0.5313	0.8960	0.0952
211	0.7813	0.5313	1.0240	0.1088	236	0.7500	0.5000	1.1111	0.1111
212	0.7813	0.5000	1.2500	0.1250	237	0.7500	0.4688	1.3611	0.1276
213	0.7813	0.4688	1.5123	0.1418	238	0.7500	0.4375	1.6529	0.1446
214	0.7813	0.4375	1.8182	0.1591	239	0.7500	0.4063	1.9955	0.1621
215	0.7813	0.4063	2.1769	0.1769	240	0.7500	0.3750	2.4000	0.1800
216	0.7813	0.3750	2.6000	0.1950	241	0.7500	0.3438	2.8809	0.1981
217	0.7813	0.3438	3.1025	0.2133	242	0.7500	0.3125	3.4568	0.2160
218	0.7813	0.3125	3.7037	0.2315	243	0.7500	0.2813	4.1522	0.2336
219	0.7813	0.2813	4.4291	0.2491	244	0.7500	0.2500	5.0000	0.2500
220	0.7813	0.2500	5.3125	0.2656	245	0.7500	0.2188	6.0444	0.2644
221	0.7813	0.2188	6.4000	0.2800	246	0.7500	0.1875	7.3469	0.2755
222	0.7813	0.1875	7.7551	0.2908	247	0.7500	0.1563	8.9941	0.2811
223	0.7813	0.1563	9.4675	0.2959	248	0.7500	0.1250	11.1111	0.2778
224	0.7813	0.1250	11.6667	0.2917	249	0.7500	0.0938	13.8843	0.2603
225	0.7813	0.0938	14.5455	0.2727	250	0.7500	0.0625	17.6000	0.2200

Table 1.39: CSTR Reactors 6

i	$x(i)$	$y(i)$	$\tau(i)$	$\Delta C_c(i)$	i	$x(i)$	$y(i)$	$\tau(i)$	$\Delta C_c(i)$
251	0.7500	0.0313	22.7160	0.1420	276	0.6875	0.6563	0.0951	0.0125
252	0.7500	0.0000	30.0000	0.0000	277	0.6875	0.6250	0.2041	0.0255
253	0.7188	0.6875	0.0889	0.0122	278	0.6875	0.5938	0.3292	0.0391
254	0.7188	0.6563	0.1902	0.0250	279	0.6875	0.5625	0.4734	0.0533
255	0.7188	0.6250	0.3061	0.0383	280	0.6875	0.5313	0.6400	0.0680
256	0.7188	0.5938	0.4390	0.0521	281	0.6875	0.5000	0.8333	0.0833
257	0.7188	0.5625	0.5917	0.0666	282	0.6875	0.4688	1.0586	0.0992
258	0.7188	0.5313	0.7680	0.0816	283	0.6875	0.4375	1.3223	0.1157
259	0.7188	0.5000	0.9722	0.0972	284	0.6875	0.4063	1.6327	0.1327
260	0.7188	0.4688	1.2098	0.1134	285	0.6875	0.3750	2.0000	0.1500
261	0.7188	0.4375	1.4876	0.1302	286	0.6875	0.3438	2.4377	0.1676
262	0.7188	0.4063	1.8141	0.1474	287	0.6875	0.3125	2.9630	0.1852
263	0.7188	0.3750	2.2000	0.1650	288	0.6875	0.2813	3.5986	0.2024
264	0.7188	0.3438	2.6593	0.1828	289	0.6875	0.2500	4.3750	0.2188
265	0.7188	0.3125	3.2099	0.2006	290	0.6875	0.2188	5.3333	0.2333
266	0.7188	0.2813	3.8754	0.2180	291	0.6875	0.1875	6.5306	0.2449
267	0.7188	0.2500	4.6875	0.2344	292	0.6875	0.1563	8.0473	0.2515
268	0.7188	0.2188	5.6889	0.2489	293	0.6875	0.1250	10.0000	0.2500
269	0.7188	0.1875	6.9388	0.2602	294	0.6875	0.0938	12.5620	0.2355
270	0.7188	0.1563	8.5207	0.2663	295	0.6875	0.0625	16.0000	0.2000
271	0.7188	0.1250	10.5556	0.2639	296	0.6875	0.0313	20.7407	0.1296
272	0.7188	0.0938	13.2231	0.2479	297	0.6875	0.0000	27.5000	0.0000
273	0.7188	0.0625	16.8000	0.2100	298	0.6563	0.6250	0.1020	0.0128
274	0.7188	0.0313	21.7284	0.1358	299	0.6563	0.5938	0.2195	0.0261
275	0.7188	0.0000	28.7500	0.0000	300	0.6563	0.5625	0.3550	0.0399

Table 1.40: CSTR Reactors 7

i	$x(i)$	$y(i)$	$\tau(i)$	$\Delta C_c(i)$	i	$x(i)$	$y(i)$	$\tau(i)$	$\Delta C_c(i)$
301	0.6563	0.5313	0.5120	0.0544	326	0.6250	0.3750	1.6000	0.1200
302	0.6563	0.5000	0.6944	0.0694	327	0.6250	0.3438	1.9945	0.1371
303	0.6563	0.4688	0.9074	0.0851	328	0.6250	0.3125	2.4691	0.1543
304	0.6563	0.4375	1.1570	0.1012	329	0.6250	0.2813	3.0450	0.1713
305	0.6563	0.4063	1.4512	0.1179	330	0.6250	0.2500	3.7500	0.1875
306	0.6563	0.3750	1.8000	0.1350	331	0.6250	0.2188	4.6222	0.2022
307	0.6563	0.3438	2.2161	0.1524	332	0.6250	0.1875	5.7143	0.2143
308	0.6563	0.3125	2.7160	0.1698	333	0.6250	0.1563	7.1006	0.2219
309	0.6563	0.2813	3.3218	0.1869	334	0.6250	0.1250	8.8889	0.2222
310	0.6563	0.2500	4.0625	0.2031	335	0.6250	0.0938	11.2397	0.2107
311	0.6563	0.2188	4.9778	0.2178	336	0.6250	0.0625	14.4000	0.1800
312	0.6563	0.1875	6.1224	0.2296	337	0.6250	0.0313	18.7654	0.1173
313	0.6563	0.1563	7.5740	0.2367	338	0.6250	0.0000	25.0000	0.0000
314	0.6563	0.1250	9.4444	0.2361	339	0.5938	0.5625	0.1183	0.0133
315	0.6563	0.0938	11.9008	0.2231	340	0.5938	0.5313	0.2560	0.0272
316	0.6563	0.0625	15.2000	0.1900	341	0.5938	0.5000	0.4167	0.0417
317	0.6563	0.0313	19.7531	0.1235	342	0.5938	0.4688	0.6049	0.0567
318	0.6563	0.0000	26.2500	0.0000	343	0.5938	0.4375	0.8264	0.0723
319	0.6250	0.5938	0.1097	0.0130	344	0.5938	0.4063	1.0884	0.0884
320	0.6250	0.5625	0.2367	0.0266	345	0.5938	0.3750	1.4000	0.1050
321	0.6250	0.5313	0.3840	0.0408	346	0.5938	0.3438	1.7729	0.1219
322	0.6250	0.5000	0.5556	0.0556	347	0.5938	0.3125	2.2222	0.1389
323	0.6250	0.4688	0.7561	0.0709	348	0.5938	0.2813	2.7682	0.1557
324	0.6250	0.4375	0.9917	0.0868	349	0.5938	0.2500	3.4375	0.1719
325	0.6250	0.4063	1.2698	0.1032	350	0.5938	0.2188	4.2667	0.1867

Table 1.41: CSTR Reactors 8

i	$x(i)$	$y(i)$	$\tau(i)$	$\Delta C_c(i)$	i	$x(i)$	$y(i)$	$\tau(i)$	$\Delta C_c(i)$
351	0.5938	0.1875	5.3061	0.1990	376	0.5313	0.5000	0.1389	0.0139
352	0.5938	0.1563	6.6272	0.2071	377	0.5313	0.4688	0.3025	0.0284
353	0.5938	0.1250	8.3333	0.2083	378	0.5313	0.4375	0.4959	0.0434
354	0.5938	0.0938	10.5785	0.1983	379	0.5313	0.4063	0.7256	0.0590
355	0.5938	0.0625	13.6000	0.1700	380	0.5313	0.3750	1.0000	0.0750
356	0.5938	0.0313	17.7778	0.1111	381	0.5313	0.3438	1.3296	0.0914
357	0.5938	0.0000	23.7500	0.0000	382	0.5313	0.3125	1.7284	0.1080
358	0.5625	0.5313	0.1280	0.0136	383	0.5313	0.2813	2.2145	0.1246
359	0.5625	0.5000	0.2778	0.0278	384	0.5313	0.2500	2.8125	0.1406
360	0.5625	0.4688	0.4537	0.0425	385	0.5313	0.2188	3.5556	0.1556
361	0.5625	0.4375	0.6612	0.0579	386	0.5313	0.1875	4.4898	0.1684
362	0.5625	0.4063	0.9070	0.0737	387	0.5313	0.1563	5.6805	0.1775
363	0.5625	0.3750	1.2000	0.0900	388	0.5313	0.1250	7.2222	0.1806
364	0.5625	0.3438	1.5512	0.1066	389	0.5313	0.0938	9.2562	0.1736
365	0.5625	0.3125	1.9753	0.1235	390	0.5313	0.0625	12.0000	0.1500
366	0.5625	0.2813	2.4913	0.1401	391	0.5313	0.0313	15.8025	0.0988
367	0.5625	0.2500	3.1250	0.1563	392	0.5313	0.0000	21.2500	0.0000
368	0.5625	0.2188	3.9111	0.1711	393	0.5000	0.4688	0.1512	0.0142
369	0.5625	0.1875	4.8980	0.1837	394	0.5000	0.4375	0.3306	0.0289
370	0.5625	0.1563	6.1538	0.1923	395	0.5000	0.4063	0.5442	0.0442
371	0.5625	0.1250	7.7778	0.1944	396	0.5000	0.3750	0.8000	0.0600
372	0.5625	0.0938	9.9174	0.1860	397	0.5000	0.3438	1.1080	0.0762
373	0.5625	0.0625	12.8000	0.1600	398	0.5000	0.3125	1.4815	0.0926
374	0.5625	0.0313	16.7901	0.1049	399	0.5000	0.2813	1.9377	0.1090
375	0.5625	0.0000	22.5000	0.0000	400	0.5000	0.2500	2.5000	0.1250

Table 1.42: CSTR Reactors 9

i	$x(i)$	$y(i)$	$\tau(i)$	$\Delta C_c(i)$	i	$x(i)$	$y(i)$	$\tau(i)$	$\Delta C_c(i)$
401	0.5000	0.2188	3.2000	0.1400	426	0.4375	0.3438	0.6648	0.0457
402	0.5000	0.1875	4.0816	0.1531	427	0.4375	0.3125	0.9877	0.0617
403	0.5000	0.1563	5.2071	0.1627	428	0.4375	0.2813	1.3841	0.0779
404	0.5000	0.1250	6.6667	0.1667	429	0.4375	0.2500	1.8750	0.0938
405	0.5000	0.0938	8.5950	0.1612	430	0.4375	0.2188	2.4889	0.1089
406	0.5000	0.0625	11.2000	0.1400	431	0.4375	0.1875	3.2653	0.1224
407	0.5000	0.0313	14.8148	0.0926	432	0.4375	0.1563	4.2604	0.1331
408	0.5000	0.0000	20.0000	0.0000	433	0.4375	0.1250	5.5556	0.1389
409	0.4688	0.4375	0.1653	0.0145	434	0.4375	0.0938	7.2727	0.1364
410	0.4688	0.4063	0.3628	0.0295	435	0.4375	0.0625	9.6000	0.1200
411	0.4688	0.3750	0.6000	0.0450	436	0.4375	0.0313	12.8395	0.0802
412	0.4688	0.3438	0.8864	0.0609	437	0.4375	0.0000	17.5000	0.0000
413	0.4688	0.3125	1.2346	0.0772	438	0.4063	0.3750	0.2000	0.0150
414	0.4688	0.2813	1.6609	0.0934	439	0.4063	0.3438	0.4432	0.0305
415	0.4688	0.2500	2.1875	0.1094	440	0.4063	0.3125	0.7407	0.0463
416	0.4688	0.2188	2.8444	0.1244	441	0.4063	0.2813	1.1073	0.0623
417	0.4688	0.1875	3.6735	0.1378	442	0.4063	0.2500	1.5625	0.0781
418	0.4688	0.1563	4.7337	0.1479	443	0.4063	0.2188	2.1333	0.0933
419	0.4688	0.1250	6.1111	0.1528	444	0.4063	0.1875	2.8571	0.1071
420	0.4688	0.0938	7.9339	0.1488	445	0.4063	0.1563	3.7870	0.1183
421	0.4688	0.0625	10.4000	0.1300	446	0.4063	0.1250	5.0000	0.1250
422	0.4688	0.0313	13.8272	0.0864	447	0.4063	0.0938	6.6116	0.1240
423	0.4688	0.0000	18.7500	0.0000	448	0.4063	0.0625	8.8000	0.1100
424	0.4375	0.4063	0.1814	0.0147	449	0.4063	0.0313	11.8519	0.0741
425	0.4375	0.3750	0.4000	0.0300	450	0.4063	0.0000	16.2500	0.0000

Table 1.43: CSTR Reactors 10

i	$x(i)$	$y(i)$	$\tau(i)$	$\Delta C_c(i)$	i	$x(i)$	$y(i)$	$\tau(i)$	$\Delta C_c(i)$
451	0.3750	0.3438	0.2216	0.0152	476	0.3125	0.2188	1.0667	0.0467
452	0.3750	0.3125	0.4938	0.0309	477	0.3125	0.1875	1.6327	0.0612
453	0.3750	0.2813	0.8304	0.0467	478	0.3125	0.1563	2.3669	0.0740
454	0.3750	0.2500	1.2500	0.0625	479	0.3125	0.1250	3.3333	0.0833
455	0.3750	0.2188	1.7778	0.0778	480	0.3125	0.0938	4.6281	0.0868
456	0.3750	0.1875	2.4490	0.0918	481	0.3125	0.0625	6.4000	0.0800
457	0.3750	0.1563	3.3136	0.1036	482	0.3125	0.0313	8.8889	0.0556
458	0.3750	0.1250	4.4444	0.1111	483	0.3125	0.0000	12.5000	0.0000
459	0.3750	0.0938	5.9504	0.1116	484	0.2813	0.2500	0.3125	0.0156
460	0.3750	0.0625	8.0000	0.1000	485	0.2813	0.2188	0.7111	0.0311
461	0.3750	0.0313	10.8642	0.0679	486	0.2813	0.1875	1.2245	0.0459
462	0.3750	0.0000	15.0000	0.0000	487	0.2813	0.1563	1.8935	0.0592
463	0.3438	0.3125	0.2469	0.0154	488	0.2813	0.1250	2.7778	0.0694
464	0.3438	0.2813	0.5536	0.0311	489	0.2813	0.0938	3.9669	0.0744
465	0.3438	0.2500	0.9375	0.0469	490	0.2813	0.0625	5.6000	0.0700
466	0.3438	0.2188	1.4222	0.0622	491	0.2813	0.0313	7.9012	0.0494
467	0.3438	0.1875	2.0408	0.0765	492	0.2813	0.0000	11.2500	0.0000
468	0.3438	0.1563	2.8402	0.0888	493	0.2500	0.2188	0.3556	0.0156
469	0.3438	0.1250	3.8889	0.0972	494	0.2500	0.1875	0.8163	0.0306
470	0.3438	0.0938	5.2893	0.0992	495	0.2500	0.1563	1.4201	0.0444
471	0.3438	0.0625	7.2000	0.0900	496	0.2500	0.1250	2.2222	0.0556
472	0.3438	0.0313	9.8765	0.0617	497	0.2500	0.0938	3.3058	0.0620
473	0.3438	0.0000	13.7500	0.0000	498	0.2500	0.0625	4.8000	0.0600
474	0.3125	0.2813	0.2768	0.0156	499	0.2500	0.0313	6.9136	0.0432
475	0.3125	0.2500	0.6250	0.0313	500	0.2500	0.0000	10.0000	0.0000

Table 1.44: CSTR Reactors 11

i	$x(i)$	$y(i)$	$\tau(i)$	$\Delta C_c(i)$	i	$x(i)$	$y(i)$	$\tau(i)$	$\Delta C_c(i)$
501	0.2188	0.1875	0.4082	0.0153	515	0.1563	0.0938	1.3223	0.0248
502	0.2188	0.1563	0.9467	0.0296	516	0.1563	0.0625	2.4000	0.0300
503	0.2188	0.1250	1.6667	0.0417	517	0.1563	0.0313	3.9506	0.0247
504	0.2188	0.0938	2.6446	0.0496	518	0.1563	0.0000	6.2500	0.0000
505	0.2188	0.0625	4.0000	0.0500	519	0.1250	0.0938	0.6612	0.0124
506	0.2188	0.0313	5.9259	0.0370	520	0.1250	0.0625	1.6000	0.0200
507	0.2188	0.0000	8.7500	0.0000	521	0.1250	0.0313	2.9630	0.0185
508	0.1875	0.1563	0.4734	0.0148	522	0.1250	0.0000	5.0000	0.0000
509	0.1875	0.1250	1.1111	0.0278	523	0.0938	0.0625	0.8000	0.0100
510	0.1875	0.0938	1.9835	0.0372	524	0.0938	0.0313	1.9753	0.0123
511	0.1875	0.0625	3.2000	0.0400	525	0.0938	0.0000	3.7500	0.0000
512	0.1875	0.0313	4.9383	0.0309	526	0.0625	0.0313	0.9877	0.0062
513	0.1875	0.0000	7.5000	0.0000	527	0.0625	0.0000	2.5000	0.0000
514	0.1563	0.1250	0.5556	0.0139	528	0.0313	0.0000	1.2500	0.0000

CHAPTER 2

IDEAS based synthesis of reactor networks featuring minimum number of units using Mixed Integer Linear Programing (MILP)

2.1 Introduction

As seen in the previous chapter solving the reactor network synthesis problem involves selecting the required reactors, determining stream flow rates and designing stream interconnections from a variety of options available. Such selection, is done by using the tools of reactor network optimization to study the impact of process properties (reactor volume and number of reactors) and stream properties (temperature, pressure, entropy, enthalpy and concentration). Reactor networks design provide optimal solutions to many industrially meaningful optimization problems such as operating cost, volume, yield and selectivity. Solving reactor networks optimization problems can lead to two types of optimal solutions: local optimums and global optimums [44]. A *global optimum* is a feasible solution that satisfies the objective function better than all other points in the feasible region. A *local optimum* is a feasible solution that satisfies the objective function better than all other nearby points but there might exist other better solutions within the feasible region. In problems where the objective function and constrains are *convex*, a local optimum is a global optimum [45]. The same statement does not hold for *non convex* problems due to the existence of multiple local optimums, making such problems more difficult to solve. Our ability to obtain global optimality depends on the optimization problem, which can be Linear Programing (LP), Mixed-Integer Linear Programing (MILP), Nonlinear Programing (NLP) or Mixed-Integer

Nonlinear Programing(MINLP). The optimization frameworks where global optimality is possible, examines rigorous trade offs among an objectives and various constraints within a process to determine a globally optimal solution. In the previous chapter we have introduce solutions to the reactor network synthesis problem using linear programing, here we will shift our focus to incorporate mixed integer linear programing formulation into solving the reactor networks synthesis problem.

George B. Dantzig first presented the simplex method as a solution for linear programing problems in 1947[46], which a game changer and opened the door to addressing many challenges that revolutionized the field of mathematical optimization. The method enabled solving large dynamic linear systems subject to a linear objective function and a finite set of linear constraints[47]. With the never-ending growth in the field of mathematical optimization many recognized the value of enhancing our ability to model real life problems by using integer variables and constraints. In cases where the objective function is linear and include integer-based variables, such programs are very similar to typical linear programs with the only exception being that certain variables can't result in real values making Mixed Integer Linear Programming (MILP) problem a special case of Linear Programing (LP). One of the most common problems at that time was the traveling salesman problem (TSP) which proved to be the challenge needed by the brightest scientists of the 1950s to develop the concepts of *linear relaxation*, *branch and bound* and *cutting planes* which were the basis of solving Mixed Integer Linear Programing problems[48]. Adding the integrality constraints (Integer Programing) significantly enhanced the chances of modeling a wider spectrum of real life problems[49] (e.g., planning and scheduling). Due to the similarities linear programing and mixed integer linear programing one would argue that such problems could be solve like typical linear programs followed by rounding up the resulting variables into the next integer digit, following such approach will not result in optimal solutions and these problems require more complex solution methods. Such cases where LPs fail to model realistic scenarios will require the use of MILPs, which offers solutions methods that enable practical modeling.

To synthesize reactor networks system we need to analyze individual reactors performance

using Residence Time Distribution (RTD) which was introduced MacMullin and Weber in 1935[7]. the concept was later developed by Danckwerts in 1953 by developing the RTD function for multiple reactors[16]. Over the last century many RTDs of different reactor systems have been calculated and presented in reaction engineering textbooks[11, 12, 13, 14]. Most researchers approached reactor network synthesis using two methodologies, *superstructure optimization* and *attainable region targeting*. The superstructure approach synthesize reactor networks using a priori determined set that include multiple reactor configurations while attainable region targeting doesn't use a priori-determined sets. Horn introduced the concept of AR for reactor networks and showed the possibility of constructing reactor networks using a collection of objective variables[43]. Glasser demonstrated the attainable region targeting of a reactor network featuring plug-flow reactor (PFR) and continuous stirred tank reactor (CSTR)[21]. Hocine and coworkers used the superstructures optimization approach to minimize PFR and CSTR to model known RTDs using Mixed Integer Non Linear Programming (MINLP)[22].

A process network synthesis methodology that guarantees global optimality has been put forward by Manousiouthakis and coworkers and has been termed the Infinite Dimensional State Space (IDEAS) approach to process network synthesis. IDEAS has been applied to reactor networks synthesis problem using infinite linear programing in the previous chapter. The objectives of this chapter are to introduce: 1-the reactor network synthesis problem for the minimum number of units 2-applications of mixed integer linear programing in IDEAS. We will review the fundamental theoretical concepts of mixed integer linear programming. Further, we will analyze solving large scale mixed integer liner programing formulations based on the reactor networks synthesis problem using commercial solvers.

The originality of this work is that we pursue for the first time the synthesizing reactor networks that features a minimum number of reactors. We want to enrich the methodology presented by demonstrating that IDEAS can address this objective of a minimum number of units and the formulation presented carries that exactly. We will identify optimal reactor networks that results in global optimality to guaranty the model reliability and authentica-

tion. The remaining sections of this chapter continue as follows. First, the basic concepts of Mixed Integer Linear Programing(MILP) are introduced. Next, the IDEAS conceptual framework of multiple residence time distribution (MRTD) is presented. Then, mathematical framework of solving MILP problems is explained. Finally, the IDEAS framework is then applied and solved for a globally optimal solution of the MILP problem in case study of a reactor network featuring a combination of PFR/CSTR reactors.

2.2 Mixed Integer Linear Programming algorithms

Mixed Integer Linear Programming (MILP) is an optimization problem where several of the involved variables are restricted to integer values (e.g. -1,0,3). Such restrictions greatly enhance the scope of real life application as well as the complexity of finding globally optimal solution. In this section we will consider MILP problems of the following general form[1]:

$$\begin{aligned} \text{minimize} \quad & Gx_i + Qy_j \\ \text{subject to} \quad & Ax_i + Hy_j \leqslant b \\ & lb \leqslant (x_i, y_j) \leqslant ub \\ & x \in \mathbb{Z}_+^n \; y \in \mathbb{R}_+^p \end{aligned}$$

Integer variables which are represented by the vector x while y contains the non integer variables. A_{eq} is the matrix where all the integer and non integer information associated with the equality constraints are stored while A_{in} represent the information of the inequality constraints. Bot matrices combine to form an $m \times n$ matrix A where m is the number of the constraints while n is the number of variables. Vectors b_{eq} and b_{in} are where the lower and upper bounds (lb and ub) associated with the equality and inequality constraints are stored. If all variables in the objective are constrained to be nonnegative integer variables, the objective function becomes Gx_i instead of $Gx_i + Qy_j$ resulting in a Pure Integer Linear Program(PILP). A *pure integer linear set* shown in Figure 2.1 below is the set of feasible solutions to a pure integer linear program $S := \{x \in \mathbb{Z}_+^n : Ax \leqslant b\}$[1].

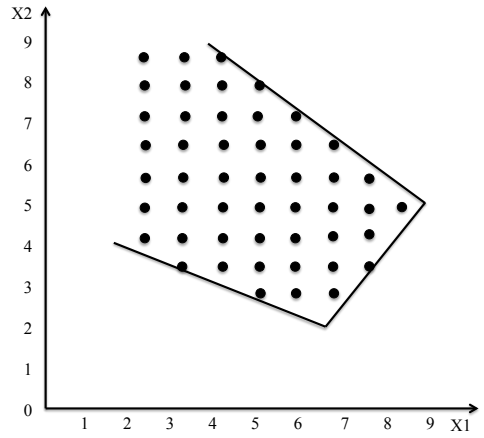

Figure 2.1: Pure integer linear set[1]

The case where x is constrained to nonnegative integer variables while y can take any non negative real value then the problem becomes a Mixed Integer Linear Program (MILP). A *mixed integer linear set* shown in Figure 2.2 is the set of feasible solutions to a mixed integer linear program: $S := \{(x, y) \in \mathbb{Z}^n_+ \times \mathbb{R}^p_+ : Ax + Hy \leqslant b\}$[1].

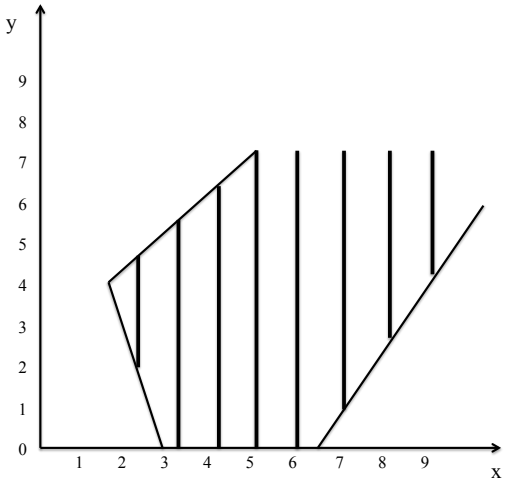

Figure 2.2: Mixed integer linear set[1]

A special case of this is the (0,1) MILP problem where variables are restricted to be 0 and 1 as shown below:

$$\begin{aligned} \text{minimize} \quad & Gx_i \\ \text{subject to} \quad & Ax_i \leqslant b \\ & x \in \{0,1\}^n \end{aligned}$$

A *(0,1) mixed integer linear set* is the set of feasible solutions to a (0,1) mixed integer linear program: $S := \{(x) \in \{0,1\}^n \times \mathbb{R}^p_+ : Ax \leqslant b\}$.

Unlike Linear Programing problems the feasible region of Mixed Integer Linear Programing problems is not a convex set which makes the solution methods developed in the previous chapter not directly applicable to this class of problems[50]. Integer programming is NP-hard which makes developing algorithms to solve large scale Mixed Integer Linear Programing problems a difficult task. Such difficulty can be addressed using a two-way solution targeting approach: using *linear relaxation* to set lower bounds on the objective function, then trying to find upper bound to find feasible solution of the primal side [51]. Such approach solves the problem numerically which enable us to come with sound approximations. We can improve the chances of obtaining an optimal solutions using the two-way targeting solution by implementing the following methods: *linear relaxation*, *branch and bound*, *cutting planes* and *heuristics*[52].

2.2.1 Linear relaxation

NP-complete optimization problems can be reduced to Integer Programs and then to a series of Linear Programming problems using *linear relaxation* where the resulting sequence of LPs are solved to approximate a solution of the mixed integer linear set S. The *linear relaxation* of S is the set: $P_0 := \{(x,y) \in \mathbb{R}^n_+ \times \mathbb{R}^p_+ : Ax + Hy \leqslant b\}$[1]. The constraints to a mixed integer linear programing (MILP) problem comes in the form of a *polyhedron* which can be defined as the set $P := \{x \in \mathbb{R}^n : Ax \leqslant b\}$ in $\mathbb{R}^n$. The feasible region is the set of integer points within the convex hull of the *mixed integer set* S which can be defined as $conv(S) := \{x \in \mathbb{R}^n : x = \sum_{i=1}^k \lambda_i x^i, \sum_{i=1}^k \lambda_i = 1\}$ where $k \geq 1, \lambda \in \mathbb{R}^k_+$ and $x^1, ..., x^k \in S$[46]. Hence, solutions are found by locating the extreme points within the

convex hull $conv(S)$ rather than the extreme points of the entire polyhedron. The feasible region of the LP is larger compared to the feasible region of the MILP. This guarantees that the optimal solution of the MILP problem lies within the LP feasible region. This also indicates that the solution of the LP can act as a new lower bound for the MILP minimization problem. In MILP minimization problems the solution of the relaxed LP problem will have a higher value than solution to the MILP: $Z_{LR} > Z_{MILP}$. Next, we introduce the Integrality constraints and examine $A_{in}x \leqslant b_{in}$ to simplify the branch and bound analysis [53].

2.2.2 Branch and bound

.

Branch and bound is the most used technique to find optimum solutions of Mixed Integer Linear Programing problems[54]. Branch and bound recursively partition the mixed integer set S into a sequence smaller sets S_i which translate into subproblems that are solved numerically. The lower bound of the first sub problem will be the solution to the relaxed LP problem while the upper bound will be any feasible solution. The technique described above searches for an optimal solutions by branching the set S into subsets $S_1, S_2, \ldots S_i$ and numerically bounding the objective function of generated subproblems[1]. The two new subproblems are: $S_1 = S \cap \{(x, y)\} : x_i \leqslant \lfloor f \rfloor$ and $S_2 = S \cap \{(x, y)\} : x_i \geq \lceil f \rceil$[1]. The subproblems are formed in a search tree format where each node of the tree consist of a linear relaxation version of the Mixed Integer Linear Programing problem with addition upper and lower limit constraints to induce integer solutions[55]. If original node S_1 is the linear relaxation which produces a non integer solution $x1 = Z1$ then the node is branched into two sub problems each with an additional specific constraint: $x1 \geq |Z1|$, $x1 \leqslant |Z1|$[56]. The new subproblems at the branch are solved, if the solution is either infeasible or an optimal integer then the branch terminates. However, if one of the sub problems produces an non integer optimal solution then the node is used to create a new branch with two new subproblems with the constraints $x2 \geq |Z2|$, $x1 \leqslant |Z2|$[57].

2.2.3 Cutting planes

As shown earlier P_0 is the linear relaxation of the mixed integer set$S$ resulting in the solution (x_1, y_1). If $(x_1, y_1) \notin S$ then we will use the following inequality constraint $C_1x + C_2y \leqslant \beta$ to trim the feasibility region of the linear relaxation and cut (x_1, y_1) out. The resulting *cutting plane* can be defined as: $P_1 = P_0 \cap \{(x_1, y_1) : C_1x + C_2y \leqslant \beta\}$ with $S \subseteq P_1 \subseteq P_0$ which makes the linear relaxation of the the set P_1 a better approximation of the optimal solution set S than the linear relaxation of the set P_0[1]. To further improve the efficiency the branch and bound method we will use *cutting planes* algorithm to tighten the linear relaxation of the Mixed Integer Linear Programing problem by reducing the feasible region[57]. Cuts reduce the linear relaxation feasible region with aim of reaching a convex hull that guarantees an optimal solution. All solutions of the Mixed Integer Linear Programing problem satisfies the cuts while the solution of the linear relaxation will not satisfy the latest cut as we seen above. Hence, cuts will eliminate optimal linear relaxation solution from the feasible region but will not eliminate the optimal solution of the Mixed Integer Programing problem[54]. The most common cuts used in solving Mixed Integer Linear Programing problems are[55, 58, 59, 60]:

- Gomory cuts
- Cover cuts
- MIR cuts
- Implication cuts

2.2.4 Heuristics

Heuristics are used to improve the efficiency of Mixed Integer Linear Programing solvers. Unlike the previous solutions methods presented in this section, heuristics doesn't have the ability to identify when the method has reached an optimal solution that satisfies the integrality constraints. However, coupled with the branch and bound method heuristic could produce suboptimal solutions faster than branching by it self which will improve the

computing time for finding the optimal solution[61]. Two of the most common heuristics are: the nearest-neighbor heuristic (NNH) and the cheapest insertion heuristic (CIH). The nearest-neighbor heuristic begins at any solution in the feasible region of the relaxed LP problem and then visits the nearest point then goes to a new unvisited point closest to the solution recently obtained. The cheapest insertion heuristic start with a small subset of the feasible region that includes some of the tree nodes and expand on this by adding more nodes to the initial subset. To measure the effectiveness of a heuristic the following methods are used[54]:

- Performance Guarantee:
- Probabilistic Analysis
- Empirical Analysis

The objective function of the Mixed Integer Linear Programing problem that minimizes the number of units in a reactor network assumes the following form:

$$\text{minimize} \quad \sum_{i=1}^{N_R} \lambda(i) \qquad \forall\, \lambda \in \{0,1\}$$

Definition 2.1 *$\lambda(i)$ represent switches where 0 indicates a non-active reactor while 1 indicates an active reactor in the network*

In this chapter, we will use a combination of branch and bound, cuts and heuristics to solve Mixed Integer Linear Programing problems. But first, we will present the first time realization of using the IDEAS Mixed Integer Linear Programing formulation to synthesize globally optimum reactor network with minimum number of units.

2.3 Infinite Dimensional State Space (IDEAS): modeling principles

The IDEAS conceptual framework was proposed by Manousiouthakis and coworkers as a globally optimal network synthesis methodology to solve Infinite Linear Programs(ILP). All

the previous formulations capitalized on IDEAS ability to solve ILPs, here we are going to extend this argument to Mixed Integer Linear Programing problems. IDEAS consist of two subnetworks: the operator network (OP) consisting of an infinite number of units, and a distribution network (DN), where all stream interconnections are split, mixed, and recycled.

The new formulation capitalize on the basic concepts of IDEAS of using linear maps which are the projections of the information map of a process onto a linear variety. A vector space is the infinite equivalent of a union of lower dimensional varieties. The input-output information map is shown below:

$B : D_1 \times D_2 \subset \mathbb{R}^{n+1} \times \mathbb{R} \to \mathbb{R}^{n+1} \times \mathbb{R}^2$

$$B: \quad u = \begin{bmatrix} u_1 \\ u_2 \end{bmatrix} \to y = \begin{bmatrix} y_1 \\ y_2 \end{bmatrix} = B\left(u_1, u_2\right) = \begin{bmatrix} B_1\left(u_1, u_2\right) \\ B_2\left(u_1, u_2\right) \end{bmatrix}$$

Property 1. $y_1 = B_1\left(u_1, u_2\right) = \bar{B}_1\left(u_2\right) u_1$, i.e. the first part y_1 of the output vector y is related in a linear manner to the first part u_1 of the input vector u, through an operator $\bar{B}_1$ that maps the second part u_2 of the input vector u to a mixed integer linear matrix $\bar{B}_1(u_2)$ that then pre-multiplies u_1 to y_1 form .

Property 2. $y_2 = B_2\left(u_1, u_2\right) = \bar{B}_2\left(u_2\right)$, i.e. the first part y_2 of the output vector y is related to the first part u_2 of the input vector u, under a (possibly nonlinear) operator $\bar{B}_2$.

This unit's input-output information map satisfies the above properties, since:

$$u \triangleq \begin{bmatrix} F \\ C_1^{in} \\ \vdots \\ C_n^{in} \\ \bar{t} \end{bmatrix}, u_1 \triangleq \begin{bmatrix} F \end{bmatrix}, u_2 \triangleq \begin{bmatrix} C_1^{in} \\ \vdots \\ C_n^{in} \\ \bar{t} \end{bmatrix}, y_1 \triangleq \begin{bmatrix} F \\ V \end{bmatrix}, y_2 \triangleq \begin{bmatrix} C_1^{out} \\ \vdots \\ C_n^{out} \\ \tau \end{bmatrix} = \begin{bmatrix} C_1\left(\lambda = 0\right) \\ \vdots \\ C_n\left(\lambda = 0\right) \\ \bar{t} \end{bmatrix}$$

Where,

$$u_1 \in D_1 \triangleq \{u_1 = [F] \in \mathbb{R} : F \geq 0\}$$

And,

$$u_2 \in D_2 \triangleq \left\{ u_2 = \left[\begin{array}{cccc} C_1^{in} & \cdots & C_n^{in} & \bar{t} \end{array} \right]^T \in \mathbb{R}^{n+1} : \; C_i^{in} \geq 0 \; \forall i = 1, n, \; \bar{t} \geq 0 \right\}$$

$$u \triangleq \left[\begin{array}{c} F \\ C_1^{in} \\ \vdots \\ C_n^{in} \\ \bar{t} \end{array} \right], u_1 \triangleq \left[\begin{array}{c} F \end{array} \right], u_2 \triangleq \left[\begin{array}{c} C_1^{in} \\ \vdots \\ C_n^{in} \\ \bar{t} \end{array} \right], y_1 \triangleq \left[\begin{array}{c} F \\ V \end{array} \right], \bar{B}_1(u_2)u_1 = \left[\begin{array}{c} 1 \\ \bar{t} \end{array} \right] \left[\begin{array}{c} F \end{array} \right]$$

,

$$y_2 \triangleq \left[\begin{array}{c} C_1^{out} \\ \vdots \\ C_n^{out} \\ \tau \end{array} \right] = \left[\begin{array}{c} \int_0^\infty C_1(t) \frac{1}{\bar{t}} E\left(\frac{t}{\bar{t}}\right) dt \\ \vdots \\ \int_0^\infty C_n(t) E\left(\frac{t}{\bar{t}}\right) dt \\ \bar{t} \end{array} \right]$$

Where,

$$u_1 \in D_1 \triangleq \{u_1 = [F] \in \mathbb{R} : F \geq 0\}$$

And,

$$u_2 \in D_2 \triangleq \left\{ u_2 = \left[\begin{array}{cccc} C_1^{in} & \cdots & C_n^{in} & \bar{t} \end{array} \right]^T \in \mathbb{R}^{n+1} : \; C_i^{in} \geq 0 \; \forall i = 1, n, \; \bar{t} \geq 0 \right\}$$

Having established the applicability of IDEAS to the Mixed Integer Programing problem under consideration, we next present the resulting IDEAS Mixed Integer Linear Programing formulation.

	F^I	$F^{\hat{I}}$	$F^{I\hat{I}}$	F^{OI}	F^O	$F^{\hat{O}}$	$F^{\hat{I}\hat{O}}$	$F^{\hat{O}\hat{O}}$
OBJ	0	λ	0	0	0	0	0	0
FBIN	1	0	-1	-1	0	0	0	0
FBOUT	0	0	0	-1	1	0	0	1
CBOUT	0	0	0	-C_A^I	C_A^O	1	1	-C_A^O
SFB1	0	1	-1	0	0	0	-1	0
SFB2	0	0	0	0	0	1	-1	-1
SCB	0	C_A^I	-C_A^I	0	0	0	-C_A^O	0

Table 2.1: Constraint Matrix (A)

2.3.1 IDEAS Mixed Integer Linear Programing formulation

The problems solved in this chapter will have a single network inlet and outlet. Network inlet flow has two choices once it enters the network, it can bypass the states (and thus all possible reactors) and leave the network (this is represented by F^{OI}) or it can travel to any number of different states (this is represented by $F^{I\hat{I}}$). Table 2.3.1 shows the state crossflows $F^{\hat{I}\hat{O}}$, the reactor flows $F^{\hat{I}}$ and the network interconnection.

The objective function for the minimum number of units problem is:

$$min \ \sum_{i=1}^{\infty} \lambda(i) \ \forall \lambda \in \{0,1\} \tag{2.1}$$

DN total mass balance mixing equations:

$$F^O(i) = \sum_{j=1}^{N_I} F^{OI}(i,j) + \sum_{j=1}^{\infty} F^{O\hat{O}}(i,j) \forall i = 1, ..., N_O \tag{2.2}$$

$$F^{\hat{I}}(i) = \sum_{j=1}^{N_I} F^{\hat{I}I}(i,j) + \sum_{j=1}^{\infty} F^{\hat{I}\hat{O}}(i,j) \forall i = 1, ..., \infty \tag{2.3}$$

DN total mass balance splitting equations:

$$F^{I}(j) = \sum_{i=1}^{N_O} F^{OI}(i,j) + \sum_{i=1}^{\infty} F^{\hat{I}I}(i,j) \forall j = 1, ..., N_I \tag{2.4}$$

$$F^{\hat{O}}(j) = \sum_{i=1}^{N_O} F^{O\hat{O}}(i,j) + \sum_{i=1}^{\infty} F^{\hat{I}\hat{O}}(i,j) \forall j = 1, ..., \infty \tag{2.5}$$

DN component mass balance mixing equations:

$$C_A^{\hat{I}}(i) F^{\hat{I}}(i) = \sum_{j=1}^{N_I} C_A^{I}(j) F^{\hat{I}I}(i,j) + \sum_{j=1}^{\infty} C_A^{\hat{O}}(j) F^{\hat{I}\hat{O}}(i,j) \quad \forall i = 1, ..., \infty \tag{2.6}$$

OP balance equations:

$$F^{\hat{O}}(i) = F^{\hat{I}}(i) \forall i = 1, ..., \infty \tag{2.7}$$

Overall network component mass balance mixing equations:

$$C_A^{O}(i) F^{O}(i) = \sum_{j=1}^{N_I} C_A^{I}(j) F^{OI}(i,j) + \sum_{j=1}^{\infty} C_A^{\hat{O}}(j) F^{O\hat{O}}(i,j) \ \ \forall k = 1, ..., n \ \ \forall i = 1, ..., N_O \tag{2.8}$$

DN outlet specifications:

$$\left(F^{O}(i)\right)^{l} \leq F^{O}(i) \leq \left(F^{O}(i)\right)^{u} \ \ \forall i = 1, ..., N_O \tag{2.9}$$

$$\left(C_C^{O}(i)\right)^{l} F^{O}(i) \leq \sum_{j=1}^{N_I} C_C^{I}(j) F^{OI}(i,j) + \sum_{j=1}^{\infty} C_C^{\hat{O}}(j) F^{O\hat{O}}(i,j) \leq \left(C_C^{O}(i)\right)^{u} F^{O}(i) \quad \forall i = 1, ..., N_O \tag{2.10}$$

MILP constraints:

$$0 \leqslant \sum_{i=1}^{\infty} \tau(i) F^{\hat{I}}(i) \leqslant V^{U} \tag{2.11}$$

$$\sum_{i=1}^{N_i} F^{\hat{I}}(i) - V^U \frac{\sum_{i=1}^{N_i} \lambda(i)}{\sum_{i=1}^{N_i} \tau(i)} \leqslant 0 \tag{2.12}$$

Non-negativity constraints:

$$F^I \geq 0;\ F^O \geq 0; F^{\hat{I}} \geq 0; F^{\hat{O}} \geq 0; F^{OI} \geq 0; F^{\hat{I}I} \geq 0; F^{\hat{I}\hat{O}} \geq 0; F^{O\hat{O}} \geq 0 \tag{2.13}$$

2.4 Case Study

In this section we will use the methods used in the previous sections to develop a solution procedure for the minimum number of units Mixed Integer Linear Programing problem using IDEAS mathematical framework of network synthesis. The formulation consist of an integer objective function with integer,linear and linearized non-linear constraints. The Trambouze reaction scheme is taking place inside the reactor units under consideration. The corresponding kinetic rate, and reactor network inlet information is:

$$A \xrightarrow{k_1} B\ ,\ k_1 = 0.025\,\frac{kmol}{m^3 \cdot s};$$
$$A \xrightarrow{k_2} C\ ,\ k_2 = 0.2\,\frac{1}{s};$$
$$A \xrightarrow{k_3} D\ ,\ k_3 = 0.4\frac{}{m^3} kmol \cdot s$$

where,

$$k_2{}^2 = 4k_1k_3;\quad \alpha = \frac{k_2}{2k_3} = 0.25 > 0$$

And

$$C_A^I = 1\frac{kmol}{m^3},\ C_C^I = 0\frac{kmol}{m^3}$$

As we showed earlier the advantage of IDEAS is that it overcomes the nonlinearity of problem constraints by utilizing the linearity properties that the process variables naturally follow. IDEAS solve an infinite number of Mixed Integer Linear Programming problems

using a finite number of grid points which are obtained by discretizing the concentration space. Based on the discretization scheme (specific number of intervals) IDEAS determines the number of available reactors, number of constraints (m) and the number of variables (n). All constraints and variables are stored in an A matrix of size ($m \times n$). In this case study our choice of discretization is 16 intervals which results in 272 reactors (136 PFRs and 136 CSTRs), 75073 variables and 1096 constraints (277 inequalities and 819 equalities). The resulting A matrix will have a size of (1096×75073), some commercial solvers elect the choice of splitting the A matrix into two matrices based on type of constraints (A_{eq} and A_{in}). The matrix can be separated into three sections, the first one contains parameters and variables related to the objective function (the first row). The second contains parameters and variables related to equality constraints (A_{eq}) while the third covers inequality constraints(A_{in}).

$$
A = \begin{bmatrix}
\lambda(1) & \lambda(2) & \lambda(3) & \lambda(4) & \lambda(5) & \lambda(6) & \dots & \lambda(n) \\
 & & & \cdots\cdots\cdots\cdots\cdots\cdots\cdots\cdots & & & & \\
0 & 0 & 0 & 0 & 0 & 0 & 0 & 0 \\
1 & 0 & 0 & 0 & 0 & 0 & 0 & 0 \\
0 & 1 & 0 & 0 & 0 & 0 & 0 & 0 \\
0 & 0 & 1 & 0 & 0 & 0 & 0 & 0 \\
0 & 0 & 0 & 1 & 0 & 0 & 0 & 0 \\
0 & 0 & 0 & 0 & 1 & 0 & 0 & 0 \\
0 & 0 & 0 & 0 & 0 & 1 & 0 & 0 \\
0 & 0 & 0 & 0 & 0 & 0 & \ddots & 0 \\
0 & 0 & 0 & 0 & 0 & 0 & 0 & 1 \\
 & & & \cdots\cdots\cdots\cdots\cdots\cdots\cdots\cdots & & & & \\
C_A^I(1) & 0 & 0 & 0 & 0 & 0 & 0 & 0 \\
0 & C_A^I(2) & 0 & 0 & 0 & 0 & 0 & 0 \\
0 & 0 & C_A^I(3) & 0 & 0 & 0 & 0 & 0 \\
0 & 0 & 0 & C_A^I(4) & 0 & 0 & 0 & 0 \\
0 & 0 & 0 & 0 & C_A^I(5) & 0 & 0 & 0 \\
0 & 0 & 0 & 0 & 0 & C_A^I(6) & 0 & 0 \\
0 & 0 & 0 & 0 & 0 & 0 & \ddots & 0 \\
0 & 0 & 0 & 0 & 0 & 0 & 0 & C_A^I(n) \\
\Delta Cc(1) & \Delta Cc(2) & \Delta Cc(3) & \Delta Cc(4) & \Delta Cc(5) & \Delta Cc(6) & \dots & \Delta Cc(n) \\
\Delta Cc(1) & \Delta Cc(2) & \Delta Cc(3) & \Delta Cc(4) & \Delta Cc(5) & \Delta Cc(6) & \dots & \Delta Cc(n)
\end{bmatrix}
$$

The bound matrix (b) contains lower and upper bound on the problem constrains and the relationship between the two matrices is based on $Ax \leqslant b$ and $x \geqslant lb$. Where x is contains all the flow rates variables of the problem that will change within the problem according to the way the interconnections are shaped between the DN and OP:

$$x = \begin{bmatrix} F^{\hat{I}}{}_{(1\to n)} & F^{OI} & F^{\hat{I}I}{}_{(1\to n)} & F^{O\hat{O}}{}_{(1\to n)} & F^{\hat{I}\hat{O}}{}_{(1\to n,1\to n)} \end{bmatrix}$$

In carrying out the IDEAS methodology, the inlet and outlet concentrations for the PFRs/CSTRs are specified ($C_A^{\hat{I}} = 1$ and $C_A^{\hat{O}} = 0$) . For the considered case study, the IDEAS solutions for minimum units number problem with an ($V_{max} = 30$) are presented for the three aforementioned cases:

Case 1: $C_A^{\hat{O}} = 0 \ \frac{kmol}{m^3}$ **and** $0.40 \leqslant C_C^{\hat{O}} \leqslant 0.45 \ \frac{kmol}{m^3}$

First, the initial linear relaxation of the Mixed Integer Linear Programing problem resulted in an objective function value of 0.266667. Then, 2 gomory cuts, 10 implication cuts and one mir cut were applied which results in a lower bound=0.888889. Heuristics were used to obtain an upper bound=2.000 with a relative gap=0.05%. After that a gomory cut and 4 implication cuts were performed resulting in lower bound=0.888889 and a relative gap=5.60%. Two rounds of branch and methods explored 368 and 440 nodes to find the final solution. The optimal network consist of one unit, a PFR (unit 1) with a residence time is τ_1= 8.00 and $C_C^{\hat{O}} = 0.4047$ as shown below in Table 2.4.

Unit Number	$C_A^{in}(\frac{kmol}{m^3})$	$C_A^{out}(\frac{kmol}{m^3})$	ΔC_C	$\tau(s)$	$V(m^3)$
1	1.00	0	0.4047	8.00	8.00

Table 2.2: Case1: IDEAS reactor network information

Case 2: $C_A^{\hat{O}} = 0 \ \frac{kmol}{m^3}$ **and** $0.30 \leqslant C_C^{\hat{O}} \leqslant 0.40 \ \frac{kmol}{m^3}$

First, the initial linear relaxation of the Mixed Integer Linear Programing problem resulted in an objective function value of 0.273463. Then, 11 gomory cuts, 42 implication cuts, 2 flow cover cuts and 9 mir cuts were applied which resulted in a lower bound=0.962090. Heuristics were used to obtain an upper bound=2.000 with a relative gap=0.05%. After that

a gomory cut and 3 implication cuts were performed resulting in lower bound=0.968398 and a relative gap=1.63%. Branch and bound explored 198 nodes to reach the final solution. The optimal network consist of two units, a PFR (unit 1) and a CSTR (unit 2). The residence times are τ_1= 7.33 and τ_2= 20.80. The OP network inlet flow rates are $F^{\hat{I}}{}_1 = 1.0435$ and $F^{\hat{I}}{}_2 = 0.3478$. The flow rates from the network outlet to the OP inlet are $F^{\hat{I}I}{}_1 = 0.6957$ and $F^{\hat{I}I}{}_2 = 0.3043$. The flow rate from the OP outlet to the network outlet is $F^{O\hat{O}}{}_1 = 1.000$. The flow rates from OP outlet to the network outlet are $F^{\hat{I}\hat{O}}{}_{(1,2)} = 0.3043$ and $F^{\hat{I}\hat{O}}{}_{(2,1)} = 0.0435$ as shown below in Table 2.4.

Unit Number	$C_A^{in}(\frac{kmol}{m^3})$	$C_A^{out}(\frac{kmol}{m^3})$	ΔC_C	$\tau(s)$	$V(m^3)$
1	0.6875	0	0.2942	7.33	7.65
2	0.8750	0.0625	0.2600	20.80	7.23

Table 2.3: Case2: IDEAS reactor network information

Case 3: $C_A^{\hat{O}} = 0\ \frac{kmol}{m^3}$ **and** $0.20 \leqslant C_C^{\hat{O}} \leqslant 0.30\ \frac{kmol}{m^3}$

First, the initial linear relaxation of the Mixed Integer Linear Programing problem resulted in an objective function value of 0.450301. Then, 10 gomory cuts, 30 implication cuts, 2 flow cover cuts and 10 mir cuts were applied which resulted in a lower bound=1.186799. Heuristics were used but there was no need to apply branch and bound in this case. The optimal network consist of two units, a PFR (unit 1) and a CSTR (unit 2). The residence times are τ_1= 7.65 and τ_2= 27.50. The OP network inlet flow rates are $F^{\hat{I}}{}_1 = 0.8795$ and $F^{\hat{I}}{}_2 = 0.4151$. The flow rates from the network outlet to the OP inlet are $F^{\hat{I}I}{}_1 = 0.7146$ and $F^{\hat{I}I}{}_2 = 0.2854$. The flow rates from the OP outlet to the network outlet are $F^{O\hat{O}}{}_1 = 0.7498$ and $F^{O\hat{O}}{}_2 = 0.2502$. The flow rates from OP outlet to the network outlet are $F^{\hat{I}\hat{O}}{}_{(1,2)} = 0.1649$ and $F^{\hat{I}\hat{O}}{}_{(2,1)} = 0.1297$ as shown below in Table 2.4.

Unit Number	$C_A^{in}(\frac{kmol}{m^3})$	$C_A^{out}(\frac{kmol}{m^3})$	ΔC_C	$\tau(s)$	$V(m^3)$
1	0.8125	0	0.3411	7.65	6.73
2	0.6875	0	0	27.50	11.42

Table 2.4: Case3: IDEAS reactor network information

Case 4: $C_A^{\hat{O}} = 0\ \frac{kmol}{m^3}$ **and** $0.10 \leqslant C_C^{\hat{O}} \leqslant 0.20\ \frac{kmol}{m^3}$

First, the initial linear relaxation of the Mixed Integer Linear Programing problem resulted in an objective function value of 0.682045. Then, 5 gomory cuts, 40 implication cuts, a flow cover cut and 13 mir cuts were applied which resulted in a lower bound=1.440165. Heuristics were used to obtain an upper bound=3.000 with a relative gap=0.03%. After that 3 implication cuts were applied that resulted in a lower bound=1.440914 and a relative gap=18.66%. Branch and bound explored 227 nodes to reach the final solution. The optimal network consist of two units, a PFR (unit 1) and a CSTR (unit 2). The residence times are τ_1= 7.90 and τ_2= 25.00. The OP network inlet flow rates are $F^{\hat{I}}{}_1 = 0.3840$ and $F^{\hat{I}}{}_2 = 1.0240$. The flow rates from the network outlet to the OP inlet are $F^{\hat{I}\hat{I}}{}_1 = 0.3600$ and $F^{\hat{I}\hat{I}}{}_2 = 0.6400$. The flow rateâĂĺfrom the OP outlet to the network outlet is $F^{O\hat{O}}{}_2 = 1.000$. The flow rates from OP outlet to the network outlet are $F^{\hat{I}\hat{O}}{}_{(1,2)} = 0.0240$ and $F^{\hat{I}\hat{O}}{}_{(2,1)} = 0.3840$ as shown below in Table 2.4.

Unit Number	$C_A^{in}(\frac{kmol}{m^3})$	$C_A^{out}(\frac{kmol}{m^3})$	ΔC_C	$\tau(s)$	$V(m^3)$
1	0.9375	0	0.3843	7.8947	3.03
2	0.6250	0	0	25.00	25.60

Table 2.5: Case4: IDEAS reactor network information

Case 5: $C_A^{\hat{O}} = 0\ \frac{kmol}{m^3}$ **and** $0 \leqslant C_C^{\hat{O}} \leqslant 0.10\ \frac{kmol}{m^3}$

First, the initial linear relaxation of the Mixed Integer Linear Programing problem resulted in an objective function value of 0.973033. Then, 4 gomory cuts, 25 implication cuts and 4 mir cuts were applied which resulted in a lower bound=1.915089. Heuristics were used to obtain an upper bound=3.000 with a relative gap=0.03%. After that 4 implication cuts were applied that resulted in a lower bound=1.915089 and a relative gap=2.86%. Branch and bound explored 376 nodes to reach the final solution. The optimal network consist of three units, a PFR (unit 1) and two CSTRs (units 2 and 3). The residence times are τ_1=0.667 , τ_2=25.000 and τ_3=2.500 . The OP network inlet flow rates are $F^{\hat{I}}{}_1 = 0.9049$, $F^{\hat{I}}{}_2 = 1.0369$. and $F^{\hat{I}}{}_3 = 1.1061$. The flow rates from the network outlet to the OP inlet are $F^{\hat{I}I}{}_1 = 0.9049$, $F^{\hat{I}I}{}_2 = 0.0260$ and $F^{\hat{I}I}{}_3 = 0.0691$. The flow rate from the OP outlet to the network outlet is $F^{O\hat{O}}{}_3 = 1.000$. The flow rates from OP outlet to the network outlet are $F^{\hat{I}\hat{O}}{}_{(2,1)} = 0.9049$, $F^{\hat{I}\hat{O}}{}_{(2,3)} = 0.1061$ and $F^{\hat{I}\hat{O}}{}_{(3,2)} = 1.0369$ as shown below in Table 2.4.

Unit Number	$C_A^{in}(\frac{kmol}{m^3})$	$C_A^{out}(\frac{kmol}{m^3})$	ΔC_C	$\tau(s)$	$V(m^3)$
1	1.000	0.6875	0.1105	0.6667	0.60
2	0.6250	0	0	25.00	25.92
3	0.0625	0	0	2.50	2.77

Table 2.6: Case5: IDEAS reactor network information

2.5 Discussion and conclusions

Here we have demonstrated that Mixed Integer Linear Programing formulations can potentially provide an advantage in solving the minimum number of units problem featuring multiple normalized residence time density/distribution models(MRTD). The advantage depends on the types of consideration that are incorporated into the design procedure. The

use of MRTD enable flexibility, but we can see through some of the case studies that the MRTD emulates the behavior of one residence time distribution model mixing pattern or that one RTD is emulated by another RTD mixing pattern. For example a Continuous Stirred Tank Reactor is emulated with Plug Flow Reactor with a large recycle. A Plug Flow Reactor is emulated by a sequence of Continuous Stirred Tank Reactors. however, when other consideration are incorporated into the design producer such as concentration the emulation capabilities of various technologies may be limited and this is shown in Case 5. The residence time disruption belongs to a reactor who's contents are considered to be specially uniform and who's dimensionless. The Continuous Stirred Tank Reactor and Plug Flow Reactor models are shown to satisfy the requirements necessary for the application of the Infinite Dimensional State Space (IDEAS) framework to address the problem at hand, yet the proposed methodology is applicable to arbitrary residence time distributions that can be experimentally obtain and thus can aid the designer to synthesize reactor networks that are not limited to ideal models such as Plug Flow Reactors and Continuous Stirred Tank Reactors only.

2.6 Appendix A

Table 2.7: CSTR Reactors 1

i	$x(i)$	$y(i)$	$\tau(i)$	$\Delta C_c(i)$	i	$x(i)$	$y(i)$	$\tau(i)$	$\Delta C_c(i)$
1	1.0000	0.9375	0.1053	0.0204	28	0.9375	0.1875	3.6090	0.3188
2	1.0000	0.8750	0.2222	0.0416	29	0.9375	0.1250	4.5614	0.3483
3	1.0000	0.8125	0.3529	0.0636	30	0.9375	0.0625	5.8947	0.3728
4	1.0000	0.7500	0.5000	0.0866	31	0.9375	0.0000	7.8947	0.3843
5	1.0000	0.6875	0.6667	0.1105	32	0.8750	0.8125	0.1307	0.0220
6	1.0000	0.6250	0.8571	0.1355	33	0.8750	0.7500	0.2778	0.0450
7	1.0000	0.5625	1.0769	0.1615	34	0.8750	0.6875	0.4444	0.0689
8	1.0000	0.5000	1.3333	0.1887	35	0.8750	0.6250	0.6349	0.0939
9	1.0000	0.4375	1.6364	0.2171	36	0.8750	0.5625	0.8547	0.1200
10	1.0000	0.3750	2.0000	0.2466	37	0.8750	0.5000	1.1111	0.1472
11	1.0000	0.3125	2.4444	0.2770	38	0.8750	0.4375	1.4141	0.1755
12	1.0000	0.2500	3.0000	0.3081	39	0.8750	0.3750	1.7778	0.2050
13	1.0000	0.1875	3.7143	0.3392	40	0.8750	0.3125	2.2222	0.2355
14	1.0000	0.1250	4.6667	0.3687	41	0.8750	0.2500	2.7778	0.2666
15	1.0000	0.0625	6.0000	0.3931	42	0.8750	0.1875	3.4921	0.2976
16	1.0000	0.0000	8.0000	0.4047	43	0.8750	0.1250	4.4444	0.3271
17	0.9375	0.8750	0.1170	0.0212	44	0.8750	0.0625	5.7778	0.3516
18	0.9375	0.8125	0.2477	0.0432	45	0.8750	0.0000	7.7778	0.3631
19	0.9375	0.7500	0.3947	0.0662	46	0.8125	0.7500	0.1471	0.0230
20	0.9375	0.6875	0.5614	0.0901	47	0.8125	0.6875	0.3137	0.0469
21	0.9375	0.6250	0.7519	0.1151	48	0.8125	0.6250	0.5042	0.0719
22	0.9375	0.5625	0.9717	0.1412	49	0.8125	0.5625	0.7240	0.0979
23	0.9375	0.5000	1.2281	0.1684	50	0.8125	0.5000	0.9804	0.1251
24	0.9375	0.4375	1.5311	0.1967	51	0.8125	0.4375	1.2834	0.1535
25	0.9375	0.3750	1.8947	0.2262	52	0.8125	0.3750	1.6471	0.1830
26	0.9375	0.3125	2.3392	0.2566	53	0.8125	0.3125	2.0915	0.2134
27	0.9375	0.2500	2.8947	0.2878	54	0.8125	0.2500	2.6471	0.2445

Table 2.8: CSTR Reactors 2

i	$x(i)$	$y(i)$	$\tau(i)$	$\Delta C_c(i)$	i	$x(i)$	$y(i)$	$\tau(i)$	$\Delta C_c(i)$
55	0.8125	0.1875	3.3613	0.2756	82	0.6250	0.5625	0.2198	0.0261
56	0.8125	0.1250	4.3137	0.3050	83	0.6250	0.5000	0.4762	0.0533
57	0.8125	0.0625	5.6471	0.3295	84	0.6250	0.4375	0.7792	0.0816
58	0.8125	0.0000	7.6471	0.3411	85	0.6250	0.3750	1.1429	0.1111
59	0.7500	0.6875	0.1667	0.0239	86	0.6250	0.3125	1.5873	0.1416
60	0.7500	0.6250	0.3571	0.0489	87	0.6250	0.2500	2.1429	0.1727
61	0.7500	0.5625	0.5769	0.0750	88	0.6250	0.1875	2.8571	0.2037
62	0.7500	0.5000	0.8333	0.1022	89	0.6250	0.1250	3.8095	0.2332
63	0.7500	0.4375	1.1364	0.1305	90	0.6250	0.0625	5.1429	0.2577
64	0.7500	0.3750	1.5000	0.1600	91	0.6250	0.0000	7.1429	0.2692
65	0.7500	0.3125	1.9444	0.1905	92	0.5625	0.5000	0.2564	0.0272
66	0.7500	0.2500	2.5000	0.2216	93	0.5625	0.4375	0.5594	0.0556
67	0.7500	0.1875	3.2143	0.2526	94	0.5625	0.3750	0.9231	0.0850
68	0.7500	0.1250	4.1667	0.2821	95	0.5625	0.3125	1.3675	0.1155
69	0.7500	0.0625	5.5000	0.3066	96	0.5625	0.2500	1.9231	0.1466
70	0.7500	0.0000	7.5000	0.3181	97	0.5625	0.1875	2.6374	0.1777
71	0.6875	0.6250	0.1905	0.0250	98	0.5625	0.1250	3.5897	0.2071
72	0.6875	0.5625	0.4103	0.0510	99	0.5625	0.0625	4.9231	0.2316
73	0.6875	0.5000	0.6667	0.0782	100	0.5625	0.0000	6.9231	0.2432
74	0.6875	0.4375	0.9697	0.1066	101	0.5000	0.4375	0.3030	0.0284
75	0.6875	0.3750	1.3333	0.1361	102	0.5000	0.3750	0.6667	0.0578
76	0.6875	0.3125	1.7778	0.1665	103	0.5000	0.3125	1.1111	0.0883
77	0.6875	0.2500	2.3333	0.1976	104	0.5000	0.2500	1.6667	0.1194
78	0.6875	0.1875	3.0476	0.2287	105	0.5000	0.1875	2.3810	0.1505
79	0.6875	0.1250	4.0000	0.2581	106	0.5000	0.1250	3.3333	0.1799
80	0.6875	0.0625	5.3333	0.2826	107	0.5000	0.0625	4.6667	0.2044
81	0.6875	0.0000	7.3333	0.2942	108	0.5000	0.0000	6.6667	0.2160

Table 2.9: CSTR Reactors 3

i	$x(i)$	$y(i)$	$\tau(i)$	$\Delta C_c(i)$
109	0.4375	0.3750	0.3636	0.0295
110	0.4375	0.3125	0.8081	0.0599
111	0.4375	0.2500	1.3636	0.0910
112	0.4375	0.1875	2.0779	0.1221
113	0.4375	0.1250	3.0303	0.1516
114	0.4375	0.0625	4.3636	0.1760
115	0.4375	0.0000	6.3636	0.1876
116	0.3750	0.3125	0.4444	0.0305
117	0.3750	0.2500	1.0000	0.0616
118	0.3750	0.1875	1.7143	0.0926
119	0.3750	0.1250	2.6667	0.1221
120	0.3750	0.0625	4.0000	0.1466
121	0.3750	0.0000	6.0000	0.1581
122	0.3125	0.2500	0.5556	0.0311
123	0.3125	0.1875	1.2698	0.0622
124	0.3125	0.1250	2.2222	0.0916
125	0.3125	0.0625	3.5556	0.1161
126	0.3125	0.0000	5.5556	0.1277
127	0.2500	0.1875	0.7143	0.0311
128	0.2500	0.1250	1.6667	0.0605
129	0.2500	0.0625	3.0000	0.0850
130	0.2500	0.0000	5.0000	0.0966
131	0.1875	0.1250	0.9524	0.0295
132	0.1875	0.0625	2.2857	0.0540
133	0.1875	0.0000	4.2857	0.0655
134	0.1250	0.0625	1.3333	0.0245
135	0.1250	0.0000	3.3333	0.0361
136	0.0625	0.0000	2.0000	0.0116

Table 2.10: PFR Reactors 1

i	$x(i)$	$y(i)$	$\tau(i)$	$\Delta C_c(i)$	i	$x(i)$	$y(i)$	$\tau(i)$	$\Delta C_c(i)$
137	1.0000	0.9375	0.1108	0.0208	164	0.9375	0.1875	9.7959	0.3673
138	1.0000	0.8750	0.2469	0.0432	165	0.9375	0.1250	14.4444	0.3611
139	1.0000	0.8125	0.4152	0.0675	166	0.9375	0.0625	22.4000	0.2800
140	1.0000	0.7500	0.6250	0.0938	167	0.9375	0.0000	37.5000	0.0000
141	1.0000	0.6875	0.8889	0.1222	168	0.8750	0.8125	0.1384	0.0225
142	1.0000	0.6250	1.2245	0.1531	169	0.8750	0.7500	0.3125	0.0469
143	1.0000	0.5625	1.6568	0.1864	170	0.8750	0.6875	0.5333	0.0733
144	1.0000	0.5000	2.2222	0.2222	171	0.8750	0.6250	0.8163	0.1020
145	1.0000	0.4375	2.9752	0.2603	172	0.8750	0.5625	1.1834	0.1331
146	1.0000	0.3750	4.0000	0.3000	173	0.8750	0.5000	1.6667	0.1667
147	1.0000	0.3125	5.4321	0.3395	174	0.8750	0.4375	2.3140	0.2025
148	1.0000	0.2500	7.5000	0.3750	175	0.8750	0.3750	3.2000	0.2400
149	1.0000	0.1875	10.6122	0.3980	176	0.8750	0.3125	4.4444	0.2778
150	1.0000	0.1250	15.5556	0.3889	177	0.8750	0.2500	6.2500	0.3125
151	1.0000	0.0625	24.0000	0.3000	178	0.8750	0.1875	8.9796	0.3367
152	1.0000	0.0000	40.0000	0.0000	179	0.8750	0.1250	13.3333	0.3333
153	0.9375	0.8750	0.1235	0.0216	180	0.8750	0.0625	20.8000	0.2600
154	0.9375	0.8125	0.2768	0.0450	181	0.8750	0.0000	35.0000	0.0000
155	0.9375	0.7500	0.4688	0.0703	182	0.8125	0.7500	0.1563	0.0234
156	0.9375	0.6875	0.7111	0.0978	183	0.8125	0.6875	0.3556	0.0489
157	0.9375	0.6250	1.0204	0.1276	184	0.8125	0.6250	0.6122	0.0765
158	0.9375	0.5625	1.4201	0.1598	185	0.8125	0.5625	0.9467	0.1065
159	0.9375	0.5000	1.9444	0.1944	186	0.8125	0.5000	1.3889	0.1389
160	0.9375	0.4375	2.6446	0.2314	187	0.8125	0.4375	1.9835	0.1736
161	0.9375	0.3750	3.6000	0.2700	188	0.8125	0.3750	2.8000	0.2100
162	0.9375	0.3125	4.9383	0.3086	189	0.8125	0.3125	3.9506	0.2469
163	0.9375	0.2500	6.8750	0.3438	190	0.8125	0.2500	5.6250	0.2813

Table 2.11: PFR Reactors 2

i	$x(i)$	$y(i)$	$\tau(i)$	$\Delta C_c(i)$	i	$x(i)$	$y(i)$	$\tau(i)$	$\Delta C_c(i)$
191	0.8125	0.1875	8.1633	0.3061	218	0.6250	0.5625	0.2367	0.0266
192	0.8125	0.1250	12.2222	0.3056	219	0.6250	0.5000	0.5556	0.0556
193	0.8125	0.0625	19.2000	0.2400	220	0.6250	0.4375	0.9917	0.0868
194	0.8125	0.0000	32.5000	0.0000	221	0.6250	0.3750	1.6000	0.1200
195	0.7500	0.6875	0.1778	0.0244	222	0.6250	0.3125	2.4691	0.1543
196	0.7500	0.6250	0.4082	0.0510	223	0.6250	0.2500	3.7500	0.1875
197	0.7500	0.5625	0.7101	0.0799	224	0.6250	0.1875	5.7143	0.2143
198	0.7500	0.5000	1.1111	0.1111	225	0.6250	0.1250	8.8889	0.2222
199	0.7500	0.4375	1.6529	0.1446	226	0.6250	0.0625	14.4000	0.1800
200	0.7500	0.3750	2.4000	0.1800	227	0.6250	0.0000	25.0000	0.0000
201	0.7500	0.3125	3.4568	0.2160	228	0.5625	0.5000	0.2778	0.0278
202	0.7500	0.2500	5.0000	0.2500	229	0.5625	0.4375	0.6612	0.0579
203	0.7500	0.1875	7.3469	0.2755	230	0.5625	0.3750	1.2000	0.0900
204	0.7500	0.1250	11.1111	0.2778	231	0.5625	0.3125	1.9753	0.1235
205	0.7500	0.0625	17.6000	0.2200	232	0.5625	0.2500	3.1250	0.1563
206	0.7500	0.0000	30.0000	0.0000	233	0.5625	0.1875	4.8980	0.1837
207	0.6875	0.6250	0.2041	0.0255	234	0.5625	0.1250	7.7778	0.1944
208	0.6875	0.5625	0.4734	0.0533	235	0.5625	0.0625	12.8000	0.1600
209	0.6875	0.5000	0.8333	0.0833	236	0.5625	0.0000	22.5000	0.0000
210	0.6875	0.4375	1.3223	0.1157	237	0.5000	0.4375	0.3306	0.0289
211	0.6875	0.3750	2.0000	0.1500	238	0.5000	0.3750	0.8000	0.0600
212	0.6875	0.3125	2.9630	0.1852	239	0.5000	0.3125	1.4815	0.0926
213	0.6875	0.2500	4.3750	0.2188	240	0.5000	0.2500	2.5000	0.1250
214	0.6875	0.1875	6.5306	0.2449	241	0.5000	0.1875	4.0816	0.1531
215	0.6875	0.1250	10.0000	0.2500	242	0.5000	0.1250	6.6667	0.1667
216	0.6875	0.0625	16.0000	0.2000	243	0.5000	0.0625	11.2000	0.1400
217	0.6875	0.0000	27.5000	0.0000	244	0.5000	0.0000	20.0000	0.0000

Table 2.12: PFR Reactors 3

i	$x(i)$	$y(i)$	$\tau(i)$	$\Delta C_c(i)$
245	0.4375	0.3750	0.4000	0.0300
246	0.4375	0.3125	0.9877	0.0617
247	0.4375	0.2500	1.8750	0.0938
248	0.4375	0.1875	3.2653	0.1224
249	0.4375	0.1250	5.5556	0.1389
250	0.4375	0.0625	9.6000	0.1200
251	0.4375	0.0000	17.5000	0.0000
252	0.3750	0.3125	0.4938	0.0309
253	0.3750	0.2500	1.2500	0.0625
254	0.3750	0.1875	2.4490	0.0918
255	0.3750	0.1250	4.4444	0.1111
256	0.3750	0.0625	8.0000	0.1000
257	0.3750	0.0000	15.0000	0.0000
258	0.3125	0.2500	0.6250	0.0313
259	0.3125	0.1875	1.6327	0.0612
260	0.3125	0.1250	3.3333	0.0833
261	0.3125	0.0625	6.4000	0.0800
262	0.3125	0.0000	12.5000	0.0000
263	0.2500	0.1875	0.8163	0.0306
264	0.2500	0.1250	2.2222	0.0556
265	0.2500	0.0625	4.8000	0.0600
266	0.2500	0.0000	10.0000	0.0000
267	0.1875	0.1250	1.1111	0.0278
268	0.1875	0.0625	3.2000	0.0400
269	0.1875	0.0000	7.5000	0.0000
270	0.1250	0.0625	1.6000	0.0200
271	0.1250	0.0000	5.0000	0.0000
272	0.0625	0.0000	2.5000	0.0000

CHAPTER 3

Steam methane based hydrogen production using low cost/temperature renewable energy

3.1 Introduction

Worldwide production of hydrogen is 50 million tons per year[2]. As can be seen in Figure 3.1, 96% of this production comes from fossil fuels, while only 1% comes from renewable resources[2, 62]. Hydrogen has numerous uses (see figure 3.2), as an industrial feedstock [2] (e.g., for methanol, ammonia, and subsequently fertilizer production), as an upgrading agent [62] (e.g., for converting heavier feed-stocks to lighter fuels in the refining industry), as gaseous fuel [63](e.g. in fuel cells for both electricity generation & hydrogen fueled vehicles), and as liquid fuel [64] (e.g. in space craft for propulsion).

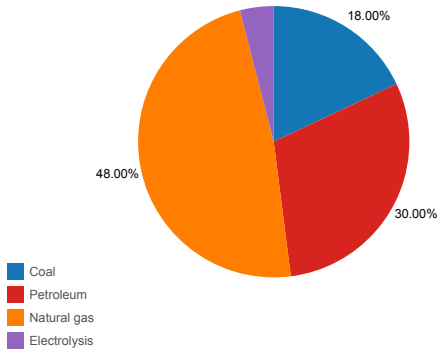

Figure 3.1: Worldwide Hydrogen Production[2]

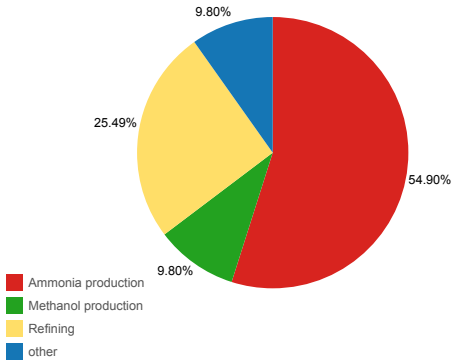

Figure 3.2: Worldwide Hydrogen Utilization [2]

Increasing the percentage of renewable energy used in hydrogen production is a major challenge, whose successful resolution can yield significant benefits, such as increased sustainability of the energy supply, and reduced carbon dioxide (CO_2) emissions to the atmosphere [65]. To better understand how this goal may be pursued, it is instructive to briefly review the evolution of hydrogen production methods.

The steam-iron hydrogen production process, developed in early days of the 20^{th} century, is one of the oldest commercial hydrogen production methods [66, 67].

Industrially hydrogen was first produced from coke and steam, using the Haber Bosch process [68].

Over the past forty years, the evolution of hydrogen production technologies has culminated into processes with increased efficiency, enhanced profitability, and reduced environmental impact. Figure 3.3, illustrates the currently prevalent hydrogen production pathways, using a variety of technologies and multiple energy resources. Electrolysis splits water into oxygen and hydrogen using electricity which can come from nuclear or renewable energy sources (e.g., solar, wind, hydro and geothermal) [69]. Its main advantage is the high purity of the obtained hydrogen (which enable its utilization in fuel cells), while its disadvantages include low efficiency, and consumption of a high quality energy form (electricity). Biomass can be used to generate hydrogen either through a hydrolysis/fermentation combination, or through pyrolysis and/or gasification, whereby syngas and bio gas are first generated as raw

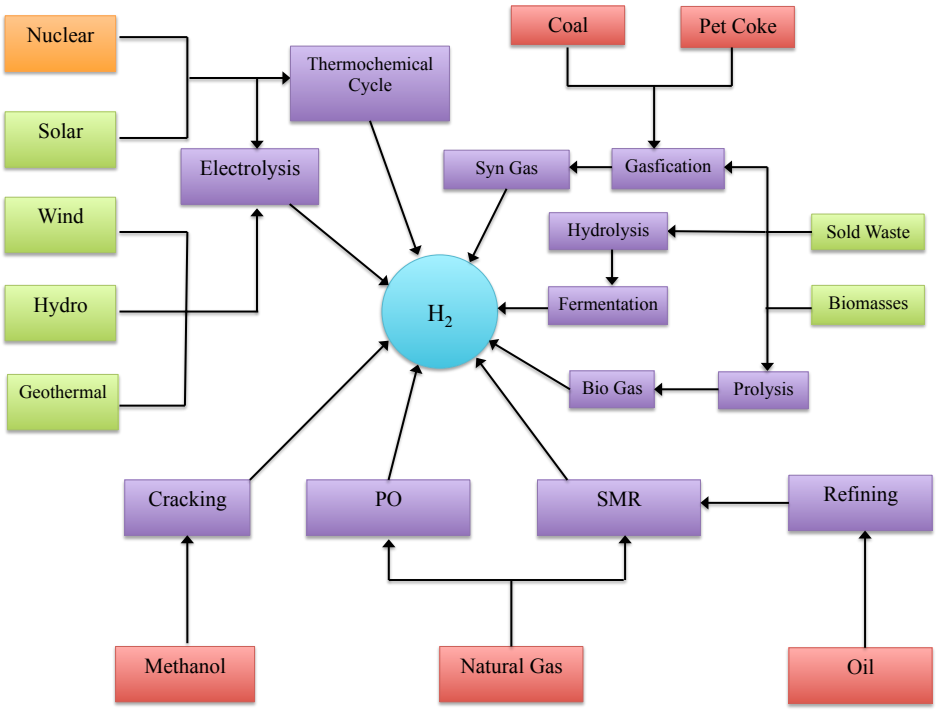

Figure 3.3: Hydrogen Production Pathways [3, 4]

material for subsequent hydrogen production [70]. A lot of work have been done on developing biomass conversion routes, however we are still far away from the day where biomass would replace fossil fuels. Water-splitting thermo-chemical cycle based hydrogen production, utilizing either nuclear or concentrated solar energy, is a zero CO_2 emission process undergoing significant technological development, but yet to be commercialized [71]. Coal based hydrogen production is one of the most economically efficient methods of hydrogen production, but is burdened with high CO_2 emission rates.[70]. Partial oxidation (POX) is a catalytic process in which oxygen is mixed with methane or low quality feeds(e.g. low value natural as, coal, coke)[72, 2], to generate hydrogen with no external heat input, but its faced with the major safety concern of the wide explosive range of the oxygen/hydrogen mixture.

Natural gas has become the main source of hydrogen, due to cost effectiveness, high hydrogen to carbon ratio, and wide availability[72]. Steam Methane Reforming (SMR) is

the most commonly used process to produce hydrogen from natural gas[2, 73].

The first steam reforming plant was built in 1930s, by BASF and Standard Oil, as part of the Baton Rouge Refinery[74, 75]. During the early days of 20^{th} century BASF played a major role in the development and industrialization of the steam methane reforming (SMR) process. The process has been undergoing continuous technological development, which led to more efficient catalysts, and improved reactor and separation designs. The process is highly endothermic and its external energy needs are typically supplied by burning a portion of the natural gas in a furnace[76]. BASF was the first to carry out the SMR in multiple reactor tubes within a heated furnace, where natural gas was burned to provide the aforementioned endothermic load. The process operates near equilibrium(950 to 1,250 K and 25-30 bar[77]), and utilizes a nickel-alumina catalyst[77].

The aforementioned use of natural gas as both raw material and fuel in SMR based hydrogen production, suggests that a straightforward strategy to increase the percentage of renewable energy used in hydrogen production is to reduce or eliminate the use of natural gas as fuel in reforming. Past experience (see SO_x, NO_x emission reductions) indicates that technological developments are often coupled to the enactment of legislation. Worldwide carbon tax legislation is currently either being contemplated or enacted. Several categories of carbon related taxation are considered, with some focusing on carbon dioxide emissions (carbon emission taxes), and others focusing on taxing the "burning" of fossil fuels, while leaving untaxed their use as raw materials. Thus in a world where fossil fuel "burning" is taxed, the SMR process will be partially taxed for its portion of natural gas used as fuel. The position put forward in this work, is that a means of reducing (or even avoiding) such taxation is to reduce the high temperature reformer's endothermic load (or even to alter it to being exothermic). In this way the reformer fuel requirements will be reduced or eliminated. Of course, the transformation of methane to hydrogen still necessitates energy input. However, such energy input need not be provided at the high temperature conditions of the reformer, but rather at a lower temperature, where alternative, renewable energy sources may be brought to bear. Indeed, such a reconfiguration of the energy input would open the

way for hybrid fossil-fuel/renewable designs of the SMR process, where the natural gas is used predominantly as raw material, while the renewable energy resource is used to meet the process energy needs. Such a potential renewable energy resource is concentrated solar power (CSP), whereby reflectors are used to concentrate the sun's radiation and transform it to heat [78]. CSP is typically implemented in solar trough, solar tower and solar dish configurations[78]. A variety of working fluids can be used, including molten salts and synthetic oils, and low operating cost energy can be delivered at a variety of temperature levels. According to the National Renewable Energy Laboratory, solar towers can currently deliver temperatures of 835K, and are expected to reach 920K by 2020. This is also confirmed by [78], who states that CSP tower plants using molten salts can deliver temperatures around 820K. Similarly, solar troughs can currently deliver 720K, and are expected to reach 773K by 2020. It thus becomes apparent that hot utilities at 770 K, and 420 K, can be delivered by concentrated solar power (CSP) tower and trough plants. CSP is eligible for fixed interest rate government bonds (loans) and feed- in tariffs (FIT). Fixed interest loans ease the financial burden of the capital cost associated with installing and maintaining solar power equipment. FIT is an energy policy tool designed to motivate the deployment of renewable energy resources in the form of payments for electricity produced. in Cyprus CSP is entitled to a FIT at the rate of 0.26 €/kWh as part of the government plan to produce 13% of total electricity consumed from renewable resources by 2020[78].

The remainder of this chapter is structured as follows. First, the status of carbon tax legislation around the world is surveyed. The main idea is next presented, in a section where the basics of steam methane reforming (SMR) are first reviewed, and then transitioning a reformer from being endothermic to being exothermic is presented. Subsequently, the proposed energetically enhanced steam methane reforming process is presented, including alternative process designs with varying levels of endothermicity. Heat integration for each of these designs is then carried out, so that their real energy consumption needs are properly quantified. Energy cost rates for which the proposed process is superior to traditional reforming are then identified. Finally, the presented process is discussed and conclusions are

drawn.

3.2 Worldwide status of carbon pricing legislation

Legislation aiming to reduce Green House Gas (GHG) emissions is currently being contemplated and/or enacted around the world, including the Kyoto (1990s), Paris (2015) and Marrakesh (2016) international agreements on climate change. Carbon pricing programs aim to accomplish two basic objectives: reduce the burning of fossil fuels and boost the deployment rate of renewable energy resources. To realize such objectives two legislative approaches have been put forward. Carbon tax is an explicit surcharge on carbon emissions set by governments, this format is similar to the way central banks set interest rates to reach specific inflation target (setting a price to reach an emissions target in this case). The implementation of carbon taxes started in the Nordic countries in the early 1990s (Denmark (1992), Finland (1990), Norway (1991) and Sweden (1991) and later in the UK (2001). On the other hand, in cap-and-trade based systems carbon price is determine by the trading of quotas (emission permits) generated by auctioning or free allocations (benchmarking or grandfathering)[79, 80]. In such systems, emitters have the choice of strategically placing the emissions reductions under an overall quota objective rather than the restriction of an explicit carbon tax. However, such flexibility results in longer emissions reduction periods compared to carbon taxes. Income from both programs provides a reliable revenue stream due to its dependence on an inelastic commodity (fossil fuel emissions)[81].

Close examination of the aforementioned carbon legislation reveals a differentiation between *combustion processes* where fossil fuels are burned and *non-combustion processes* where fossil fuels is used as a feed. Fossil fuel combustion accounts for 68% of the global GHG emissions of which 90% is carbon dioxide (CO2), while industrial processes (non-combustion sources) account for 7% of the global GHG emissions [82]. 42% of the CO2 from fossil fuels combustion comes from electricity and heat generation. Due to the importance of such products a consistent pattern of emission taxation exemption is observed around the world,

the results of such exemptions will be presented in details later in this section. However, when it comes to *non-combustion processes* a universal agreement is yet to be reached with carbon legislations around the world coming up with different answers.

The European Union's carbon legislation (EU ETS) is a cap-and-trade system first established in 2005[83]. EU ETS covers only 45% of the entire EU greenhouse gas (GHG) emissions, [84], where the rest of the emissions are either exempt (transportation), under other regional carbon legislations (carbon tax) or need to reach a certain threshold (instillation size) to be counted against the cap. Another reason is coverage since the EU ETS covers emissions from the following GHG only:: carbon dioxide (CO_2), nitrous oxide (N_2O), perfluorocarbons ($PFCs$). The structure of the system allows for an overall GHG emissions target to be met even if some individual countries fail to maintain their targets3.1[6]. Under the EU ETS legislative directive, a *broad interpretation* of combustion installations is defined as "All combustion installations that produce electricity, heat or steam, even if their main purpose is not energy production, but e.g. the production of ethylene or ammonia (e.g. naphtha crackers or ammonia plants)." [84]. This broad interpretation is used in the following countries: Austria, Belgium, Denmark, Finland, Ireland, Latvia, Portugal and Sweden [85]. An alternative *medium interpretation* states: "All combustion installations that produce electricity, heat or steam, with the purpose of energy production, including those that are process-integrated, e.g. a steam plant integrated in e.g. chemical industry is included, but process furnaces such as crackers in the petrochemical industry are excluded." [84]. This interpretation is used in Estonia, Germany, Lithuania, Luxembourg and the UK [85]. Finally, a *narrow interpretation* states: "Only combustion installations that produce electricity, heat or steam and supply that to third parties." [84] and is used in France, Italy and Spain [85].

The above three EU ETS interpretations make clear that within this EU legislation not all CO_2 emissions are equal. Indeed CO_2 emissions not directly resulting from electricity, heat or steam generation may be excluded from regulation. Due to the combined use of the EU ETS and the climate change levy in the UK and the transparent legislative exemptions the

picture is clearer. Natural gas used in the production of hydrogen via steam reforming is an example of fossil fuels being used as a feed in industrial processes. The UK exempts natural gas fed to reformers for the production of hydrogen from the climate change levy[86]. Such exemption aligns with the UK adoption of the *medium interpretation*. In the EU ETS *broad interpretation* similar industrial feed stocks would count against the emission cap. With the emergence of carbon legislations worldwide, a major point of emphasis is *carbon leakage*, where high emissions industries would decide to move their operations to countries with no carbon legislations. To compensate for the effect of losing business competitiveness under *carbon leakage*, certain carbon legislations offers offsets it terms of free allocations (permits). Sector by sector eligibility takes place where industries are benchmarked to determine the free allocations (permits). The New Zealand Emissions Trading Scheme offers such free allocations (permits) to high emissions industrial emissions to cover the trade exposure and avoid losing any competitive advantage[87].

Emissions reductions in Denmark was a result of the implementation of carbon tax in May 1992, the current irate is $31 per ton of CO_2 which sum up to $ 1 billion in annual revenues part of which is used to refund carbon emissions covered by the EU emissions trading system (EU ETS)[5, 6, 88]. Norway introduced the carbon tax in 1991 with a variable rate between $ 4-60 per ton of carbon dioxide that results now in $ 1.58 billion of annual revenues [89, 88]. The upper limit of the varying rate is applied on Norway oil & gas sector which generates most of the county's gross domestic product(GDP) and the fact that the industry is Norway's biggest carbon dioxide emitter [90]. Sweden established a carbon tax in 1991 as part of a reform package to the energy tax legislations to reduce oil dependence and carbon dioxide emissions , the current rate is $ 168 per ton of carbon dioxide and results in annual revenues of $ 3.68 billion [6, 89, 88, 91]. Carbon emissions covered by the EU emissions trading system (EU ETS) are carbon tax exempt in Norway and Sweden. The implementation of carbon taxes in Noridc countries resulted in a positive economical impact, based on world bank GDP data the economy of Denmark grow by 93.3 % and the economy of Sweden grow by 82.2% while the economy of Norway grow by a staggering 219% [6]. Meanwhile between the carbon

tax implementation and 2008, emission data shows that carbon dioxide emissions dropped in Denmark and Sweden by 18.1% and 15.1% while an increase of 64.6% was reported in Norway[6]. The emissions reductions in Denmark and Sweden can be attributed to the government subsides for renewable energy and energy efficiency coupled with the effect of the carbon tax implementation[90]. The equity of carbon taxes in the Nordic countries can be examined by comparing the ratio of carbon taxes to total energy taxes which is 15.4% for Denmark, 28.6% for Norway and 25% for Sweden[81].

The EU emissions trading system (EU ETS) enabled reduction of carbon emissions but it faced some criticisms which was used by the US senate to reject a similar proposal of implementation in 2009[92, 79]. One of the reasons used to turn down the proposal was China which is the US main economic competitor did not act on reducing industrial emissions[92]. China passed the US as the world number one carbon dioxide emitter in 2006 and as of 2013 China is responsible for 30% of the world carbon dioxide emissions[93]. Like the US, China did not implement a full scale carbon pricing programs at the time. However, this is expected to change in 2017 when China will role out the world largest carbon cap-and-trade system. China dependence on cheap electricity from coal will change in 2017 with an expected shift to natural gas and nuclear power plants[92]. The program offers incentives to cleaner power generation plants that leaves lower Greenhouse Gases (GHG) footprint with a target of reducing emissions by more than 40% of 2005 levels [5, 92]. With such changes in China the US is expected to follow suit by introducing a carbon pricing program in the next few years. Meanwhile, Japan introduced carbon tax in October 2012 as a measure of reducing carbon dioxide emissions and a main component of the tax policy will focus of taxing fossil fuels burned within chemical process. The carbon tax rate is 2.89 $ per ton of carbon dioxide and will end up costing each Japanese household 1.3 $ per month[94]. the revenues generated from the tax legislations will be directed to climate change mitigation efforts, improving energy efficiency and finance renewable energy projects[94].

In terms of market size, The EU emissions trading system (EU ETS) is the world largest carbon pricing program with with 2,000 million metric tons (MMT) of GHG emissions and

a price of $ 7 per ton. The largest carbon tax program is in Japan which governs 800 MMT (70% of Japan emissions) at a price of $ 3 per ton [5]. in 2017, after experimenting with several pilot program China will roll out the largest GHG emissions quota trading system. China's cap and trade system will control 5,000 MMT , to put this number in perspective this program will control and price 13% of the world's total emissions. Table 3.1 show that countries with carbon pricing programs have achieved reductions in carbon dioxide emissions compared to 1990 levels. Such reductions can be attributed to fuel switching(Coal to Natural gas), deployment of renewable energy technologies, improved energy efficiency and the economic slowdown of 2008.

Table 3.1: World Emission Data (1900-2011)[6]

CO2 Emissions	1990	2011	% Change
China	2,460,744	9,019,518	72.72%
Denmark	50,231	40,377	-24.40%
European Union	4,081,647	3,574,100	-14.20%
Finland	51,745	54,767	5.52%
France	375,633	338,805	-10.87%
Germany	930,000	729,000	-27.57%
India	690,577	2,074,345	66.71%
Ireland	31,243	36,069	13.38%
Japan	1,094,288	1,187,657	7.86%
Netherlands	158,403	168,007	5.72%
Norway	31,386	45,533	31.07%
Portugal	42,196	49,725	15.14%
Spain	218,597	270,676	19.24%
Sweden	51,947	52,145	0.38%
United Kingdom	555,903	448,236	-24.02%
United States	4,823,557	5,305,570	9.09%

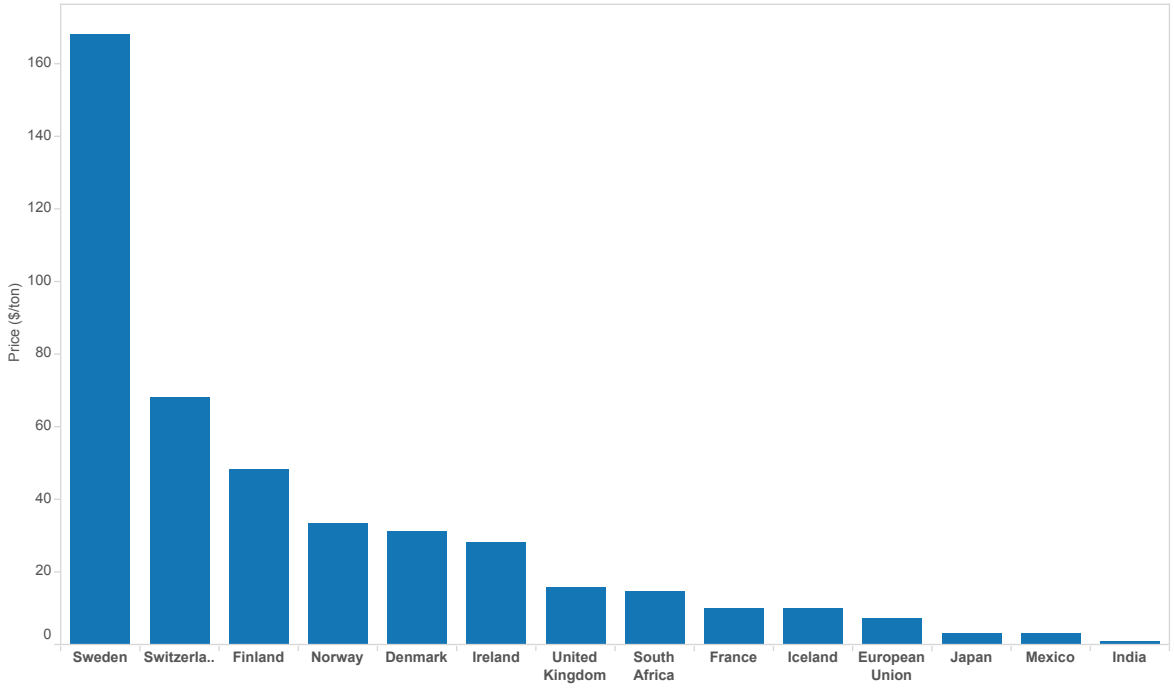

Figure 3.4: CO2 emissions prices worldwide [5]

In terms of prices, Figure 3.4 show carbon prices world wide. Sweden, is where we have the world highest carbon price with $ 168 per ton of carbon dioxide emitted. Japan, is where we find the lowest carbon price with $ 2.89 per ton of carbon dioxide emitted.

3.2.1 Fossil fuels combustion

Before going through the details of carbon pricing programs it's imperative to explain the effect of such programs on the technology presented in this chapter. Certain carbon pricing programs target fossil fuel processing by distinguishing between *combustion processes* where fossil fuels are burned and *non-combustion processes* where fossil fuels are not burned. Burning fossil fuels is the main contributor to carbon emissions world wide (99% of total carbon dioxide emissions cite(2016)) with 42% coming from electricity and heat generation, which depends on a fuel mix consisting mainly of coal and natural gas. Electricity and heat generation carbon dioxide emissions shows high dependence on coal in the following countries: China(97%) , India (95%) , Japan(54%) and the US(75%) [82]. Hence a special considera-

Table 3.2: Carbon dioxide emissions from fuel combustion (2005-2013)

	CO_2 Fuel Combustion (Mt CO_2)			Total Primary Energy Supply (TPES)	
Country	2005	2013	% change	TPES (PJ)	CO_2/TPES (tCO_2 per TJ)
China	5359.72	8977.1	67.5%	126000.58	71.25
Czech Republic	118.46	101.13	-14.6%	1756.41	57.58
Denmark	48.43	38.81	-19.9%	730.45	53.13
Germany	786.76	759.6	-3.5%	13299.72	57.11
India	1086.46	1868.62	72.0%	32466.34	57.56
Ireland	44.24	34.36	-22.3%	546.8	62.84
Italy	456.27	338.22	-25.9%	6505.12	51.99
Japan	1196.15	1235.06	3.3%	19035.47	64.88
Norway	34.55	35.29	2.1%	1369.35	25.77
Russia	1481.66	1543.12	4.1%	30600.9	50.43
Saudi Arabia	419.1	472.38	12.7%	8046.24	58.71
United Kingdom	476.62	448.71	-5.9%	7994.8	56.12

tion is given to *non-combustion processes* in certain carbon pricing programs. For example, in the EU emissions trading system (EU ETS) and other carbon tax programs fossil fuels are counted against the cap or taxed for *combustion processes* but not in *non-combustion processes* with exceptions to fuels used for electricity generation. The EU mandate state that fuels used in power generation are tax exempt but countries like Czech Republic and Italy place taxes on such fuels for environmental reasons[95]. To show the impact of the various carbon pricing legislative approaches reviewed in this chapter we will examine the carbon dioxide emissions data for the following countries: China, Czech Republic, Denmark, Germany, India, Ireland, Italy, Norway ,Russia, Saudi Arabia and the UK. In terms of total carbon dioxide emissions from *combustion processes* we will examine for the period 2005-2013 as shown in Table 3.2.

Carbon dioxide emissions from fuel combustion decline in all countries with carbon pric-

ing programs in this study with the exception of Japan and Norway. Following the 2011 Fukushima incident Japan moved away from nuclear power generation (27% of total power generated in 2005) to fossil fuel based power generation(31% coal and 43% natural gas in 2013). Such a switch resulted in the overall increase in carbon dioxide emissions between 2005 and 2013 as shown above. The case of Norway can be explained in two levels: consumer and corporate. In Norway, where citizens enjoy one of the highest income levels (GDP per capita) around the world behavioral economics is a key factor at the consumer level. The population of Norway simply accepted the economical penalties represented by rising transportation fuels prices associated with the implementation of carbon taxes and choose convenience over economical savings and environmental impact [90]. At the corporate level, Norway variable carbon tax rate hit the oil & gas companies hard, but since such companies are profit oriented and were enjoying a boom period; behavioral economics didn't play a critical part at the corporate level. The oil & gas companies in Norway responded by addressing the problem in a sustainable fashion by investing heavily in carbon capture and sequestration (CCS) technologies [90]. The work done by such companies in the 1990s and the early 2000s resulted in first wave of commercial CCS plants around the world. In 2008, Norway coupled its carbon tax system with the EU ETS to cover areas not covered by the existing carbon taxes system (55% of the emissions are covered by carbon tax). The environmental corporate approach and the policy changes in 2008 resulted in a reduction of carbon dioxide emissions by 6.4% between 2010 and 2013 [6]. Countries without carbon pricing legislative policy experienced a growth in emissions over the period between 2005 and 2013: China (67.5%), India (72.0%), Russia (4.1%) and Saudi Arabia (12.7%).

Table 3.3 shows that Germany experienced an increase of 1.2% in carbon dioxide emissions from the electricity & heat generation sector between 2010 and 2013. Over the same period countries taxing fuel combustion in electricity generation experienced a decline in carbon dioxide emissions: Czech Republic (-12.2%), Ireland(-14.5%) and Italy (-18.2%). This is attributed to two factor: the fuel mix used in electricity & heat generation and the country's legislative position on taxing electricity & heat generation fuels. In terms of fuel mix, Ger-

Table 3.3: Carbon dioxide emissions form electricity & heat generation (2005-2013)

	CO_2 Sector Emissions (Mt CO_2)			Electricity & Heat		
Country	2010	2013	% change	$\frac{gCO_2}{kWh}$	Output (tWh)	Fossil fuels share(%)
China	3498.26	4386.21	25.4%	680.1	6449.4	78%
Czech Republic	63.86	56.1	-12.2%	468.2	119.8	54%
Denmark	22.15	16.92	-23.6%	233.5	72.5	54%
Germany	338.22	342.32	1.2%	448.6	763.0	61%
India	790.48	944.58	19.5%	791.5	1193.5	80%
Ireland	13.13	11.23	-14.5%	435.5	25.8	78%
Italy	135.91	111.18	-18.2%	319.5	348.0	61%
Japan	477.05	594.41	24.6%	568.8	1045.1	87%
Norway	2.91	1.99	-31.6%	14.2	140.8	2%
Russia	891.93	943.5	5.8%	368.4	2561.2	67%
Saudi Arabia	178.31	206.49	15.8%	727.0	284.0	100%
United Kingdom	176.61	169.64	-3.9%	454.6	373.1	65%

many's coal share of the fuel mix increased from (44%) to (46%) with a decline in nuclear and natural gas shares of the fuel mix from (23%) and (14%) to (16%) and (12%) respectively. In the Czech Republic, coal fuel mix share declined from (58%) to (51%) while nuclear fuel mix share increased from (33%) to (35%) with an additional share coming from solar (2%). In Italy, coal and oil fuel mix shares declined from (15%) and (7%)to (14%) and (6%) with additional share coming from solar (8%). In Ireland some of the decline in carbon dioxide emission can be attributed to reduced electricity & heat demand which returned to 2004 levels but in terms of fuel mix wind share experienced an increase from (9%) to (28%)[6]. In terms of legislative position Germany does not tax fuels used in electricity & heat generation while Czech Republic and Italy tax such fuels for environmental reasons with Ireland only taxing natural gas for Combined Heat and Power (CHP) Generation. Ireland started a carbon tax in 2010 at rate of €15 per tonne of CO_2 initially that later grow to €20 per tonne of CO_2, during the first three years Ireland netted around €1 billion[96]. The tax legislations resulted in a decline of carbon dioxide emissions from fuel combustion by 22.3% since 2005, some might argue that this was a result of an economical recession but in 2011 alone the same emissions dropped by 10.45% coupled with a growing economy[97]. This kind of decline in emission is usually attributed to the use of more renewable energy resource in the fuel mix, according to the Irish Wind Energy Association 28% of Ireland electricity needs are generated via wind energy. This enabled Ireland to tax the more cleaner fossil fuels like natural gas since 2012 at a rate of €4.10 per MWh which is based tax rating of €20 per tonne of CO_2. Natural gas as a feed to the to the chemical and petrochemical industries is tax exempt[98]. The aforementioned statistics shows that improvements in the fuel mix and the legislative stance on electricity & heat generation fuels contributed favorably to reducing carbon dioxide emissions.

3.3 Transitioning from traditional to energetically enhanced reforming

The crude-oil refining industry consumes ever increasing amounts of hydrogen, mainly in its crude oil cracking operations. In fact, the reduced hydrogen content of U.S crude oil reserves is creating situations where refinery hydrogen demand exceeds hydrogen supply. Currently, the preferred method for large scale hydrogen production is steam methane reforming (SMR) of natural gas. Traditional reformers are operated industrially near equilibrium conditions around 1150K (at 950 K to 1,250 K and 25-30 bar[77]) with a high endothermic heat load that is provided through the burning of natural gas and other fossil fuel resources. The SMR process involves the following three reactions[99]:

$$CH_4 + H_2O \longrightarrow CO + 3H_2 \quad (r1) \quad \Delta H1 : 206.1\ kJmol^{-1}$$

$$CO + H_2O \longrightarrow CO_2 + H_2 \quad (r2) \quad \Delta H2 : -41.15\ kJmol^{-1}$$

$$CH_4 + 2H_2O \longrightarrow CO_2 + 4H_2 \quad (r3) \quad \Delta H3 : 164.9\ kJmol^{-1}$$

According to Le Chatelier's Principle, the forward reactions r1 and r3 are favored at low pressures, (e.g. 1 bar), but kinetic considerations necessitate the use of high pressures (e.g. 5-25 bar), and steam to methane molar ratios (e.g. α=3.1) exceeding the stoichiometric value (α=2.1), to insure high levels of methane conversion (above 90%). At equilibrium conditions, (r3) is linearly dependent on (r1) & (r2) and can thus be ignored. Tables 3.4, 3.5and 3.6 below show the inlet and resulting outlet species molar flowrates, and associated heat load, of a traditional Steam Methane Reformer operating at equilibrium, at various temperatures, and at P=5 bar. These results are obtained using the UNISIM software package, utilizing the Peng Robinson thermodynamic model, and are confirmed using total Gibbs free energy minimization calculations. They indicate that high methane conversions are attained, and that highly endothermic loads are required.

It is thus apparent that enhancing the energy consumption profile of the SMR process requires that the aforementioned endothermic heat loads be reduced. In our earlier work,

Table 3.4: Baseline case (950 K)

Inlet (Kmol/hr)			Outlet (Kmol/hr)					T=950 K
CH_4	CO	H_2O	CH_4	CO	CO_2	H_2O	H_2	Heat Load (kJ/s)
1	0	2	0.357019	0.315989	0.326992	1.030027	2.255935	36.88944639
1	0	3	0.228872	0.314748	0.456381	1.772491	2.769766	43.60485157
1	0	5	9.15E-02	0.27291	0.635569	3.455952	3.361006	50.40256858
1	0	10	1.23E-02	0.167385	0.820331	8.191954	3.783477	53.52254265
1	0	15	2.94E-03	1.15E-01	8.82E-01	13.12095	3.873162	53.49859292
1	0	20	1.02E-03	8.71E-02	0.911884	18.08913	3.90883	53.32546527

[100, 101], we established that a reactor's heat load may be possible to reduce through the use of a reactor network. In particular, we established theoretically, and demonstrated through case studies, that if the universe of possible reactor networks contains either only endothermic or only exothermic units, then the energy consumption associated with carrying out a particular set of reaction tasks does not depend on the network structure, [100]. On the other hand, if the universe of possible reactor networks contains both endothermic and exothermic units, then the energy consumption associated with carrying out a particular set of reaction tasks depends on the network structure, and can be possibly reduced through the use of an appropriate network, [101]. Close examination of the reactions taking place in the SMR quickly reveals that although the overall process is endothermic, one of the reactions taking place within the reactor is exothermic. Indeed, the reaction ($CO+H_2O \longrightarrow CO_2+H_2$) has an exothermic load of ($-41.15\ kJmol^{-1}$).

Definition 3.1: *Energetically Enhanced Steam Methane Reforming (EESMR) is a method for hydrogen production with an enhanced reaction profile resulting in reducing or entirely eliminating the associated steam methane reforming endothermic heat load*

The proposed Energetically Enhanced Steam Methane Reforming (EESMR) process aims to improve the environmental and economic profile of the SMR process, by reducing the SMR endothermic heat load. The chemistry of hydrogen production from natural gas consist of

Table 3.5: Baseline case (1050 K)

Inlet (Kmol/hr)			Outlet (Kmol/hr)					T=1050 K
CH_4	CO	H_2O	CH_4	CO	CO_2	H_2O	H_2	Heat Load (kJ/s)
1	0	2	0.111282	0.622987	0.265731	0.845552	2.931884	53.18640267
1	0	3	4.58E-02	0.547912	0.406315	1.639459	3.268995	55.93858188
1	0	5	1.14E-02	0.406976	0.581619	3.429786	3.547404	56.40386442
1	0	10	1.23E-03	0.235687	0.763078	8.238156	3.759374	55.29476117
1	0	15	2.99E-04	0.164639	0.835062	13.16524	3.834166	54.66161207
1	0	20	1.05E-04	0.126373	0.873522	18.12658	3.873206	54.30461295

Table 3.6: Baseline case (1150 K)

Inlet (Kmol/hr)			Outlet (Kmol/hr)					T=1150 K
CH_4	CO	H_2O	CH_4	CO	CO_2	H_2O	H_2	Heat Load (kJ/s)
1	0	2	1.92E-02	0.773227	0.207618	0.811538	3.150152	59.81567777
1	0	3	6.35E-03	0.652679	0.340972	1.665376	3.321926	59.37056547
1	0	5	1.50E-03	0.489838	0.508666	3.49283	3.504178	58.10331219
1	0	10	1.72E-04	0.299659	0.700169	8.300003	3.699654	56.39202126
1	0	15	4.34E-05	0.215657	0.7843	13.21574	3.784169	55.61219775
1	0	20	1.57E-05	0.168418	0.831567	18.16845	3.83152	55.17142133

Table 3.7: EESMR case (1050 K)

Inlet (Kmol/hr)			Outlet (Kmol/hr)					T=1050 K
CH_4	CO	H_2O	CH_4	CO	CO_2	H_2O	H_2	Heat Load (kJ/s)
1	1	2	0.195553	1.32241	0.482036	0.713517	2.895376	45.79983088
1	3	2	0.317363	2.890938	0.791699	0.525665	2.839609	35.15185961
1	5	2	0.399228	4.60835	0.992422	0.406807	2.794736	28.06737944
1	10	2	0.515176	9.221342	1.263482	0.251695	2.717953	18.16189217
1	15	2	0.573886	14.03173	1.394386	0.179501	2.672727	13.20782496
1	20	2	0.608667	18.92147	1.469866	0.138801	2.643865	10.29330447
1	3	5	9.43E-02	2.182369	1.723291	2.371048	4.440274	40.12149182
1	5	5	0.165924	3.619487	2.214589	1.951335	4.716816	30.86129469
1	10	5	0.330637	7.665991	3.003372	1.327265	5.011462	12.8703939
1	15	5	0.454346	12.08053	3.465127	0.989218	5.102091	0.626447093
1	20	5	0.544231	16.6931	3.762673	0.781558	5.129979	-7.901561803
1	5	10	4.73E-02	2.551045	3.401616	5.645722	6.259601	26.80974384
1	10	10	0.155172	5.909069	4.935759	4.219412	7.470244	5.155381023
1	15	10	0.282906	9.768743	5.948352	3.334554	8.099635	-12.6878066
1	20	10	0.405559	13.92542	6.669017	2.736542	8.45234	-27.37890321
1	10	15	7.61E-02	4.742091	6.181785	7.894338	8.953415	-1.95000895
1	15	15	0.169672	8.147716	7.682611	6.487061	10.17359	-22.38496694
1	20	15	0.279877	11.91671	8.803409	5.476468	10.96378	-40.17806354
1	15	20	0.103469	6.944181	8.95235	10.15112	11.64194	-30.52636747
1	20	20	0.19016	10.37335	10.43649	8.753667	12.86601	-50.36933256

Table 3.8: EESMR case (1150 K)

Inlet (Kmol/hr)			Outlet (Kmol/hr)					T=1150 K
CH_4	CO	H_2O	CH_4	CO	CO_2	H_2O	H_2	Heat Load (kJ/s)
1	1	2	3.63E-02	1.610381	0.353336	0.682948	3.244485	57.36209
1	3	2	6.32E-02	3.39136	0.545445	0.51775	3.355861	53.85461
1	5	2	8.25E-02	5.251157	0.66635	0.416144	3.418869	51.4984
1	10	2	0.112054	10.05412	0.83383	0.278224	3.497668	48.05649
1	15	2	0.128473	14.95162	0.919905	0.208568	3.534486	46.2101
1	20	2	0.138835	19.88902	0.972149	0.166685	3.555645	45.06446
1	3	5	1.15E-02	2.505102	1.483427	2.528043	4.449015	48.28266
1	5	5	2.03E-02	4.093203	1.886476	2.133846	4.825511	43.92312
1	10	5	0.04236	8.448592	2.509048	1.533313	5.381967	36.66148
1	15	5	0.060724	13.07359	2.865686	1.195038	5.683515	32.1399
1	20	5	7.52E-02	17.82781	3.096944	0.978302	5.871208	29.04316
1	5	10	5.31E-03	2.951882	3.04281	5.962497	6.026887	33.98685
1	10	10	1.68E-02	6.611587	4.371641	4.645132	7.321324	20.73264
1	15	10	3.09E-02	10.73965	5.22948	3.801393	8.136861	11.75248
1	20	10	0.04519	15.1248	5.830013	3.215177	8.694444	5.185292
1	10	15	8.12E-03	5.419378	5.572502	8.435619	8.548141	9.974855
1	15	15	1.77E-02	9.099499	6.882844	7.134814	9.829871	-2.98361
1	20	15	2.91E-02	13.12058	7.850295	6.178828	10.76293	-12.8308
1	15	20	1.08E-02	7.888105	8.101123	10.90965	11.06881	-14.017
1	20	20	1.94E-02	11.57884	9.401732	9.6177	12.34344	-26.8281

Table 3.9: CH_4 equilibrium conversion, and endothermic load temperature dependence

P=1 bar and α=3.1		
Temperature (K)	Conversion %	Heat load (kJ/s)
900	89.35%	50.9
950	96.61%	56.08
1000	99.03%	58.26
1050	99.71%	59.27
1100	99.91%	59.9
1150	99.97%	60.38
1200	99.99%	60.77

steam methane reforming (SMR), dry methane reforming(DMR) and partial oxidation of methane (POX) as shown in table 3.10. Due the complex chemistry of hydrogen production from natural gas distinctions become less clear with different reactions taking place at the same conditions. therefore, industrially its common to use different reforming routes and multiple reformers with high temperatures and steam to tailor the final products specifications. The advantages of this route is reducing the reaction residence time.

Table 3.10: Reformer reactions routes

Reaction	$\Delta H\ kJmol^{-1}$	reaction number	Process
$CH_4 + H_2O \longrightarrow CO + 3H_2$	206	$r1$	SMR
$CO + H_2O \longrightarrow CO_2 + H_2$	-41.15	$r2$	WGSR
$CH_4 + 2H_2O \longrightarrow CO_2 + 4H_2$	164.9	$r3$	SMR
$CH_4 + CO_2 \longrightarrow 2CO_2 + 2H_2$	247	$r4$	DMR
$CH_4 + \frac{1}{2}O_2 \longrightarrow CO + 2H_2$	-36	$r5$	POX

We notice in table 3.10 that the water gas shift reaction (WGSR) ($r2$) and the partial oxidation reaction (POX) ($r5$) are the only exothermic reactions from the group. Integrating WGSR or POX with the conventional SMR will lead to reduction of the reformer heat

load. POX, however, comes with inherent safety concerns (O_2/H_2 mixtures have a wide explosive range) and the need for an air separation unit to provide oxygen for the process. Integrating WGSR with SMR overcomes the aforementioned safety concerns and the need for use of an air separation unit by controlling the CO/H_2O ratio in the feed. This is accomplished by introducing into the reformer feed significantly higher amounts of water (H_2O) and significant amounts of carbon monoxide (CO). This introduction significantly enhances the reaction rate of the aforementioned reaction, which transforms carbon monoxide and water to carbon dioxide and hydrogen. Since this reaction is exothermic, its enhancement alters the endothermic nature of the overall reforming process as demonstrated in the attached closed-loop flowsheets. Implementation of this altered reforming mode requires more amounts CO than typically produced from steam methane reforming. This can be accomplished incorporating a Reverse Water Gas-Shift Reactor (RWGSR) that comes with a low temperature small endothermic heat load. This heat load can be addressed by renewable energy from concentrated solar power in order to entirely eliminate the burning of natural gas in the SMR process.

In this section we will present detailed process simulation designs examining the conventional endothermic steam methane reforming and the newly developed energetically enhanced exothermic steam methane reforming processes. The cases presented here detail the process energetic enhancement compared to conventional SMR. All process flow sheets designs are simulated with Peng-Robinson equation of state in a commercial flowsheet simulator (UNISIM by Honeywell). Heat and power integration analysis is carried out using the UCLA in-house software[38].

3.3.0.1 Case 1

The baseline production method is illustrated in Figure 3.5. It features a combined feed of H2O/CH4 at ratio of 3/1 to a reformer operating temperature and pressure of 1100K and 25 bar respectively. The reformer has **endothermic heat load of 42.6 kJ/s**. Thus **a reformer furnace is needed**. Material and energy stream data for this flowsheet are

provided in Tables 3.11 and 3.12.

The overall flowsheet inlets are 1 kmol/h methane, 0.9 kmol/h water, and 3.6 kmol/h air, and the overall flowsheet outlets are 4 kmol/h hydrogen and 1 kmol/h carbon dioxide. Following pumping to 25 bar, the water stream is mixed with a recycle stream comprised of the liquid outlets from the two flash units Flash Drum and Flash Drum-2, and then heated to 1100K. The methane stream is compressed and heated to 25 bar and 1100K, and then mixed with the water stream to form the feed to the reformer, which operates at 1100K and 25 bar. The reformer outlet is cooled to 650K and fed to a HTS reactor operating at 650K and 25 bar. The outlet of the HTS reactor is further cooled to 475K, then fed to an LTS reactor operating at 475K and 25 bar. Afterwards, the LTS reactor outlet is cooled to 313K, then fed to a flash separation unit (Flash Drum), operating at 313K and 25 bar, to recycle the water back to the inlet of the reformer. The vapor outlet from the flash separation unit is then fed to a separation unit to extract hydrogen at 20 bar from the stream. The remaining waste gas at 1 bar from the hydrogen separation unit is heated to 1100K before being fed to a combustor operating at 1115K and 1 bar. An inlet stream of 3.6 kmol/h of air at 1 bar is preheated to 1100K before being fed to the combustor along with the waste gas stream. The combustor outlet stream is cooled back to 313K and fed to a second flash separation unit operating at 313K and 1 bar to remove the H2O from the stream. The recycled H2O is pumped to 25 bar and mixed with the H2O outlet from the first flash separation unit and recycled back to the reformer inlet. Pinch analysis-based heat integration is carried out (with a ΔT_{min} of 4 K), making available three hot utilities at 1200K, 770K, and 420K, and one cold utility at 298K.

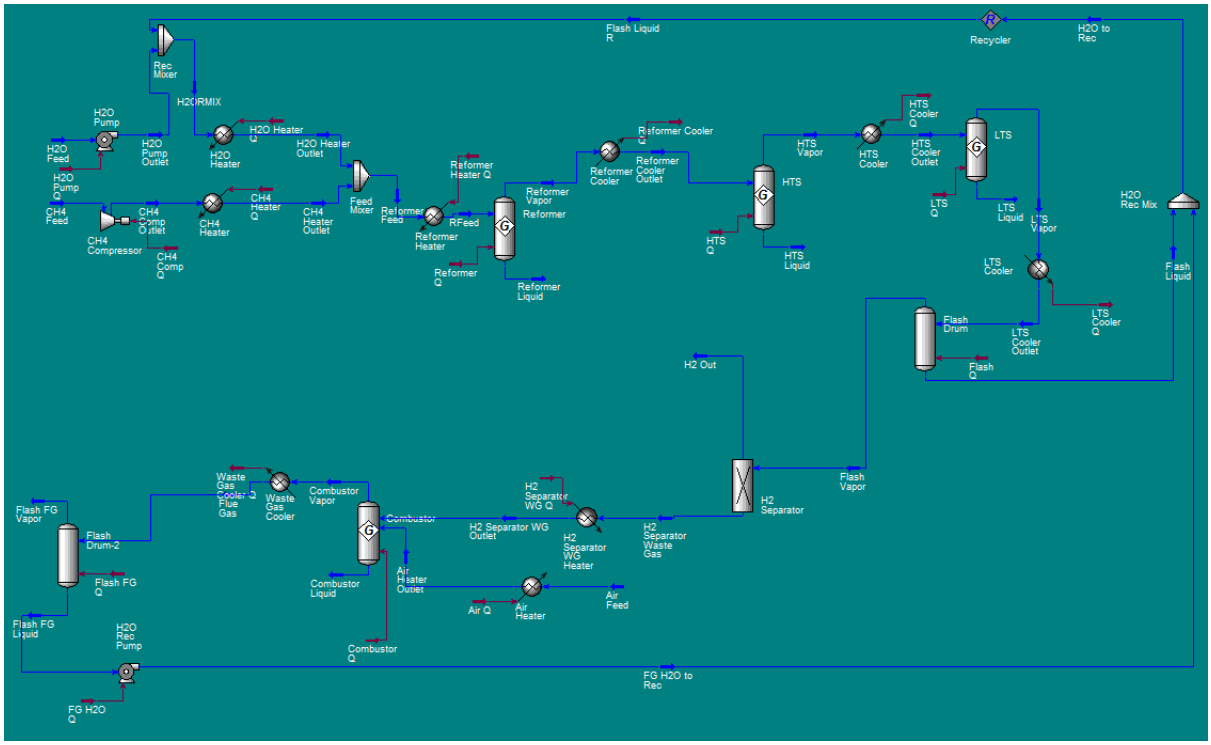

Figure 3.5: UniSim flowsheet of case 1

3.3.0.2 Case 2

The proposed production method is illustrated in Figure 3.6. Material and energy stream data for this flowsheet are provided in Tables 3.11 and 3.12. The overall flowsheet inlets are 1 kmol/h methane and 2 kmol/h water, and the overall flowsheet outlets are 4 kmol/h hydrogen and 1 kmol/h carbon dioxide. Following water pumping and methane compression to 5 bar, both streams are heated to 1140K, are mixed with a CO/H_2O recycle stream also heated to 1140K, and are then fed to the reformer, creating a reformer feed with 18/15/1 $H_2O/CO/CH_4$ ratio. The reformer operating temperature and pressure are 1140K and 5 bar respectively. The reformer has an **exothermic heat load of -0.8529 kJ/s** at 1140K. The reformer product stream is cooled to 750K and mixed with the recycle stream which is also at 750K. The resultant mixture stream is further cooled to 313K, and then fed to an adiabatic flash distillation vessel V-100 operating at 5 bar and 313 K that separates most of the liquid

water, which is then used to form the reformer recycle stream. The flash vapor product is fed to a carbon dioxide capture unit. The carbon dioxide outlet of the CO_2 capture unit is then split, at a ratio of 4.8/95.2, into the pure carbon dioxide outlet product of the overall flowsheet, and a carbon dioxide stream fed to the reverse water gas-shift reactor (RWGSR). The carbon dioxide-lean product emanating from the carbon dioxide capture unit is then fed into a hydrogen separation process which separates the hydrogen gas, and recycles the remaining gases to the reformer feed stream. The pure hydrogen outlet of the separation process is then split, at a ratio of 15/85, into the pure hydrogen outlet product of the overall flowsheet, and an hydrogen stream fed to the reverse water gas-shift reactor (RWGSR). The resulting carbon dioxide/hydrogen mixture is then heated to 750K and fed to reverse water gas-shift reactor (RWGSR). The RGS reactor has an endothermic heat load need of 62.46 kJ/s at 750K. The RWGSR exit stream is recycled to the inlet of the aforementioned adiabatic flash. Pinch analysis-based heat integration is carried out (with a ΔT_{min} of 4K) making available three hot utilities at 1200K, 770K, and 420K, and one cold utility at 298K.

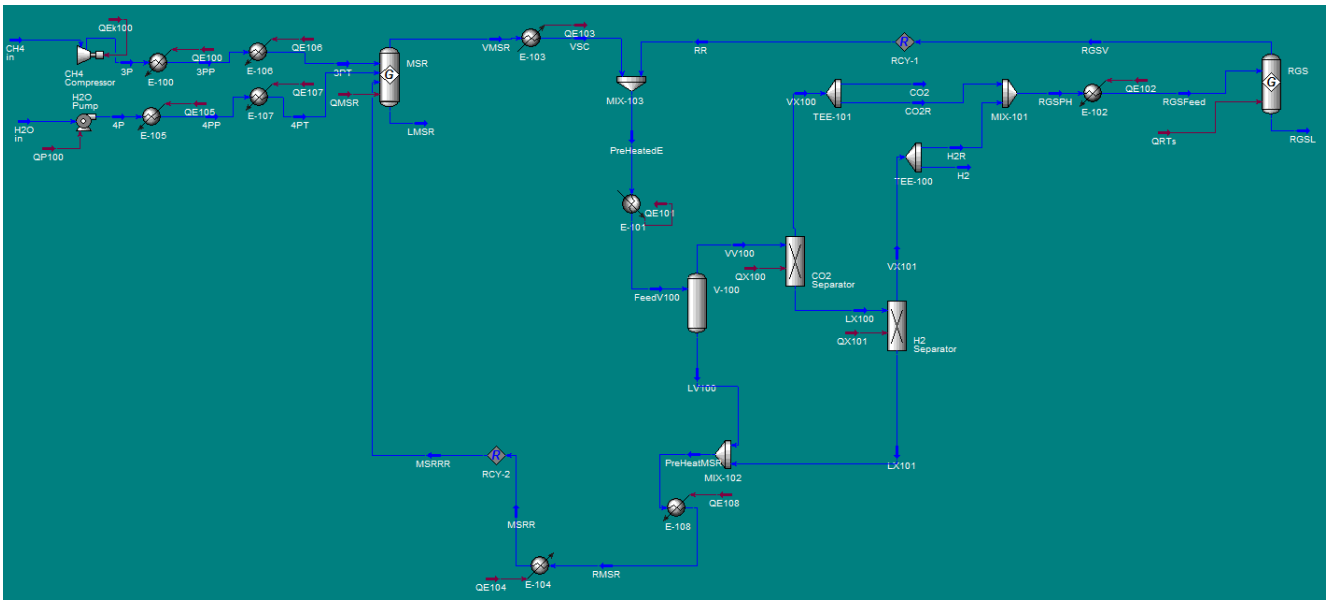

Figure 3.6: UniSim flowsheet of cases 2 & 5

3.3.0.3 Case 3

The proposed production method is illustrated in Figure 3.7. Material and energy stream data for this flowsheet are provided in Tables 3.11 and 3.12. The overall flowsheet inlets are 1 kmol/h methane and 1.1 kmol/h water, and the overall flowsheet outlets are 3.1 kmol/h hydrogen and 1 kmol/h carbon dioxide. This process is basically the same as case study 2, except that part of the hydrogen stream is now burned with air in a combustor operating at 1200K. The **heat load generated in the combustor (61.7 kJ/s)** is such that the endothermic needs of the process are met, so that heat integration analysis indicates no need for hot utility use at 1200K. The combustor outlet is then cooled and processed through a flash separator to remove water. The flash vapor outlet is a nitrogen-rich stream which is released to the environment. The flash liquid outlet is then heated first to 740K and then to 1140K and finally recycled to the reformer. Pinch analysis-based heat integration is carried out (with a ΔT_{min} of 4K) making available three hot utilities at 1200K, 770K, and 420K, and one cold utility at 298K.

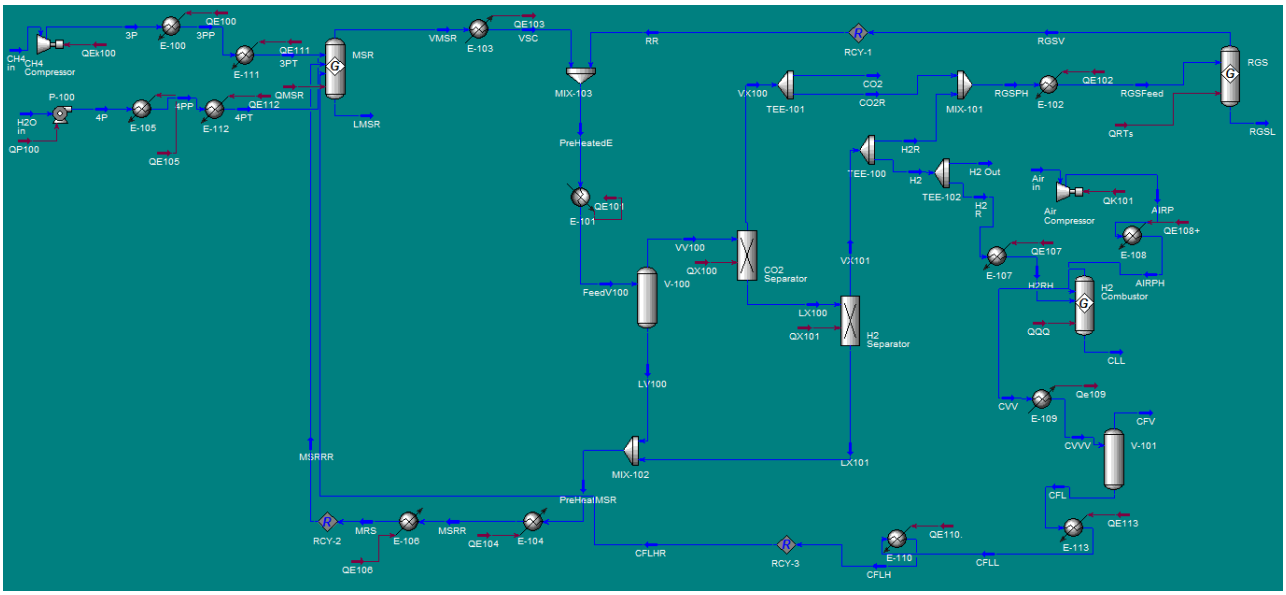

Figure 3.7: UniSim flowsheet of cases 3 & 4

3.3.0.4 Case 4

This process is basically the same as case study 3, except the fact that the**reformer is now endothermic with a heat load of 24.04 kJ/s** and this load is matched by the output of**the combustor which produces 26.38 kJ/s in an exothermic heat load**. The minimum utility cost solution reveals that **no 1200K or 420K hot utility is needed while 114.5898 kJ/s of 770K hot utility is needed (36.25 kJ/s of which is used to meet the reverse water gas-shift reactor (RWGSR) endothermic heat load and 66.2738 kJ/s of 298K cold utility is needed**.The proposed production method is illustrated in Figure 3.7. Material and energy stream data for this flowsheet are provided in Tables 3.11 and 3.12. The overall flowsheet inlets are 1 kmol/h methane and 1.6 kmol/h water, and the overall flowsheet outlets are 3.6 kmol/h hydrogen and 1 kmol/h carbon dioxide. This process is basically the same as case study 3, except the fact that the reformer is now **endothermic with a heat load of 24.04 kJ/s** and this load is matched by the output of the combustor which produces **26.38 kJ/s in an exothermic heat load**.

3.3.0.5 Case 5

This process is basically the same as case study 2, except for the fact that an amine-based carbon dioxide separator unit is selected as the carbon dioxide separation technology. As such, the proposed production method is illustrated in Figure 2, material and energy stream data for this flowsheet are provided in Tables 3.11 and 3.12. Since the amine-based carbon dioxide separator unit employs its own reboiler and condenser, additional hot and cold utility loads must be employed.

3.3.0.6 Case 6

This process is basically the same as case study 2, except for the fact that we are quantifying the effect of the combustor by replacing it with external utilities. Another target is also to study the effect of temperature pressure and temperature against the rest of the cases. It

features a combined feed of H_2O/CH_4 at ratio of 2.82 to a reformer operating temperature and pressure of 1145K and 5 bar respectively.

The design inlets are 1 kmol/h methane, 2.0 kmol/h water and the overall flowsheet outlets are 4 kmol/h hydrogen and 1 kmol/h carbon dioxide. Following pumping to 5 bar, the water stream is mixed with a recycle stream and then heated to 1145K. The methane stream is compressed and heated to 5 bar and 1145K, and then mixed with the water and recycle streams to form the reformer feed(5 bar and 1145K). The reformer product outlet is cooled to 650K and fed to a High Temperature Shift (HTS) reactor (650K and 5 bar). The product outlet of the HTS reactor is cooled to 475K, then fed to a Low Temperature Shift (HTS) reactor operating (475K and 5 bar). Afterwards, the LTS reactor outlet is cooled to 313K, then fed to a flash separation unit (313K and 5 bar) from which water is recycled back to the inlet of the reformer. The vapor outlet from the flash separation unit is then fed to an hydrogen separation unit to extract hydrogen from the stream. The remaining waste gas from the hydrogen separation unit is fed to a second flash separation unit operating(313K and 5 bar) to remove the water from the stream. The recycled water is mixed with the water outlet from the first flash separation unit and recycled back to the reformer inlet.

3.3.0.7 Case 7

As illustrated in case 2, Energetically Enhanced Steam Methane Reforming(EESMR) is capable of altering the endothermic needs of a reformer by eliminating the associated heat load. Here, we will show that a minor energetic enhancement is enough to reduce the endothermic heat load. As we have shown earlier that the change of the heat load is mostly associated with the water and the carbon monoxide in the feed as shown in table 3.14.

In identifying the reboiler and condenser loads for the CO_2 amine-based capture process used in case 2,3,4 and 5 the hot and cold utility loads for the amine process, as reported in [102], are employed: Reboiler Energy to Mass Ratio: 4.49 $\frac{GJ}{ton}$ CO_2 captured Condenser Energy to Mass Ratio: 2.49 $\frac{GJ}{ton}$ CO_2 captured Since for case 2 the amount of carbon dioxide

Table 3.11: Process material and energy stream data 1

Description	Case1	Case2	Case3	Case4	Case5
Overall CH_4 inlet (kmol/h)	1.00	1.00	1.00	1.00	1.00
Overall H_2O inlet (kmol/h)	0.90	2.00	1.10	1.60	2.00
Overall AIR inlet (kmol/h)	3.60	0.00	3.40	1.00	0.00
Overall H_2 outlet (kmol/h)	2.60	4.00	3.10	3.60	4.00
Overall CO_2 outlet (kmol/h)	1.00	1.00	1.00	1.00	1.00
HU (1200K) energy consumption (kJ/s)	0.00	0.00	0.00	0.00	0.00
HU (770K) energy consumption (kJ/s)	0.00	62.64	0.00	114.59	62.57
HU (420K) energy consumption (kJ/s)	0.00	18.49	0.90	0.00	1157.60
CU (298K) energy consumption (kJ/s)	40.20	2.99	3.73	66.27	633.58
mol CH_4 fed to reformer (kgmol/h)	1.00	1.03	1.03	1.01	1.03
mol CO fed to reformer (kgmol/h)	0.00	14.64	14.64	6.61	14.64
mol H_2O fed to reformer (kgmol/h)	2.90	17.70	17.70	17.46	17.70
mol CO_2 fed to reformer (kgmol/h)	0.00	0.22	0.22	0.30	0.22
mol H_2 fed to reformer (kgmol/h)	0.00	0.27	0.27	0.36	0.27
mol CH_4 from reformer (kgmol/h)	0.28	0.03	0.03	0.01	0.03
mol CO from reformer (kgmol/h)	4.14	8.70	8.70	3.33	8.70
mol H_2O from reformer (kgmol/h)	1.87	9.76	9.76	12.18	9.76
mol CO_2 from reformer (kgmol/h)	0.31	7.17	7.17	4.58	7.17
mol H_2 from reformer (kgmol/h)	2.48	10.22	10.22	7.64	10.22
Reformer heat load (kJ/s)	42.56	-0.85	-0.85	24.04	-0.85

captured by the amine process is 20.65 kmol CO_2 /hr, it then holds: Reboiler Load: (4.49 $\frac{GJ}{ton}$ CO_2) * (0.044 ton CO_2/kmol CO_2) * (20.65 kmol CO_2/hr) / (3600 $\frac{s}{hr}$)= 1.13 MJ/s Condenser Load: (2.49 $\frac{GJ}{ton}$ CO_2) * (20.65 $\frac{kmol}{hr}$) * (0.044 ton CO_2/kmol CO_2)/ (3600 $\frac{s}{hr}$)=-0.633 $\frac{MJ}{s}$. Both designs 1 and 2 has the added advantage that it generates carbon dioxide as a pure product that is ready for carbon sequestration or for any other use. The minimum work

Table 3.12: Process material and energy stream data 2

Description	Case1	Case2	Case3	Case4	Case5
Reformer heat load per mol CH4 fed to reformer	42.56	-0.83	-0.81	23.90	-0.83
mol CH_4 fed to RWGSR-CO_2 reactor (kgmol/h)	n/a	0.00	0.00	0.00	0.00
mol CO fed to RWGSR-CO_2 reactor (kgmol/h)	n/a	0.14	0.14	0.06	0.14
mol H_2O fed to RWGSR-CO_2 reactor (kgmol/h)	n/a	0.00	0.00	0.00	0.00
mol CO_2 fed to RWGSR-CO_2 reactor (kgmol/h)	n/a	19.66	19.66	27.82	19.66
mol H_2 fed to RWGSR-CO_2 reactor (kgmol/h)	n/a	22.95	22.95	31.08	22.95
mol CH_4 from RWGSR-CO_2 reactor (kgmol/h)	n/a	0.00	0.00	0.00	0.00
mol CO from RWGSR-CO_2 reactor (kgmol/h)	n/a	6.08	6.08	3.36	6.08
mol H_2O from RWGSR-CO_2 reactor (kgmol/h)	n/a	5.94	5.94	3.29	5.94
mol CO_2 from RWGSR-CO_2 reactor (kgmol/h)	n/a	13.72	13.72	24.53	13.72
mol H_2 from RWGSR-CO_2 reactor (kgmol/h)	n/a	17.01	17.01	27.78	17.01
RWGSR CO_2 Reactor heat load (kJ/s)	n/a	62.46	62.46	36.25	62.46
Combustor heat load (kJ/s)	-81.41	n/a	-61.70	-26.38	n/a
Total work of compression (kJ/s)	3.49	1.77	8.13	3.64	1.77
Total work of pumping (kJ/s)	0.02	0.01	0.00	0.00	0.01
mol of CO_2 captured in Amine system(kmol/hr)	n/a	20.65	20.65	20.84	20.65
Minimum work for H_2 separation (kJ/s)	-2.21	17.57	17.57	12.05	17.57
Amine reboiler heat load (kJ/s), [3]	n/a	0.00	0.00	0.00	1142.00
Amine system condenser heat load (kJ/s) [3]	n/a	0.00	0.00	0.00	-633.00
Minimum Work for CO_2 separation (kJ/s)	n/a	25.48	25.48	29.83	25.48

of separation for the carbon dioxide separator and hydrogen separator units are determined using the equation $W_{min} = \sum nb_o - \sum nb_i$, where b is the work availability function, $b = H - T_oS$

3.4 Results and discussion

For all designs, we perform pinch analysis-based heat integration (with a ΔT_{min}=4 K), [103], to determine the minimum hot/cold utility energy consumption. Table 3.13 provides a summary comparison of the minimum utility cost solution for three case studies. The proposed heat exchange network can utilize four available utilities. There are three hot utilities available at 1200K, 770K and 420K respectively and one cold utility at 298K.

Table 3.13: Minimum utility cost solution (kJ/s)

	Case 2	Case 6	Case 7
Hot utility (1200K)	0	60.68	14.79
Hot utility (770K)	62.64	9.58	54.24
Hot utility (420K)	18.49	0.29	14.31
Cold utility (298K)	2.99	0	5.59
Refomer heat load	-0.85	60.68	13.93

A comparison between the conventional steam methane reforming (SMR) and energetically enhanced reforming (EESMR) is done by comparing the CO/H_2O ratios, reformer heat loads and utility needs in cases 2,6 and 7. Case 2 eliminate the reformer heat load while case 7 improves the minimum utility cost requirement of the reformer without entirely eliminating the reformer endothermic heat load. A comparison between these cases 6 and 7 show a reduction in the reformer endothermic heat load from 60.680 kJ/s to 13.93 kJ/s. For case 6 the minimum utility cost solution reveals that **60.68 kJ/s 1200K hot utility is needed while 9.58 kJ/s of 770K hot utility and 0.29 kJ/s of 420K hot utility is needed and no 298K cold utility is needed**. Case 7, the minimum utility cost solution reveals that **14.79 kJ/s 1200K hot utility is needed while 54.24 kJ/s of 770K hot utility and 14.31 kJ/s of 420K hot utility is needed and 5.59 kJ/s of 298K cold utility is needed**.

Energetic enhancements is at full display in case 2 the minimum utility cost solution

Table 3.14: Reformer heat load (kJ/s)

CO (kmol/hr) \ H_2O (kmol/hr)	1	5	10	15	20
1	50.31	55.00	52.08	50.61	49.83
5	41.45	44.43	36.26	30.96	27.43
10	39.39	36.30	23.15	13.75	6.88
15	38.55	31.01	13.81	1.02	-8.77
20	38.17	27.34	6.71	-8.98	-21.32

reveals that **no 1200K hot utility is needed (eliminating the need for a reformer furnace), 62.6441 kJ/s of 770K hot utility is needed (62.40 kJ/s of which is used to meet the RWGSR endothermic heat load, and the remainder ensures that the flowsheet's hot composite curve is above the cold composite curve in pinch analysis), 18.4920 kJ/s of 420K hot utility is needed, and 2.9870 kJ/s of 298K cold utility is needed**.

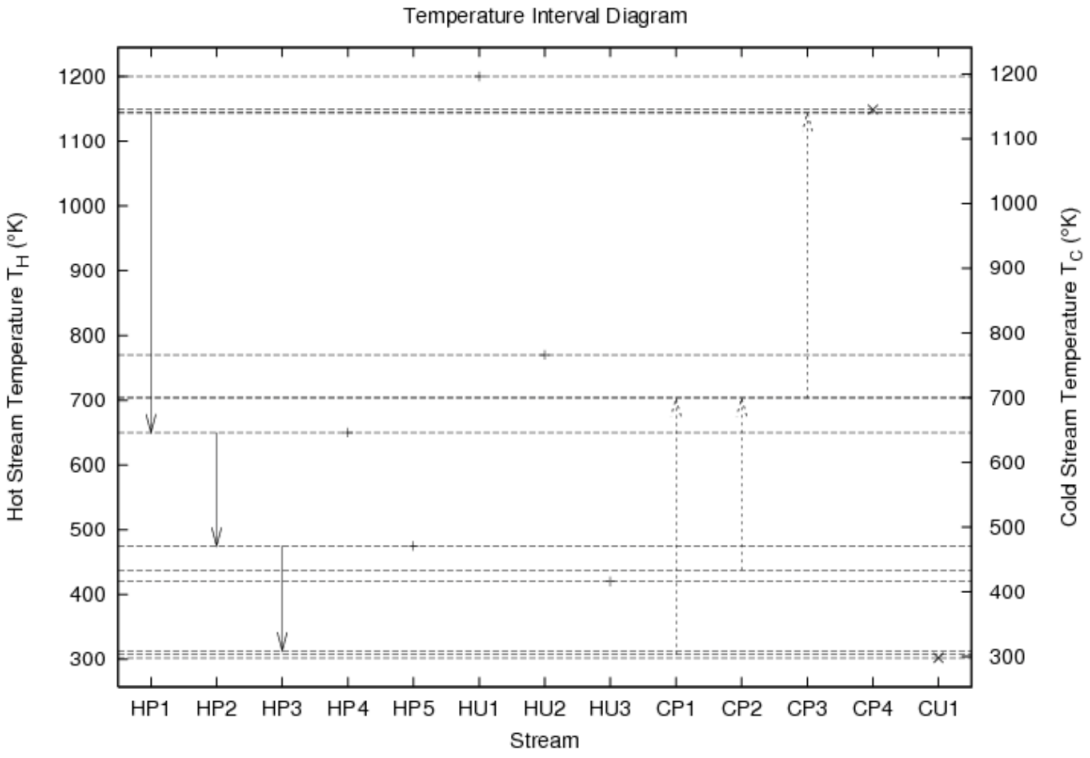

Figure 3.8: Temperature Interval Diagram CASE 2

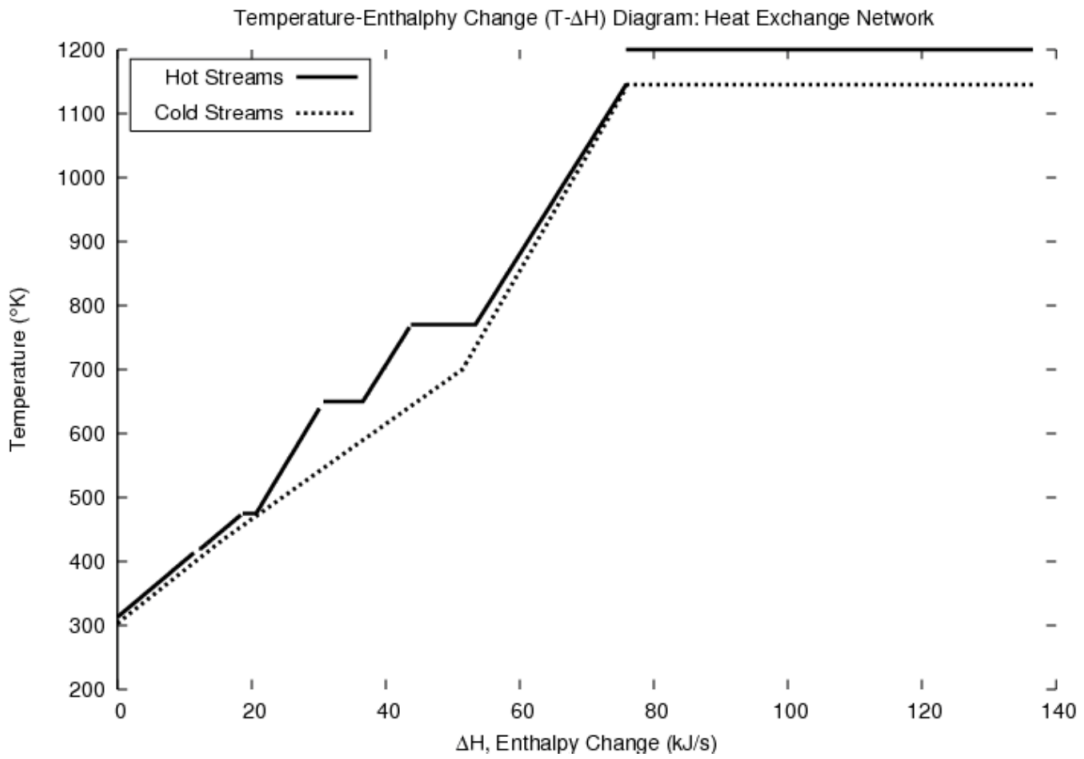

Figure 3.9: Temperature-Enthalpy Diagram CASE 2

For case 1 the minimum utility cost solution reveals that **no 1200K hot utility is needed, in addition to the heat provided by the combustor in a furnace. No 770K hot utility, and no 420 K hot utility is needed. However, 40.2022 kJ/s of 298K cold utility is needed. The amount of hydrogen produced is 2.6 kmol/hr, for a methane feed of 1 kmol/hr**.

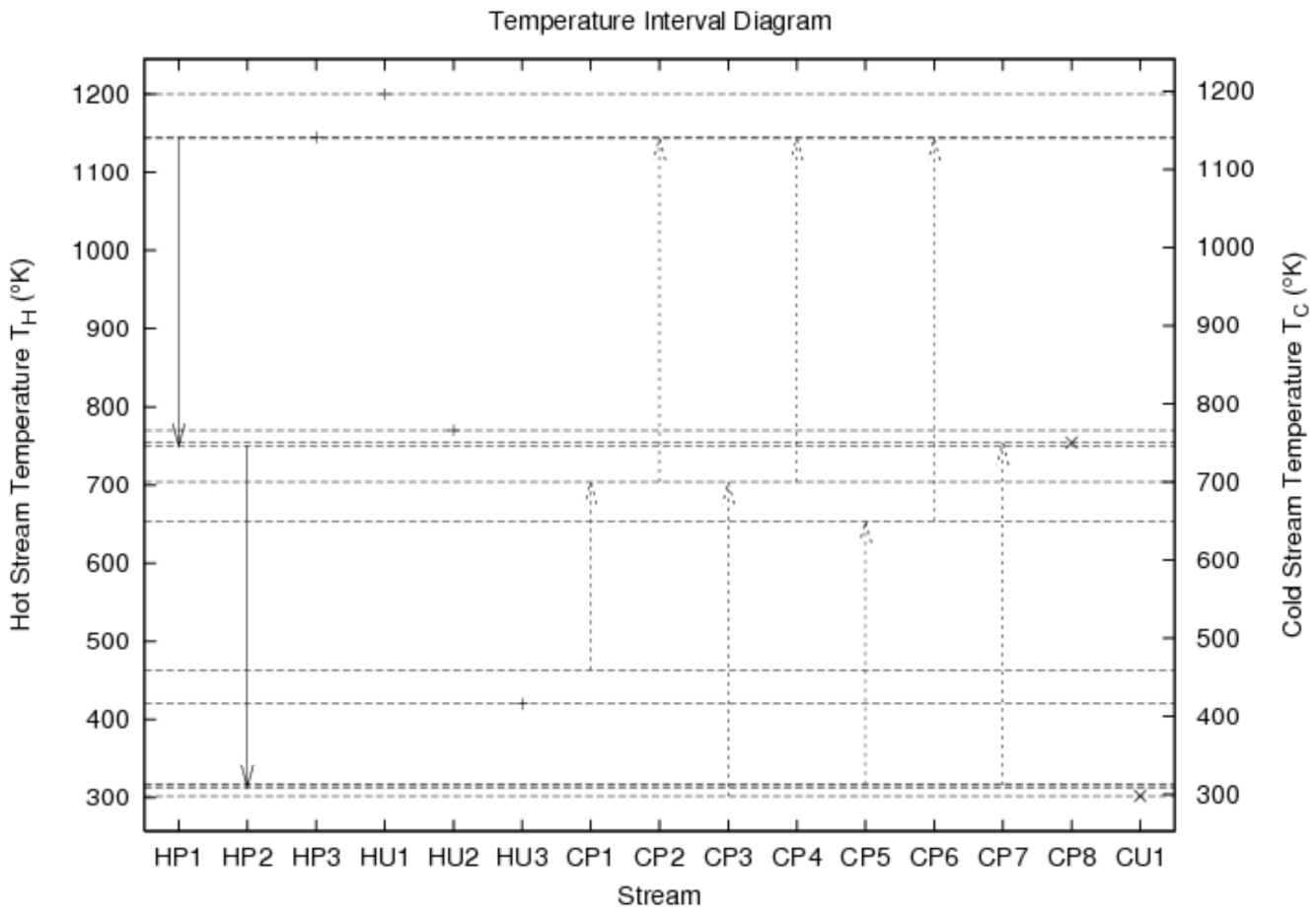

Figure 3.10: Temperature Interval Diagram CASE 6

For case 3 the minimum utility cost solution reveals that **no 1200K hot utility is needed (eliminating the need for a reformer furnace), no 770K hot utility is needed** , 0.9023 kJ/s 420K hot utility is needed, and 3.7294 kJ/s of 298K cold utility is needed.

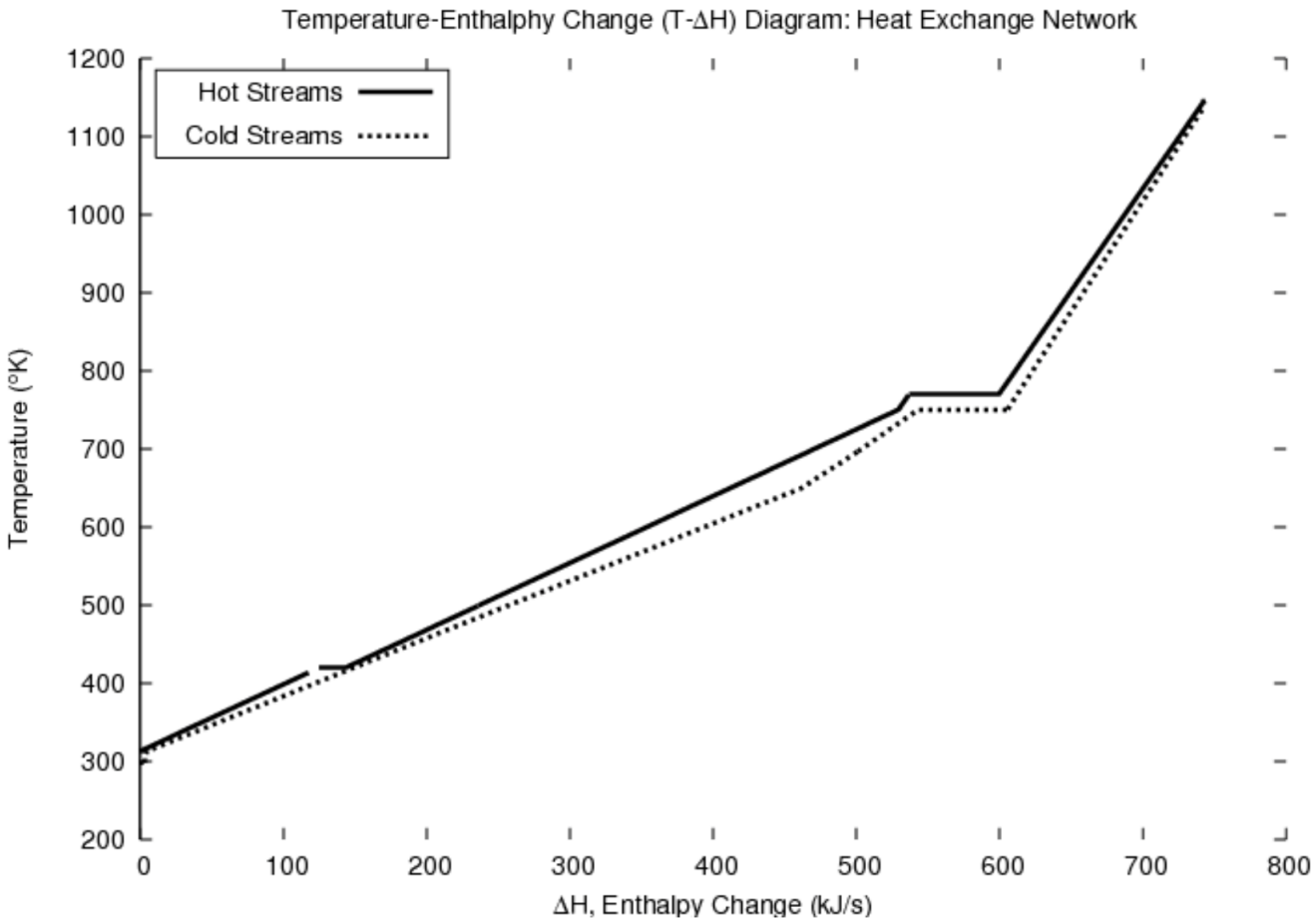

Figure 3.11: Temperature-Enthalpy Diagram CASE 6

For case 4 the minimum utility cost solution reveals that **no 1200K or 420K hot utility is needed while 114.5898 kJ/s of 770K hot utility is needed (36.25 kJ/s of which is used to meet the RWGSR endothermic heat load and 66.2738 kJ/s of 298K cold utility is needed.**

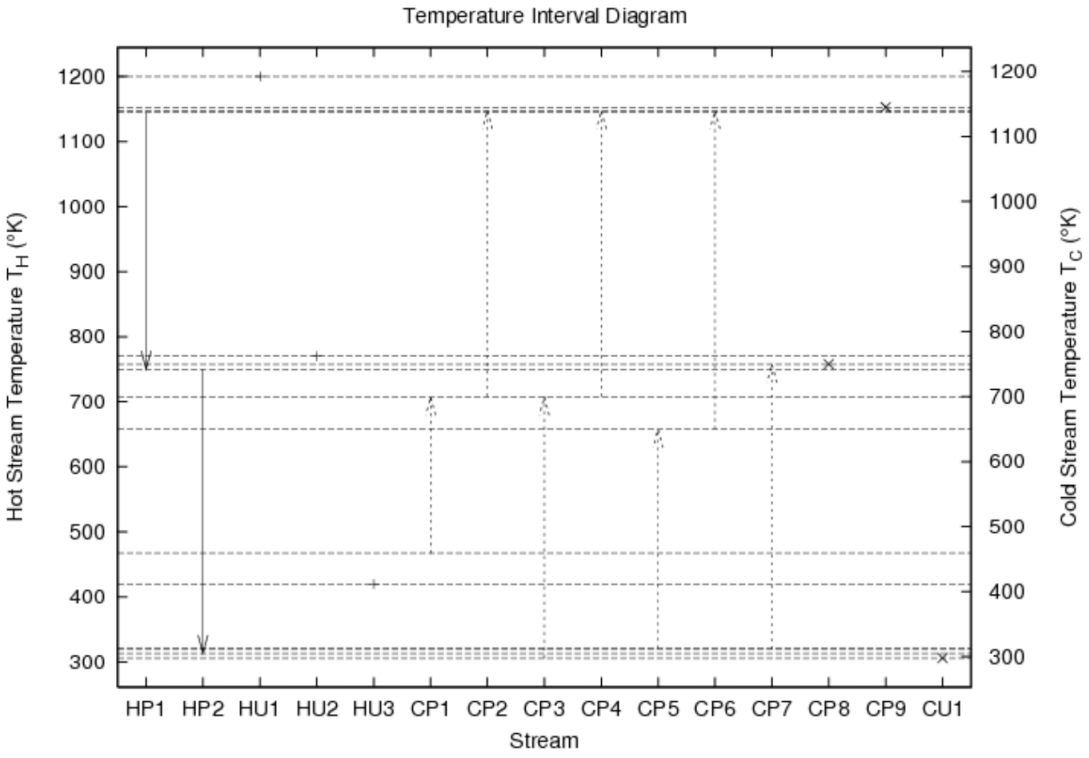

Figure 3.12: Temperature Interval Diagram CASE 7

For case 5 the minimum utility cost solution reveals that **no 1200K hot utility is needed while 62.5686 kJ/s of 770K hot utility and 1157.5990 kJ/s of 420K hot utility is needed and 633.5785 kJ/s of 298K cold utility is needed.**

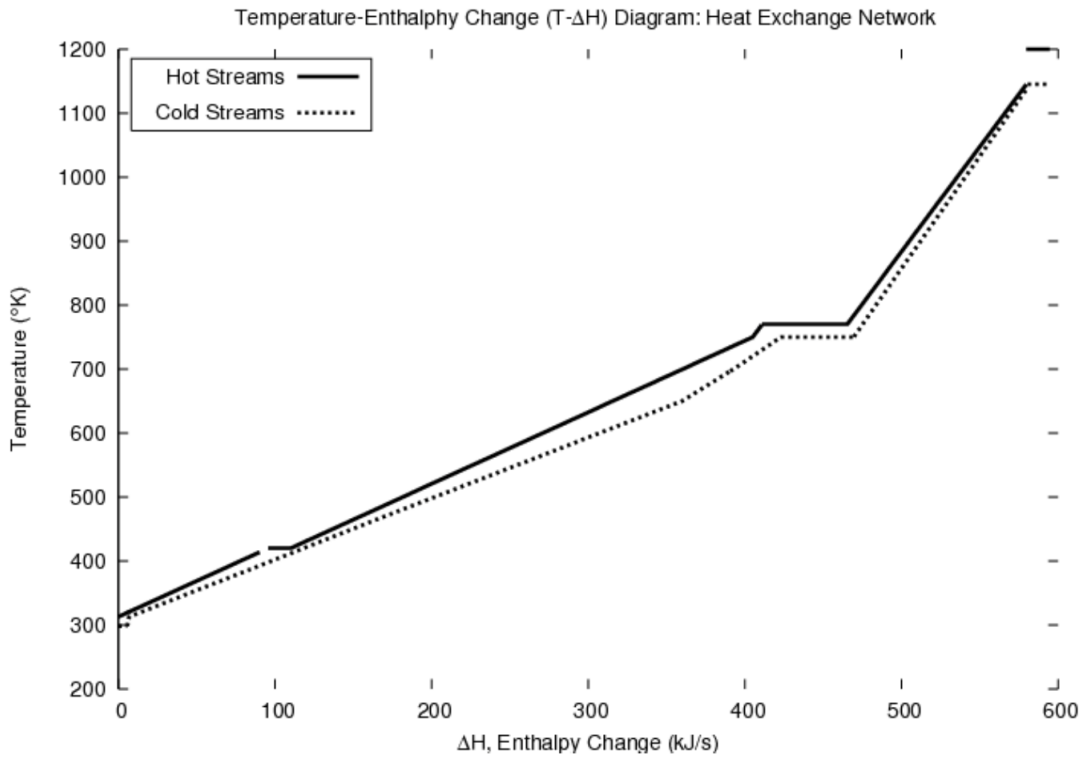

Figure 3.13: Temperature-Enthalpy Diagram CASE 7

Case 2 energetic features can be even further improved compared to the case 6 design by using renewable energy resources to supply the utilities at 770K and 420K respectively this is not applicable in case 6 due to the need of 1200K utility. A potential renewable energy resource that can be brought to bear as a hot utility for the above described energetically enhanced steam methane reforming processes is concentrated solar power (CSP) and trough plants[78, 104]. Another advantage of the case 2 flowsheet is that it requires no high energy (1200K) furnace, thus significantly reducing the capital cost of the overall reforming process and eliminates the need for burning fossil fuels in the process. By using renewable energy instead burning fossil fuels to supply the needed utilities, case 2 (EESMR) delivers a hydrogen production method thats immune to current and future carbon taxes related to burning fossil fuels.

Countries tend to sanction tax exemptions to emissions from electricity/heat generation in their respective carbon pricing programs. In the US electricity/heat generation is not

subjected to any carbon dioxide emission taxes. The EU energy taxation directive states that burning fuels in electricity generation and heating in chemical process is tax exempt in member counties. However, countries can circumvent this directive if there are environmental justifications. Worldwide fossil fuels burning is taxed in Denmark, Estonia, Hungary, Ireland, Italy, Japan, Latvia, Lithuania, Norway, Spain , Sweden and the UK[95]. From the list above only Ireland and Spain the fuels are taxed based on carbon dioxide emissions while other countries use other emissions measures like sulfur and nitrogen emission taxes or direct taxes on burned fuels[95]. The United Kingdom imposes a direct carbon tax on natural gas used as a utility fuel for electricity generation sector at a rate $0.0027 per kWh [89]. Ireland started a carbon tax in 2010 at rate of €15 per tonne of carbon dioxide initially that later grow to €20 per tonne of carbon dioxide[96]. According to the Irish Wind Energy Association 24% of Ireland electricity needs are generated via wind energy. This enabled Ireland to even tax the more cleaner fossil fuels like natural gas. Ireland has had a natural gas tax since 2012 at a rate of €4.10 per mWh that is based on a tax rating of €20 per tonne of carbon dioxide. Natural gas as a feed for industrial processes is tax exempt in Ireland but the burning of natural gas is taxed and generally not eligible for tax relief subsides [98]. In Finland, which was the first country to introduce carbon taxes in 1990 natural gas is taxed at reduced rate $3.02 (€2.016) per mWh as feed material power generation. However, the burning of natural gas as a utility fuel for electricity generation is tax exempt by decree 309/2003 of the Finnish Ministry of Trade and Industry[95]. In the US, electricity/heat generation in the US account for 30% of total carbon dioxide emissions where coal and natural gas are the main contributers [105]. A 2013 study by the EPA estimates that emissions related to natural gas (methane) used in the US can be reduced by 6.4% at zero cost and 21.4% at carbon tax rate of $45 per ton of carbon dioxide[106, 107]. In a world where carbon pricing programs are growing its important to for mature technologies to adapt to the changing polices. Energetically enhanced steam methane reforming process (EESMR) is merely a simple example of how we can use process intensification and energy efficiency to adapt to a future where there is a price tag associated with carbon emissions. Figure 3.14 shows the

change in carbon dioxide emissions from electricity/heat generation between 1990 and 2013. Group 1 are countries that set an explicit price on the carbon dioxide emissions from burning fossil fuels or set a direct tax on such fuels in electricity/heat generation under carbon pricing programs and includes: Japan, Ireland, Italy, Lithuania, Norway, Spain and the UK. Group 2 are countries that place emissions related taxes on other pollutants like sulfur and nitrogen but not carbon dioxide and includes: Denmark, Estonia, Hungary and Sweden.

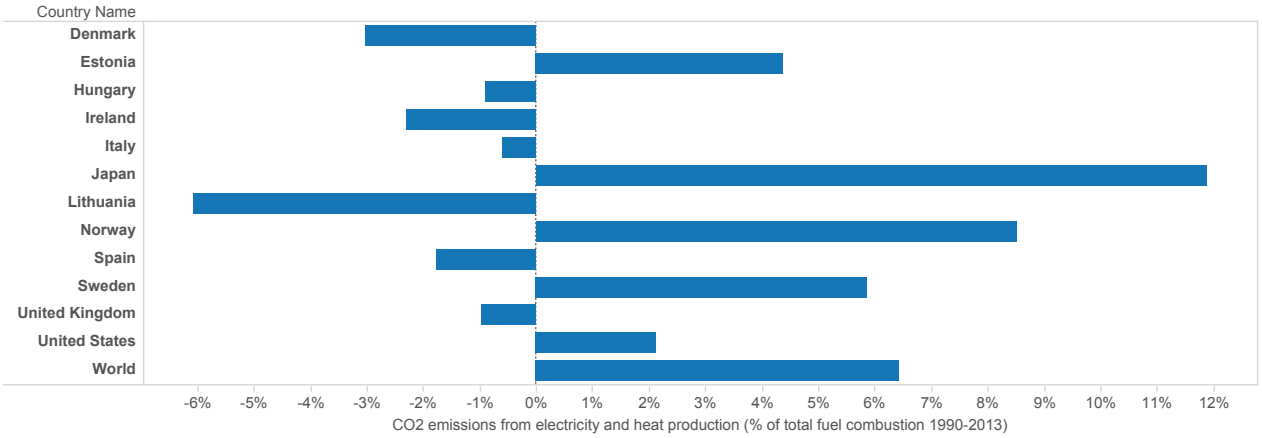

Figure 3.14: Carbon dioxide emissions from electricity and heat production, total (% of total fuel combustion) [1990-2013] [6]

Group 1 with the exception of Japan and Norway shows that proposed policy had a positive impact by reducing carbon dioxide emissions from electricity/heat generation. The increase in Norway can be explained by the fact that almost all of the country electricity generation comes from hydro-power which means that the policy had a minimum impact due to the marginally small size of the fossil fuels market share in the electricity/heat generation sector. Meanwhile, Japan increase in emission is due to the switch from Nuclear power plants to fossil fuels after the fukushima disaster in 2011. Group 2 shows mixed result as reductions occurred in Denmark and Hungary while increases took place in Estonia and Sweden. Its to be noted that the sharp decrease in the Denmark can be attributed to the fact that Denmark post one of the highest electricity consumption taxes in Europe. Meanwhile, the increase carbon dioxide emissions in Estonia is attributed to its dependence on oil for 90% of its

electricity/heat production unlike the rest of the EU member countries that uses natural gas and renewable energy resources. In future scenarios with higher carbon taxes rate Estonia would import electricity since local oil based production from wont be economically feasible. The increase in Sweden is attributed to the increased demand of electricity in the country with no addition in power generation capacity which resulted in electricity imports from countries without carbon taxing programs.

3.5 Conclusions

An energetically enhanced steam methane reforming process (EESMR) was developed. The process use natural gas to feed the reformer but does not require the burning natural gas to produce hydrogen. The heat integration featuring minimum cold/power utility of the process shows that the heating and cooling requirements of the process can be met by using concentrated solar power. The designed The heat exchange network generates enough power to supply all the electricity needs of the flowsheet, including pumps, compressors and separation systems. The proposed methodology leads to better economical and environmental performance when compared to conventional Steam Methane Reforming . Indeed, the developed designs show that and exothermic reformer is a achievable. Also, energetic enhancement can deliver lower reformer heat load without eliminating the endothermic heat load entirely if needed. Through design and application, we have conformed that the reformer heat load is directly dependent on the amount of water and carbon monoxide fed to the reformer. The exothermic reformer reduces the process capital cost by eliminating the need for a process furnace typically associated with hydrogen production industrially. The energetically enhanced process use utilities at 770 K and 420 K while conventional reforming use utilities at 1200 K, 770 K and 420K. Eliminating the use of a 1200K (combustor) reduce the plant daily fuel costs by 18.5% compared to conventional reforming plants, reducing the impact of natural gas prices by 18.5% hence make the process economics less dependent of natural gas prices. In terms of environmental performance the new process produce carbon

dioxide at higher purity which makes it ready for post processing sequestration. Energetically Enhanced Steam Methane Reforming doesn't burn any fossil fuels which makes it an environmental superior to Steam Methane Reforming. In turn, this implies that the proposed process is a sustainable hydrogen production method in a world where carbon pricing programs blossoming. Current trends show that a direct carbon tax on the burning of fossil fuels in electricity/heat generation is growing worldwide and that scientific developments are needed to find solutions that can strive in a world where carbon is priced. Revenues coming from carbon pricing programs are used to promote the renewable energy which would ultimately support the policy target of reducing emissions.

CHAPTER 4

Zero carbon emissions chemical power systems

4.1 Introduction

Human society is faced with two indisputable facts: carbon dioxide concentrations in the earth's atmosphere (03-03-13 weekly average of 397.30 ppm at Mauna Loa, [108]), are the highest they have ever been [109]; and the carbon containing, energetically dense, fossil fuels used to meet societal energy needs will be depleted. It is now commonly accepted that steps should be taken to both reduce anthropogenic carbon dioxide emissions, and increase use of renewable energy resources. This dual goal is even more imperative given projected reductions in worldwide nuclear electric power (from 7.1 % in 2011, to 6.2%-6.7% in 2020, 4.7%-6.2% in 2030, and 2.3%-5.7% in 2050,[110]). Following the 2011 Fukushima incident, and Germany's decision to abandon nuclear power, the use of green energy subsidies (1% of German GDP) led, within months, to an increase of renewables from 20% to 25% of total power. Furthermore, renewables are projected to grow to 40% by 2020, and 80% by 2050,[111]. Climate protection, protection from nuclear risks, a changeover to a post-fossil fuel world economy, and Germany's technological capabilities and innovative strengths, are identified as the reasons for the nuclear to renewable transition. According to [112], renewables will grow from 19% (3800 TWh) of worldwide electricity production in 2008, to between 23% and 45% (7400 TWh and 14 500 TWh) in 2035, matching coal-fired generation. Concentrating solar power (CSP) electricity in particular will grow at much faster rates, from 1 TWh (1.4 GW capacity) in 2008, to 340 TWh (90 GW capacity) in 2035.

At present, however, fossil fuels are used at more than 70% of the world's power plants

[113]. In China, for example, coal is the primary contributor to power generation due to its wide availability and flexibility in environmental regulation. In the United States, more than 40% of energy associated with CO_2 emissions-equivalent to 2.035 billion metric tons of CO_2âĂŤcomes from power generation [114] and is expected to increase to 12% by 2040 [115]. In terms of emissions intensity, CO_2 released from coal power plants is 60% greater than that emitted from natural gas power plants per kW/h produced [115]. In terms of overall cost, the US power sector spends more than USD $30 billion on fossil fuels [113]. Of course, certain states have sought to increase the market share of renewable energy in the power generation sector. California, for example, has set the target to reduce greenhouse gas (GHG) emissions by 33% by 2020. Currently, 45% of electricity generated in California comes from natural gas and 17% from renewable energy resources (e.g., solar power, wind power, and hydropower) [116]. In particular, natural gas has experienced extraordinary growth in the United States, given the ongoing shale gas boom that contributed to 23.1% of US natural gas production in 2010 compared to 1.6% in 2000 [117]. Correspondingly, the market share of natural gas in the US energy sector grew from 12% in 1990 to 33% in 2015. Meanwhile, natural gas production reached a record 80.2 bcf/d in 2016, with an expected growth of 3.0% by 2017 [118]. The ready availability of natural gas and its superior environmental emission patterns compared to those of other fossil fuels both support such market share growth.

In general, carbon emissions management drives the development of new sustainable power generation technologies. The early 1990s, for example, demonstrated a global trend in which worldwide coal power generation capacities started to decline while those of natural gas soared. Following the oil crisis in the 1970s, great emphasis has been placed on improving the economics of power generation [119] and been shaped by competing economic and environmental interests. Economically, fossil fuel (e.g., oil, coal, and natural gas) prices and peak demand-based electricity potentially constrain improvements; environmentally, short-term CO_2 emissions primarily complicate the production of electricity from fossil fuels due to long-term concerns over future carbon tax legislation.

To improve fossil fuel-based power generation, two problems need to be addressed: CO2

emissions and the inflexibility of electrical supply. The problem of CO2 emissions has been tackled in industry by using two approaches: carbon capture and sequestration (CCS) and carbon use. On the one hand, CCS has repeatedly succeeded as a tool to counter potential carbon tax scenarios worldwide, as the situation in Norway has demonstrated. On the other, carbon use provides a solution to convert CO_2 to high-value carbon-containing chemicals that can enable the coproduction of electricity and chemicals (e.g., formic acid) without emitting CO_2 into the environment.

In this chapter, we introduce a natural gas-based chemical-power coproduction system (NGCPS) with zero CO_2 emissions that produces electricity, formic acid, and water with flexible switching options. During off-peak times, power plants are typically shut down, as long as the plant allows flexible shut downs and restarts, which prompts the loss of economic potential during off-peak hours. However, the NGCPS would not lose such economic potential due to its ability to switch from producing formic acid and electricity to formic acid and hydrogen. In turn, the economic flexibility and the zero CO2 emissions enable a wide range of applications for the coproduction of power and chemicals.

The remainder of this chapter is structured as follows. To begin, we present the thermodynamic processes and cycles of power generation, after which we examine the feasibility of the proposed NGCPS and describe the various subcomponents. Next, we detail heat and power integration to show the economic potential of the NGCPS, followed by an analysis of the concomitant economic and environmental trade-offs of the system. In closing, we discuss our results and draw some conclusions.

4.2 Thermodynamics of power generation:

An important aspect of studying power plants is the analysis of how thermodynamic processes and cycles involved in power generation behave. Ultimately, such analysis informs the selection of thermodynamic cycles in power generation plants, which depends on environmental regulations, capital and operational costs, fuel costs, and efficiency- and load-related

considerations. In general, a *thermodynamic cycle* is a series of thermodynamic processes that a system undergoes in returning to its original state in terms of thermodynamic properties [120]. By extension, a *thermodynamic process*, is the path between states that a system takes to achieve changes in its thermodynamic properties [120]. Certain thermodynamic properties remain constant during a thermodynamic process, including temperature (i.e., isothermal processes), pressure (i.e., isobaric processes), and volume (i.e., isochoric processes). Within the cycle, the working fluid exhibits changes in its thermodynamic states that allow for the transfer of heat between the system and its boundaries using *heat engines*. Heat (Q) represents the energy transferred to the system by the surroundings, whereas work (W) represents work done by the system. The relationship between the quantities is explained by the first law of thermodynamics [121, 120]:

$$J \oint \delta Q = \oint \delta W \tag{4.1}$$

In what follows, we address the thermodynamic fundamentals of power generation required to develop high-performance plant designs. Such designs depend on the selection of available thermodynamic cycles in specific configurations. We start by presenting the Rankine cycle (i.e., used in steam engine power plants), the Brayton cycle (i.e., used in gas turbine power plants), and the Rankine-Brayton cycle (i.e., used in combined cycle power plants).

4.2.1 Rankine cycle

Named after William J. Rankine, the Rankine cycle ranks among the most commonly used thermodynamic cycles to model steam turbine performance in power generation plants. Water in the form of steam typically serves as the working fluid in the Rankine cycle, which runs in a closed loop format. Water is heated in a boiler to produce sub- or supercritical steam that is fed into the turbine in order to generate the work needed to produce electricity. The rest of the cycle consists of a consider used to saturate the vapor exiting the turbine. The saturated product is then fed into a pump for pressurization before returning it to the

boiler to complete the cycle. The cycle can be summarized as the following processes [120]:

- 1-2: A pump is used to pressurize the working fluid (reversible adiabatic process);
- 2-3: The pressurized working fluid is heated in the boiler (isobaric process);
- 3-4: Turbine expansion occurs to generate the work and power (reversible adiabatic process); and
- 4-1: Heat transfer in a condenser completes the cycle (isobaric process).

Major factors governing the efficiency of the Rankine cycle are the temperatures at which heat is provided to and dumped from the cycle. Controlling the aforementioned temperature differential by increasing the former and reducing the latter promotes improvements in the cycle's thermal efficiency. The Rankine cycle has been favorable in early power generation applications because it completely condenses the turbine vapors into liquids before pumping instead of feeding the liquid-vapor mixture into the pump, which is more difficult to control. The thermal efficiency of the Rankine cycle is given by [121]:

$$\eta = \frac{W_{net}}{Q_H} \tag{4.2}$$

In modern applications, the Rankine cycle is used as a heat recovery bottoming cycle in combined cycle power generation plants. In combined cycles, heat is released by the combustion of fuels (e.g., natural gas) and converted to heat, which is later used to generate work at the turbine's topping cycle. The exhaust of the topping cycle includes heat that would normally be released into the system's surroundings. The quality of heat recovered by the Rankine cycle depends on the conditions of the exhaust discharge from the topping process, which is used to generate the steam that will power the turbine in the cycle. Heat recovery using the Rankine cycle improves the combined cycle performance and efficiency, which primarily explains why combined cycle power generation has experienced such commercial success.

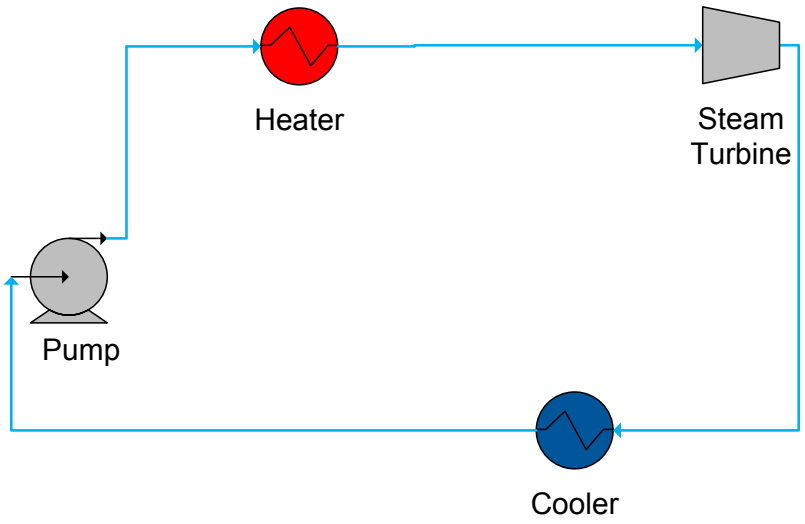

Figure 4.1: Rankine cycle

4.2.2 Brayton cycle

Named after George Brayton, the Brayton cycle, by contrast, is a gas-based thermodynamic cycle that represents the operation of a constant pressure gas turbine heat engine. The process occurs in two forms: as an open-loop cycle mostly used in airplane jet engines and as a closed loop cycle for power plant operations. The ideal Brayton cycle consists of the following four processes [120]:

- 1-2: Reversible adiabatic pressurization of the inlet air occurs in the compressor (isentropic process);
- 2-3: The compressed air is mixed with fuel and burned in a combustion process (isobaric process);
- 3-4: The reversible diabatic expansion of the heated and pressurized air in the turbine produces work (isentropic process); and
- 4-1: Heat is rejected by cooling the air back into its initial condition (isobaric process).

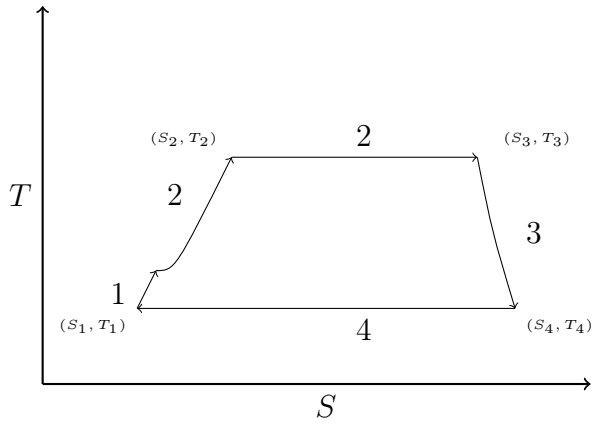

Figure 4.2: Rankine cycle T-S diagram

Designing a Brayton cycle requires that special attention be paid to the compressor, since its efficiency determines the amount of back work that it will consume. Back work can require from 40% to 80% of the amount of work generated in the gas turbine in order to run the compressor [121], which will be deducted from the power generation potential of the cycle. However, with high compressor and gas turbine efficiencies coupled with combined cycle configuration, that requirement should not be a problem. By comparison with the Rankine cycle, the pump uses approximately 1% of back work, since the specific volume of the liquid in the steam turbine is far lower than the gas-specific volume in the gas turbine. The thermal efficiency of the Brayton cycle is given by [121]:

$$\eta = 1 - \frac{Q_L}{Q_H} \tag{4.3}$$

Most real-world applications of the Brayton cycle depend on air as the working fluid. However, to improve the environmental performance of the cycle and avoid SO_x and NO_x pollutants, gases that burn cleaner than air can be used, such as noble gases (e.g., Ar), which can serve as a working fluid in a Brayton cycle with minimal environmental emissions [122].

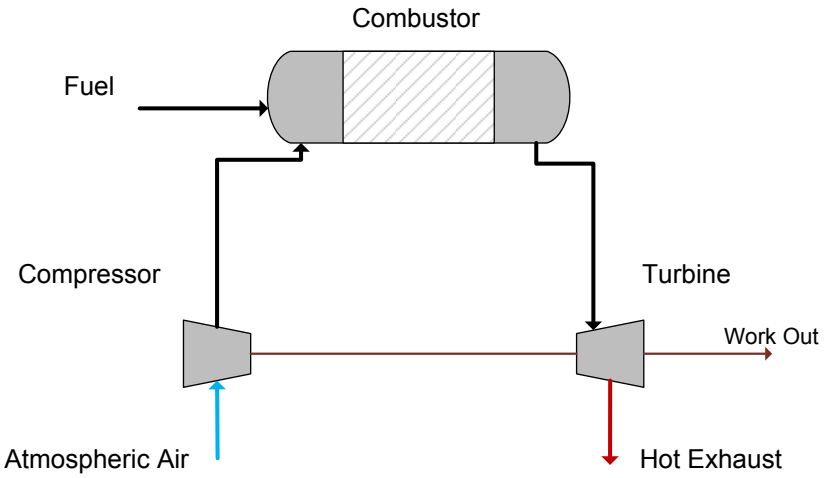

Figure 4.3: Brayton open loop cycle

4.2.3 Combined cycle

A combined cycle natural gas power plant benefits from lower capital costs, shorter construction times, greater flexibility, and superior efficiency than single cycle natural gas power plants [123]. Natural gas power plants can reach thermal efficiencies of 54% in combined cycle mode compared to 35% in single cycle mode [124], since joining two thermodynamic cycles affords an improved combined cycle configuration that yields greater efficiency. Briefly, excess energy in the exhaust gases in certain thermodynamics cycles, usually released into the environment, can be used in a secondary cycle to improve the efficiency of power generation. The design employs two cycles: a topping cycle, which is usually a gas turbine cycle, and a bottoming cycle for heat recovery (e.g., steam cycle).

Among current developments that have improved the performance of combined cycle power generation, gas turbines in topping cycles can now produce exhaust gas with temperatures as low as $T = 750\ K$, and steam cycles can operate at high pressures ($P = 165\ bar$) [113], which better enables the integration of two thermodynamics cycles. The difference between the exhaust temperature and bottoming cycle temperature is the pinch temperature,

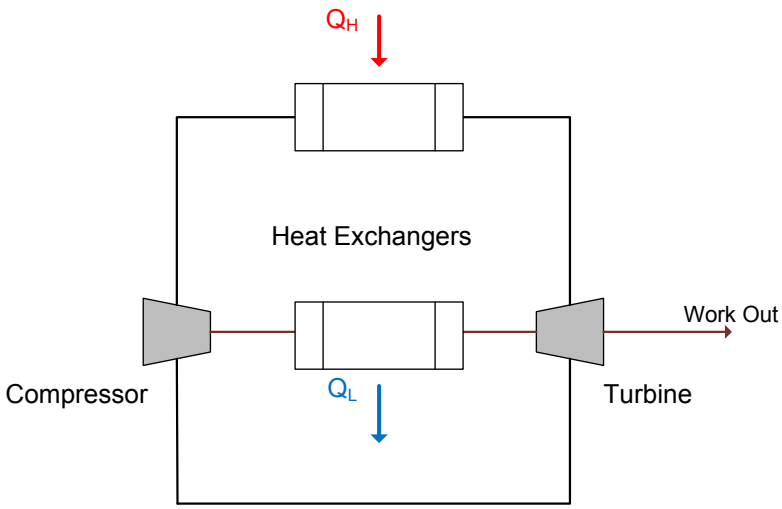

Figure 4.4: Brayton closed loop cycle

ranging from 5 to 15 K; the less the difference, the more efficient the heat transfer. However, as the pinch point decreases, the surface area needed for heat transfer decreases as well [113]. At present, a combination of Brayton (topping cycle) and Rankine cycles (bottoming cycle) is the most common method to produce electricity from natural gas. Natural gas is burned with air or a noble gas in a combustor, and the products are relayed to a gas turbine (Brayton cycle), the exhaust of which travels through a steam engine (Rankine cycle) that acts as a heat recovery subsystem. The Brayton cycle operates at high temperatures that align with natural gas combustion temperatures (1,000-1,600 K) with a exhaust gas (700-900 K), which can sufficiently feed the Rankine cycle. The temperature difference is a chief factor in improving the efficiency of heat's conversion to work. Currently, thermal efficiency is restricted by material limitations that stipulate a cap of 925 K on steam generated in the process. Furthermore, a lower temperature constraint restricts the bottoming cycle (Rankine cycle) by the temperature of the cooling water (298 K).

Natural gas provides the cheapest overall costs for combined cycle electricity production from fossil fuels. For example, the natural gas-based combined cycle electricity production cost is 58.9 mills/kWh, compared to 76.3 mills/kWh for a coal-based integrated gasification

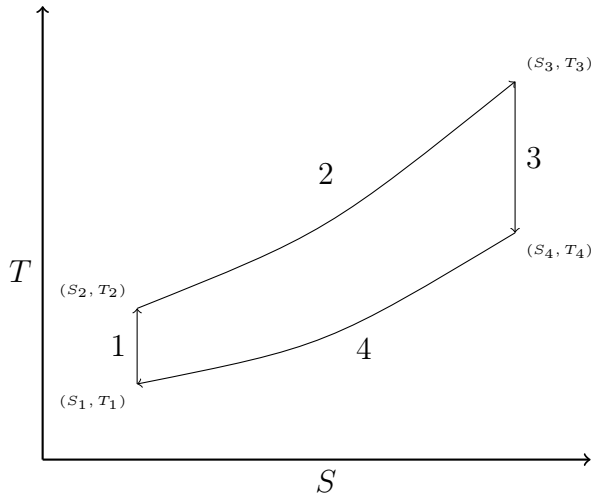

Figure 4.5: Brayton cycle T-S diagram

combined cycle [124]. Moreover, a natural gas combined cycle demands shorter construction-to-production times and offers a better emissions pattern than coal-based combined cycle plants. The chief argument against natural gas power generation is thus the fluctuation of natural gas prices observable in today's markets.

4.2.4 Heat and power integration:

Industrial processes involving chemical reactions result in internal temperature gradients that require the use of external utilities and result in additional costs. Accordingly, allocating the minimum utility and its associated costs gives raise to the problem of minimum utility optimization. A popular early method called *pinch analysis* was used to solve the problem by controlling internal temperature gradients in chemical processes using *heat engines* and the following utilities [125, 126]:

- Hot utility from an external heat source (e.g., fossil fuels or steam);
- Cold utility from a heat sink (e.g., cooling water); and
- Work utility used to transform heat loads within the system (e.g., electricity).

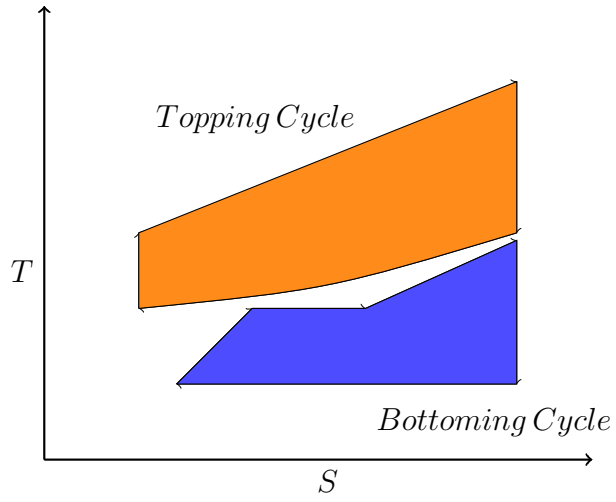

Figure 4.6: Combined Brayton-Rankine cycle T-S diagram

In pinch analysis, streams are defined as hot and cold streams; each stream that increases in temperature is a cold stream, whereas one that decreases in temperature is a hot stream. The efficiency of heat flows in the process determines how much utility the process consumes. The significance of the pinch is that we may not transfer heat across the pinch, use cold utilities above the pinch, or use hot utilities below the pinch. The lowest allowable temperature difference is the *pinch temperature* (ΔT_{min}), which is the point that divides the minimum utility problem into two segments: a heat sink, which is located above the pinch, and a heat source, which is located below [125]. Figure 4.7 shows the interactions of streams and utilities above and below the pinch at a composite heat and enthalpy curve. The figure reveals that in pinch analysis, heat can be transferred from high to low to temperature streams, but not vice versa. We therefore conclude that the full capabilities of heat and power integration are not used in pinch analysis without the use of heat pumps.

Definition 4.1: *Heat engines are devices in which a working fluid performs thermodynamic processes to transfer thermal energy in the form of heat from a heat source (high temperature) to a heat sink (low temperature) while producing work.*

The heat engine model can be described using the first and second laws of thermody-

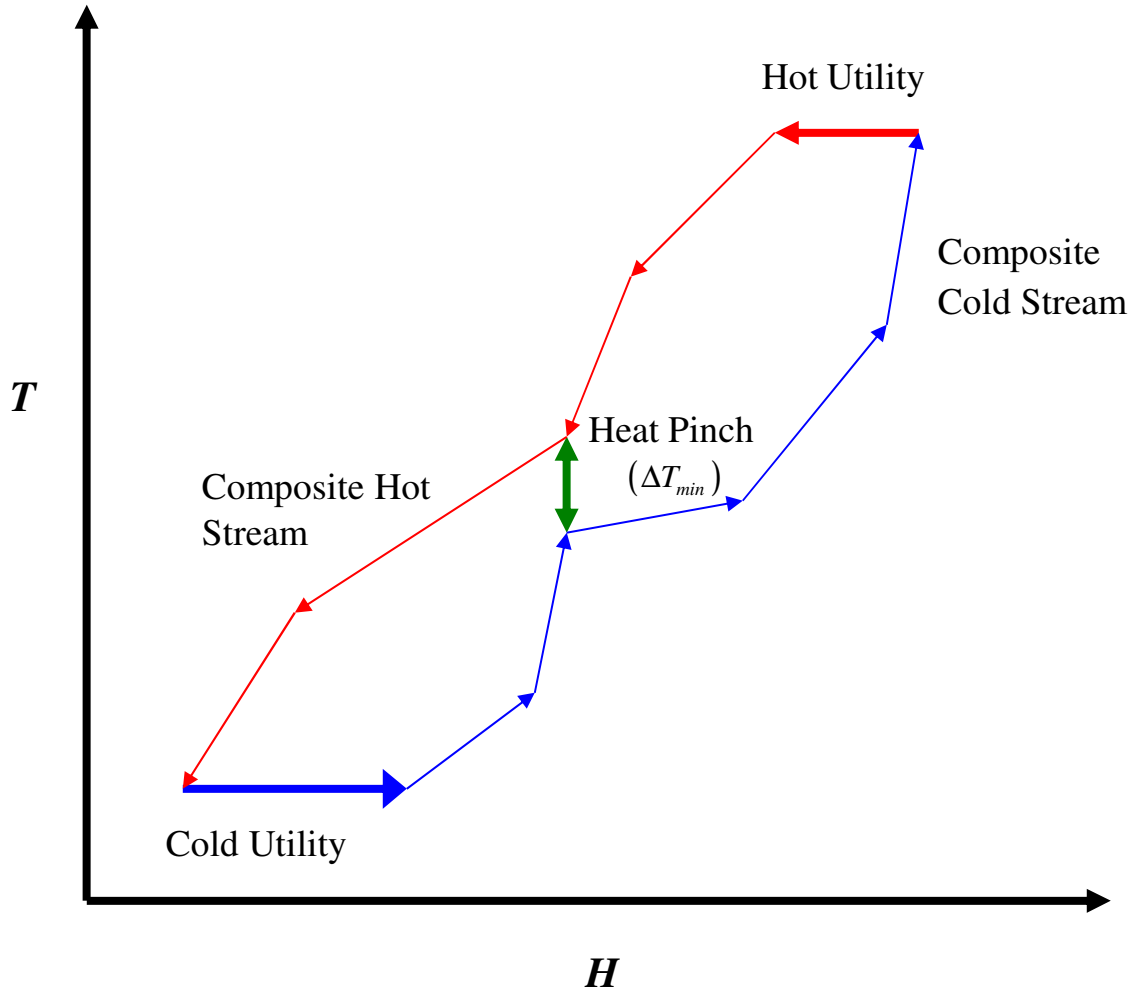

Figure 4.7: Pinch diagram

namics:

$$Q_H^{engine} - Q_C^{engine} - W^{engine} = 0 \tag{4.4}$$

$$(F\rho c_p)_C \ln(\frac{T_{fin}^C}{T_{in}^C}) + (F\rho c_p)_H \ln(\frac{T_{fin}^H}{T_{in}^H}) = 0 \tag{4.5}$$

Heat engines (e.g., internal combustion engines) first connect a high-entropy heat source with a lower-entropy heat sink to generate work. Although increasing the temperature

differential between the source and sink increases the amount of work generated, that amount is bounded by the entropy increase in the sink. Heat pumps use work to force the flow of heat against the temperature gradient (e.g., refrigeration). Unlike heat engines, heat pumps necessarily consume more work as the temperature differential between the heat source and heat sink increases.

Definition 4.2: *Heat pumps are devices that transfer heat from cold to hot reservoirs while consuming work.*

As such, heat pumps can upgrade the quality of heat transferred within the system and allow for heat and power integration, as described in a model using the following equations:

$$Q_C^{pump} - Q_H^{pump} + W^{pump} = 0 \tag{4.6}$$

$$Q_C^{pump} = (F\rho c_p)_H (T_{in}^H - T_{fin}^H) > 0 \tag{4.7}$$

$$Q_H^{pump} = (F\rho c_p)_C (T_{fin}^C - T_{in}^C) > 0 \tag{4.8}$$

With the heat pump and heat engine models defined, we use both to perform heat and power integration using the heat engineâĂŞpump (HEP) network, originally presented by Hasliastos and Manousiouthakis [126]. A HEP network is used to solve the minimum utility cost problem via the integration of heat exchangers, heat engines, and heat pumps without any previous commitment to the network structure. Energy flows are distributed between a heat exchange (HE) network and HEP network by using the aforementioned utilities. The heat used by the HEP network from the hot utility is denoted as δ_H^{HEP}, whereas the heat transferred to the cold utility by the HEP network is denoted as δ_C^{HEP}

We first present the objective function that minimizes the overall cost of hot, cold, and electrical utilities:

$$min \quad \sum_{i=1}^{N_{HUV}} c_{HUV,i} F_{HUV,i} + \sum_{i=1}^{N_{CUV}} c_{CUV,i} F_{CUV,i} + \sum_{i=1}^{N_{HUC}} c_{HUC,i} q_{HUC,i} F_{HUC,i} + \sum_{i=1}^{N_{CUC}} c_{CUC,i} q_{CUC,i} F_{CUC,i} + c_W W \quad (4.9)$$

The minimum utility problem presented in Equation 4.9 is described by the following utility streams:

- Hot utility with variable temperature (HUV);
- Cot utility with variable temperature (CUV);
- Hot utility with constant temperature (HUC); and
- Cold utility with constant temperature (CUC).

The optimization problem is governed by four constraints. The first is an energy balance on the k_{th} temperature interval:

$$\begin{aligned} &\delta_k + \left(\eta_k \sum_{i=1}^{N_{HPV}} \lambda_{HPV,i,k} F_{HPV,i} (c_P)_{HPV,i} + \sum_{i=1}^{N_{HUV}} \lambda_{HUV,i,k} F^{HEN}_{HUV,i,k} (c_P)_{HUV,i} \right) \\ &\quad \left(T^H_k - T^H_{k+1}\right) + \left(\eta_k \sum_{i=1}^{N_{HPC}} \lambda_{HPC,i,k} F_{HPC,i} q_{HPC,i} + \sum_{i=1}^{N_{HUC}} \lambda_{HUC,i,k} F^{HEN}_{HUC,i,k} q_{HUC,i} \right) \\ &= \delta_{k+1} + \left(\theta_k \sum_{i=1}^{N_{CPV}} \lambda_{CPV,i,k} F_{CPV,i} (c_P)_{CPV,i} + \sum_{i=1}^{N_{CUV}} \lambda_{CUV,i,k} F^{HEN}_{CUV,i,k} (c_P)_{CUV,i} \right) \left(T^C_k - T^C_{k+1}\right) \\ &\quad + \left(\theta_k \sum_{i=1}^{N_{CPC}} \lambda_{CPC,i,k} F_{CPC,i} q_{CPC,i} + \sum_{i=1}^{N_{CUC}} \lambda_{CUC,i,k} F^{HEN}_{CUC,i,k} q_{CUC,i} \right) \quad \forall k = 0, n-1 \quad (4.10) \end{aligned}$$

Heat loads are correlated to the available energy denoted by δ_k and δ_{k+1}. Meanwhile, η_k is the fraction of the hot stream enthalpy that goes to the cold stream in the heat engine network (HEN), while the remaining fraction $1 - \eta_k$ will go to the cold stream in the heat engine-pump network (HEP). θ_k is the fraction of enthalpy increase accomplished by the

heat exchange. Overall, this constraint balances the energy leaving the interval k and the the amount of energy that a cold stream can absorb. The next set of constraints showen in Equations 4.11 and 4.12 governs the total use of hot utilities in the problem:

$$F^{HEN}_{HUV,i,k} + F^{HEP}_{HUV,i,k} = F_{HUV,i} \quad \forall k = 0, n-1 \ ; \quad \forall i = 1, N_{HUV} \tag{4.11}$$

$$F^{HEN}_{CUV,i,k} + F^{HEP}_{CUV,i,k} = F_{CUV,i} \quad \forall k = 0, n-1 \ ; \quad \forall i = 1, N_{CUV} \tag{4.12}$$

Equation 4.13 shows the overall entropy balance in the HEP network, which illustrates the effect of hot and cold utilities on entropy input to the HEP network by taking into account the entropy associated with δ_k and δ_{k+1}. This dynamic is illustrated by using ε_k, in which $\varepsilon_k \geq 0$ for HE networks, or $\varepsilon_k \leq 0$ for HEP networks and is free otherwise. The entropy equality constraint is as follows:

$$\begin{aligned}
&\varepsilon_k + \left((1-\eta_k) \sum_{i=1}^{N_{HPV}} \lambda_{HPV,i,k} F_{HPV,i} (c_P)_{HPV,i} + \sum_{i=1}^{N_{HUV}} \lambda_{HUV,i,k} F^{HEP}_{HUV,i,k} (c_P)_{HUV,i} \right) \\
&\ln(\frac{T^H_k}{T^H_{k+1}}) + \left((1-\eta_k) \sum_{i=1}^{N_{HPC}} \lambda_{HPC,i,k} F_{HPC,i} q_{HPC,i} + \sum_{i=1}^{N_{HUC}} \lambda_{HUC,i,k} F^{HEP}_{HUC,i,k} q_{HUC,i} \right) (\frac{1}{T^H_k}) \\
&= \varepsilon_{k+1} + \left((1-\theta_k) \sum_{i=1}^{N_{CPV}} \lambda_{CPV,i,k} F_{CPV,i} (c_P)_{CPV,i} + \sum_{i=1}^{N_{CUV}} \lambda_{CUV,i,k} F^{HEP}_{CUV,i,k} (c_P)_{CUV,i} \right) \ln(\frac{T^C_k}{T^C_{k+1}}) \\
&+ \left((1-\theta_k) \sum_{i=1}^{N_{CPC}} \lambda_{CPC,i,k} F_{CPC,i} q_{CPC,i} + \sum_{i=1}^{N_{CUC}} \lambda_{CUC,i,k} F^{HEP}_{CUC,i,k} q_{CUC,i} \right) (\frac{1}{T^C_{k+1}}) \quad \forall k = 0, n-1
\end{aligned} \tag{4.13}$$

Such that:

$$\delta_0 = \delta_n = 0; \quad \delta_k \geq 0 \ \ \forall k = 0, n \tag{4.14}$$

and

$$\varepsilon_0 = \varepsilon_n = 0 \tag{4.15}$$

Work (W) consists of the difference of enthalpies in the process streams instead of entropy since entropy does not enter or leave the system. The work consumption/generation can be calculated by using Equation 4.16:

$$W = \sum_{k=0}^{n-1} \left((1-\eta_k) \sum_{i=1}^{N_{HPV}} \lambda_{HPV,i,k} F_{HPV,i} (c_P)_{HPV,i} + \sum_{i=1}^{N_{HUV}} \lambda_{HUV,i,k} F^{HEP}_{HUV,i,k} (c_P)_{HUV,i} \right)$$
$$\left(T^H_k - T^H_{k+1}\right) + \left((1-\eta_k) \sum_{i=1}^{N_{HPC}} \lambda_{HPC,i,k} F_{HPC,i} q_{HPC,i} + \sum_{i=1}^{N_{HUC}} \lambda_{HUC,i,k} F^{HEP}_{HUC,i,k} q_{HUC,i} \right)$$
$$- \left((1-\theta_k) \sum_{i=1}^{N_{CPV}} \lambda_{CPV,i,k} F_{CPV,i} (c_P)_{CPV,i} + \sum_{i=1}^{N_{CUV}} \lambda_{CUV,i,k} F^{HEP}_{CUV,i,k} (c_P)_{CUV,i} \right) \left(T^C_k - T^C_{k+1}\right)$$
$$- \left((1-\theta_k) \sum_{i=1}^{N_{CPC}} \lambda_{CPC,i,k} F_{CPC,i} q_{CPC,i} + \sum_{i=1}^{N_{CUC}} \lambda_{CUC,i,k} F^{HEP}_{CUC,i,k} q_{CUC,i} \right) \quad (4.16)$$

4.3 Feasibility of proposed Chemical/Power system:

In this section, we demonstrate the fundamentals of a multi objective process integration strategy for developing a zero CO_2 emissions Chemical/Power system (NGCPS). Such systems are sustainable carbon management solutions in which natural gas is transformed to valuable chemicals while producing power. Table 4.1 shows some possible reaction routes to produce high-value chemicals in hybrid NGCPS.

Table 4.1: Typical carbon dioxide conversion routes

Chemical Compound	Net Reaction
Formic Acid	$H_2 + CO_2 \longrightarrow HCOOH$
Acetic acid	$4H_2 + 2CO_2 \longrightarrow CH_3COOH + 2H_2O$
Urea	$2NH_3 + CO_2 \longrightarrow NH_2CONH_2$

To produce high-value chemicals, natural gas needs to be partially converted to either hydrogen (H_2) to produce formic and acetic acids or to ammonia (NH_3) to produce urea. We focus on the production of formic acid as the high-value chemical given the lower amount

of hydrogen required than acetic acid and since it does not require the production of NH_3.

Lopez and Manousiouthakis introduced a energy self-sufficient system for producing hydrogen and formic acid from natural gas[99]. A system is energy self-sufficient if its steady-state open system has inlets in

F_I and outlets in F_O, no heat transferred from the surroundings to the system, heat possibly transferred from the system to the surroundings ($\dot{Q}_j \leq 0,\ \ j \in S_Q$) at the uniform surroundings temperature ($T_{\sigma,j} = T_0$) , and the system's net shaft work can be produced or consumed by the system, if not both, as long as the net rate of work is non-positive $\dot{W}_j \leq 0\ \ j \in S_W$. Energetic self-sufficiency (Ω) requires a system to satisfy the following conservation laws:

$$\sum_{i\in\ S_I} \dot{m}_i - \sum_{i\in\ S_O} \dot{m}_i = 0 \tag{4.17}$$

$$\sum_{i\in\ S_I} H_i\dot{m}_i - \sum_{i\in\ S_O} H_i\dot{m}_i + \sum_{j\in S_Q} \dot{Q}_j + \sum_{j\in S_W} \dot{W}_{s,j} = 0 \tag{4.18}$$

$$\sum_{i\in\ S_I} S_i\dot{m}_i - \sum_{i\in\ S_O} S_i\dot{m}_i + \sum_{j\in S_Q} \frac{\dot{Q}_j}{T_{\sigma,j}} + \dot{S}_G = 0,\ \ \dot{S}_G \geq 0 \tag{4.19}$$

Based on those laws, the work produced by the system can be reversibly used to meet any of the system's work needs. In our case, such work is used to produce electricity. The definition of energetic self-sufficiency can be mathematically stated as [99]:

$$\dot{Q}_0 \leq 0,\ \dot{W}_{s,j} \leq 0\ \forall j \in S_W \tag{4.20}$$

$$T \cdot \dot{S}_G = T \cdot \left(\sum_{i\in\ S_O} S_i\dot{m}_i - \sum_{i\in\ S_I} S_i\dot{m}_i \right) - \dot{Q}_0 \geq 0 \tag{4.21}$$

The above equations imply that necessary conditions, independent of $\dot{S}_G$, for a system to be energetically self-sufficient are [99]:

$$-\dot{Q}_0 - \sum_{j \in S_W} \dot{W}_j = \sum_{i \in S_I} H_i \dot{m}_i - \sum_{i \in S_O} H_i \dot{m}_i \geq 0 \tag{4.22}$$

$$\sum_{i \in S_I} (H_i - T \cdot S_i)\, \dot{m}_i - \sum_{i \in S_O} (H_i - T \cdot S_i)\, \dot{m}_i \geq 0 \tag{4.23}$$

Figure 4.8 shows an energetically self sufficient open steady state $NGCPS$ with streams F_I coming in and streams F_O coming out. The system produces electricity in the amount of the work generated in the system W. It is important to study the power chemical production potential, and a more detailed analysis will require the study of individual species involved, as well as of the related reaction cluster.

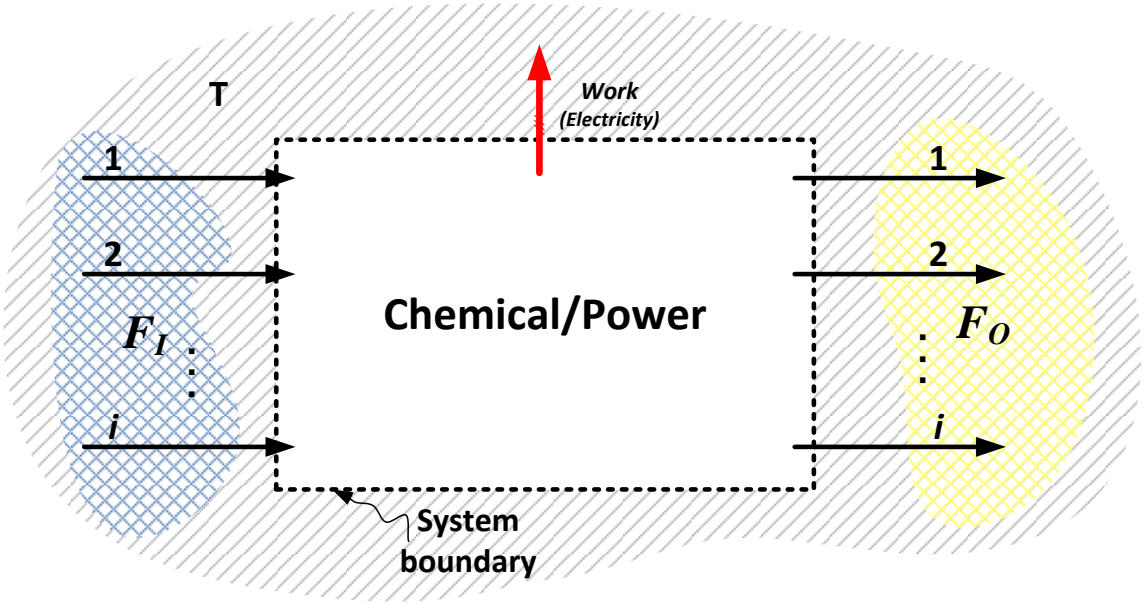

Figure 4.8: Energetically self-sufficient open steady-state system Ω

For a reaction cluster to be considered thermodynamically feasible each reaction in the cluster must be thermodynamically feasible at the given temperature and satisfy a mass balance governing the species. Furthermore, the reaction cluster must be economically feasible

as part of the requirement for a $NGCPS$ design. The Gibbs free energy of reaction (ΔG) needs to be negative for the reaction to be spontaneous, while equilibrium takes place when ΔG=0. The reaction cluster consists of the following reactions:

$$(0.5 - 0.25X)CH_4 + 2(0.5 - 0.25X)O_2 \longrightarrow (0.5 - 0.25X)CO_2 + 2(0.5 - 0.25X)H_2O$$

$$(Y)CH_4 + 2(Y)H_2O \longrightarrow (Y)CO_2 + 4(Y)H_2$$

$$(0.5 + 0.25X - Y)CH_4 + (0.5 + 0.25X - Y)H_2O \longrightarrow (0.5 + 0.25X - Y)CO + (0.5 + 0.25X - Y)H_2$$

$$(0.5 + 0.25X - Y)CO + (0.5 + 0.25X - Y)H_2O \longrightarrow (0.5 + 0.25X - Y)CO_2 + (0.5 + 0.25X - Y)H_2$$

$$CO_2 + H_2 \longrightarrow HCOOH$$

Which results in the following overall reaction:

$$CH_4 + (1 - \frac{X}{2})O_2 \longrightarrow HCOOH + (-\mathrm{X})H_2O(1+\mathrm{X})H_2$$

The reaction cluster reveals that reactions include methane (CH_4) combustion, which fuels the energy needs for the process. The cluster also includes steam methane reforming (SMR) used to produce hydrogen (H_2), which in sufficient amounts can convert (CO_2),the emission of which can be eliminated by producing formic acid ($CHOOH$). The design strategy of the NGCPS process is exceptionally valuable for coupling multiple product options

(formic acid, hydrogen, and electricity), and flexibility plays an important role in determining what configuration should be used in running the process. Varying demand for any commodity or product is best addressed by using an integrated process with multiple flexible subcomponents. The NGCPS process consists of:

- SMR;
- CH_4 Combustion;
- Chemical Conversion of CO_2; and
- A natural gas combined cycle.

The interaction between the different process subcomponents is shown in Figure 4.9 below.

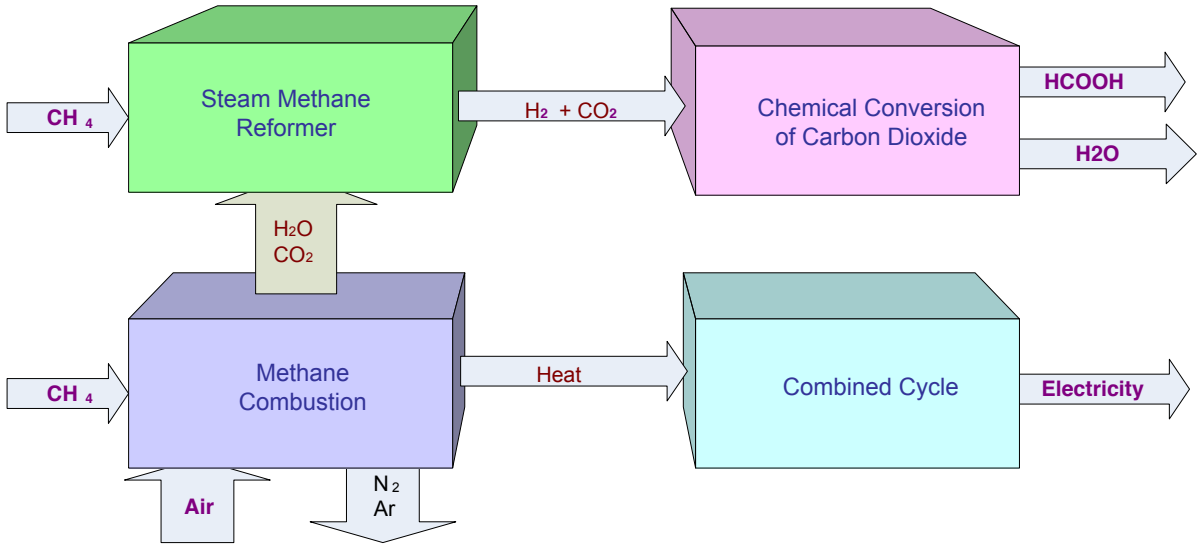

Figure 4.9: Power-chemical co-production process

4.3.1 Steam methane reforming(SMR)

Natural gas consists primarily of methane (CH_4) and other impurities in ratios that differs depending on the source of the natural gas. For this process, we assume that natural gas consists of pure methane (CH_4). for producing hydrogen and uses the following endothermic reactions of natural gas and water (steam) to produce hydrogen, carbon dioxide and carbon monoxide.

$$CH_4 + 2H_2O \longrightarrow CO_2 + 4H_2 \quad (\Delta H : 164.9\ kJmol^{-1}) \text{ (Endothermic)}$$

$$CH_4 + H_2O \longrightarrow CO + 3H_2 \quad (\Delta H : 206.1\ kJmol^{-1}) \text{ (Endothermic)}$$

Methane (CH_4) is fed to the process at the following conditions(1 kmole/s, 298 K, 1 atm), this methane is partially feed to the reformer (0.25 kmole/s), whereas the rest is used to generate the processâĂŹs energy needs. Steam (H_2O) is fed into the reformer through a recycle stream, along with the CH_4 stream, after which the feed is heated and pressurized to (1230 K, 21 atm) in preparation for the H_2 production at the reformer. The steam to methane ratio at the reformer is set to $\alpha = 3.19$ in order to maintain the required CH_4 conversion levels. The reformer products are then cooled to 350 K before entering the first flash column, where the liquid stream consisting of H_2O is split in two streams; the first is recycled back to the reformer at the rate of 0.80 kmole/s, whereas the second is the water stream leaving the process at a rate of 1.00 kmole/s. The vapor outlet of flash column 1 consisting primarily of H_2 and CO, among other species, is then sent to the chemical conversion section.

4.3.2 CH_4 combustion

Combustion systems operate at high temperatures ($T = 1300\ K$)and release a large amount of heat, which allows for the oxidation of CH_4 to CO_2 and H_2O. Since combustion systems

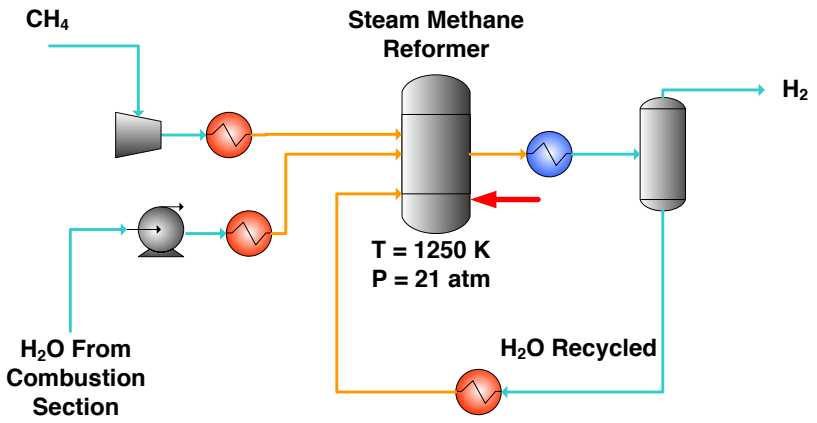

Figure 4.10: Flowsheet of Power-chemical co-production process distillation section

are rarely operated with precise stoichiometric ratios due to complexities in fuel-oxygen mixing, such systems are designed with a margin for error. Here, we assume perfect mixing to simplify the analysis. The air separation plant feed on air (298 K, 1 atm) and consists of two pressure swing absorber units that are used to separate N_2, Ar and O_2. The rest of CH_4 fed into the process (0.75 kmole/s) is fed into the combustion reactor where it reacts with O_2 extracted from the air separation plant at following conditions (1.5 kmole/s, 298 K and 1 atm). Both streams are then mixed with H_2O recycled from the chemical conversion section and heated to 1250 K before being fed into the combustion reactor (1300 K) and burnt according the following reaction:

$$CH_4 + 2O_2 \longrightarrow CO_2 + 2H_2O$$

The combustion reaction is assumed to convert completely in order to produce CO_2 and H_2O which are then cooled to 300 K. After the combustor products are sent to flash column 2, where CO_2 and H_2O are separated. The H_2O stream is then recycled back to the reformer, whereas the CO_2 stream is sent to the chemical conversion section.

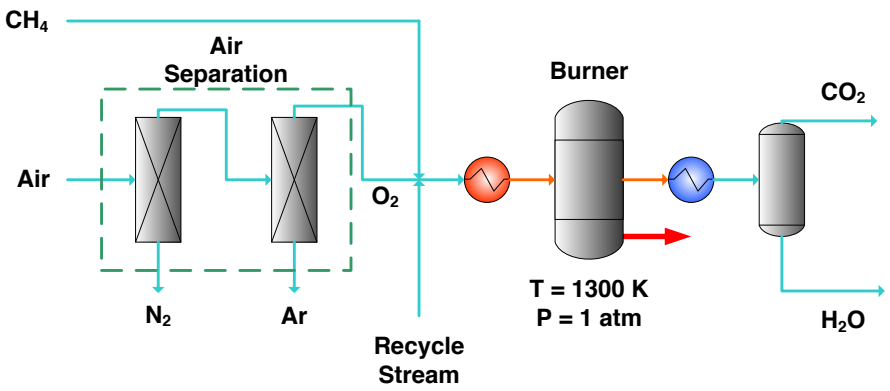

Figure 4.11: Flowsheet of Power-chemical co-production process steam methane reformer section

4.3.3 Chemical conversion of CO_2

CO_2 and H_2 coming from the SMR and the combustor, are compressed and cooled down (353 K, 40 atm) before entering the formic acid reactor react, as follows:

$$CO_2 + H_2 \longrightarrow HCOOH$$

The products of the formic acid reactor pass through a valve to reduce its pressure to (1 atm) are heated before entering the distillation column (368 K, 1 atm). There, high-purity formic acid is separated from the rest of the components, whereas the bottom products of the column are recycled back to feed the combustor.

4.3.4 Natural gas combined cycle

Heat is transfered from the combustion plant to the combined Brayton-Rankine cycle using an argon/steam as the working fluid. In that design, the topping cycle is the Brayton cycle (Argon), whereas the bottoming cycle is the Rankine Cycle (Steam). Argon (Ar) is compressed and fed into a combustor running on CH_4 and then fed into the gas turbine[127]. As the hot mixture enters the gas turbine, it rotates the turbine's blades to generate work in

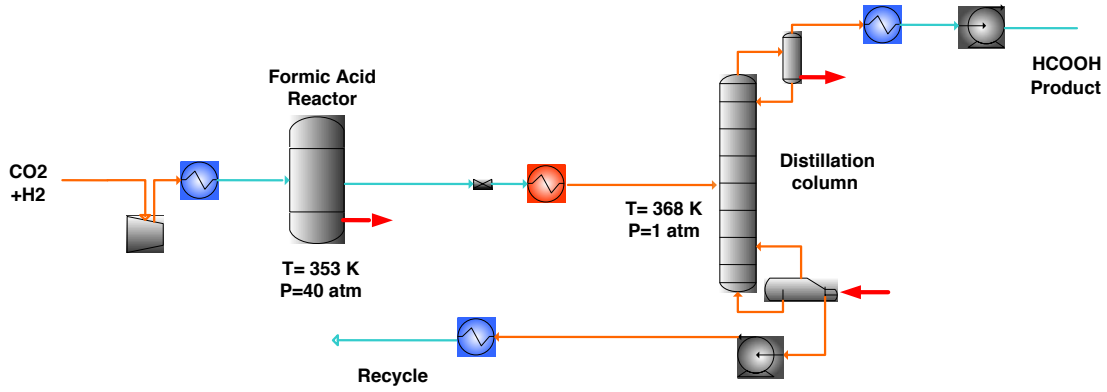

Figure 4.12: Flowsheet of Power-chemical co-production process burner section

order to complete the Brayton cycle, and the resulting hot exhaust (low entropy) is moved to the Rankine cycle, starting with the heat recovery boiler. The heat recovery boiler consists of a series of heat exchangers used to create superheated steam by passing the hot exhaust through the heat exchangers. The superheated steam then enters the steam turbine, where it expands to generate additional work by rotating the turbine blades, which improves the overall efficiency of the cycle. The Brayton cycle operates in open-loop mode, whereas the Rankine cycle operates in closed-loop mode. The water exiting the steam turbine is fed into a cooling tower before pumped to a high pressure and sent to the heat recovery boiler to close the cycle loop, as shown in figure 4.13.

4.4 Results and discussion

The chemical-power system can be analyzed by evaluating its economic impact, measured according to power generation potential and the value of the chemicals produced. The primary factor contributing to the power generation potential is the difference between the heat generated by burning natural gas (Q_C) and the heat load of the reformer Q_{SMR} (hereafter Q_D). For each iteration adjusting the CH_4 split ratio between the combustor and the reformer will require adjusting the oxygen feed to the combustor and the water to CH_4

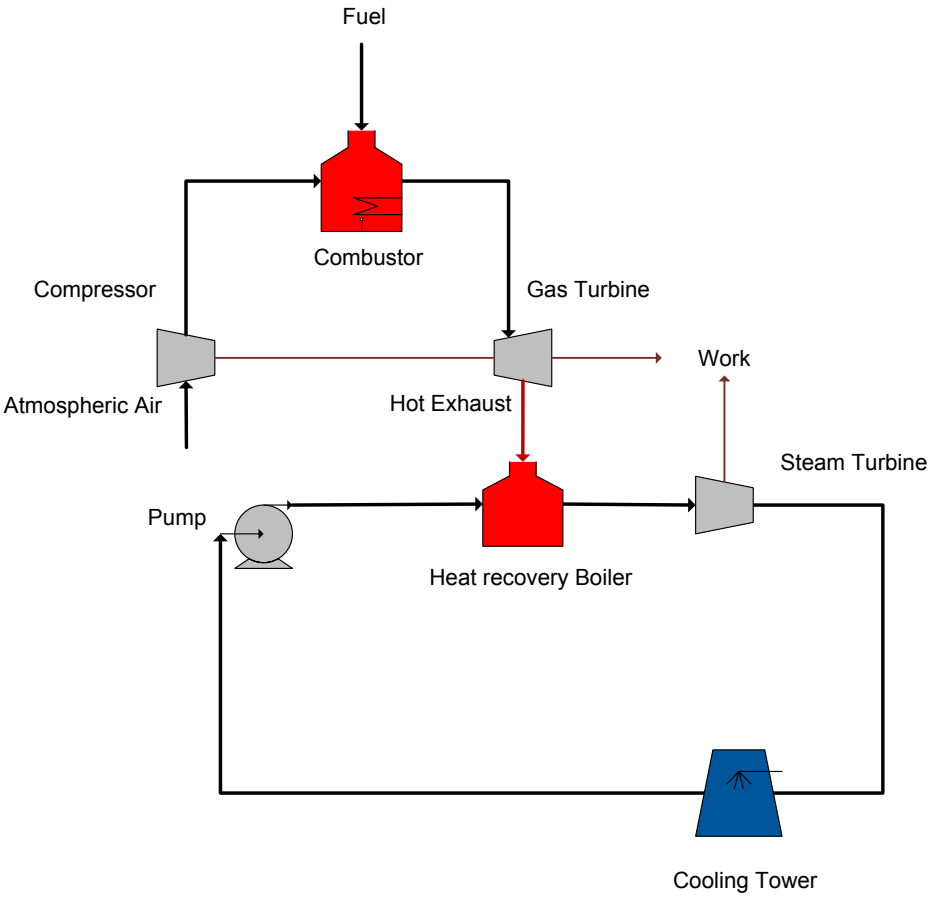

Figure 4.13: Combined Brayton-Rankine Cycle

ratio in the reformer to calculate a new Q_D. Table 4.2 shows how the quantities of natural gas sent to both the reformer and the combustor affect the decision-making process. A balance needs to be struck between maximizing the power generation potential Q_D and meeting the production targets of formic acid. Sending 90% of the natural gas to the combustor will maximizes Q_D; however, we cannot produce enough hydrogen to neutralize the carbon dioxide emissions.

The aforementioned reaction cluster features two degrees of freedom $X \geq -1$ and $Y \geq 0$[99], controlling both parameters X and Y will enable the control of the system to be optimized for hydrogen (H_2), formic acid($CHOOH$) or power production. Here, we will avoid producing hydrogen (H_2) to maximize the power production, we set $X = -1$ and

Table 4.2: Power Generation Potential (Q_D)

CH_4 to reformer (% feed)	CH_4 to combustor (% feed)	Q_D ($\frac{kJ}{s}$)
10	90	6.942×10^5
25	75	5.418×10^5
40	60	3.907×10^5
60	40	1.883×10^5
75	25	3.660×10^4

$Y = 0.125$, which resulted in sending 75% of the natural gas to the combustor and 25% to the reformer. The result is the following reaction:

$$CH_4 + \frac{3}{2}O_2 \longrightarrow HCOOH + H_2O$$

In what follows, we perform heat and power integration analysis in order to calculate the minimum utility cost needed for a heat engine network based on the formulation presented earlier. In doing so, we consider an inclusive thermodynamic approach including all heating and cooling units in the process. Notably, the HEN network has access to cold utilities only. Figure. 4.14 shows the temperature interval diagram that characterize the flow of heat across the pinch and determines segments where the use of utility is needed without prior contentment to the power operations (heat engines & heat pumps). Such an approach can maximize the efficiency by which we meet the minimum energy required to design an energetically self sufficient system.

The pinch temperature (ΔT_{min}) is the segment of the diagram in which the heat flow is not continuous. (ΔT_{min}) wont appear as a singular point but as a bottlenecking segment where heat transfer is most challenging. Studying the area around (ΔT_{min}) can improve the chances of designing an efficient power operations as well as the overall work (W) produced by the process as shown in table. 4.3.

Figure. 4.15 shows the HEPN temperature entropy diagram ($T - \Delta S$) featuring mini-

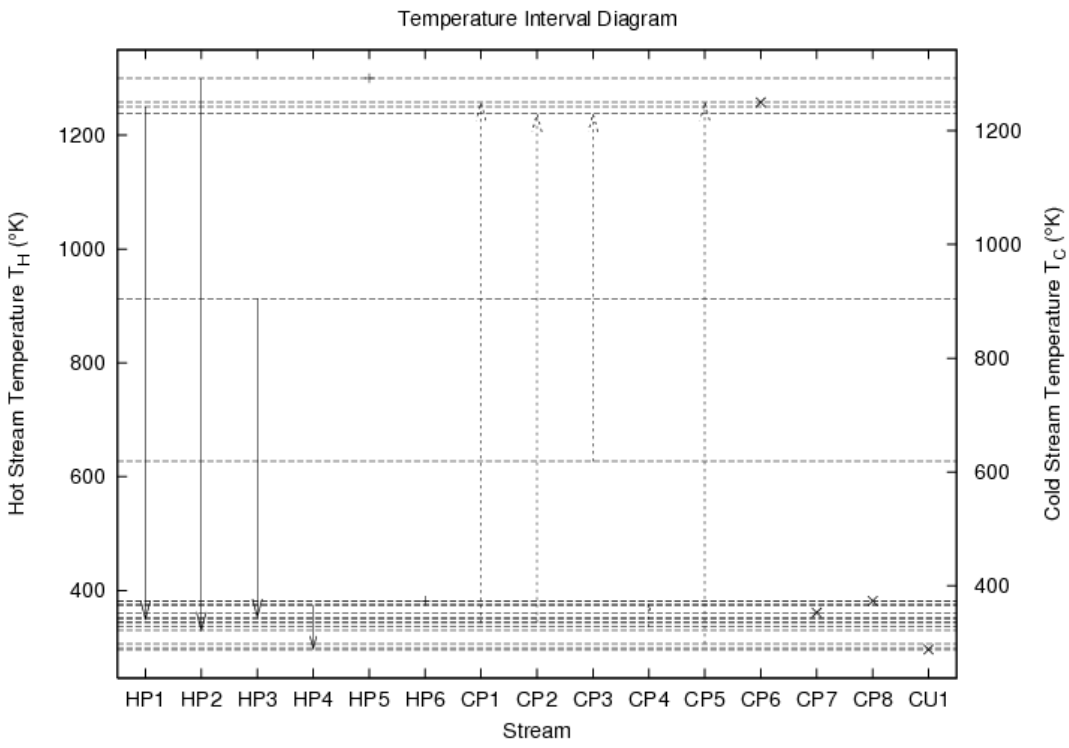

Figure 4.14: Temperature Interval Diagram

mum cold utility; the diagram is used to describe the temperatures that shape the power operations. Segments of the temperature entropy diagram where the hot stream curve is below the cold stream curve show the operations of the heat pump, whereas segments where the hot curve is above the cold curve shows the operations of the heat engine. The figure shows no segments in which the hot stream curve is above the cold stream curve, meaning that the power operation does not require the use of heat pumps, as explained by the fact that sufficient heat is generated within the process to avoid the need to transfer heat against the temperature gradient. To operate, the process depends on one heat engine to produce the needed change in entropy between the process streams.

Figure. 4.16 shows the HEP network temperature enthalpy diagram ($T - \Delta H$) featuring minimum cold utility, in which the exact temperature separating the power operation segments is not defined on the enthalpy scale[126]. However, Figure. 4.16 can be used to determine the amount of work generated, represented on an enthalpy scale as the difference

Table 4.3: W as a function of ΔT_{min}

ΔT_{min} (K)	W (kJ/s)
1	5.19×10^5
2	5.17×10^5
3	5.14×10^5
4	5.12×10^5
5	5.09×10^4

between the hot stream and cold stream curves, as shown by the red column.

For this process, we propose a natural gas combined cycle for electricity and chemical production. Brayton cycle acts as the topping cycle with Argon (Ar) as its working fluid, whereas the Rankine cycle acts the bottoming cycle with steam (H_2O) as its working fluid. The topping cycle runs a gas turbine at $P = 3.5atm$ with a flu gas at $T = 950K$, whereas the bottoming cycle recovers the heat from the flu gas to run a steam turbine at $P = 217.1atm$. Electricity is generated by the combined cycle at a rate of 244,300 kW. To put that number into perspective, we compare it with an actual natural gas combined cycle plant that generates electricity at a rate of 555,000 kW [124]. The decline stems from the fact that part of the methane fed into the process is used to produce formic acid, which is another revenue stream.

Having established the power generation potential of the process, we can use heat and power integration to conduct a cost-revenue analysis of the converged flowsheet. The system's operating cost consists only of the cost of natural gas, which equals conventional power generation and NGCPS; thus, we focus on the revenue streams generated from each process. All calculations in our analysis are on a mole of natural gas basis. A typical natural gas power plant would generates a revenue of \$13.23 /mol CH_4 while an NGCPS generates \$7.09 /mol CH_4 for the electricity generated. That difference derives from the fact that part of the natural gas fed into the NGCPS is used to generate the hydrogen required to neutralize the carbon dioxide emission. Based on the current price of formic acid of \$0.70 /kg [99], ,

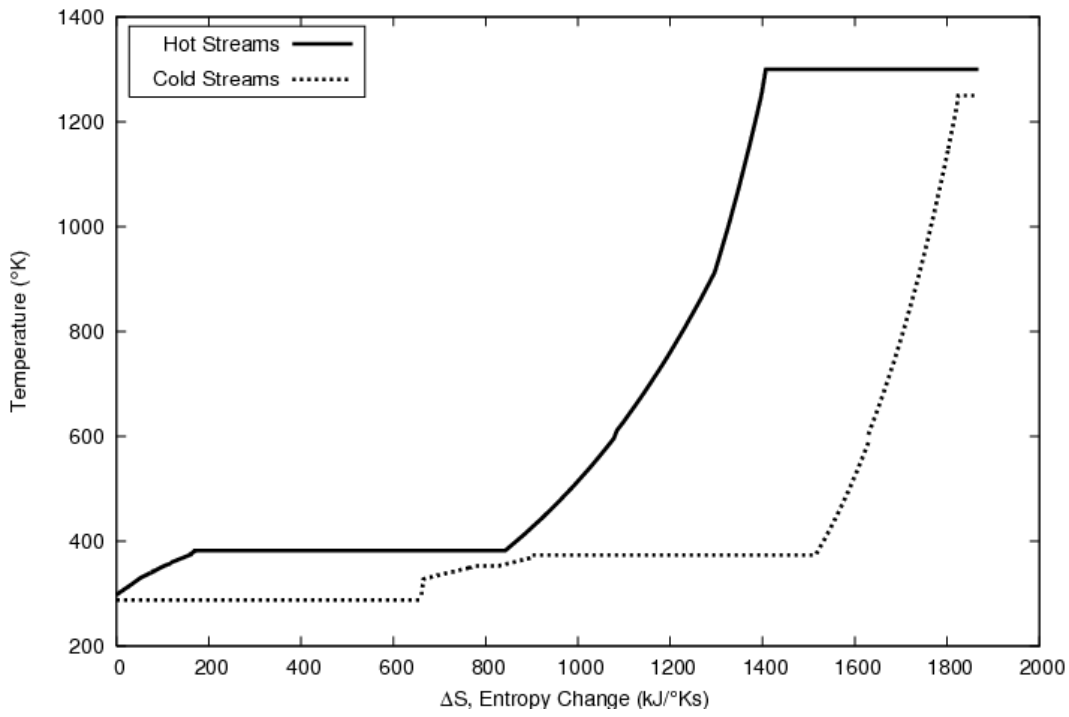

Figure 4.15: HEPN Temperature Entropy Diagram ($T - \Delta S$)

the NGCPS produces \$32.22 /mol CH_4 worth of formic acid. That result brings the total economic potential of the NGCPS to \$39.3 /mol CH_4 , a 297% increase over the economic potential of conventional natural gas power generation.

In the event that future legislation pushes for carbon pricing programs such as carbon taxes or carbon cap and trade systems, the cost of carbon-emitting chemicals or power generation processes would increase with the cost associated with carbon emissions. Such additional costs will be depend on the emissions profile of fossil fuels used in the process, and cleaner fuels such as natural gas will pose lower penalty costs than other fuels such as oil and coal [124]. Processes with carbon use technologies such as chemical-power generation would be immune to such legislation due to their environmental-friendly nature. Although carbon emission prices are currently deregulated in the United States, there is an increasing push to set targets and prices for such them.

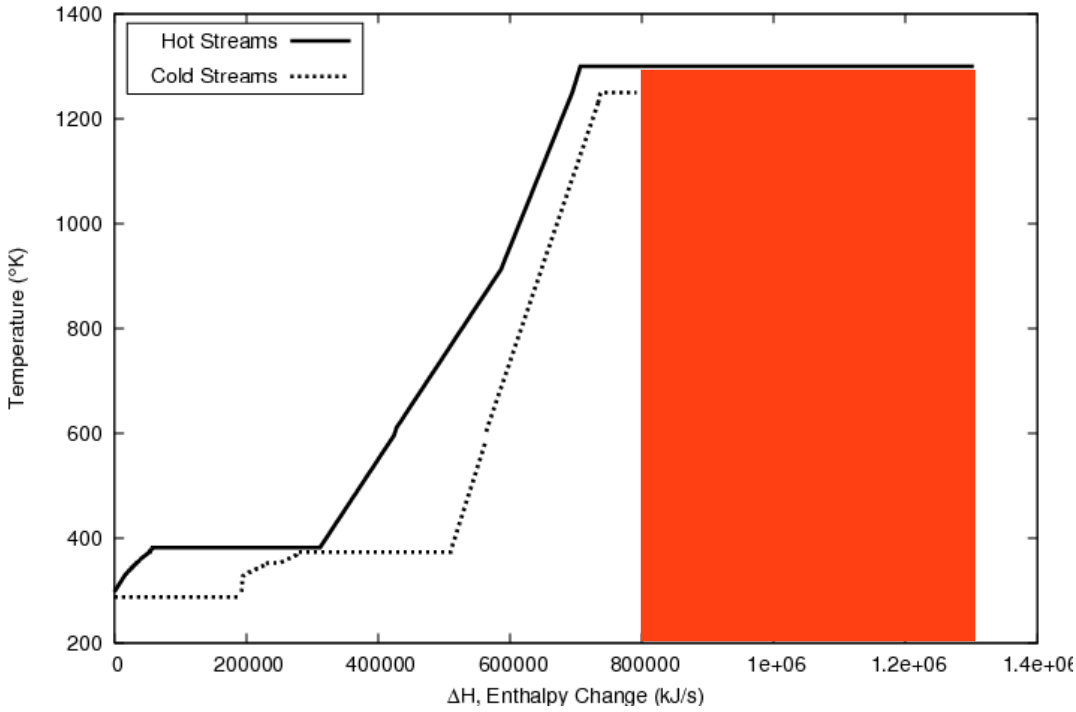

Figure 4.16: HEPN Temperature Enthalpy Change Diagram ($T - \Delta H$)

4.5 Conclusions

The proposed NGCPS is a novel, sustainable way of using natural gas to produce electricity and formic acid. The system shows the hydrogenation of CO_2 to be an environmentally friendly formic acid production method. Using or converting CO_2 is a better economical alternative to CCS in power generation, since it enables avoiding permanent CO_2 storage costs endured by power generation with carbon capture. The NGCPS produces 1 kmol of formic acid and 244,300 kW of electricity for every kmol of natural gas, and our operating cost analysis of the system suggests a return of 297%. The novelty of this work is that it combines two unique and profitable industries (power and high-value chemicals), whose union opens a path for new sustainable designs for the coproduction of different high-value specialty chemicals and electricity using the framework presented in this chapter.

Nomenclature

η thermal effiency

$\overline{C}_A(\tau)$ SLFR concentration of A at residence time τ

$\overline{C}_A(\tau)$ SLFR concentration of C at residence time τ

$\tau(i)$ residence time of the ith OP unit

τ_c critical value of the residence time τ

$C_k^I(j)$ kth component concentration in the jth network inlet

$C_k^O(i)$ kth component concentration in the ith network outlet

$C_k^{\overline{I}}(i)$ kth component concentration in the ith OP inlet

$C_k^{\overline{O}}(i)$ kth component concentration in the ith OP outlet

$C_A(\tau)$ PFR concentration of A at residence time τ

$C_C(\tau)$ PFR concentration of C at residence time τ

E residence time density function

$E(\theta)$ normalized residence time density (NRTd) function value at normalized time θ

F volumetric flow rate ($\frac{m^3}{s}$)

$F^I(j)$ jth network inlet flow rate

$F^O(i)$ ith network outlet flow rate

$F^{\hat{I}\hat{O}}(i,j)$ jth OP outlet flow rate to the ith OP network outlet

$F^{\hat{I}I}(i,j)$ jth network outlet flow rate to the ith OP inlet

$F^{\hat{I}}(j)$ jth OP inlet flow rate

$F^{\hat{O}}(i)$ ith OP outlet flow rate

F^{in} inlet volumetric flow rate ($\frac{m^3}{s}$)

$F^{O\hat{O}}(i,j)$ jth OP outlet flow rate to the ith network outlet

$F^{OI}(i,j)$ jth network inlet flow rate to the ith network outlet

F^{out} outlet volumetric flow rate ($\frac{m^3}{s}$)

N_I IDEAS network inlet streams

N_O IDEAS network outlet streams

V volume (m^3)

W Work

References

[1] M. Conforti, G. Cornuéjols, and G. Zambelli, *Integer programming*, vol. 271. Springer, 2014.

[2] P. Zakkour and G. Cook, "Ccs roadmap for industry: High-purity co2 sources," *Sectoral Assessment-Final Draft Report. Global Technology Roadmap for CCS in Industry*, 2010.

[3] R. M. Navarro, M. C. Sanchez-Sanchez, M. C. Alvarez-Galvan, J. L. G. Fierro, and S. M. Al-Zaharani, "H2 production from renewables," *Energy Production and Storage: Inorganic Chemical Strategies for a Warming World*, p. 3, 2013.

[4] M. Conte, A. Iacobazzi, M. Ronchetti, and R. Vellone, "Hydrogen economy for a sustainable development: state-of-the-art and technological perspectives," *Journal of Power Sources*, vol. 100, no. 1, pp. 171–187, 2001.

[5] K. Eberhard, "All the world's carbon pricing systems in one animated map," *Sightline Daily*, vol. 44, 2014.

[6] W. B. Group, "World development indicators 2015," 2015.

[7] R. MacMullin and M. Weber, "The theory of short-circuiting in continuous-flow mixing vessels in series and the kinetics of chemical reactions in such systems," *Trans. Am. Inst. Chem. Eng*, vol. 31, no. 2, pp. 409–458, 1935.

[8] E. L. Paul, V. A. Atiemo-Obeng, and S. M. Kresta, *Handbook of industrial mixing: science and practice*. John Wiley & Sons, 2004.

[9] M. J. Cheah, I. G. Kevrekidis, and J. B. Benziger, "Water slug formation and motion in gas flow channels: the effects of geometry, surface wettability, and gravity," *Langmuir*, vol. 29, no. 31, pp. 9918–9934, 2013.

[10] E. B. Nauman, "Residence time theory," *Industrial & Engineering Chemistry Research*, vol. 47, no. 10, pp. 3752–3766, 2008.

[11] O. Levenspiel, "Chemical reaction engineering," *Industrial & engineering chemistry research*, vol. 38, no. 11, pp. 4140–4143, 1999.

[12] E. B. Nauman and B. Buffham, *Mixing in continuous flow systems*. John Wiley & Sons Inc, 1983.

[13] J. B. Rawlings and J. G. Ekerdt, *Chemical reactor analysis and design fundamentals*. Nob Hill Pub, Llc, 2002.

[14] H. S. Fogler, *Elements of chemical reaction engineering*. Prentice-Hall International London;, 1999.

[15] J. Bałdyga, J. Bourne, and S. Hearn, "Interaction between chemical reactions and mixing on various scales," *Chemical Engineering Science*, vol. 52, no. 4, pp. 457–466, 1997.

[16] P. Danckwerts, "Continuous flow systems: distribution of residence times," *Chemical Engineering Science*, vol. 2, no. 1, pp. 1–13, 1953.

[17] T. N. Zwietering, "The degree of mixing in continuous flow systems," *Chemical Engineering Science*, vol. 11, no. 1, pp. 1–15, 1959.

[18] S. C. Tseng, N. B. Jackson, and J. G. Ekerdt, "Isosynthesis reactions of coh2 over zirconium dioxide," *Journal of Catalysis*, vol. 109, no. 2, pp. 284–297, 1988.

[19] S. Chauhan, J. Bell, and R. Adler, "On optimum mixing in continuous homogeneous reactors," *Chemical Engineering Science*, vol. 27, no. 3, pp. 585–591, 1972.

[20] J. D. Paccione, D. M. Follansbee, P. L. Young, and D. M. Dziewulski, "Analytical determination of the baffle factor for disinfection contact systems based on hydraulic analysis, disinfection kinetics, and c t tables," *Journal of Environmental Engineering*, p. 04016026, 2016.

[21] D. Glasser, C. Crowe, and D. Hildebrandt, "A geometric approach to steady flow reactors: the attainable region and optimization in concentration space," *Industrial & Engineering Chemistry Research*, vol. 26, no. 9, pp. 1803–1810, 1987.

[22] S. Hocine, L. Pibouleau, C. Azzaro-Pantel, and S. Domenech, "Modelling systems defined by rtd curves," *Computers & Chemical Engineering*, vol. 32, no. 12, pp. 3112–3120, 2008.

[23] Z. Al-Husseini and V. I. Manousiouthakis, "Ideas based synthesis of minimum volume reactor networks featuring residence time density/distribution models," *Computers & Chemical Engineering*, vol. 60, pp. 124–142, 2014.

[24] J. F. Burri, S. D. Wilson, and V. I. Manousiouthakis, "Infinite dimensional state-space approach to reactor network synthesis: application to attainable region construction," *Computers & chemical engineering*, vol. 26, no. 6, pp. 849–862, 2002.

[25] V. I. Manousiouthakis, A. M. Justanieah, and L. A. Taylor, "The shrink–wrap algorithm for the construction of the attainable region: an application of the ideas framework," *Computers & chemical engineering*, vol. 28, no. 9, pp. 1563–1575, 2004.

[26] A. Posada and V. Manousiouthakis, "Multi-feed attainable region construction using the shrink–wrap algorithm," *Chemical Engineering Science*, vol. 63, no. 23, pp. 5571–5592, 2008.

[27] J. A. Conner and V. I. Manousiouthakis, "Global optimality properties of total annualized and operating cost problems for compressor sequences," *AIChE Journal*, vol. 60, no. 12, pp. 4134–4149, 2014.

[28] B. J. Davis, L. A. Taylor, and V. I. Manousiouthakis, "Identification of the attainable region for batch reactor networks," *Industrial & Engineering Chemistry Research*, vol. 47, no. 10, pp. 3388–3400, 2008.

[29] W. Zhou and V. I. Manousiouthakis, "Non-ideal reactor network synthesis through ideas: Attainable region construction," *Chemical engineering science*, vol. 61, no. 21, pp. 6936–6945, 2006.

[30] W. Zhou and V. I. Manousiouthakis, "Global capital/total annualized cost minimization of homogeneous and isothermal reactor networks," *Industrial & Engineering Chemistry Research*, vol. 47, no. 10, pp. 3771–3782, 2008.

[31] V. I. Manousiouthakis, "On dimensionality of attainable region construction for isothermal reactor networks," *Computers & Chemical Engineering*, vol. 32, no. 3, pp. 439–450, 2008.

[32] W. Zhou and V. I. Manousiouthakis, "Automating the ar construction for non-isothermal reactor networks," *Computers & Chemical Engineering*, vol. 33, no. 1, pp. 176–180, 2009.

[33] W. Zhou and V. I. Manousiouthakis, "Variable density fluid reactor network synthesisâĂŤconstruction of the attainable region through the ideas approach," *Chemical Engineering Journal*, vol. 129, no. 1, pp. 91–103, 2007.

[34] S. Wilson and V. Manousiouthakis, "Ideas approach to process network synthesis: Application to multicomponent men," *AIChE journal*, vol. 46, no. 12, pp. 2408–2416, 2000.

[35] A. M. Justanieah and V. Manousiouthakis, "Ideas approach to the synthesis of globally optimal separation networks: application to chromium recovery from wastewater," *Advances in Environmental Research*, vol. 7, no. 2, pp. 549–562, 2003.

[36] L. L. Martin and V. I. Manousiouthakis, "Globally optimal power cycle synthesis via the infinite-dimensional state-space (ideas) approach featuring minimum area with fixed utility," *Chemical engineering science*, vol. 58, no. 18, pp. 4291–4305, 2003.

[37] J. F. Burri and V. I. Manousiouthakis, "Global optimization of reactive distillation networks using ideas," *Computers & chemical engineering*, vol. 28, no. 12, pp. 2509–2521, 2004.

[38] K. Holiastos and V. Manousiouthakis, "Infinite-dimensional state-space (ideas) approach to globally optimal design of distillation networks featuring heat and power integration," *Industrial & engineering chemistry research*, vol. 43, no. 24, pp. 7826–7842, 2004.

[39] J. E. Drake and V. Manousiouthakis, "Ideas approach to process network synthesis: minimum plate area for complex distillation networks with fixed utility cost," *Industrial & engineering chemistry research*, vol. 41, no. 20, pp. 4984–4992, 2002.

[40] J. E. Drake and V. Manousiouthakis, "Ideas approach to process network synthesis: minimum utility cost for complex distillation networks," *Chemical engineering science*, vol. 57, no. 15, pp. 3095–3106, 2002.

[41] R. Sargent and K. Gaminibandara, "Optimum design of plate distillation columns," *Optimization in action*, pp. 267–314, 1976.

[42] I. E. Grossmann and R. Sargent, "Optimum design of heat exchanger networks," *Computers & Chemical Engineering*, vol. 2, no. 1, pp. 1–7, 1978.

[43] F. Horn, "Attainable and non-attainable regions in chemical reaction technique," in *CHIMICA & L INDUSTRIA*, vol. 47, p. 235, Polo Vle Abruzzi 5, 20131 Milan, Italy, 1965.

[44] J.-B. Hiriart-Urruty, "From convex optimization to nonconvex optimization. necessary and sufficient conditions for global optimality," in *Nonsmooth optimization and related topics*, pp. 219–239, Springer, 1989.

[45] D. G. Luenberger, *Introduction to linear and nonlinear programming*, vol. 28. Addison-Wesley Reading, MA, 1973.

[46] M. Jünger, T. M. Liebling, D. Naddef, G. L. Nemhauser, W. R. Pulleyblank, G. Reinelt, G. Rinaldi, and L. A. Wolsey, *50 Years of integer programming 1958-2008: From the early years to the state-of-the-art*. Springer Science & Business Media, 2009.

[47] G. B. Dantzig, "Application of the simplex method to a transportation problem," *Activity analysis of production and allocation*, vol. 13, pp. 359–373, 1951.

[48] G. Dantzig, R. Fulkerson, and S. Johnson, "Solution of a large-scale traveling-salesman problem," *Journal of the operations research society of America*, vol. 2, no. 4, pp. 393–410, 1954.

[49] G. Stephanopoulos and G. V. Reklaitis, "Process systems engineering: From solvay to modern bio-and nanotechnology.: A history of development, successes and prospects for the future," *Chemical engineering science*, vol. 66, no. 19, pp. 4272–4306, 2011.

[50] M. R. Garey and D. S. Johnson, "A guide to the theory of np-completeness," *WH Freemann, New York*, 1979.

[51] A. Fügenschuh and A. Martin, "Computational integer programming and cutting planes," *Handbooks in Operations Research and Management Science*, vol. 12, pp. 69–121, 2005.

[52] K. L. Hoffman and T. K. Ralphs, "Integer and combinatorial optimization," in *Encyclopedia of Operations Research and Management Science*, pp. 771–783, Springer, 2013.

[53] M. W. Savelsbergh, "Preprocessing and probing techniques for mixed integer programming problems," *ORSA Journal on Computing*, vol. 6, no. 4, pp. 445–454, 1994.

[54] W. L. Winston and J. B. Goldberg, *Operations research: applications and algorithms*, vol. 3. Duxbury press Belmont, CA, 2004.

[55] M. A. Branch and A. Grace, *MATLAB: optimization toolbox: user's guide version 1.5*. The MathWorks, 1996.

[56] E. Klotz and A. M. Newman, "Practical guidelines for solving difficult mixed integer linear programs," *Surveys in Operations Research and Management Science*, vol. 18, no. 1, pp. 18–32, 2013.

[57] H. Stadtler and C. Kilger, "Supply chain management and advanced planning," 2002.

[58] E. D. Andersen and K. D. Andersen, "Presolving in linear programming," *Mathematical Programming*, vol. 71, no. 2, pp. 221–245, 1995.

[59] R. E. Gomory, "Outline of an algorithm for integer solutions to linear programs and an algorithm for the mixed integer problem," in *50 Years of Integer Programming 1958-2008*, pp. 77–103, Springer, 2010.

[60] R. E. Gomory and T. C. Hu, "Multi-terminal network flows," *Journal of the Society for Industrial and Applied Mathematics*, vol. 9, no. 4, pp. 551–570, 1961.

[61] B. Golden, L. Bodin, T. Doyle, and W. Stewart Jr, "Approximate traveling salesman algorithms," *Operations research*, vol. 28, no. 3-part-ii, pp. 694–711, 1980.

[62] S. El Azzeh, M. Sarshar, and R. Fayaz, "Hydrogen economy and the built environment," in *World Renewable Energy Congress-Sweden; 8-13 May; 2011; Linköping; Sweden*, no. 057, pp. 1986–1995, Linköping University Electronic Press, 2011.

[63] K. Kendall, "Hydrogen and fuel cells in city transport," *International Journal of Energy Research*, vol. 40, no. 1, pp. 30–35, 2016.

[64] J. Stephens and W. Cartagena, "Liquid hydrogen propellant tank sub-surface pressurization with gaseous helium," 2015.

[65] I. Dincer and C. Acar, "Review and evaluation of hydrogen production methods for better sustainability," *international journal of hydrogen energy*, vol. 40, no. 34, pp. 11094–11111, 2015.

[66] A. Messerschmitt, "Verfahren zur erzeugung von wasserstoff durch abwechselnde oxidation und reduktion von eisen in von außen beheizten, in den heizraeumen angeordneten zersetzern," *German Patent DE*, vol. 266863, 1911.

[67] V. Hacker, R. Fankhauser, G. Faleschini, H. Fuchs, K. Friedrich, M. Muhr, and K. Kordesch, "Hydrogen production by steam–iron process," *Journal of Power Sources*, vol. 86, no. 1, pp. 531–535, 2000.

[68] J. W. Erisman, M. A. Sutton, J. Galloway, Z. Klimont, and W. Winiwarter, "How a century of ammonia synthesis changed the world," *Nature Geoscience*, vol. 1, no. 10, pp. 636–639, 2008.

[69] D. Gardner, "Hydrogen production from renewables," *Renewable Energy Focus*, vol. 9, no. 7, pp. 34–37, 2009.

[70] S. E. Hosseini and M. A. Wahid, "Hydrogen production from renewable and sustainable energy resources: Promising green energy carrier for clean development," *Renewable and Sustainable Energy Reviews*, vol. 57, pp. 850–866, 2016.

[71] T. Riis, E. F. Hagen, P. J. Vie, and Ø. Ulleberg, "Hydrogen production and storage–r&d priorities and gaps," *IEA Hydrogen Implementing Agreement (HIA)*, 2006.

[72] B. on Energy, E. S. N. R. Council, D. on Engineering, P. S. N. R. Council, and W. N. A. of Engineering, *The hydrogen economy: Opportunities, costs, barriers, and R&D needs*. National Academies Press, 2004.

[73] B. Metz, O. Davidson, H. De Coninck, M. Loos, L. Meyer, *et al.*, "Carbon dioxide capture and storage," 2005.

[74] P. Farnell, "Engineering aspects of hydrocarbon steam reforming catalysts," *Topics in Catalysis*, vol. 59, no. 8-9, pp. 802–808, 2016.

[75] F. Beyer, J. Brightling, P. Farnell, and C. Foster, "Steam reforming–50 years of development and the challenges for the next 50 years," in *AIChE 50th Annual Safety in Ammonia Plants and Related Facilities Symposium, Toronto, Canada*, 2005.

[76] L. J. Christiansen, "Use of modeling in scale-up of steam reforming technology," *Catalysis Today*, vol. 272, pp. 14–18, 2016.

[77] J. Xu and G. F. Froment, "Methane steam reforming, methanation and water-gas shift: I. intrinsic kinetics," *AIChE Journal*, vol. 35, no. 1, pp. 88–96, 1989.

[78] A. Poullikkas, "Economic analysis of power generation from parabolic trough solar thermal plants for the mediterranean regionâĂŤa case study for the island of cyprus," *Renewable and sustainable Energy reviews*, vol. 13, no. 9, pp. 2474–2484, 2009.

[79] N. H. Stern, S. Peters, V. Bakhshi, A. Bowen, C. Cameron, S. Catovsky, D. Crane, S. Cruickshank, S. Dietz, N. Edmonson, *et al.*, *Stern Review: The economics of climate change*, vol. 30. Cambridge University Press Cambridge, 2006.

[80] M. L. Weitzman, "Prices vs. quantities," *The review of economic studies*, vol. 41, no. 4, pp. 477–491, 1974.

[81] S. C. Bhattacharyya, *Energy economics: concepts, issues, markets and governance*. Springer Science & Business Media, 2011.

[82] International Energy Agency, "co_2 emissions from fuel combustion," 2016.

[83] I. Bailey, "The eu emissions trading scheme," *Wiley Interdisciplinary Reviews: Climate Change*, vol. 1, no. 1, pp. 144–153, 2010.

[84] E. C. Action, "The eu emissions trading system (eu ets)," 2013.

[85] A. Gilbert, J.-W. Bode, and D. Phylipsen, *Analysis of the national allocation plans for the EU emissions trading scheme*. Ecofys, 2004.

[86] GOV.UK, "Excise notice ccl1/3: Climate change levy - reliefs and special treatments for taxable commodities," 2015.

[87] Ministry for the environment, "Environmental reporting on atmosphere and climate," 2016.

[88] J. Carl and D. Fedor, "Tracking global carbon revenues: A survey of carbon taxes versus cap-and-trade in the real world," *Energy Policy*, vol. 96, pp. 50–77, 2016.

[89] J. Sumner, L. Bird, and H. Dobos, "Carbon taxes: a review of experience and policy design considerations," *Climate Policy*, vol. 11, no. 2, pp. 922–943, 2011.

[90] L. Abboud, "An exhausting war on emissions: NorwayâĂ§ s efforts to contain greenhouse gases move forward–and backfire," *Wall Street Journal*, 2008.

[91] B. Johansson, "Economic instruments in practice 1: Carbon tax in sweden," in *workshop on innovation and the environment, OECD, Paris*, vol. 19, 2000.

[92] J. H. Davis and C. Davenport, "China to announce cap-and-trade program to limit emissions," *The New York Times*, vol. 24, 2015.

[93] Carbon Tax Center, "Where carbon is taxed," 2010.

[94] "Japan introduces new tax on carbon emissions," Jan 2013.

[95] Finnish Energy, "Energy taxation in europe, japan and the united states," 2011.

[96] F. J. Convery, L. Dunne, D. Joyce, *et al.*, "Ireland's carbon tax and the fiscal crisis: Issues in fiscal adjustment, environmental effectiveness, competitiveness, leakage and equity implications," tech. rep., OECD Publishing, 2013.

[97] E. Rosenthal, "Carbon taxes make ireland even greener," *New York Times*, 2012.

[98] Irish Tax and Customs, "Guide to natural gas carbon tax," June 2009.

[99] J. A. P. Lopez and V. I. Manousiouthakis, "Natural gas based hydrogen production with zero carbon dioxide emissions," *international journal of hydrogen energy*, vol. 36, no. 20, pp. 12853–12868, 2011.

[100] P. G. Ghougassian and V. Manousiouthakis, "Attainable composition, energy consumption, and entropy generation properties for isothermal/isobaric reactor networks," *Industrial & Engineering Chemistry Research*, vol. 52, no. 9, pp. 3225–3238, 2013.

[101] P. G. Ghougassian and V. Manousiouthakis, "Minimum entropy generation for isothermal endothermic/exothermic reactor networks," *AIChE Journal*, vol. 61, no. 1, pp. 103–117, 2015.

[102] F. A. Tobiesen, H. F. Svendsen, and K. A. Hoff, "Desorber energy consumption amine based absorption plants," *International Journal of Green Energy*, vol. 2, no. 2, pp. 201–215, 2005.

[103] A. Posada and V. Manousiouthakis, "Hydrogen and dry ice production through phase equilibrium separation and methane reforming," *Journal of power sources*, vol. 156, no. 2, pp. 480–488, 2006.

[104] C. Turchi, M. Mehos, C. K. Ho, and G. J. Kolb, "Current and future costs for parabolic trough and power tower systems in the us market," in *Proceedings of the 16th SolarPACES Conference, Perpignan, France*, 2010.

[105] "Inventory of U.S. greenhouse gas emissions and sinks: 1990-2014," tech. rep., US Environmental Protection Agency, 2016.

[106] "Global mitigation of non-co_2 greenhouse gases: 2010-2030," tech. rep., US Environmental Protection Agency, 2013.

[107] G. E. Metcalf and D. Weisbach, "Design of a carbon tax, the," *Harv. Envtl. L. Rev.*, vol. 33, p. 499, 2009.

[108] ESRL, NOAA, "National oceanic & atmospheric administration, earth system research laboratory: Mauna loa co2 annual mean data," 2015.

[109] ESRL, NOAA, "National oceanic & atmospheric administration: Earth system research laboratory. time history of atmospheric carbon dioxide from 800,000 years ago until january 2012.," 2015.

[110] International Atomic Energy Agency, "Energy, electricity and nuclear power estimates for the period up to 2050," 2015.

[111] D. Buchan, *The Energiewende-Germany's gamble*. Oxford Institute for Energy Studies Oxford, 2012.

[112] International Energy Agency, "World energy outlook," 2010.

[113] D. Y. Goswami and F. Kreith, *Energy conversion*. CRC press, 2007.

[114] Environmental Protection Agency, "Regulatory impact analysis: Clean power plan proposed rule," 2014.

[115] Energy Information Administration, "Power sector co2 emissions sensitive to policy changes and natural gas supply," 2015.

[116] California Energy Commission, "Energy almanac: California electricity statistics & data," 2015.

[117] Z. Wang and A. Krupnick, "A retrospective review of shale gas development in the united states: What led to the boom?," *Resources for the Future DP*, pp. 13–12, 2013.

[118] Energy Information Administration, "Short Term Energy Outlook," 2016.

[119] T. Colmenares and W. Seider, "Heat and power integration of chemical processes," *AIChE journal*, vol. 33, no. 6, pp. 898–915, 1987.

[120] M. M. Abbott, J. M. Smith, and H. C. Van Ness, "Introduction to chemical engineering thermodynamics," *McGraw-Hill, Boston*, pp. 619–626, 2001.

[121] R. E. Sonntag and G. J. Van Wylen, *Introduction to thermodynamics: classical and statistical*. 1971.

[122] J. Tarlecki, N. Lior, and N. Zhang, "Analysis of thermal cycles and working fluids for power generation in space," *Energy Conversion and Management*, vol. 48, no. 11, pp. 2864–2878, 2007.

[123] A. Polyzakis, C. Koroneos, and G. Xydis, "Optimum gas turbine cycle for combined cycle power plant," *Energy conversion and management*, vol. 49, no. 4, pp. 551–563, 2008.

[124] J. Black *et al.*, "Cost and performance baseline for fossil energy plants volume 1: bituminous coal and natural gas to electricity," *National Energy Technology Laboratory: Washington, DC, USA*, 2010.

[125] B. Linnhoff and J. R. Flower, "Synthesis of heat exchanger networks: I. systematic generation of energy optimal networks," *AIChE Journal*, vol. 24, no. 4, pp. 633–642, 1978.

[126] K. Holiastos and V. Manousiouthakis, "Minimum hot/cold/electric utility cost for heat exchange networks," *Computers & chemical engineering*, vol. 26, no. 1, pp. 3–16, 2002.

[127] B. Zauderer, "Fossil fuel fired, closed cycle mhd generator in parallel with steam turbine cycle with zero emissions and co2 sequestration," 2012. US Patent 8,277,543.